THE EFFECT OF RECASTING NICKEL CHROMIUM AND COBALT CHROMIUM ALLOYS ON THE QUALITY OF FIXED PROSTHODONTIC DEVICES

NR MCHOUH

PhD **2015**

THE EFFECT OF RECASTING NICKEL CHROMIUM AND COBALT CHROMIUM ALLOYS ON THE QUALITY OF FIXED PROSTHODONTIC DEVICES

NAJIBEH RAJAB MCHOUH

A thesis submitted in partial fulfilment of the requirements
of the
Manchester Metropolitan University for the degree of Doctor of Philosophy

School of Healthcare Science
Manchester Metropolitan University
2015

Abstract

Base metal dental alloys are among the oldest restorative dental materials used in dentistry. They are still widely applied and are expected to remain in demand in the coming years. They demonstrate adequate properties required to meet the needs of wide and variable applications. Base metal alloys can be used alone or in combination with other dental materials to construct a dental restoration. Due to environmental and financial factors, variable practices have emerged in the processing of these alloys. Among these practices is the reuse of surplus alloys. The aim of this study was to evaluate the effect of recycling nickel-chromium and cobalt-chromium alloys on the quality of dental restorations employing a suggested test protocol where the correlation between the different factors tested was investigated.

Wax patterns of different shapes were prepared for the different tests conducted. For each alloy type, five different combinations of new and surplus alloys were prepared to cast the wax patterns using an induction casting machine. Castings were subjected to different quality assessment investigations; (i) the microstructure was assessed for the presence of pores and inclusions and the chemical composition was evaluated for the amount of elements present (mass%), castings produced from new alloy were used as a control; (ii) castings were subjected to a polishing procedure simulating the technique used in dental laboratories. Surface roughness (Ra) was analysed prior to and after the polishing procedure using light profilometer; (iii) a metal to ceramic bond strength test was conducted following the requirements of ISO 9693: 2000. ISO standardised test pieces were subjected to a three-point bending test using a universal testing machine and bond strength evaluated; and (iv) ions released from castings were measured, where castings were placed into artificial saliva at pH 4 and 6 for five weeks. The mean amounts released were measured using inductively coupled plasma atomic emission spectroscopy (ICP/OES).

The findings of this study imply that although microstructure and chemical composition of castings containing surplus alloy varied from those produced entirely from new alloys, these variations were not always significant and depended on the alloy type and restoration type. Surface roughness evaluation suggests that consecutive laboratory procedures, such as

finishing and polishing procedures can considerably enhance surface topography of casting produced partially and entirely from surplus alloy. For the bonding test investigation, all test groups demonstrated bond strength values higher than that recommended by ISO 9693: 2000. A similar observation was documented for the ion release test; despite the increase in the amount of ions released from castings containing surplus alloys, the detected amount of ions was however very small compared to those documented in the literature.

Although some of the tested characteristics of castings containing 100% recycled alloys were marginally inferior to those produced from new alloy, the former castings gave acceptable results and would be expected to function and perform appropriately in the patient's mouth in the equivalent manner to castings produced from new alloys. However the addition of a small amount of new alloy, as low as 25%, has been shown to enhance the performance of castings compared to those containing 100% recycled alloy in the different tests conducted.

Declaration

This thesis contains no material which has been accepted for the award of any other degree or diploma in any university, to the best of my knowledge and belief, contains no materials previously published or written by another, except where due reference has been made in the text. In addition, no parts of this thesis have been copied from other sources. I understand that any evidence of plagiarism and/or the use unacknowledged third party data will be dealt with as a very serious matter.

Signiture: Najibeh Mchouh Date: 15.07.2015

Acknowledgement

I would like to express my sincere thanks to Dr Rebecca Taylor, my director of studies and first supervisor for her continuous guidance, encouragement and support during the course of this work. My very sincere thanks also to my second supervisor, Dr Stephen Horne for his immense knowledge and precious help.

I would also like to thank my third supervisor and previous director of study, Mr Christopher Maryan, for his help and guidance even after his retirement, a few months before the submission of this thesis.

My special thanks to Mr Michael Green for his help and training on metallographic preparations, Dr Anthony Scallan for his kind help and assistance with the statistics of this research and Hayley Andrews for offering her time and expertise in training me on the use of scanning electronic microscopy. I would also like to thank Mr Tom Carly from the Skillbond Company for providing all the materials needed for this research.

My sincere appreciation to the Faculty of Science and Engineering at Manchester Metropolitan University for funding this research.

My thanks to my parents, Rajb Mchouh and Mahdiah Rasheed, for their encouragement and my husband Muhamad Aljahmi, for his patience and understanding.

Table of contents

List of figures

List of tables

Nomenclature

NiCr-AM-0	Nickel-chromium, all-metal crowns made out of 100% new alloy
NiCr-AM-25	Nickel-chromium, all-metal crowns made out of 25% new alloy+75% once-recast alloy
NiCr-AM-50	Nickel-chromium, all-metal crowns made out of 50% new alloy +50% once-cast alloy
NiCr-AM-75	Nickel-chromium, all-metal crowns made out of 75% new alloy+25% once-recast alloy
NiCr-AM-100	Nickel-chromium, all-metal crowns made out of 100% once-cast alloy
NiCr-CB-0	Nickel-chromium, ceramic-bonded crowns made out of 100% new alloy
NiCr-CB-25	Nickel-chromium, ceramic-bonded crowns made out of 25% new alloy +75% once-cast alloy
NiCr-CB-50	Nickel-chromium, ceramic-bonded crowns made out of 50% new alloy +50% once-cast alloy
NiCr-CB-75	Nickel-chromium, ceramic-bonded crowns made out of 75% new alloy +25% once-cast alloy
NiCr-CB-100	Nickel-chromium, ceramic-bonded crowns made out of 100% once-cast alloy
CoCr-AM-0	Cobalt-chromium, all-metal crowns made out of 100% new alloy
CoCr-AM-25	Cobalt-chromium, all-metal crowns made out of 25% new alloy +75% once-cast alloy
CoCr-AM-50	Cobalt-chromium, all-metal crowns made out of 50% new alloy +50% once-cast alloy
CoCr-AM-75	Cobalt-chromium, all-metal crowns made out of 75% new alloy +25% once-cast alloy
CoCr-AM-100	Cobalt-chromium, all-metal crowns made out of 100% once-cast alloy
CoCr-CB-0	Cobalt-chromium, ceramic-bonded crowns made out of 100% new alloy
CoCr-CB-25	Cobalt-chromium, ceramic-bonded crowns made out of 25% new alloy +75% once-cast alloy
CoCr-CB-50	Cobalt-chromium, ceramic-bonded crowns made out of 50% new alloy

	+50% once-cast alloy
CoCr-CB-75	Cobalt-chromium, ceramic-bonded crowns made out of 75% new alloy +25% once-cast alloy
CoCr-CB-100	Cobalt-chromium, ceramic-bonded crowns made out of 100% once-cast alloy
SEM	Scanning electron microscopy
EDAX	Energy-dispersive X-Ray Spectroscopy
SPSS	Statistical Package for Social Sciences

1.1 Aims of study

The aim of this study was to identify, evaluate and understand the effect of the re-casting procedure on the quality of nickel-chromium and cobalt-chromium dental alloys. Five different proportions of new and re-cast alloys were used (100% new alloy, 75% new alloy +25% re-cast alloys, 50% new alloy +50% re-caste alloys, 25% new alloy +75% re-caste alloy and 100% re-cast alloy). The associated microstructure topography, chemical composition, surface roughness and ion release of castings were investigated. Metal to ceramic bond strength was also evaluated.

1.2 Outline of the thesis

Chapter 1 provides an overview of the study

Chapter 2 reviews the main categories of dental alloys and their properties. Factors relating to the casting procedure and their effect on the quality of castings are contained. It also summarizes defects that can occur in castings. Recasting procedure and its effect on the quality of castings are reviewed.

Chapter 3 presents porosity occurrence in base metal cast alloys and their chemical composition. It focuses on the different types of porosity and segregation and factors causing these defects in cast alloys. Methods used to assess castings' quality are described; the findings of microstructural and chemical analyses are discussed.

Chapter 4 reviews the effect of finishing and polishing procedures on surface roughness of castings. It describes the finishing and polishing mechanisms including the different types and composition of abrasives and factors affecting the efficacy of finishing and polishing procedures. Methods used to assess surface roughness are described and findings are discussed.

Chapter 5 presents the metal to ceramic bond strength. The nature of the bonding is explained in detail including factors affecting bonding of metal to ceramic and methods used to evaluate this bond. This chapter details the different influences that recasting surplus alloys can have on bond strength. Methods used in this study to evaluate metal-ceramic bond strength are described and results are discussed.

Chapter 6 contains details on ion release from castings. Biomaterials and biocompatibility of dental alloys are defined. Corrosion and ion release from alloys is presented. Biological and non-biological tests used to measure the ion release from alloys are summarized. Methods used to assess ion release from alloys are described and results are discussed.

Chapter 7 contains an overall discussion and Recommendations of the present research including the strengths and limitations. Suggestions for future studies are also highlighted.

Chapter 8 presents conclusions of the study

1.3 Overview

Since being introduced to dentistry in 1929, cast base metal alloys have been widely used in the construction of fixed and removable partial dentures, orthodontic appliances and metallic components on acrylic dentures. Despite the presence of more aesthetic materials and the emergence of new computer aided design and manufacturing methods, which allow the use of a variety of new dental materials, the demand for these alloys is still high, especially by the National Health Service (NHS). A recent UK based survey revealed that for the fabrication of fixed prostheses, base metal alloys are the most commonly used (52%), with high gold content alloys only used in 8% of the cases [1]. Low cost and adequate physical and mechanical properties, such as low density, high strength and high modulus of elasticity have enabled these alloys to gradually replace noble and semi-noble alloys.

When selecting an alloy for a dental application, a number of factors influence the selection decision. Biocompatibility, physical properties and cost are the main factors. However, over the last two decades, cost has become more influential. A recent survey by an oral health professional association identified that up to 60% of custom-made devices in the area of crowns and bridges, were imported from other countries [2]. In addition, laboratories do not always use alloys corresponding to the dentist prescription, and use cheaper alloys instead [3, 4]. A UK based survey revealed that in 24% of cases, the selection of material was made by dental technicians [1]. Other practices include mixing different brands of alloys, and recycling surplus base metal alloys [5]. The increased prevalence of these practices has made the quality of dental castings questionable, and emphasized the need for vigilance and quality control of custom made dental prostheses.

According to the available literature [5–8] the reuse of surplus base metal alloys is one of the most common practices in dental laboratories. However, no documented figures are available with regard to the amount of recycled or reused surplus alloys; e.g. a report about recycling and recovery in the UK stated cobalt and titanium as elements included in alloys. However, the scale of recycling of these alloys in the UK is unknown [9] .The casting procedure results in surplus alloy, in the form of sprues, buttons and defective parts. By mass, these parts can occupy up to 50-60 % of the casting mass depending on the size of the

casting and the design of sprues [10]. By reusing these parts, the estimated cost can be reduced by 30-40% [11]. From economic and environmental aspects, reusing alloys is highly beneficial because of the reduced amount of natural resources used, and minimizing the pollution which can be caused by the mining works required to extract minerals. However, the implications of this procedure on the quality of dental restorations are not yet fully understood and needs further investigation. This study will evaluate the effect of reusing base metal alloys on the casting quality.

Although there have been several studies on recycling base metals alloys, results of the effect of reusing surplus alloys on the quality of castings are conflicting [12,13], and do not provide a comprehensive understanding of the effect of recycling base alloys. For example, some studies have documented changes in the microstructural characteristics and elemental composition of castings produced from recycled material [14]. However, they have not demonstrated if these changes will compromise the dental device quality and adversely affect cast properties [15]. In contrast, other studies have documented changes in the physical and mechanical properties of castings produced from recycled alloys; however, the microstructural and elemental deviations that might have contributed to these changes were not investigated [16–18].

A few studies have investigated the microstructure amongst other properties of restorations. However, the reason for selecting a particular property to test, and the relation between the microanalysis and characteristics tested were not made clear [19]. In addition, results of the different investigations were not clearly related nor logically presented. No firm conclusion can be drawn from the available literature and there remains an open question on how and why recasting base metal alloys can affect casting quality. The uncertainty surrounding the answers to these questions might explain why manufacturers of base metal alloys, unlike noble and semi-noble alloys do not provide recommendations with regard to the reuse of the surplus casting. For noble and semi-noble alloys, most researchers have recommended the reuse of surplus alloys without compromising alloy quality [19,20].

For a full investigation of the effect of reusing base metal alloys on castings' quality to be provided, both the microstructure and chemical composition of recycled castings and the influence of structure on function must be studied. As different restorations vary in their applications and because it is not practical to evaluate all the mechanical, physical and biological properties of a dental casting, properties chosen to be tested have to contribute to the casting application. A dental restoration is a medical device; it replaces a tooth tissue in the oral cavity. Hence, for bonded castings and all other types of castings of different applications, biocompatibility is an essential requirement. Surface characteristics of castings contribute to its biocompatibility. In addition to biocompatibility, bonded castings must demonstrate adequate bond strength with the quality of the bond relying extensively on the surface characteristics of castings.

In this study, the microstructure, chemical composition, surface roughness, bond strength and ion release of castings produced from surplus alloys at the different stages of restoration fabrication will be evaluated. This combined approach will contribute to the understanding the effect of re-casting on the properties of base metal alloys' castings.

Previous studies have not followed the same comprehensive approach adopted in this study which will evaluate the quality of dental castings. The knowledge derived will benefit alloy manufacturers, dental technicians, dentists and patients; and impacts on biological, financial and environmental issues.

2 Literature review

2.1 Dental alloys

2.1.1 Brief history

The history of dental restorations dates back to the time of the ancient Egyptians and the Etruscans. Among currently-available restorative dental materials, gold has the oldest and longest history of use in dentistry; it has been used for dental repairs for more than 4000 years, when the prime aim of restoring or repairing tissues was aesthetic rather than functional**.** Gold wires were used by the Phoenicians after 2500 BC, and modern gold crowns were described by Mouton in 1746. Amalgam was introduced into dentistry in 1833, and has been widely used in the 19th century. The development of base metal alloys was established during the early years of the 20th century. Due to their superior mechanical properties and low density, these have primarily been used for the fabrication of metal frameworks of removable dentures. Subsequently, due to their adequate properties and reasonable cost, they have gradually replaced gold base alloys [10][21].

2.1.2 Shaping dental alloys

Elements are combined together to produce an alloy with adequate properties for a given application. In dentistry, alloys have extensive applications; they are used for the construction of inlays, crowns, bridges, orthodontic devices, including metallic brackets, arch wires, bands, springs and ligature wires, denture implants and many endodontic instruments and devices. Three methods are used to shape dental alloys; (i) amalgamation, in which material is backed into a tooth cavity while it is still in the plastic state; (ii) cold working, in which alloy is mechanically shaped into the desired shape at a temperature below its crystallisation temperature; and (iii) casting, which involves heating the alloy to its melting temperature and forcing it into a preheated mould [22], (iv) milling, in which alloys, such as titanium and Co-Cr alloys are processed on dental CAD/CAM devices, (v) sintering, where metal powder is melted, with an electric beam for example, to construct a restoration from 3D model data [23].

2.2 Types of dental alloys

According to ISO 22674: 2006 [24], alloys are categorized according to their mechanical properties. These requirements should be met by the metallic material after the recommended processing techniques, e.g. casting and machining (Table 2-1).

Table 2-1 Categories of dental alloys according to their mechanical properties [24].

Type	Proof strength of 0.2%, non-proportional extension MPa, Minimum	Elongation after fracture (%), Minimum
0*	-	-
1	80	18
2	180	10
3	270	5
4	360	2
5	500	2

* Metallic materials for ceramic-metal crowns produced by electroforming or sintering belong to type 0.

2.3 Cast alloys

According to the American Dental Association (ADA) [25], dental casting alloys are designated according to chemical composition or mechanical properties. Classification by chemical composition is based on the weight content of gold and other noble metals. If the gold content is ≥ 40% and the noble metals content is ≥ 60%, the alloy will be classed as a high noble alloy. When the noble metals content exceeds 25%, the alloy will be classed as a noble alloy. If the noble metals are less than 25%, it is considered a base metal alloy. The mechanical properties used for classifying alloys are yield strength (MPa) and percentage elongation (%). Accordingly, alloys are categorised into four groups: (i) soft alloys with a strength of more than 140 MPa, and an elongation of 18%; (ii) medium alloys whose strength is 140-200 MPa, and elongation is 18%; (iii) hard alloys whose strength is 200-340 MPa, and elongation is 12%; (iv) extra hard strength where strength is more than 340 MPa, and elongation is 10% [10, 26].

2.3.1 High noble alloys

According to the ADA specifications No.5 [25], high noble alloys are categorised into three main groups. The first group comprises the gold- platinum alloys, which can be used for full cast and ceramic-metal restorations, and may contain silver as hardeners and zinc as oxygen

scavenger. The second group comprises the gold-palladium alloys, which can be used for the same applications. These contain tin, indium or gallium as oxide-forming elements. The third group comprises the gold-copper-silver-palladium alloys, which are used for full cast restorations. High noble alloys are easy to manipulate, and have the key advantage of resistance to corrosion compared to other cast alloys [26].

2.3.2 Noble alloys

Noble alloys are categorised into four main types, namely gold, copper, silver, and palladium alloys. These alloys contain more silver than the high noble alloys, palladium-copper alloys contain gallium, which lowering the liquidus temperature and increases strength. Palladium-silver alloys cover a wide range of compositions, as the palladium content can lie in the range 26-70 mass%, and the silver content between 20-60 mass%. This produces a range of available properties and applications. These alloys have high strength (400-690 MPa), good hardness (230-275 kg/mm^2), and moderate elongation (10-20%). Moreover, the modulus of elasticity is 93-127 GPa, which is greater than that of high noble alloys, but lower than that of base alloys [10, 26].

2.3.3 Base metal alloys

Base metal alloys are free of gold, platinum or palladium. Examples of base metal alloys used in dentistry are the stainless steels, titanium base materials, nickel-chromium, and cobalt-chromium. The latter two are the commonest base metal alloys, used extensively for the fabrication of a variety of instruments, appliances and restorations.

2.3.3.1 Nickel-chromium alloys

It was in the 1930s when nickel alloys were first introduced for the fabrication of crowns, bridges and partial denture frameworks. Based on the content of chromium, molybdenum and beryllium, Wataha [27] classified Ni-Cr alloys into three groups, Ni-Cr-Be (14% Cr), Ni-Cr (14% Cr) , and Ni-high-Cr (16%-27% Cr and 6% Mo).

Most of the nickel-chromium alloys for fixed prosthesis contain 60-80 mass% nickel, 10-27 mass% chromium and 2-14 mass% molybdenum [26]. Beryllium used to be included in the Ni-Cr alloys composition. However, a report from the CEN/TC (European Committee for

Standardisation, Technical Committees) [28], recommended against the use of beryllium in dental alloys. Beryllium is considered hazard to dental technician who is exposed to its dust and vapour during grinding, polishing and casting of dental alloys. Exposure to Be is associated with the occurrence of different serious skin and lung diseases. In addition, the ADA recommends against the use of beryllium in dental alloys. ISO standards limits Be content to 0.02 mass% [26].

These alloys can be used for full cast and removable restorations. However, due to their adequate properties of high hardness and modulus of elasticity when compared to gold alloys, they are mostly used for bonded restorations. These properties allow for a reduction in the thickness of the cast, so more space is available for porcelain, while still maintaining appropriate strength. In addition, the coefficient of thermal expansion is close to that of veneering ceramics; indeed, a compatible coefficient of thermal expansion is essential to minimise the possibility of metal to ceramic failure. Hence, molybdenum is added to decrease the thermal expansion coefficient. In addition to molybdenum, titanium and manganese enhance corrosion resistance, while beryllium acts as a grain refiner and lowers the melting temperature. Aluminium addition increases strength and hardness. For partial denture frameworks, carbon is added to enhance yield strength and hardness, however it reduces ductility [29]. The properties of nickel alloys can be affected by the heat treatment during casting and ceramic firing cycles. Winkler [30] and Morris [31] reported a reduction in hardness of nickel chromium alloys after exposure to ceramic firing cycles. The main drawback of these alloys, which may restrict their application, is that nickel-containing alloys can be harmful to people with nickel contact allergy. In addition, repeated small dose exposures can cause toxic reactions, while long-term exposure may adversely affect both human monocytes and oral mucosal cells [32].

2.3.3.2 Cobalt-chromium alloys

The first cobalt chromium alloy was introduced to dentistry in the 1930s, in medical implants [33]. These alloys are mainly used for removable appliances, where high rigidity is essential. Cobalt chromium alloys contain 53-67 mass% cobalt, 25-30 mass% chromium, and 2-6 mass% molybdenum. Chromium is considered the key component of this alloy because it confesses corrosion resistance. However, the presence of more than 30 mass% chromium

in a dental alloy makes it difficult to cast and results in the formation of brittle phases within the alloy [29]. Cobalt, which is the major component, adds strength and enhances the modulus of elasticity. Molybdenum provides corrosion resistance and lowers the thermal expansion coefficient. Tungsten also increases corrosion resistance. Other alloying elements are also added, such as silicon, carbon, manganese and iron. Compared to nickel-chromium alloy, this alloy demonstrates superior strength and hardness, however it is less ductile and its thermal expansion coefficient is not as compatible with veneering ceramics as nickel chromium alloys. Comparable properties of cobalt-chromium and nickel-chromium alloys make them a possible alternative to patients, who are sensitive to nickel. however, chromium is also considered an allergen, and patients should also be tested for chromium allergies [26]. Both alloys might contain a small amount of aluminium, carbon, copper and manganese.

2.3.4 Other alloy systems

The third group of base alloys consists of titanium alloys, which are mostly used for implants due to their superior biocompatibility and enhanced corrosion resistance [34]. Titanium is the main component of the alloy, which may also contain vanadium, aluminium, iron, carbon, and nitrogen in appropriate proportions. Their superior biocompatibility is the most favourable property. However, the need for special casting equipment and investment materials to address their low density and high affinity to gases has limited its use as a cast alloy. Stainless steel alloys were one of the first base alloys introduced to dentistry, and their application can be traced back to 1912. They are mainly used in orthodontic instruments and endodontic appliances. The main components of these alloys are chromium and carbon [29].

2.3.4.1 Base metal alloys for ceramic bonded restorations

In addition to basic properties governing the suitability of alloys for fixed and removable frameworks, an essential requirement is that the coefficient of thermal expansion is comparable with that of the ceramic used in ceramic-metal systems. This must be slightly higher for alloys to ensure that ceramic is under compressive loading. In addition, a bonding alloy must have a higher melting temperature than ceramic, and be able to provide adequate roughness for mechanical bonding with veneering materials. It must also have

adequate strength, in that the high strength of the casting reduces deflection, in turn, reducing stresses in the ceramic. High yield strength is required to avoid plastic deformation, high modulus of elasticity is essential to minimise elastic deformation e.g. in bending [10,35].

The design of metal core is critical to provide a space for a suitable ceramic thickness for aesthetic purposes. Colour of the alloy oxides should be masked with opaque ceramics with no complications. Indeed, light coloured oxides are favourable as they are easy to mask with opaque ceramics. High-noble alloys have relatively light-coloured oxides, which can be easily masked with opaque ceramic. However, most nickel and cobalt-based alloys have darker, grey oxides that require thicker layers of opaque ceramic to mask [36].

2.3.5 Selection of base metal alloys

Given the wide variety of available alloys, selection is governed by a number of factors in relation to patient satisfaction and health, and laboratory technique. Alloys should be available and relatively inexpensive. They should harmonise in both function and appearance with the surrounding oral tissues while in use. In addition, it must be adequate for a specific application, as illustrated in the following examples: for a posterior bridge, where restoration is subjected to high loads, the alloy is required to have a high modulus of elasticity; for a clasp in a removable denture, ductility is the prime property, needed to cope with the repeated removal and insertion of the restoration; moreover, these can be made thinner with adequate rigidity [29,35].

2.3.6 Manipulation of base metal alloys

The properties and quality of castings are highly dependent on the manipulation of materials. The melting temperatures encounters in base metal alloys (1300-1450 ˚C) are higher than those of noble alloys (970-1200 ˚C). As a result, melting methods used for noble metal alloys, such as gas-air mixture, are not suitable for base metal alloys, where more controlled conditions are required. Furthermore, investment materials should maintain the integrity at such high casting temperatures. Hence, phosphate bonded and silica bonded investment material are favourable. Gypsum bonded material is less stable at temperatures

higher than 1200 °C, and forms sulphur dioxide, which can be absorbed by the alloy, decreasing its ductility [22].

The density of base metal alloys is half that of noble metal alloys; this low density may lead to inadequate filling of the mould, and sufficient casting force must be applied. Moreover, the porosity of investment material has to be sufficient to allow trapped air to escape. Castings have to be sandblasted with alumina particles to remove residual investment material and oxides formed on the surface. Due to the hardness of these alloys and the low elongation values in comparison to noble cast alloys, in addition to the roughness of investment material used to mould wax patterns, polishing procedures are always expected to be performed with difficulty [22].

2.3.7 Properties of base metal alloys

2.3.7.1 Physical properties

Chromium alloys are lustrous and silvery-white, while nickel alloys are less silvery with a slight golden tinge. Casting shrinkage is 2.05-2.33%. The density of these alloys lies between 8-9 g/cm^3, and elongation is relatively low (3%) [37].

2.3.7.2 Mechanical properties

Base metal alloys have superior mechanical properties to noble metal alloys. The modulus of elasticity is about 145-220 GPa for CoCr alloys, and 150-210 GPa for Ni-Cr alloys, which is twice as much as for noble metal alloys. This allows reduction in the thickness of interproximal connectors and metal copings of anterior bonded restorations. Yield strength is 460-640 MPa for CoCr alloys, and 255-730 MPa for Ni-Cr alloys. Base metal alloys hardness is about 370 kg/mm^2. Although hardness protects thin margins from destruction during polishing, increased hardness makes adjustments harder, while improperly polished surfaces cause greater wear to opposing teeth [10,26].

2.4 Casting process

Metal casting is a process where molten metal is poured into a mold and allowed to solidify into an object. Casting processes can be categorisd into three main groups, (i) sand casting, in which sand is used to define the cavity inside a mold and to make any cores that are

contained in the mold. (ii) die casting, in which molten metal is introduced directly into a permanent tooling and (iii) investment casting, the main advantage of this process over the other casting processes is the use of one piece mould and the absence of the partings required for pattern removal [38].

Dental castings are produced by the investment (lost-wax) process. A wax pattern replicating the object to be produced is surrounded by a heat resistant investment material forming a mould. The wax is then removed by heating. Molten metal is then introduced into the mould cavity through a channel called a sprue (Figure 2-1)

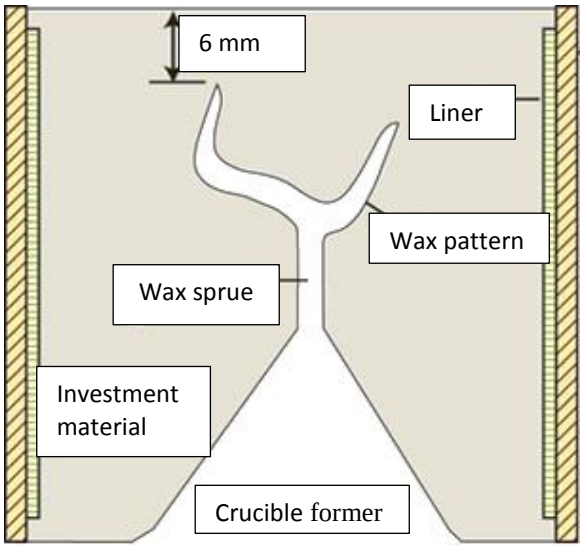

Figure 2-1 Schematic representation of a dental investment casting mould [10]

2.4.1 Factors affecting casting quality

The Investment casting method is associated with the presence of imperfections and discontinuities. These imperfections can be classified as surface or internal. Surface imperfections are visible or open to the surface, such as surface porosity, roughness, incomplete castings, finning and bubbling. Internal imperfections are not open to the surface, and include shrinkage cavities, internal inclusions and segregation. Gas porosity and inclusions can be surface or internal. Inappropriate handling of materials at the different

stages of the casting process, including wax pattern making, mould manufacturing and metal melting and casting, results in the occurrence of casting defects [38].

2.4.2 Effect of sprue design

Sprue design should meet essential requirements to achieve a casting with optimal properties. Sprue design should allow the molten metal to solidify progressively from the extremes of the mold to the sprues and reservoir. Pattern area should solidify first and thick sections feed thin sections, localised shrinkage porosity in patterns should be prevented, and an adequate and sufficient supply of molten metal should be provided with a suitable gas escape mechanism.

Two sprue designs are available, namely bar casting, in which the bar sprue acts as a reservoir for a molten metal and to feed and ensure complete filling of the mould cavity (Figure 2-2 A). It has to be more toward the centre of the mould than the alternative crown pattern. The crown pattern should stand higher than the bar and 5 mm from the top of the mould and also 5 mm away from the ring wall. For vacuum pressure casting, cast port (attachments between sprue bar and pattern) and cross bar should have the same diameter, because the impact pressure, applied through gravity only, is very low during vacuum pressure casting. However, if the centrifugal casting method is used, the connection channel between the cross bar to the cast funnel must be reduced in size. The second sprue design is the direct supply (Figure 2-2 B); in this system, each crown pattern is attached to a cast port which leads directly to the cast funnel, it can be used for crowns, partial crowns, onlays and inlays [10,22,26].

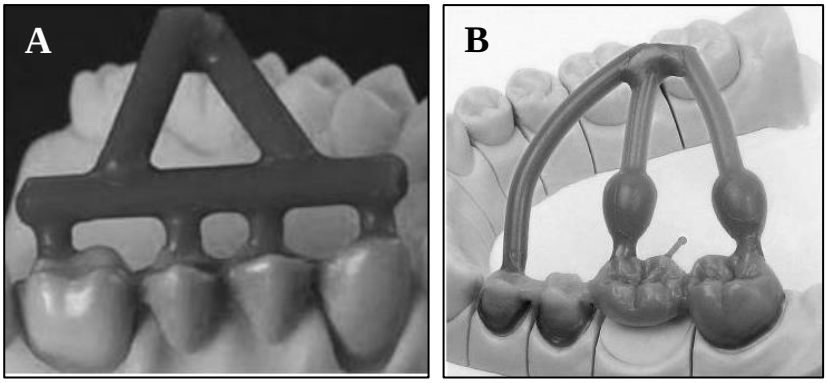

Figure 2-2 Diagrammatic representation of direct (A) and indirect spruing (B) [39]

Sprue position and configuration have been known to affect surface roughness of castings [40,41], and the accuracy of marginal fit of bridges [42]. Sprue-coping junction design has also been shown to contribute to casting quality, flared and smooth sprue attachments enhance castability and minimise porosity [43].

2.4.3 Effect of investment materials

The basic components of investment materials are refractory fillers and binders. Refractory fillers are in the form of quartz, tridymite and cristobalite. Binders can be alpha-hemihydrate for gypsum-bonded investment or magnesium oxide and phosphate for phosphate-bonded investment. Gypsum bonded investment materials can provide a smooth consistency on mixing with water which leads to the production of casting with smooth surface. The major drawbacks of this material are reactions above 700°C when sulphur dioxides and trioxide can be produced. It should therefore not be heated above 700°C, and can only be used with alloys having a maximum melting temperature of 1040 °C. This limits its application to high noble and some noble alloys. In addition, this investment material is not strong enough to tolerate the high turbulence associating with casting base dental alloys and expansion from a gypsum bonded investment is not sufficient for base metal alloys.

Phosphate-bonded investment material, on the other hand, can be used with most of the available dental alloys due to its favourable properties, such as strength, expansion control and precision. Although it is difficult to divest and sandblast castings, because of the strong adherence of oxides, increased demand for base alloys and cast ceramics make phosphate-

bonded materials the most commonly-used [10,26]. Using phosphate-bonded materials with cobalt-chromium and nickel-chromium is well documented in the literature. Work is being conducted to investigate silica-based materials for use as investment for the casting of titanium based materials. Titanium has high reactivity with some of the components of these materials, such as silicon, oxygen and phosphorus. The products of these reactions can affect corrosion resistance, and mechanical properties [44–46].

2.4.4 Effect of melting method

Melting an alloy is a critical stage of the casting process. Overheating an alloy beyond its casting temperature can affect its microstructure and result in the formation of precipitates, and consequently may adversely affect physical and mechanical properties. Two main types of crucible materials are available, namely graphite and ceramic. Graphite crucibles are not suitable for base metal alloys, which are sensitive to carbon contamination. They were primarily designed to be used with high gold content alloys, and are inexpensive, can be easily handled, and show resistance to thermal cracking [47]. Ceramic crucibles have been used as an alternate. They can be used with all cast alloys, are thermally stable and inert to molten metals [10,48]. Typical crucible ceramics are ThO_2, stabilized ZrO_2 (i.e. additions of HfO_2 and CaO to ZrO_2), Al_2O_3 , MgO, Bn, and fused silica [49].

2.4.4.1 Melting with flame

A flame is generated by gas and air, acetylene and air, or acetylene and pure oxygen. The flame has to be adjusted; a torch flame can be divided into different zones (Figure 2-3). The tip of the reduced zone is the portion which should be used to melt the alloy. It is blue in colour and is the hottest part of the flame. Using the unburned gas portion of the flame (carbon rich area) causes the inclusion of carbon into the alloy. Using the oxidizing zone causes oxygen entrapment in the molten metal [10].

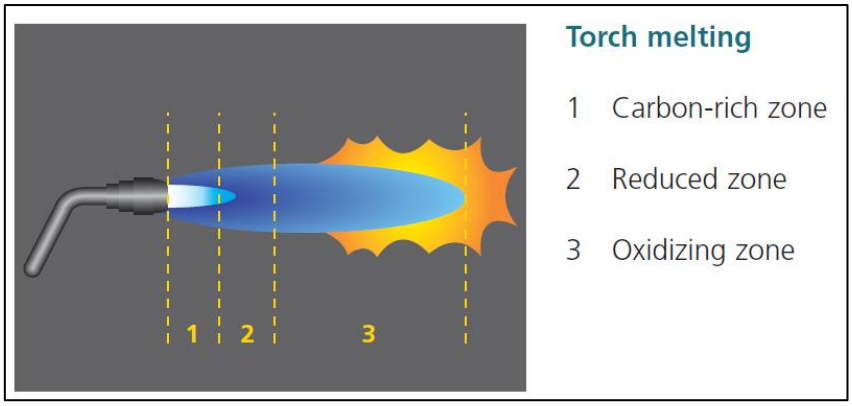

Figure 2-3 Flame casting [50]

2.4.4.2 Melting with resistance heating

When an alloy is melted in a resistance-heating furnace, the temperature is created via a power-charged resistance heating conductor coil. The coil surrounds a receiving container for the crucible. The resistance-heated conductor is warmed up by electric power. The heat emitted by the heating coil is transferred to the crucible causing the alloy to melt. Casting temperature must be set to compensate for heat loss during heat transfer [51] (Figure 2-4).

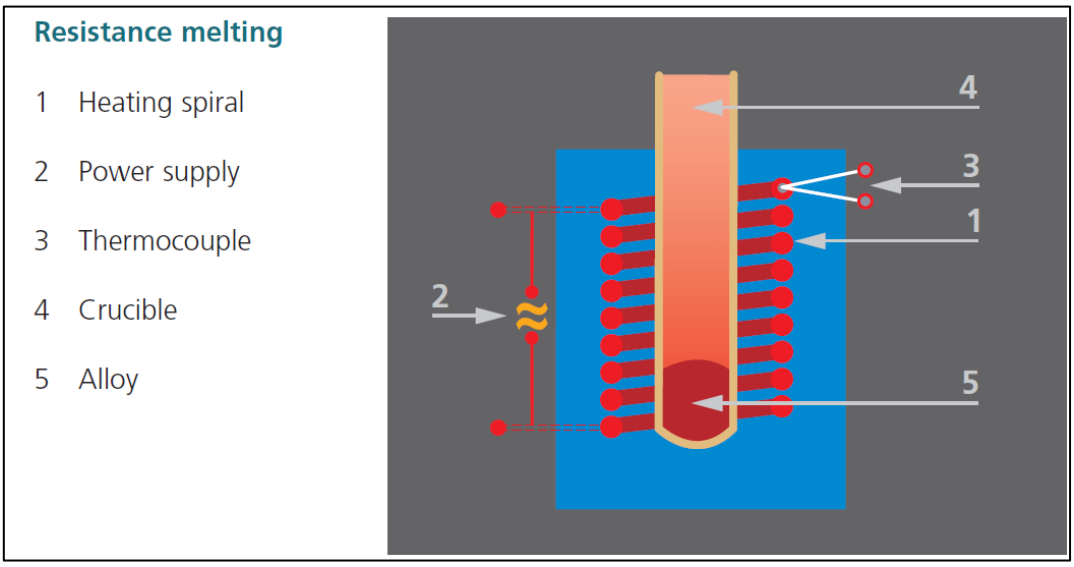

Figure 2-4 Resistance melting [51]

2.4.4.3 Melting with induction heating

The induction tension is created via a transformer, which is connected to an alternating current. Induction tension is transmitted onto the induction coil, which enfolds the crucible. To avoid burning of the coil, the induction coil is cooled with water during the casting

process. When the high frequency tension is transmitted onto the induction coil, and while the alloy melts, turbulence and a variable magnetic field develop within the alloy causing it to heat up and melt [51] (Figure 2-5).

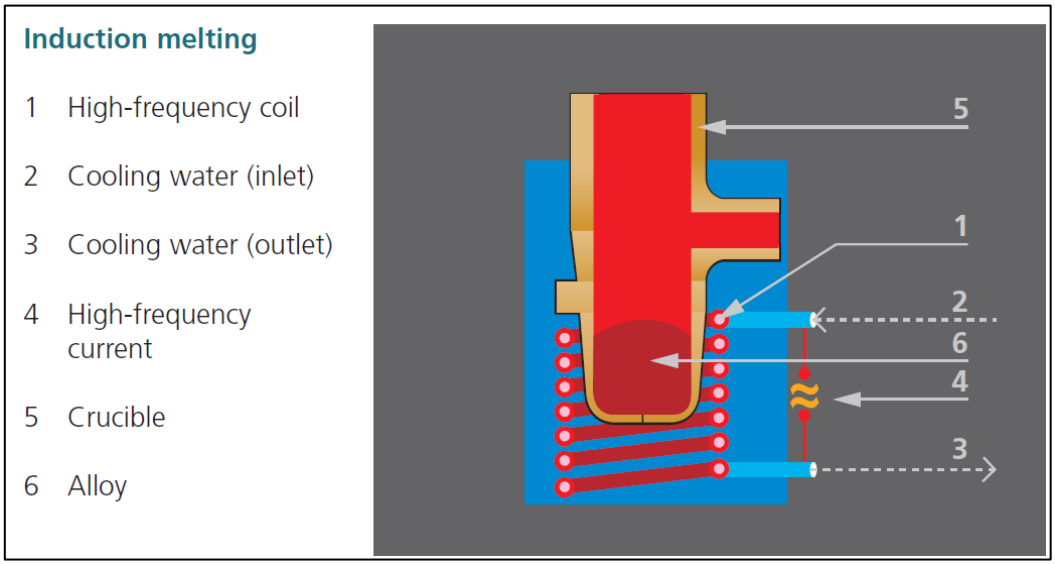

Figure 2-5 Induction melting [51]

2.4.4.4 Melting with electric arc heating

The electric arc is created by a current that continuously runs between two electrodes. One electrode (negative) is made of tungsten and represents the movable part during the melting process. The second electrode (positive) is located at the bottom of the crucible. During the melting process, both electrodes approach each other until the continuous currents cross and connect. Arc furnaces differ from induction furnaces in that the alloy is directly exposed to an electric arc, and the current in the furnace terminals passes through the charged alloy. It is used with alloys of high melting temperature, such as titanium (1800 ˚C) [51] (Figure 2-6).

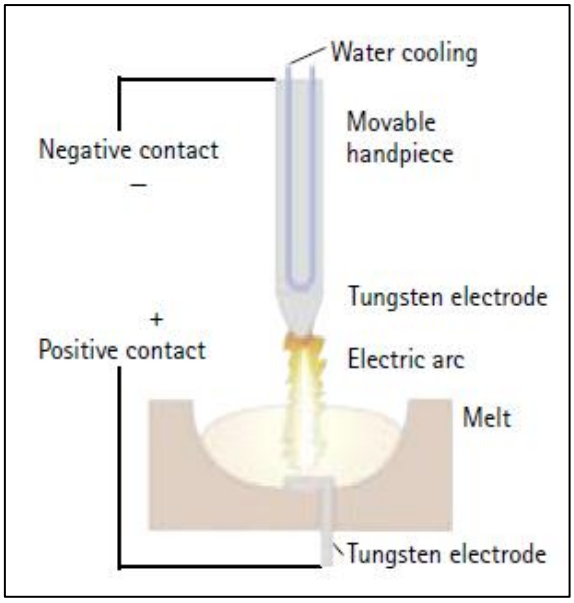

Figure 2-6 Electric arc heating [51]

Most studies have compared the effects of using a variety of melting methods on microstructure and mechanical properties of a particular alloy or a range of alloys [52]. Among all melting methods, flame melting is the least controlled. In addition, other melting systems demands less skill from the operator, and result in less errors in technique [53]. On the other hand, induction vacuum casting has been shown to produce good quality castings with regard to casting defects [54].

2.4.5 Casting methods

2.4.5.1 Centrifugal casting

This casting process uses a centrifugal force to transfer molten alloy into the preheated investment mold. The flow of molten metal is affected by a combination of forces initiated by centrifugal arm activation and gravity force, which work in a contrary direction [51] (Figure 2-7).

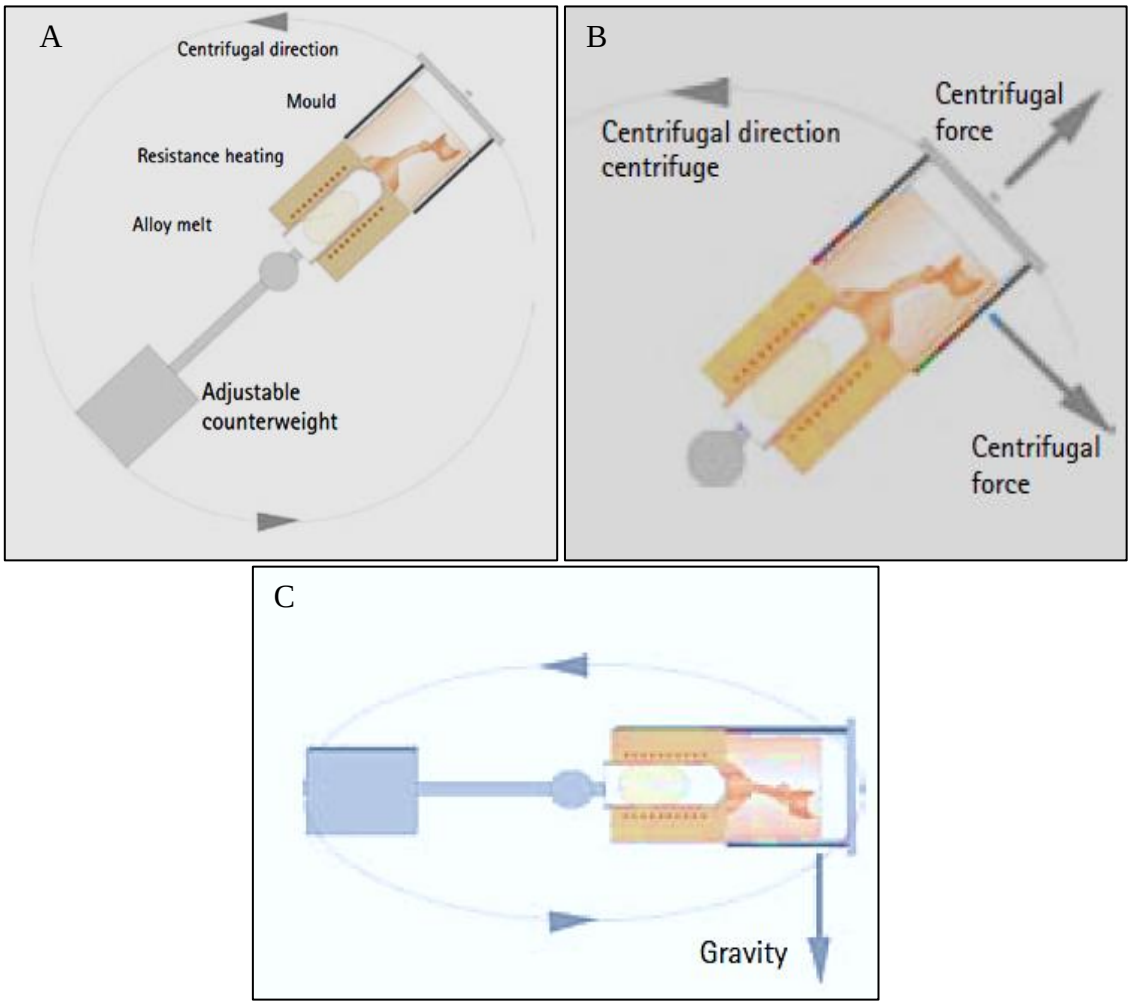

Figure 2-7 Crucible centrifuge, top view (A), centrifugal force (B), gravity (C) [51]

2.4.5.2 Vacuum pressure casting

Following resistance or induction heating, molten metal is forced into a mould by gravity and vacuum at a pressure of about 2.5 bar. The pressure is then increased to 3-3.5 bar 60 seconds. It has been documented in the literature that induction vacuum casting enhances surface characteristics of noble alloys [53] and base metal alloys [55].

2.5 Casting defects

Casting processes can result in defects, such as pores and cracks, appropriate handling of materials and strict observation of procedures can minimise casting failures.

2.5.1 Finning, bubbling and foreign particles

Rapid heating can cause the investment material to crack, allowing molten alloy to flow into these cracks resulting in fins on the casting surface. Inadequate porosity of the investment surface, due to an inaccurate liquid to powder ratio, can also result in excess nodules attaching to the casting. High liquid powder ratio results in a thick mixture and poor flow of investment over wax pattern. These casting faults can compromise quality, if present at critical areas, such as margins and fitting surfaces [10]. Contamination with foreign particles can cause surface imperfections, in terms of roughness and voids. Foreign bodies can be investment particles and debris from crucibles.

2.5.2 Incomplete castings

Among all the possible factors causing incomplete casting, insufficient permeability is the most relevant; backpressure of unvented (compressed) air has to be overcome by using sufficient pressure for the right period of time [40]. Premature solidification of sprues is another factor and can be prevented by using an adequate thickness of sprues attached to the thick sections of the wax pattern [42,43]. Moulds should be heated properly to ensure complete removal of wax and moisture, and also balance mould temperature to alloy temperature. Sufficient heating of alloy is an essential requirement, where insufficient heating results in melt of high viscosity and surface tension resulting in incomplete casting [56]. Low density of base alloys, which creates less thrust, make it more vulnerable to this type of defect [22].

2.5.3 Porous casting objects

Porosity is the most common casting defect; and cannot be entirely prevented. Porosity can spread within the casting and on its surface. Different types of porosity might exist throughout the cast. Solidification defects result in shrinkage porosity. Gases trapped during casting result in subsurface, and pinhole porosity. Inclusions suspended in the molten metal act as sites of porosity and result in gas inclusions [57]. (Porosity will be discussed in detail in Chapter three).

2.5.4 Microstructure

2.5.4.1 Microstructure of cast alloys

Nickel alloys have a face-centred cubic crystal structure at all temperatures, while cobalt alloys have a face-centred cubic crystal structure at temperatures above 417 °C, and hexagonal structure at room temperature. Elements like nickel and carbon are added to cobalt alloys to stabilise the face centred cubic crystal structure [58]. In terms of microstructure, alloys are categorised into three main groups; solid solution, eutectic and peritectic.

In solid solution alloys, liquid freezes to form a single solid phase of the same composition as the liquid. In eutectic alloys, a liquid of eutectic composition solidifies at a single temperature producing two solid phases. For peritectic alloys, two solid phases are formed, but in contrast to eutectic alloys, they do not form simultaneously, one solid phase forms, this phase then reacts with the liquid phase to form the second solid phase [59].

Base metal dental alloys mostly solidify with a dendritic microstructure, while high noble and noble alloys solidify with a polycrystalline microstructure in which the three dimensions of each crystal is similar. During solidification of alloys grain boundaries are the last microstructural feature to form. These regions of lattice disorder provide sites where low melting phases, precipitates and porosity occur [10].

Cobalt-chromium alloys in the cast condition consist of an austenitic matrix composed of a solid solution of cobalt and chromium in a cored dendritic structure. The dendritic regions are rich in cobalt, while the interdental dendritic region is a combination of different phases

[26]. Carbides formation is associated with this structure, and depends on the presence of some elements, such as molybdenum, cobalt and chromium. Carbides may be found at the grain boundaries, and can be spherical and not continuous [14]. The microstructure of nickel-chromium alloy exhibited cored dendrites with twin grain boundary and thin, elongated precipitates within the matrix [60].

2.5.5 Quantifying microstructure and image analysis

Image analysis is widely used in various disciplines, such as medicine, biology, engineering and geological science [61]. This application has been enhanced by the expansion in the use of quantitative microscopy methods. Microstructure features have been employed mainly for qualitative assessments to support further assessments. Indeed, microstructural features of alloys, such as grain size, primary and secondary dendrite arm spaces and pores, can be quantified either by a visual inspection or a semi-automatic inspection by image analysis. However, image analysis software is not extensively used in the dental alloys research sector.

Visual methods, such as the linear-intercept method and the equivalent circle diameter method, are very slow and exhaustive, while semi-automatic inspections offer greater operator independence, and a high productivity time analysis.

Diógenes [62] aimed to observe the differences between visual inspection and the semi-automatic inspection. The semi-automatic measurement methodology was more precise and faster than the visual method. Krupiński [63] investigated the effect of cooling rate on the phase structure of aluminium alloys, using an image analysis software, Krupiński employed optical micrographs for the microstructural analysis. However, using scanning electron microscopy (SEM) micrographs for the analysis gives more precise measurements as SEM provides much better focus and resolution.

Galic [64] assessed the effect of chemical composition of two gold-based alloys on the microstructure and micro-hardness of alloys, ImageJ software, similar to the one used in this study, was used to quantify the grain size and the porosity occurrence. The lake of control group was a limitation of Galic assessment. Maksimović [65] evaluated the effect of

recasting process on the quality of the microstructure of high gold content alloys and calculated the porosity percentage (%) using an image analysis software. Porosity was assessed without etching the test pieces. It is not possible to compare data documented in Maksimovic's study with other studies where surfaces of test pieces were etched for microstructural evaluations [64]. Only one study was found in the literature that used image analysis software for a quantitative assessment of the casting defects of Co-Cr alloys [66]. This study aimed to assess the intensity of casting defects using Image analysis and indicated the presence of 1.3% of pores in the cross-sections of castings.

2.6 Microstructural analysis

There are two basic methods used to generate images for testing and analysing a prepared material surface: optical images, in which all parts of the image are formed simultaneously, and scanning images, in which each point of the image is forming serially, but with high frequency, and the image appears to the operator in its entirety [67]

2.6.1 Scanning electron microscopy (SEM)

SEM is used to study the surface characteristics of a bulk specimen. When electron beams hit a solid surface, a variety of interactions occur; some beams are back-scattered, while others penetrate the solid and interact with it. This interaction results in the ejection of low energy electrons and the formation of x-ray photons. Different types of formed beams are used to characterise the material and reveal information about its external morphology, chemical composition, and crystalline structure [67] (Figure 2-8).

Characterisation of dental materials relies to a large extent on SEM; for example, in 2009, 33% of the published articles in The Journal of Dental Materials and 47% of the journal articles in the Dental Material Journal reported on studies using SEM [68].

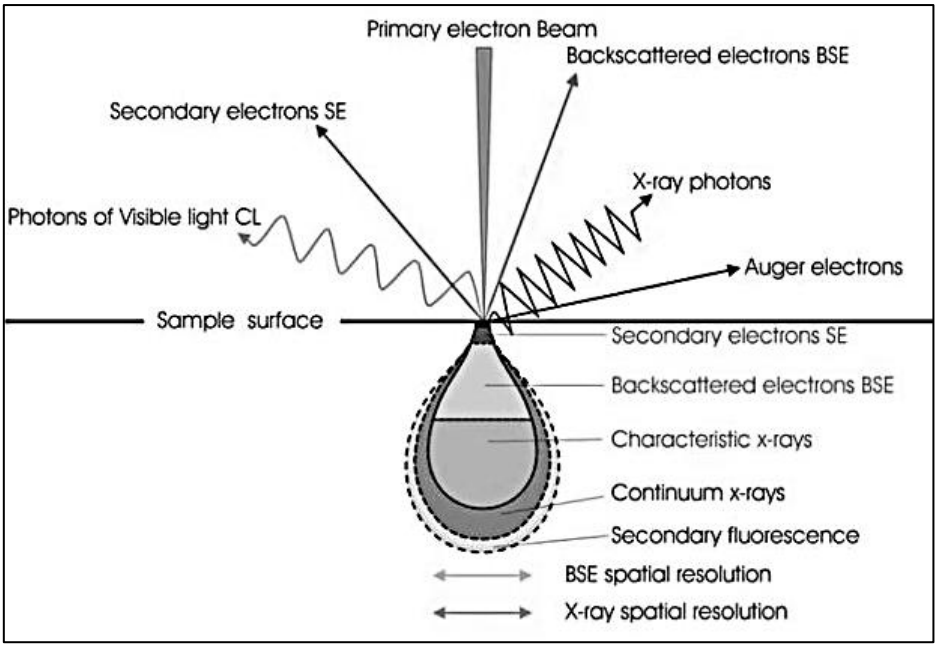

Figure 2-8 Electrons interaction with sample surface [69]

2.6.1.1 Components of SEM

A scanning electron microscope consists of an electron gun, where electrons are produced from a tungsten wire, driven toward an extractor anode and then directed towards the specimen surface. The second component comprises lenses, which are used to focus the beam of electrons on the specimen. Two types of lenses are utilised; a condenser lens, which is placed below the electron gun, and an objective lens, which is closer to the specimen. The third component is the scan coil, which drives the beam across the specimen surface. The fourth main component is the detector. Two types of detectors are used: one for the secondary electrons, and the other for back scattered electrons. SEM is mainly used for topographical analysis, while chemical microanalysis is done using Energy dispersive Spectrometer (EDAX) [70] (Figure 2-9).

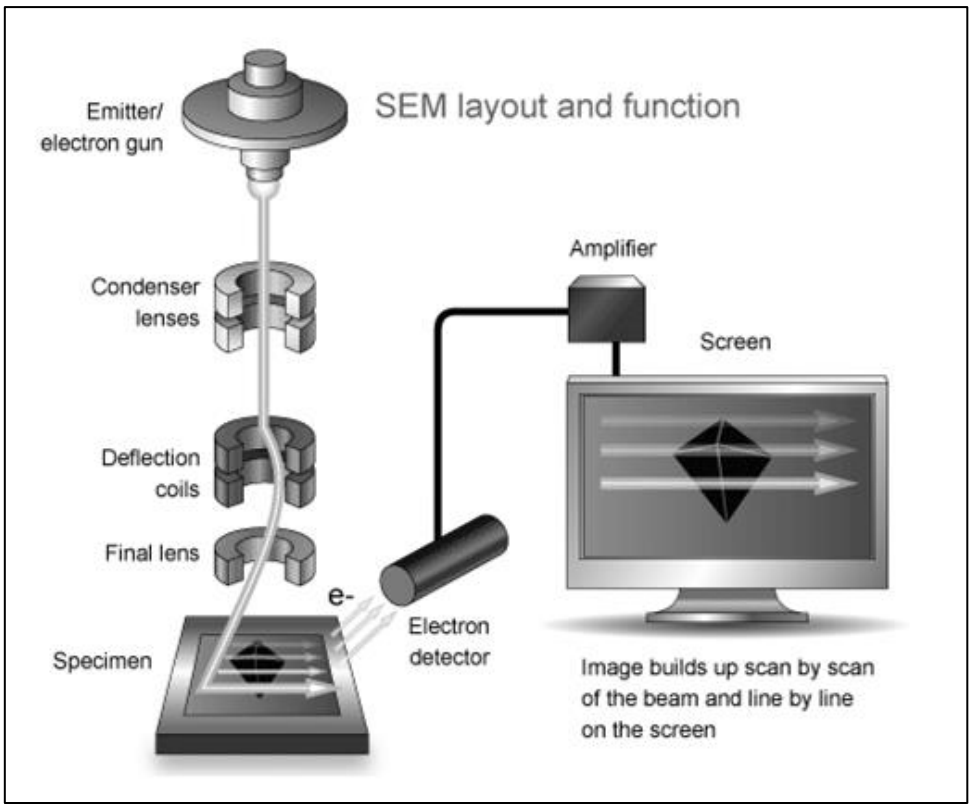

Figure 2-9 Components of scanning electron microscopy [71]

2.6.1.2 Image display

Output signals from detectors are amplified and transferred to a display unit. Scanning of the display unit is coordinated with an electron probe scan, brightness deviation, which depends on the number of secondary electrons, and appears on the monitor screen of the display unit forming an SEM image.

2.6.2 Energy dispersive X-Ray analysis (EDAX)

X-rays can derive from deeper in the sample than both secondary and backscatter electrons. A focused beam of electrons is used to generate x-rays from the specimen. The intensity of the X-rays emitted from the sample atoms is characteristic in their energy and wavelength. The various characteristic X-rays are measured using the Energy dispersive Spectrometer (EDAX). It includes a sensitive X-ray detector, liquid nitrogen for cooling and software to collect and analyse energy spectra. The detector is mounted in the sample chamber of the main instrument at the end of a long arm, which is itself cooled by liquid nitrogen. An EDAX

detector contains a crystal that absorbs the energy of incoming X-rays by ionisation, yielding free electrons in the crystal that become conductive and produce an electrical charge bias. The x-ray absorption thus converts the energy of individual x-rays into electrical voltages of proportional size; the electrical pulses correspond to the characteristic X-rays of the element. The most common detectors are made of Si(Li) crystals that operate at low voltages to improve sensitivity. Recent advances in detector technology provide detectors that operate at higher count rates without liquid nitrogen cooling. All elements from atomic number 4 (Be) to 92 (U) can be detected. EDAX can be used for qualitative analysis to identify the elements present in a specimen, and for quantitative analysis by measuring how many X-rays of a particular element are emitted per second [70].

2.6.3 Phase analysis: X-ray diffraction (XRD) and X-ray Fluorescence (XRF)

When X-rays interact with a crystalline substance, a diffraction pattern is created. The X-ray diffraction pattern of a substance can be used for quantitative determination of the various crystalline compounds; the diffraction method is thus ideally suited for characterisation and identification of polycrystalline phases. XRF is one type suited to quantitative analysis; for example, a sample may be submitted for XRF and found to contain 50% Al_2O_3 and 30% SiO_2, and this may be sufficient information. However, XRD could then distinguish between samples containing different phases; for example, quartz (SiO_2), corundum (Al_2O_3), Mullite ($Al_6Si_2O_{13}$) or kaolinite ($Al_2Si_2O_5$ $(OH)_4$) or any combination of these [67].

2.6.4 Carbon coating

Image acquisition by SEM and chemical characterisation by EDAX in samples of low electrical conductivity have the disadvantage of charge build up (Figure 2-10). Charge build up affects the generation of secondary and backscattered electrons, and the excitation of characteristic X-rays. In order to minimise this, a conductive coating is applied to the sample surface. Elements used for coating are carbon, gold, silver, platinum, palladium, and chromium [72]. The coating should be as thin as possible, of a low atomic weight, and should not contain an element, which is of prime interest in the analysis. The thickness of coating layer required for conductivity varies between different elements, and ranges from 1-10 nm. Gold coating improves SEM images quality; however its tendency to migrate on

the surface of materials and to merge into clusters might result in masking fine details of the scanned area and interfering with EDAX analysis [67].

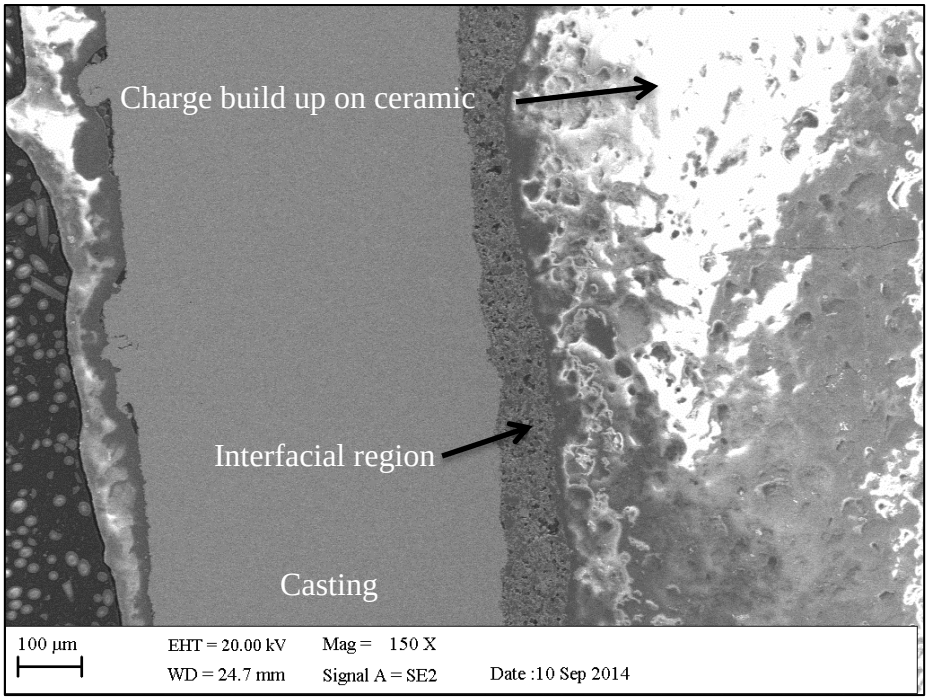

Figure 2-10 Charge build up on the ceramic side of ceramic-metal test piece.

2.6.5 SEM and image analysis systems

The vast majority of studies, which are particularly interested in the quality of dental castings, have utilised SEM and EDAX microscopy. Although SEM is primarily used for qualitative assessments, the use of image analysis software with SEM images has made it possible to gain quantitative information, and maximise the advantages of using SEM microscopy. Microstructural features of alloys, such as grain size, primary and secondary dendrite arm spaces and microstructural defects, such as pores, cracks and inclusions can be quantified [63,73].

The energy dispersive fluorescent X-ray Spectrometer (EDAX) is extensively employed in dental material research. It can be coupled with several applications, including SEM and transmission electron microscopy (TEM), making it advantageous to researchers. Some researchers have analysed the chemical composition of the bulk of alloys and investigated the effect of chemical composition on alloy properties [74,75], and some have evaluated

characterisation of materials [76,77]. Others used X-ray mapping line profile techniques to assess the concentration of elements at specific areas [78]. Most studies interested in the ceramic metal interface have used EDAX analysis [79,80].

X-ray diffraction (XRD) is mainly used to investigate crystal structure, type, and orientation, as well as the boundaries between crystals [45,81]. It is also used to assess the effect of alloying elements on phase formation and distribution [82].

2.7 Recasting dental alloys

Since 1962, studies regarding recasting of base metal alloys have been conducted by various researchers, such as Nelson [12], Hesby [13], Harcourt [83], Hong [84] and Presswood [85]. They mainly assessed properties of recast alloys, such as tensile strength, percentage elongation, modulus of elasticity, mean yield strength, micro hardness and corrosion behaviour. Some researchers investigated the microstructure and elemental composition of recast alloys [7,86].

Base metal dental alloys are super alloys, which have a specific property of melting at high temperature (1350-1500°C) [87]. Super alloys have a defining feature of demonstrating high mechanical strength and surface stability at high temperatures. The prime application of these alloys was to manufacture airfoils in the hot parts of gas turbine engines. However, optimised properties of super alloys have driven wider applications, such as mechanical containers and biomedical devices [88]. Recasting super alloys has been principally developed for aero-engine turbine vanes [89]. The manufacturing of aero engines results in an excessive amount of scraps in the form of cast gates and heads. The technique has been confirmed to construct turbine blades and vanes from recycled alloys, with the addition of at least 50% new alloy [89].

For financial and environmental reasons, dental laboratories may re-use dental alloy to manufacture metal restorations [90] . Manufacturing a metal restoration includes the use of a casting procedure, and results in a significant amount of metal surplus, such as buttons, sprues and defective castings [29], with some studies suggesting these parts of castings and the reused castings may be susceptible to the formation of microstructural defects, such as cracks and porosity [91]. Even though noble dental alloys are preferred when constructing

crown and bridge restorations, because of their biocompatibility and durability [59], base metal alloys are used because of their low cost and suitable mechanical properties [29].

Several studies have confirmed the use of recast noble and semi noble alloys [20,92] as acceptable practice providing the quantity of new material was not less than 50%. However, recommendations on the use of recast base metal alloys are in wide disagreement. While some researchers do not recommend use of re-cast alloys [93,94], others permitted the use of 100% re-used alloy for at least four generations [95], while a third group found that a combination of 50% new and 50% once-recast alloy is acceptable [96]. In addition, previously published work was restricted to investigating the mechanical and physical properties of re-cast alloy [97,98] as opposed to assessing the microstructural and elemental differences that might contribute to changes in these properties. Although variations in results obtained by researchers can be due to the different methods and techniques applied, further microstructural and chemical analyses is believed to provide a deeper understanding of the effect of re-casting on the casting quality of base metal dental alloys.

Base metal dental alloys are categorised into two groups, wrought and cast. Elemental composition, microstructure and applications are different in the two groups. Although dental technicians can control the amount of wrought alloy used to construct the metallic parts of removable orthodontic appliances, wrought alloys of high cost and significant properties, such as nickel-titanium have been subjected to recycling [99,100]. In addition to wires, metallic direct-bond orthodontic brackets have been also recycled [101,102].

2.7.1 Effect of recycling dental alloys

Re-casting might interfere with the chemical composition of alloys by changing the amount and/or the distribution of elements throughout the casting, and hence, affect the properties of alloys. In the absence of established guidelines for re-cast alloys, researchers have used different apparatus to evaluate the quality of the re-cast alloys. Some researchers evaluated the physical properties, such as marginal fit [94], castability [96] and surface roughness [103]; others evaluated metal to ceramic bond strength [104] and mechanical properties, such as hardness. Moreover, biocompatibility is the prime requirement for a dental casting, corrosion and element release tests were the main investigations by researchers to

evaluate the quality of re-cast alloys [105–107]. A few studies have evaluated the microstructure and elemental composition of base-metal re-cast alloys [19,86] , some researchers have used porosity as an evaluation parameter [108,109].

A few studies have investigated the effect of re-casting procedure of the base metal alloy on its porosity [108]. Dharmar [110] evaluated the occurrence of porosity in clasps of chromium cobalt removable partial denture frameworks. However, porosity evaluation was not precise, radiographic images were used to count defects, results of the evaluation were introduced as (number of defects), which can included different types of defects, such as pores, inclusions and cracks and not only porosity. In addition, no distinction was made between internal and external defects.

Palaskar [108] used Whitlock's method to investigate the occurrence of porosities in re-cast base metal alloys. This mesh design does not resemble the dental crown design, and so it is not a reliable indicator of the occurrence of porosity. However, it was used to evaluate the effect of different variables on alloy castability, such as sprue diameter, investing technique, and melting and casting method [111].

Mehl [112] used the number of shrinkage cavities to evaluate the alloy microstructure quality. The researcher did not include the gas porosity within the measurements. In addition, all restorations which included pores of less than 100 µm diameter were considered acceptable regardless of the repetition and surface area of these pores. However, a smaller pore size has been documented to adversely affect the yield strength of a ceramic-metal alloy [113].

2.7.2 Methods to assess quality

Castability is considered by some researchers to be a valuable factor in assessing the quality of re-cast alloys. Castability is the ability of the molten alloy to fill and reproduce the sharp detail of the mould space [29-31]. Re-casting might affect the density and flow of the alloy. Palaskar [114] assessed the effect of re-casting Ni-Cr alloys on castability using Whitlock's method. Marginal accuracy was also used to assess castability [115]. Whitlock's method is a mesh design used to evaluate alloy castability [116]. Although this method can measure the casting completeness, it does not measure the casting fit, since this design does not simulate dental restorations [117].

Dental alloys are in intimate and long-term contact with oral tissues. Variations in the oral environment, such as in saliva, temperature, plaque, and pH affect the elemental release of the alloy. Element release can cause local and systemic adverse biological effects, such as allergic reactions and mutagenicity [118]. Many researchers investigated the corrosion behaviour and element release of base metal alloys [118–120]. Peraire [19] assessed the effect of recasting process on chemical composition, microstructure and micro-hardness of noble and nickel-based alloys. No significant differences were documented among seven recast generations. In his study, Peraire stated that no casting defects were observed in any of the castings. This observation can cause the deny of the conclusions drawn by Peraire's study, it is well documented in the literature that casting process results in the presence of casting defects, such as pores and inclusions, even in castings produced from new alloys [66].

Bond strength between metal and ceramic is a critical factor for the clinical performance of restorations. Recasting alloys may affect the metal oxide layer composition and thickness at the metal-ceramic interface [121,122].

Researchers have used different approaches to investigate the effect of recasting on bond strength. Yavuz [7] observed the changes in the mass ratio of the alloy components and the occurrence of micro porosity after the re-casting procedure and suggested that these changes will have an effect on the mechanical properties and the metal-ceramic bond strength, although this was not investigated further. Mirkovic [123] evaluated the effect of recycling on the modulus of elasticity of Ni-Cr and Co-Cr alloys. Because of the decrease in the modulus of elasticity in castings containing surplus alloy, the investigator did not recommend the use of re-cast alloys for ceramic bonded restorations. However, metal-ceramic bond strength was not assessed; not evaluating bond strength is a limitation of this study.

Colour is an important factor for the success of metal-ceramic restorations; Yilmaz [124] evaluated the effects of various types of metal alloys on the color of opaque ceramic after repeated ceramic firings and concluded that subsequent firing cycles affect opaque color. However, evaluating the effect of alloy type and the number of ceramic firing cycles on the shade of the glazed ceramic gives better indication on the success of the restoration.

2.8 Evaluation of casting quality

2.8.1 Clinical and laboratory evaluations

Clinical tests involve direct observation of material performance in the oral cavity over a period of time. In contrast, laboratory tests are more involved with the material factor. These give an indication of the probability of technical quality as well. *In vitro* tests provide indirect static evaluation and description of material quality in terms of chemical, mechanical, physical, and biological properties. While *in vivo* tests observe restoration functioning, such as caries resistance, marginal integrity and surface texture [125]. In some cases, these differences between *in vivo* and *in vitro* test protocols resulted in, poor correlation between clinical observation and laboratory evaluation. Attempts to improve the correlation have been raised in combination with the increased interest in developing restorative materials, and extending the lifetime of dental restorations. Different proposals have been suggested to achieve this essentially required connection. The first proposal is testing a single property that predicts a vital clinical property, such as surface roughness. The second suggestion is evaluating a cluster of properties that is expected to cause a clinical performance change, such as ion release and surface roughness. The final proposal is simulating the oral environment and clinical condition, such as thermal cycling and mechanical fatigue [125].

2.8.2 Quality of custom made restorations

Only three studies found in the literature have aimed to evaluate the quality of custom made restorations [4,112,126]. Each researcher adopted a different approach and method.

Astudy by Ekblom [4] investigated the quality of fixed partial dentures made in China with corresponding ones made in Sweden. Marginal fit, colour, occlusal and approximal contacts and weight of castings were evaluated. It was found that although the quality of restorations made in China and Sweden were comparable, the laboratories in China did not use the alloy recommended by the dentist. Moreover, cobalt-chromium alloys used contained a small amount of nickel. The researcher used California Dental Association criteria (CDA) [127]. The criteria described by this particular association are divided into three main groups of sixteen principles. Ekblom [4], only tested five of the principles.

Although the difficulty combined with testing all the required criteria by the CDA could be the reason of this, a clarification should be provided by the researcher on why particular properties were chosen to be tested.

Another study by Mehl [112] evaluated the microstructural quality of cast noble alloy in a commercial laboratory. Mehl proposed a wiping etching as a simple method to assess microstructure. Although the researcher applied a simple method to etch the test pieces, for etching to be effective, it has to be prepared using metallographic polishing. Because researcher used a crown as a test piece, light and stereomicroscopes have been used to assess pores size and quantity. However, direct imaging can only be used for primary evaluation, and other microscopy techniques, such as SEM, provide much better focus and resolution. Image analysis was done using the circle method, and while accuracy of this visual method can be comparable to image analysis software, it is very slow and exhaustive. Microstructure of castings was compared with samples provided by the alloy manufacture. However, it would have been more realistic, if they were compared with crowns produced in a laboratory. The researcher tried to adopt a non-destructive approach to assess quality; however, accuracy and applicability of analysis should not have been compromised. The study did not explain if the observed changes in microstructure morphology would have an effect on the functional durability of restorations and compromise casting properties.

Waddell [126] investigated the elemental composition of castings manufactured in China. The presence of toxic elements in ceramic bonded restorations was the main concern of this investigation. Although no toxic elements were detected, it was identified that nickel was the dominant element in all base alloys used to manufacture low-priced crowns. In addition, a few samples contained chromium content beyond the recommended amount of 12-25%. Elemental composition of castings could have been tested against ingots of alloys provided by the manufacturer; this would help determine whether the presence of nickel in the cobalt chromium alloys had resulted from using cheap alloys or from contamination during the casting procedure. The variation in the amount of cobalt present in cobalt chromium alloys could have resulted from mixing different brands of alloys or using surplus alloys.

With the limited number of studies concerning the quality of restorations prior to the fitting in patient's mouth, further studies are needed to establish for a standard procedure.

2.9 Future of base dental alloys

Cast alloys are still extensively used presently, in spite of the recent use of all-ceramic restorations which have gained popularity due to their excellent aesthetic and development in CAD/CAM. They are used to fabricate all-metal restorations, bonded restorations, frameworks for partial dentures and metallic components of orthodontic appliances [36]. In addition, a skilled technologist can produce ceramic-bonded restorations aesthetically comparable to all-ceramic crowns. These restorations have demonstrated long-term clinical success, which is not yet available for all ceramic restorations produced using CAD/CAM systems and additive methods. The concerns about the amount of waste material associated with computer aided manufacturing and the cost combined with the limited ability of this manufacturing method to produce only one part at a time have led to the use of additive methods of manufacturing [23] such as, stereo-lithography, selective Laser Sintering (SLS) and 3-D printing. The lost wax technique can still be used, combined with some of the additive manufacturing technology, such as additive manufacturing of removable partial and full crowns, where the wax pattern is printed for conventional lost wax casting or selective laser melting [128]. However, there is still much research to be accomplished before additive manufacturing technologies become standard in the manufacturing industry. Indeed, most of these methods are expensive and technique sensitive [129].

There has been rapid progress and promising applications of digital technology, such as in orthodontics, maxillofacial and implant prosthodontics [130], and the development of additive manufacturing of indirect restorations, removable dentures and models by using wax printing and selective laser melting has added more options for the use of digital technology in dentistry [131]. However, the introduction of digital technology involves significant costs in terms of equipment purchase and staff training, which explains the reluctance of commercial companies and laboratories in contributing to deploying these technologies. A UK-based survey conducted by Chatham in 2014 [128] revealed that nearly half of UK dental schools do not have any digital dentistry in their curricula, and a high number of the graduate dentists and dental technicians are not trained on using this technology.

Current interest in recasting base metal alloys can be shown by a recent publication, in 2015, which conducted a systematic review on the influence of recasting on the quality of dental alloys [5]. In addition, other recent articles published in 2014 and 2013 [6,132] have investigated recasting process.

Although there is high potential for the worldwide replacement of the lost wax technique by digital technologies, all the above facts emphasise the expectation that base metal dental alloys and the casting method will have command for at least the short-term future.

2.9.1 Health services annual report

The National Health Service (NHS) in the UK reported that the number of patients served by the NHS dental service totalled 29.9 million patients seen in the 24 month period ending on 31 December 2013; an increase of 1.8 million on the March 2006 baseline. This represents 55.9% of the population compared with the March 2006 baseline of 55.6%. The majority of patients were classified under the band 3 treatment level [133].

In the NHS, treatments are categorised according to the level of complexity, band 3 includes complex treatments, such as crowns, dentures, and bridges. It also covers check-ups and simple treatments, such as examination [134]. According to The Health and Social Care Information centre (HSCIC) and the NHS Dental Statistics for England, the number of people in this category is increasing over time (Table 2-2). In addition, a survey of the percentage of the population served by NHS dentists demonstrated no decline within the band 3 category from 2010/11 to 2014/15 (Figure 2-11) [135]. Most people included in this category are low income individuals (Figure 2-12) [135].

Table 2-2 Number and percentage of CoTs (Case of Treatments) by treatment band at specific dates [135]

Date	Quarters	Number (000s)	Percent of total (%)
2006/07	Total	1,529	4.4
2010/11	Total	2,187	5.6
2011/12	1	515	5.3
	2	540	5.4
	3	569	5.8
	4	592	5.9
	Total	2,217	5.6
2012/13	1	518	5.4
	2	538	5.4
	3	577	6
	4	607	6
	Total	2,232	5.6

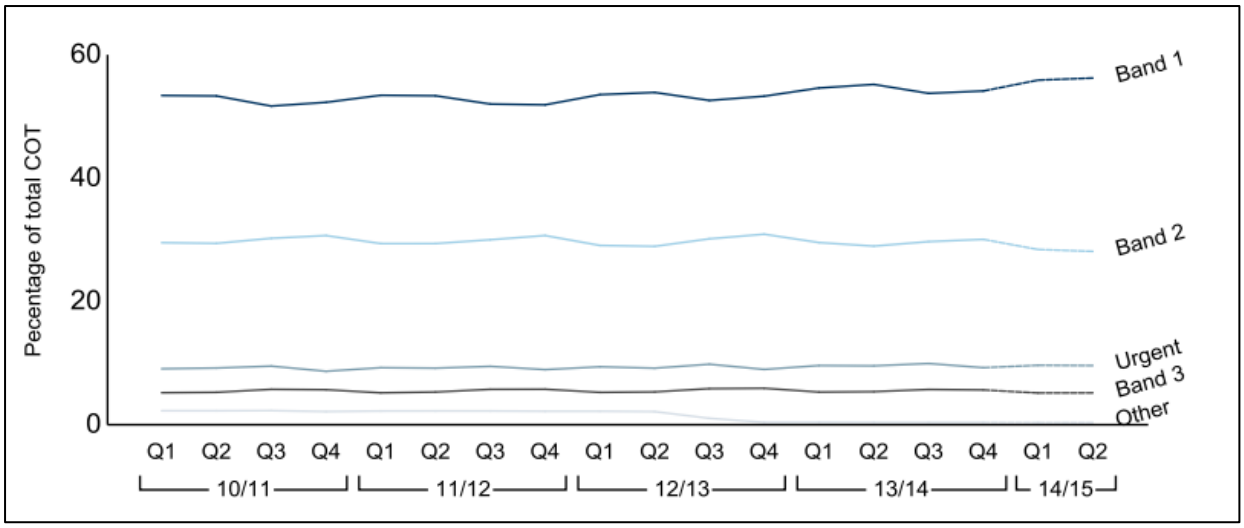

Figure 2-11 Percentage of CoTs delivered in each treatment band 2010/2011 to 2014/2015 [135]

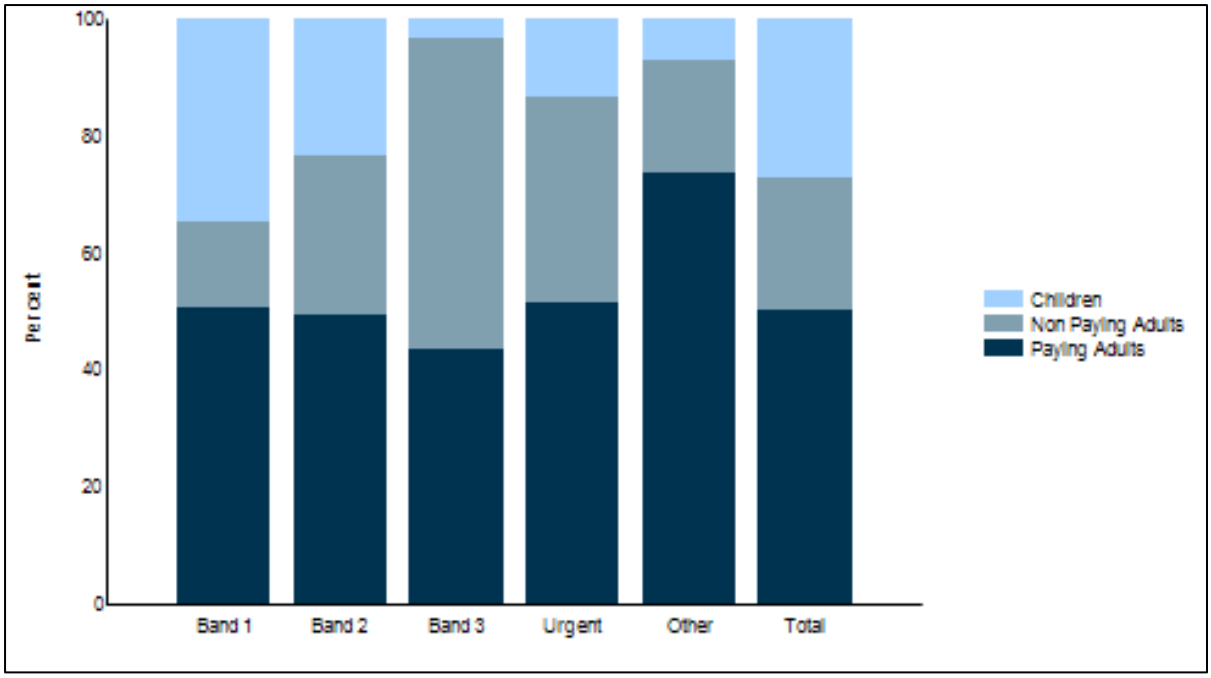

Figure 2-12 Percentage of CoTs by patient type for each treatment band, 2012/2013 [135]

2.9.1.1 Crowns and bridges

Statistics also show that the total number of crowns provided to adults by NHS dentists in 2011/2012 (821400 crowns) was similar to the total number of crowns in 2012/2013 (818400 crowns). Moreover, there has been a slight increase in the total number of bridges fitted from 196500 to 196600 in the same period.

Although there has been a small decrease in the number of adults who had crowns fitted from 773100 people in 2011/12 to 769500 people in 2012/13, there has been a marginal increase in the number of people who had bridges fitted from 85000 to 85900 during the same period of time. These figures emphasise the importance of this research and other similar research. Fixed restorations delivered by the NHS are either full cast or bonded restorations; alloys used are cobalt chromium and nickel chromium dental alloys [135]. The trend in increased demand for access to NHS services is expected to continue for the coming years [136].

2.9.2 Metal prices

The increase in noble alloys prices was always one of the reasons for the recasting process. This increase is determined by moving commodity prices. Since 2005, prices of gold have shown a gradual and steady increase up to 2013. There was then a slight drop in 2013, but since that time no further drop was reported and prices have been fluctuating within a small range. Palladium has become more expensive and so bonding alloys are back to comparable levels to those in 2010 (Figure 2-13 and Figure 2-14) [137]. It should to be noted that gold, platinum, palladium and silver are all priced in dollars per ounce, which means that the exchange rate between the dollar and the pound is very important in influencing the daily price.

For base metal alloys, in addition to the effect on the international metal market (Figure 2-15) [138], in the UK, there is a movement to large corporate practices that have joined forces and they are pushing for lower prices due to their increased buying power. This is forcing more base metal alloys to be used to reduce the price of each crown made.

Figure 2-13 Gold prices ($/ounce), over 10 years (2005-1015) [137]

Figure 2-14 Palladium prices ($/ounce), over 10 years (2005-2015) [137]

Figure 2-15 Nickel prices ($/tonne) over 6 years (2009-2015) [138]

3 Porosity and chemical analysis of alloys

3.1 Literature Review

3.1.1 Porosity

Manufacturing processes of materials, such as casting and sintering of alloys, ceramics and composites can produce porosity. The detrimental effects of porosity have been studied through mechanical, physical and chemical tests [5] or finite element analyses [139].
Porosity in cast iron have been proven to reduce its strength and ductility [140,141], while porosity in cast composites decreases their wear resistance [142]. In dental castings, porosity can compromise the restoration quality, reduces the bulk composition, and causes stress concentration in specific areas [143,144]; it can also increase the surface roughness [103] and affect corrosion behaviour of the restoration [93].

3.1.1.1 Gas porosity

Most metals, such as copper, silver and platinum absorb gases (oxygen, nitrogen and hydrogen) when exposed to melting and casting procedure. The solubility of gases decreases during solidification; subsequently, they are rejected from the melt in the form of bubbles, which may become entrapped within and between crystals at the grain boundaries and between dendrites. Figure 3.1 shows a schematic view of a section through a solidifying casting, as further growth of the dendrites occurs; gas bubbles precipitate and become trapped in the dendrite arms (Figure 3-1).

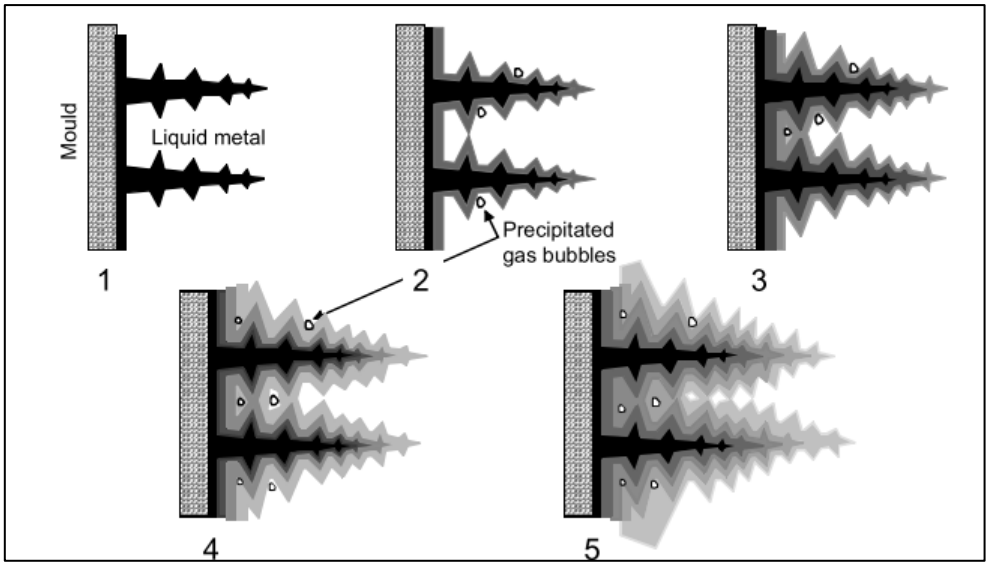

Figure 3-1 Progress of gas precipitation [145]

Dissolved gases may precipitate as simple gas bubbles but may; such as oxygen; react with melt components to form either bubbles of compound gas (e.g. CO_2) or insoluble non-metallic particles. The occurrence of this type of porosity can be increased under poor casting conditions, such as the use of a poorly adjusted torch flame. Investment material may also break down into gaseous products, which can become trapped in the molten metal. Back pressure porosity is another type of gas porosity, and results from the inability of air to escape through investment material [146]. The presence of inclusions enhances the formation of gas inclusion porosity. Inclusions can also exist from the reaction between the alloy and the investing material used to make the mould. Gas porosity is generally rounded, isolated, and well distributed [145].

3.1.1.2 Sources of gases

Gas inclusion in metals results from three main sources; firstly, atmospheric gases can be controlled by avoiding the inclusion of gases during casting. In addition, the use of small amounts of alloying elements to bind with gases and prevent their release on cooling and solidification, helps minimise gas porosity [145]. During casting, elevated temperatures enhance the reaction between components in the alloy and gases; increases in the melt temperature of 100 ˚C will double the dissolved oxygen levels. In addition to temperature, the amount of dissolved gases is also affected by time, and so alloy melting and casting has to be done in as short a time as possible. Secondly, for compound gases, such as water

vapour and carbon monoxides, the hydrogen resulting from the decomposition of water vapour is easier to be absorbed by the molten metal than hydrogen resulting from the dissociation of molecular hydrogen as the prime reaction needs less energy to happen. Finally, mould reaction products, i.e. reactions between molten metal and refractory materials can also cause porosity. Decomposition of gypsum

$$CaSO_4 + SiO_2 = CaSiO_3 + SO_3$$

happens at 960˚C; however, in the presence of silica, this might occur at 870 ˚C [147].

3.1.1.3 Solidification shrinkage and inadequate feeding

Adequate feeding of molten metal to the mould is essential to compensate for alloy shrinkage during solidification. As solidification proceeds, the volume reduces and surrounding liquid flows in to compensate for the shrinkage occurring. Geometry, sprue configuration, and dimensions all control the occurrence of porosity. Early solidification of critical areas of the cast, such as sprue to pattern attachment area can cause the flow of molten metal to be delayed or even completely blocked. When sufficient liquid cannot flow in, the solid, when it is quite soft during the early stages of solidification may flow in with the help of extra pressure from the casting machine. If neither liquid nor solid can feed the shrinkage, shrinkage porosity occurs. This shrinkage porosity can be either small-distributed pores, clustered pores or one large pore. It mainly occurs close to a sprue casting junction, and in the thicker parts of patterns [38,145].

3.1.2 Crystallisation zones

During solidification, three types of grain formation can result depending on casting conditions. Firstly, the chill zone, which is the outside layer of the casting, consisting of a thin layer of equiaxed crystals of random orientation. Secondly, columnar grains often of a dendritic shape can be produced and finally a central zone which is the last to solidify and consist of a coarser, equiaxed grains (Figure 3-2 A and B).

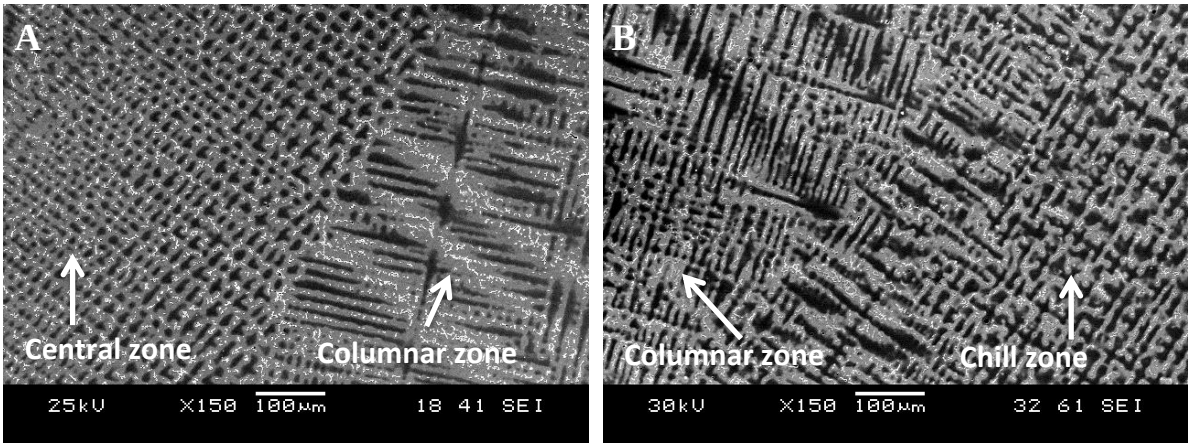

Figure 3-2 Solidification zones in Ni-Cr castings

3.1.3 Segregation

Segregation is a common phenomenon during solidification and represents the variations in composition from one point to another through the alloy structure. Two types of segregation can occur, macro-segregation and micro-segregation. In macro-segregation, changes in the chemical compositions occur at relatively large dimensions (from several millimetres to centimetres). During solidification, three phases exist: solid, liquid, and a solid–liquid phase, which is called the 'mushy zone', consisting of dendrites and interdendritic liquid.

The basic cause of segregation is that the liquid rejects solutes during freezing, because the solid phase has less solubility compared to the liquid phase [148]. Different types of macro-segregation can exist throughout the cast. Inclusions and insoluble impurities concentrate in the last part of the cast to solidify and result in normal segregation. A high concentration of later solidifying compositions near the surface of the casting results in inverse segregation. If the density of the components of solidifying metals varies, a third type called gravity segregation exists [149]. Micro-segregation however is the change in the chemical composition over a relatively small scale. Insoluble foreign particles are trapped during solidification causing segregation at the grain boundaries [150].

Porosity assessment has been utilised for casting quality control in removable dentures [110], fixed restorations [151] and welded areas of fractured components of appliances, such as clasps and orthodontic wires [152]. Most researchers used scanning electron

microscopy micrographs and X-ray micro-focus computerised tomography (micro-CT). Fewer researchers used radiographic evaluation [110,153]; radiographic examination of castings cannot detect pores of small size [153] and thin areas of casting, while uneven surfaces produce radiolucency, which may erroneously be considered as pores or defects [110].

3.2 Aims and objectives

The aim of this chapter is to report on the investigations into the effect of recasting surplus alloys on the porosity occurrence and chemical composition of nickel-chromium and cobalt-chromium test pieces produced from new and surplus alloys at different proportions.

For microstructure assessment, five different combinations of new to recast alloy were used. Two types of test pieces were prepared; all-metal crown and metal-ceramic coping. Castings were mounted into mounting compound (KonductoMet, USA), polished, etched and prepared for metallographic analysis.

Microstructure of alloys was examined with a scanning electron microscope (SEM) (JEOL, JSM-5600 LV, Japan). Casting quality was evaluated by assessing the occurrence, type, and surface area of pores. ImageJ software was used to quantify porosity. Data were presented as mean percentage area of porosity (%) and mean count of pores.

Chemical analysis, were conducted using Energy-dispersive X-Ray Spectroscopy (EDAX). Results were presented as mean of mass (mass%). For qualitative assessments, SEM micrographs and EDAX analysis were performed for the different phases of the microstructure of representing test pieces.

The data were statistically analysed using analysis of variance (ANOVA) for assessing the significance level of the differences between the experimental groups. All statistical analysis was performed with commercial statistical software IBM SPSS Statistics 19. The probability of p being below 0.05 was considered to be statistically significant. Results were represented graphically as mean values with standard deviation.

3.3 Experimental methods

3.3.1 Materials

The chemical composition of the alloys as provided by the manufacturer (Argeon-Skillbond Ltd, UK), and the EDAX analysis of alloy ingots, in unit mass%, is presented in Table 3-1 and Table 3-2

Table 3-1 The bulk composition of the Co-Cr alloy as supplied by the manufacturer and from EDAX analysis (mass%).

Element	Manufacture (mass%) (Argeloy N.P, Argen-Skillbond Ltd. UK)	EDAX (mass%)
Co	59.50	54.67
Cr	31.50	29.64
Mo	5	5.54
Si	2	2.89
Mn	<1.0	00.47
Fe	<1.0	00.46
O	-	2.39
C	<1.0	1.00

Table 3-2 The bulk composition of the Ni-Cr alloy as supplied by the manufacturer and from EDAX analysis (mass%).

Element	Manufacture (mass%) (Argeloy N.P, Argen-Skillbond Ltd. UK)	EDAX (mass%)
Ni	54	49.12
Cr	22	19.13
Mo	9	8.90
Nb	4	3.96
Ta	4	6.65
Fe	4	3.87
Al	< 1.0	1.08
Si	< 1.0	0.61
Co	< 1.0	0.60
Mn	< 1.0	-
O	-	3.10
C	< 1.0	2.00

3.3.2 Test pieces

In order to produce replicate test pieces, two silicone moulds of an upper molar acrylic die were created. One was for an upper molar full cast (0.5-3.0 mm thickness) and the other for upper molar bonded crown (0.3-0.5 mm thickness). Molten wax was poured into the moulds to create a hundred wax patterns.

3.3.2.1 Silicone mould

The acrylic die, on which the wax pattern was formed, was fixed in the centre of the lower part of a plastic mould (5.5 cm × 4.0 cm × 3.0 cm). Heavy silicone putty (MetroDent, UK) was poured into the lower part of the box surrounding the die. The silicone putty was allowed to set for twenty minutes. Two wax sprues were attached to the wax pattern (Schottlander & Davis Ltd, UK) to serve as channels for molten wax. Soft putty silicone (SheraDuosil H, UK) was used to form the top part of the mould. Silicone was poured through a hole made in the top cover of the plastic box. The silicone putty was allowed to set for thirty minutes. The two silicone putty halves were separated. Wax (Crowax-Renfert. GmbH) was melted and poured inside the mould through the sprues and allowed to cool down for three minutes Wax pattern and wax sprues were taken out of the mould. The same procedure was repeated for both silicone moulds (Figure 3-3).

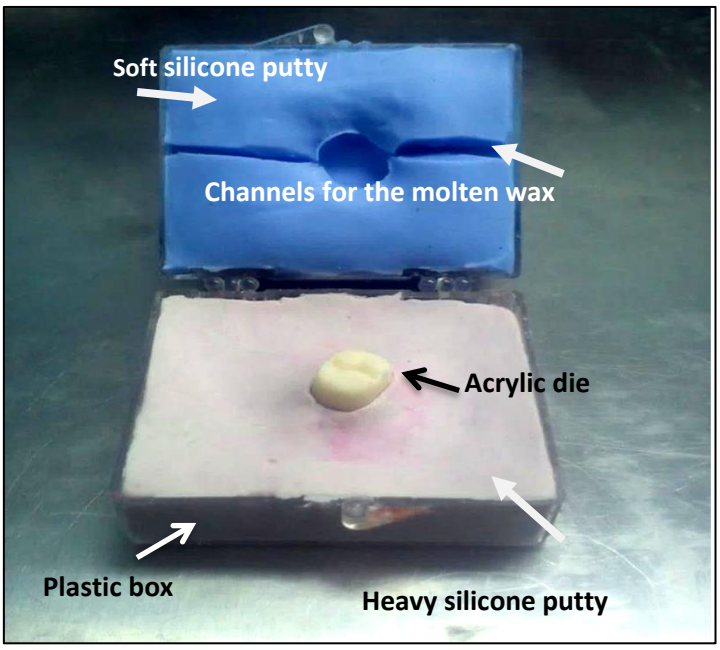

Figure 3-3 Silicone mould of an acrylic die

3.3.2.2 Experimental groups

One hundred wax patterns were fabricated and divided into two main groups (n=50), namely all-metal and ceramic-bonded crown groups. Each of the two main groups was further divided into two sub groups (n=25) of cobalt-chromium alloy (Co-Cr) and nickel-chromium alloy (Ni-Cr). Each alloy group was equally divided into five groups (n=5); the first group comprised 100% new alloy; the second group comprised 75% new alloy mixed with 25% surplus alloy; the third group comprised 50% new alloy mixed with 50% surplus alloy; the fourth group comprised 25% new alloy mixed with 75% surplus alloy; and the fifth group comprised 100% surplus alloy (Table 3-3).

Table 3-3 The experimental groups of the Co-Cr and Ni-Cr alloys with the abbreviations used to describe each test group

Alloy type	All-metal castings (AM) (0.5-1.5 mm thickness)			Ceramic-bonded castings (CB) (0.3-0.5 mm thickness)		
Cobalt-chromium (Co-Cr) (N=50)	100% new alloy	(CoCr-AM-0)	(N=5)	100% new alloy	(CoCr-CB-0)	(N=5)
	75% new + 25% re-cast	(CoCr-AM-25)	(N=5)	75% new + 25% re-cast	(CoCr-CB-25)	(N=5)
	50% new + 50% re-cast	(CoCr-AM-50)	(N=5)	50% new + 50% re-cast	(CoCr-CB-50)	(N=5)
	25% new + 75% re-cast	(CoCr-AM-75)	(N=5)	25% new + 75% re-cast	(CoCr-CB-75)	(N=5)
	100% re-cast alloy	(CoCr-AM-100)	(N=5)	100% re-cast alloy	(CoCr-CB-100)	(N=5)
Nickel-chromium (Ni-Cr) (N=50)	100% new alloy	(NiCr-AM-0)	(N=5)	100% new alloy	(NiCr-CB-0)	(N=5)
	75% new + 25% re-cast	(NiCr-AM-25)	(N=5)	75% new + 25% re-cast	(NiCr-CB-25)	(N=5)
	50% new + 50% re-cast	(NiCr-AM-50)	(N=5)	50% new + 50% re-cast	(NiCr-CB-50)	(N=5)
	25% new + 75% re-cast	(NiCr-AM-75)	(N=5)	25% new + 75% re-cast	(NiCr-CB-75)	(N=5)
	100% re-cast alloy	(NiCr-AM-100)	(N=5)	100% re-cast alloy	(NiCr-CB-100)	(N=5)

3.3.2.3 Spruing and investing

Two wax sprues (10 mm × 4 mm) were attached to a plastic crucible former and joined with a horizontal sprue (40 mm× 4 mm) (MetroDent Ltd, UK). Wax patterns were attached to the horizontal sprue with short sprues (3.5 mm× 3 mm) at an angle of 45 degrees to the wax patterns long axis to allow the incoming molten metal to flow freely to all portions of the mould (Figure 3-4). Wax patterns and crucible former were placed in a metal casting ring, about 6 mm from the top of the casting ring. Soft wax (MetroDent Ltd, UK) was used to seal around the crucible former and the casting ring. A casting ring liner (DeguDent, UK) was placed inside the ring leaving about 2.0 mm- 3.0 mm from both ends of the ring. Wax patterns were coated with a tension release agent (SheraMaster, UK).

160g of phosphate-bonded investment powder (Skillbond, UK) was mixed with 24 mL moulding liquid (Skillbond, UK) for each casting ring. Initial mixing was performed manually for 30 seconds. Vacuum mixing (Medical EXPO, Koala, UK) was then used for further mixing of 80 seconds. Investment material mix was poured into the casting rings on a vibrating table (Manfredi-Saed Pulsar-6, Torino) using the lowest vibration setting in order to avoid any distortion of wax patterns. Moulds were allowed to set for sixty minutes.

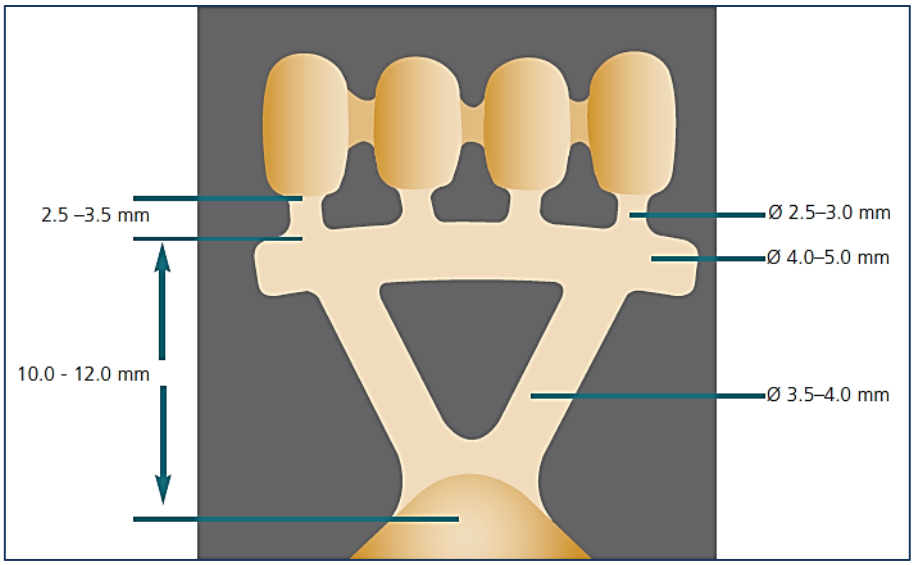

Figure 3-4 Sprue design [50]

3.3.2.4 Wax elimination and alloy casting

After the investment had set, the crucible former was removed and debris of loose investment carefully removed. The top layer was scraped off to help gases escape during wax burning and casting processes. Rings were placed in a cold furnace (Ugin, Dentaire) to burn out the wax patterns. The heating cycle was performed following the manufacturer's instructions. The temperature was raised to 290 °C; moulds were soaked at this temperature for thirty minutes. The temperature was then raised to 850 °C for sixty minutes. After removal from the furnace, the rings were transferred into an induction casting machine (Heraeus Kulzar, UK). Ingots of dental alloys (Argeloy N.P, Argen-Skillbond Ltd. UK) were heated up to their casting temperature, (1342 °C for the Ni-Cr alloy and 1400 °C for the Co-Cr alloy) and directed by centrifugal force towards the mould. Each casting was made with 28 g of the alloy. The amount of alloy required for a casting was determined by the weight of the wax pattern and sprues in grams and multiplied by the density of the alloy (8.8 g/cm^3 for the Co-Cr alloy and 8.6 g/cm^3 for the Ni-Cr alloy as provided by the manufacturer). Casts were allowed to cool down for twenty four hours, divested manually and then abraded with 50 µm Al_2O_3 abrasive under 4-bar pressure (DentalFarm, Italy) to remove the investment material.

3.3.2.5 Re-cast material preparation

Castings were separated from sprues, and sorted into groups. The oxide layer on buttons and sprues was removed by sand blasting with 50 µm Al_2O_3 abrasive under 4-bar pressure (DentalFarm, Italy). Buttons and sprues were then cut into pieces using dental separating discs (Skillbond Ltd, UK), steam cleaned, air blasted and cut into different sizes and then weighed to be mixed with new alloys in the appropriate proportion (Figure 3-5 A).

3.3.2.6 Metallographic preparation

3.3.2.6.1 Mounting

All-metal crowns were sectioned with a slow speed diamond saw (IsoMet, Buehler, USA). The section line extends through the mesiolingual cusp to the distobuccal cusp. One section of each sample was used for the investigation (Figure 3-5 B). Ceramic-bonded castings and sections of all-metal crowns were embedded in conductive filled phenolic mounting

compound (KonductoMet, USA) and cured in a mounting machine (Buehler, USA) (Figure 3-5 C).

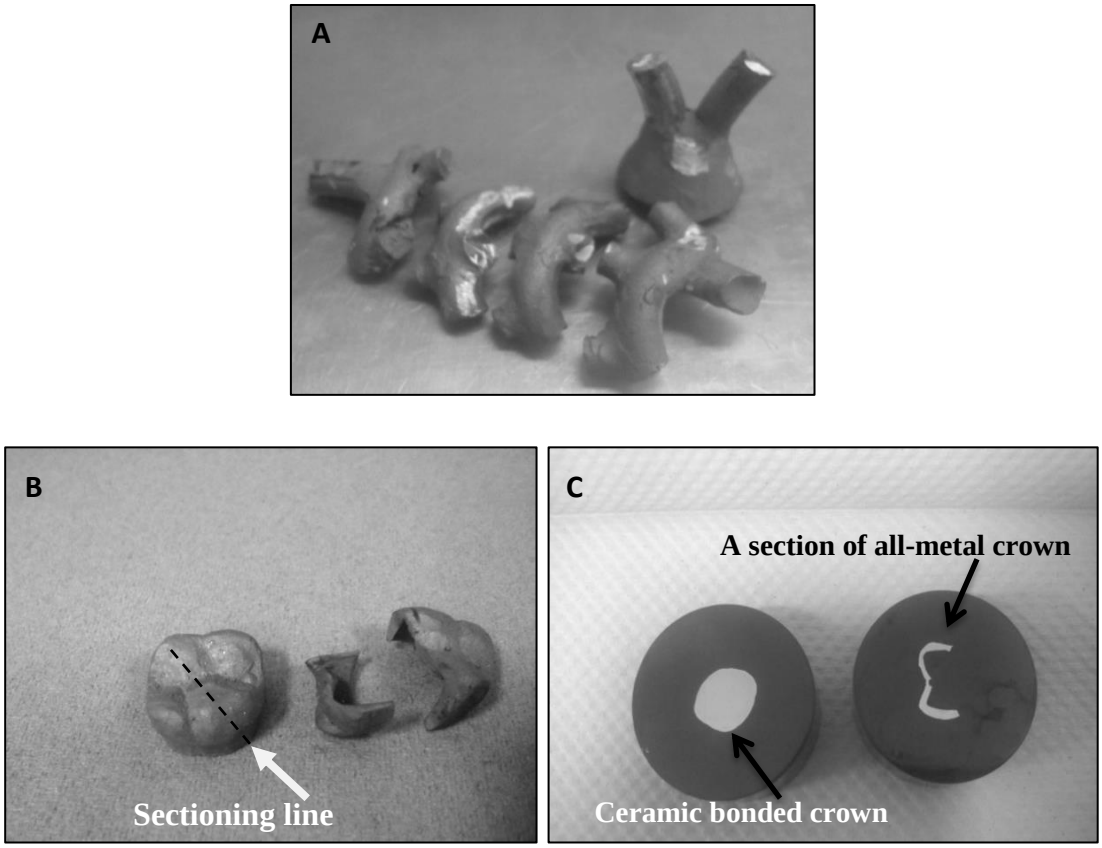

Figure 3-5 alloy surplus of casting (A), cross sections of all-metal casting (B), samples embedded in a mounting resin (C)

3.3.2.6.2 Metallographic polishing and Etching

Samples were finished automatically (Motopol12, Buehler, UK) using fine grit sandpapers to produce a flat surface, free of grooves and scratches. Grinding began with 240 grit paper followed by 2500 grit paper. Samples were then polished with 3 µm diamond paste, followed by 1µm diamond paste (MetaDi, Buehler, USA). The final polishing step was performed using 0.05 µm colloidal silica (Buehler, Lake Bluff, Illinois, USA). Specimens in the as-polished condition were examined under an optical microscope (Olympus, Vanox, UK) to assess the quality of the polishing procedure, and detect any features showing contrast. Co-Cr alloys were etched with a mixture of hydrochloric acid and distilled water in a ratio of 1:10 for 5 seconds. Ni-Cr alloys were etched with oxalic acid and distilled water in a ratio of

1:10 for 7 seconds. The etched patterns were checked with a light microscope (Olympus, Vanox, UK).

3.3.2.7 Microstructural investigations

Metallographic test pieces were examined using scanning electron microscopy (SEM) (JEOL, JSM-5600 LV, Japan), accompanied with an Energy dispersive X-Ray Spectroscopy machine (EDAX). SEM/ EDAX Analysis offered high-resolution imaging with nanometre resolution of surface structure (1024x768 Pixels). Although the field emission of SEM could be operated in low vacuum environment mode, high vacuum mode (20-25 kV) was used to optimize EDAX analysis. The test pieces were prepared for the SEM/EDAX analysis by mounting them on 12 mm pin stubs.

Porosity was micrographically determined. Five micrographs of each test piece were obtained at 150 X microscope magnification. The surface area of pores and pore count were calculated using quantitative image analysis software, ImageJ 1.45s [154].

3.3.2.7.1 Mean % area of porosity

Five SEM images were acquired for each test piece and fifty images for each test group (test group representing the restoration type all metal (AM) or ceramic bonded (CB). Surface area of pores (μm^2) and percentage surface area of pores (%) were calculated for each image, test piece and test group. Means and standard deviations of percentage surface area of porosity (%) were calculated, and presented for each test group with the scanned area being 0.45 mm^2.

To ensure accurate results, only SEM micrographs of high quality were used for image analysis, images of minor imperfections were rejected (Figure 3-6).

3.3.2.7.2 Pore count

Pores were counted on each image, test piece and test group. Pore count was presented as mean count of pores on each test group with the scanned area being 0.45 mm^2.

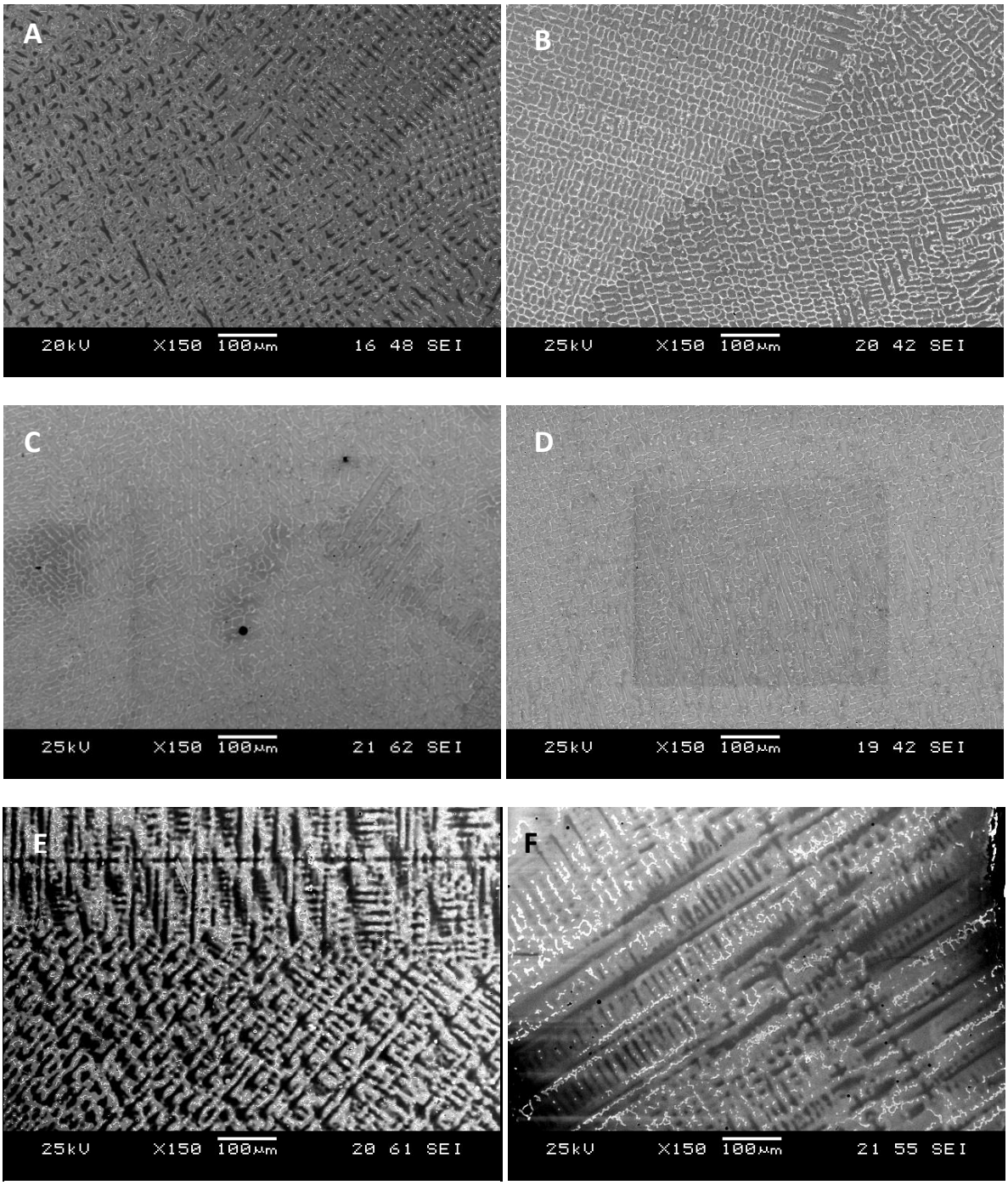

Figure 3-6 Scanning electron micrographs represent adequate (A and B) and inadequate micrographs for image analysis (C, D, E and F).

3.3.2.8 ImageJ analysis

Analysis of the metallographic images was performed in the following way:

Scale bars on the micrographs were measured, where scale was set to micrometer (Figure 3-7 A). Images were duplicated without the scale bar being present (Figure 3-7 B). Pores were identified using the threshold setting to distinguish the pores from the background (Figure 3-8 A). Images were converted to binary images. Threshold areas were measured and recorded (Figure 3-8 B).

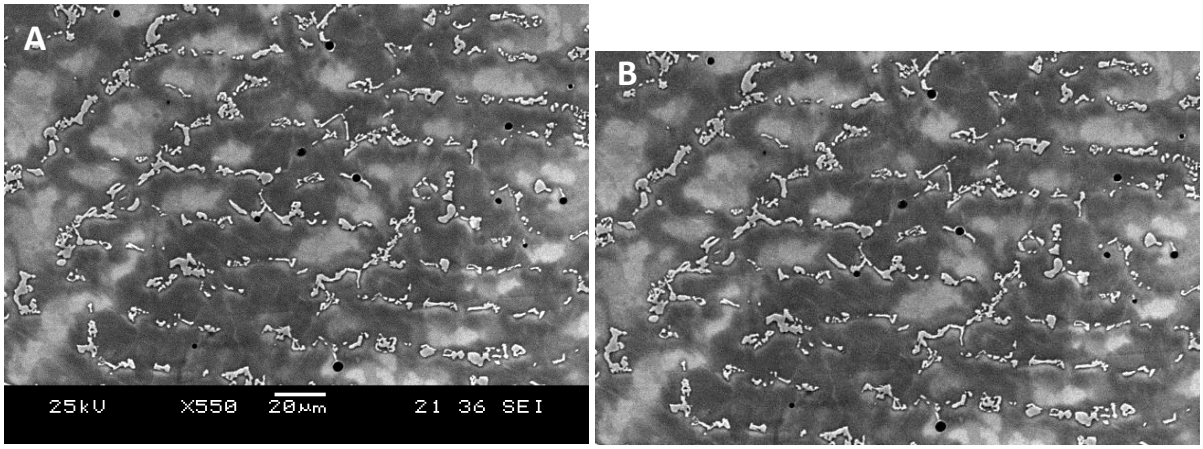

Figure 3-7 Scanning electron micrograph with a micrometer scale and an ImageJ scale bar (A), a duplication of image A (B)

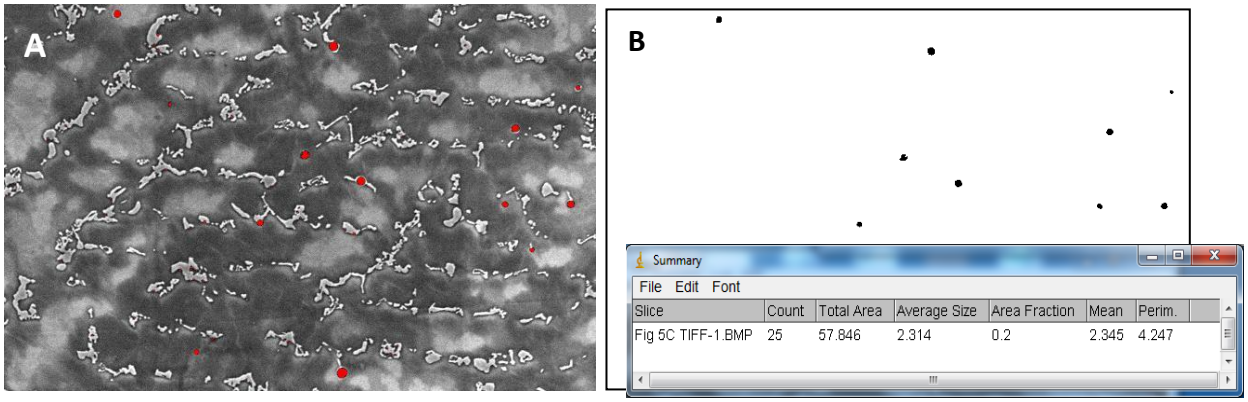

Figure 3-8 Threshold scanning electron micrograph and threshold Image J bar (A), binary scanning electron micrograph and result Image J bar (B)

The mean % area of porosity was determined by ImageJ software. The total surface area scanned was 452854.273 μm^2 for each image (Figure 3.9 A). ImageJ then measured the areas identified as porosity from which a % porosity was calculated (Figure 3.9 B). This calculation was repeated five times for each test piece and 25 times for each test group, means and standard deviation were then calculated.

Figure 3-9 Surface area of the scanned area (A), surface area of pores (B)

3.3.2.9 Energy-dispersive X-Ray Spectroscopy (EDAX) analysis

The chemical composition of castings was analysed by Energy-dispersive X-Ray Spectroscopy (EDAX). Five EDAX analyses were acquired for each test piece and twenty five for each test group. Means and standard deviations were calculated for each test group. Results were statistically analysed with one-way ANOVA and Tukey-HSD tests.

3.4 Results

3.4.1 Microstructural features of alloys

Figure 3-10 A and B, represent the microstructure of the alloys tested. Both types of the alloys demonstrated a typical dendritic solid solution structure. Figure 3-10 A represents the microstructure of a non-sectioned Co-Cr crown made out of 100% new alloy (CoCr-CB-0), it exhibits a solid solution α-phase (matrix) and an interdendritic areas. Figure 3.10 B represents the microstructure of a non-sectioned Ni-Cr crown made out of 100% new alloy (NiCr-CB-0); it exhibits cored dendrites with thin, elongated precipitates within the matrix (Figure 3-10 A and B)

3.4.2 Porosity

3.4.2.1 Types of porosity

Based on the shape and location of pores, Two types of porosity were detected, gas porosity, and shrinkage porosity. Shrinkage porosity exhibits irregular shaped pores at the sprue cast junction (Figure 3-11 A) while gas porosity and inclusion porosity exhibit spherical pores within the cast (Figure 3-11 B).

3.4.2.2 Location of pores

Pores in the Ni-Cr alloy were found at the dendrite boundaries and throughout the castings (Figure 3-12 A), while pores in the Co-Cr alloy were found mainly at the interdendritic areas of castings (Figure 3-12 B). For both types of alloys, cross sectional areas of sprues demonstrated extensive porosity (Figure 3-12 C). Castings produced from 100% recast alloys demonstrated a heterogeneous structure of less dendritic pattern with more precipitates in the matrix. Although porosity values of castings containing 75% recast alloy (AM-75%) were significantly lower than those made out of 100% recast alloys, the microstructure of these castings demonstrated heterogeneous structures where the dendrites and interdendritic areas are less defined with the presence of pores inclusions and precipitates (Figure 3-13 A-C and Figure 3-14 A-C).

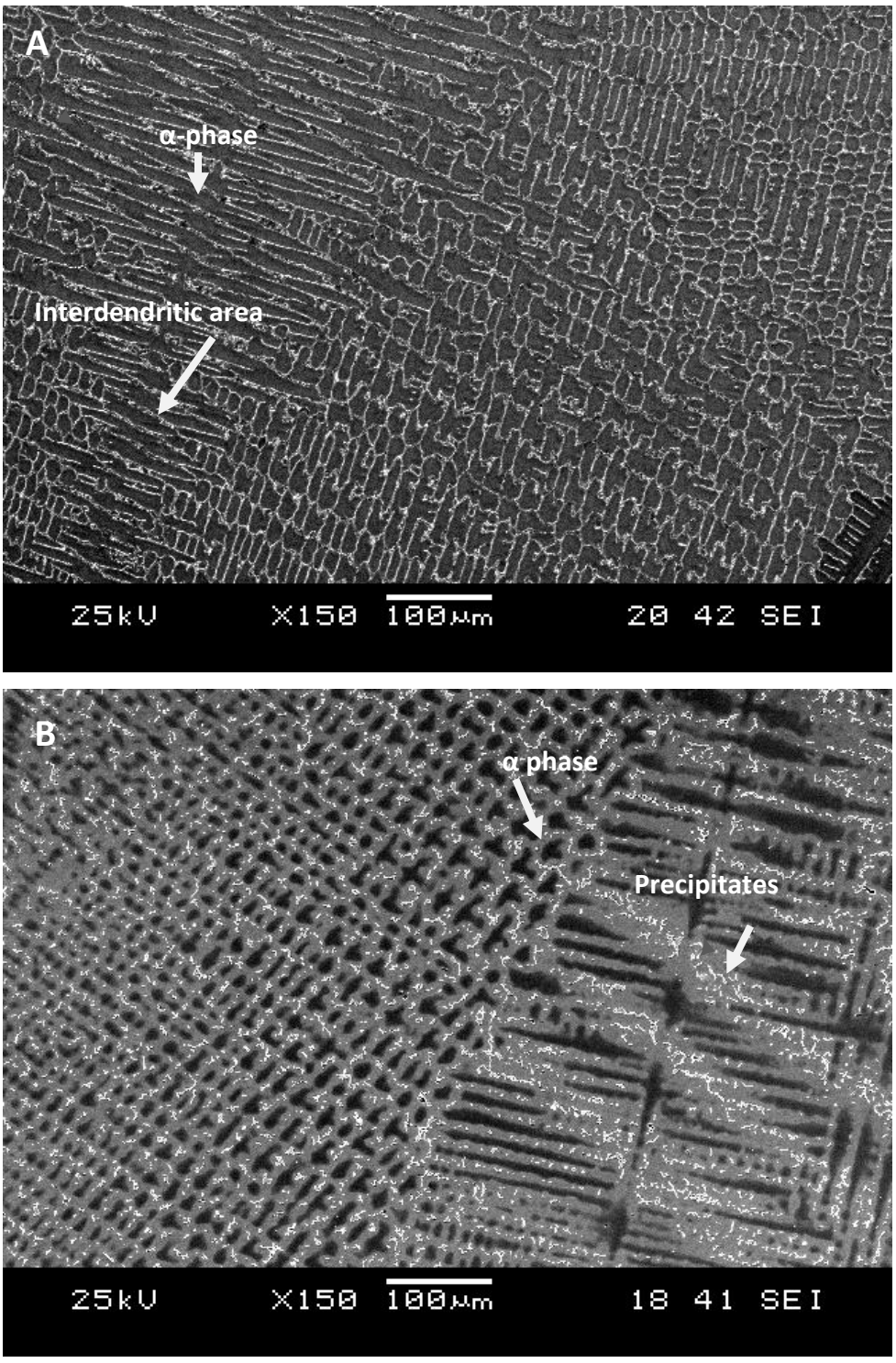

Figure 3-10 Scanning electron micrographs of as-cast microstructure of CoCr-CB-0 (A) and NiCr-CB-0 (B) revealing the dendritic solidification microstructure.

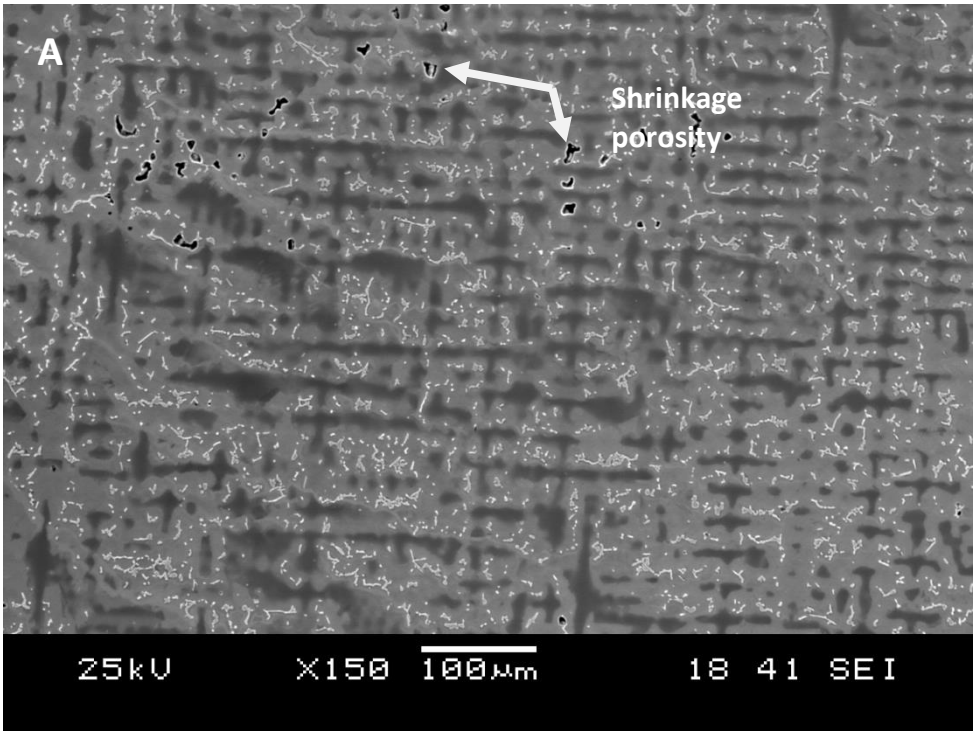

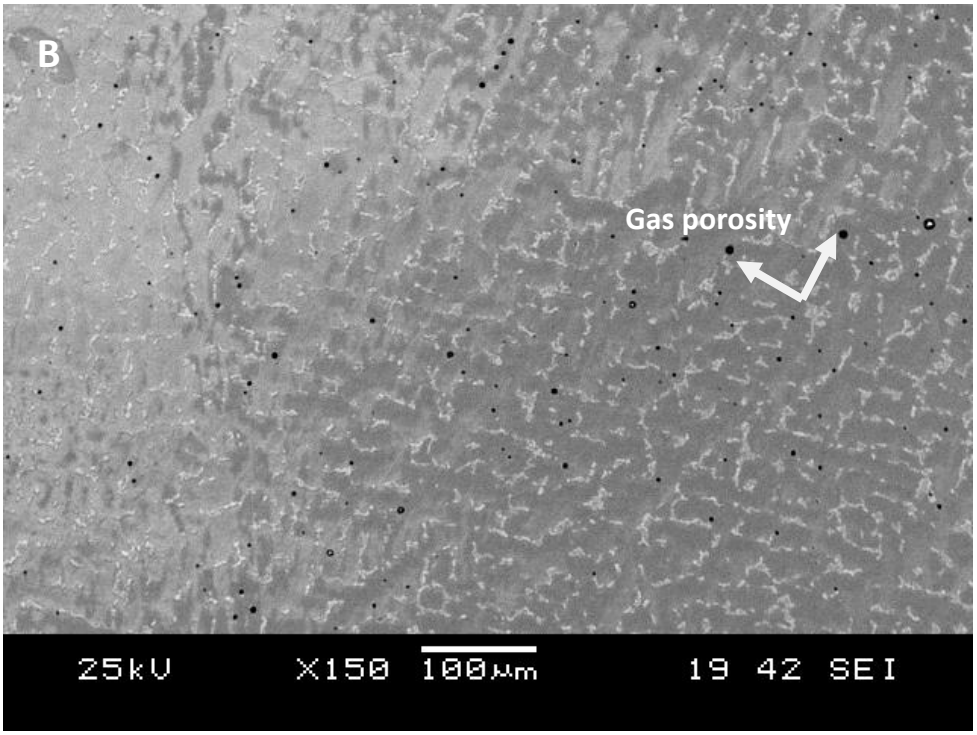

Figure 3-11 Shrinkage porosity in NiCr-AM-50 (A), gas porosity in NiCr-AM-100 (B)

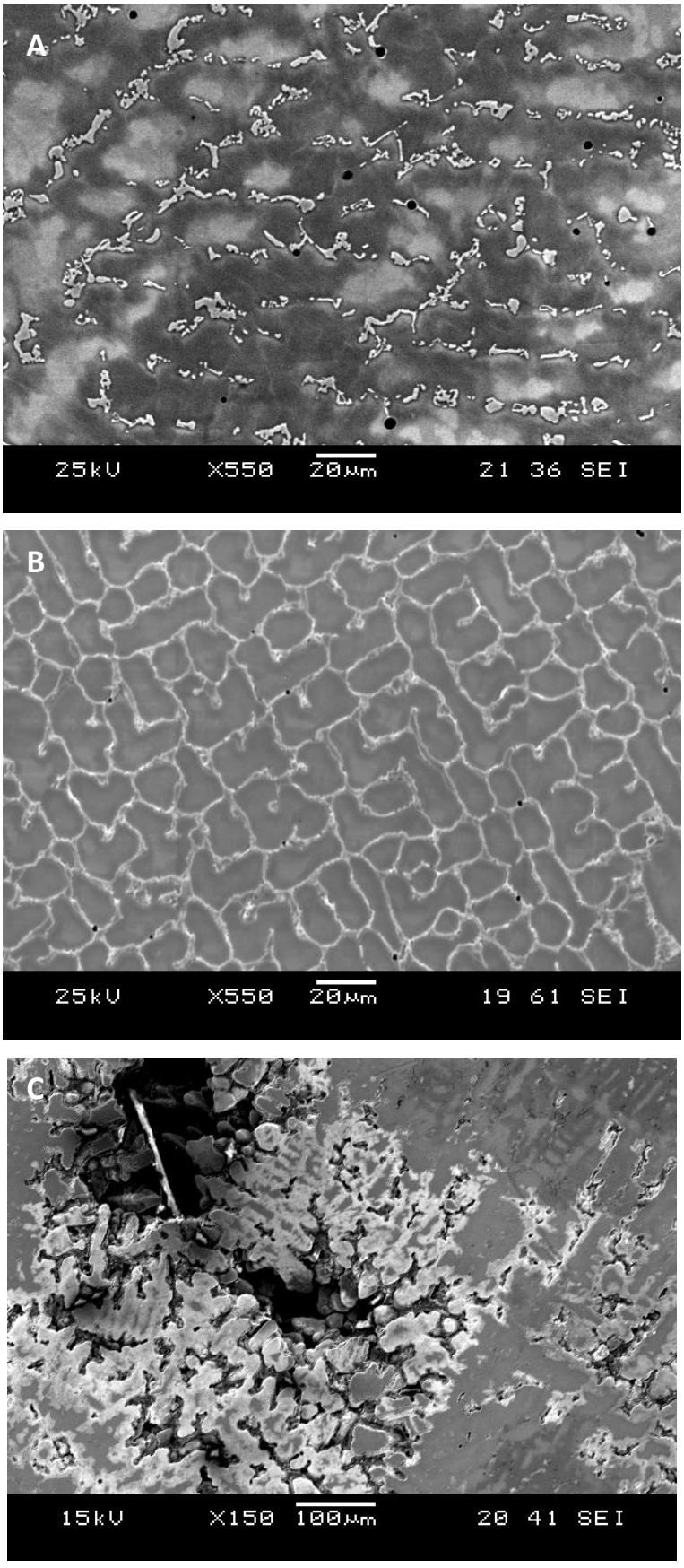

Figure 3-12 Porosity in nickel-chromium casting (A), cobalt-chromium casting (B), shrinkage porosity in a cross sectional area of cobalt-chromium sprue (C).

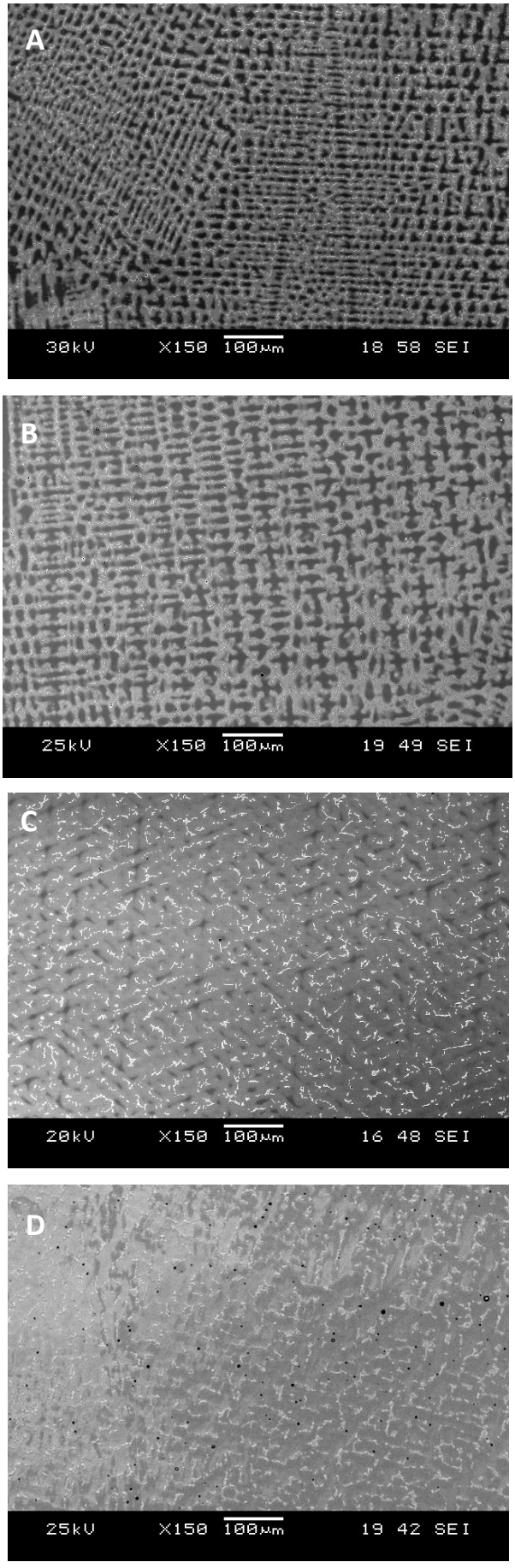

Figure 3-13 Scanning electron micrographs of microstructure of nickel-chromium castings, 0% re-cast (A), 50% re-cast (B), 75% re-cast (C), 100% re-cast (D)

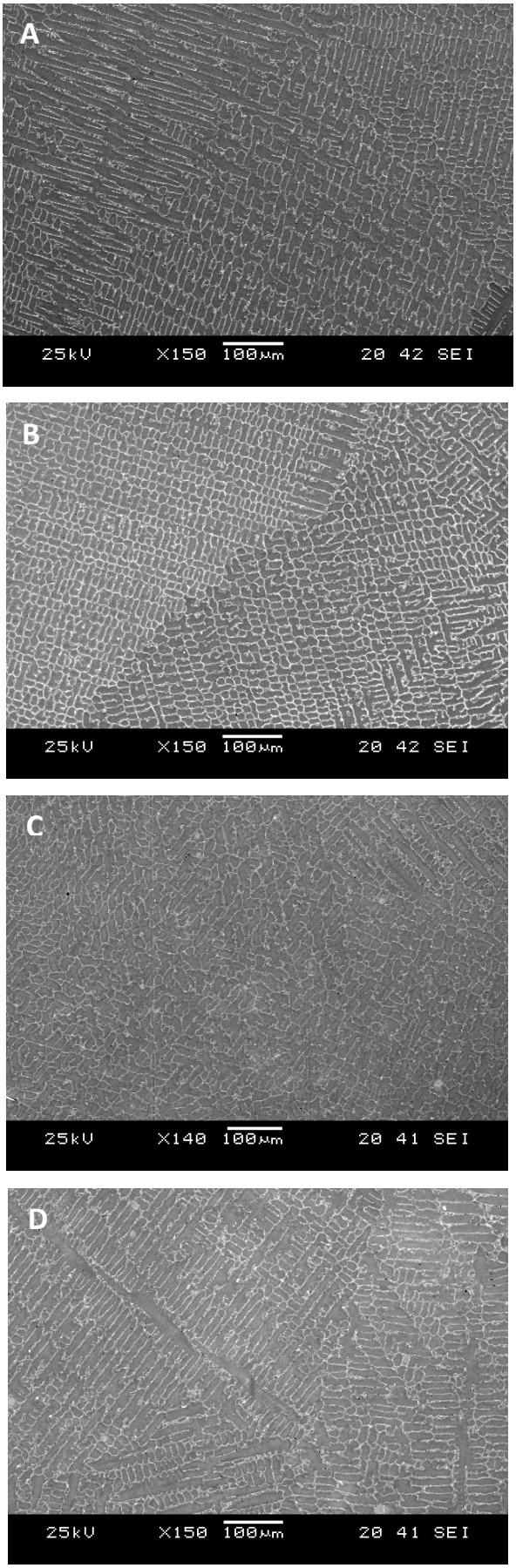

Figure 3-14 Scanning electron micrographs of microstructure of cobalt-chromium castings, 0% re-cast (A), 50% re-cast (B), 75% re-cast (C), 100% re-cast (D).

3.4.2.3 Microstructural features of castings containing recycled alloy

Microstructure of castings produced from reused alloys demonstrated irregular dendrites with increased content of participates. (Figure 3-15 A and B)

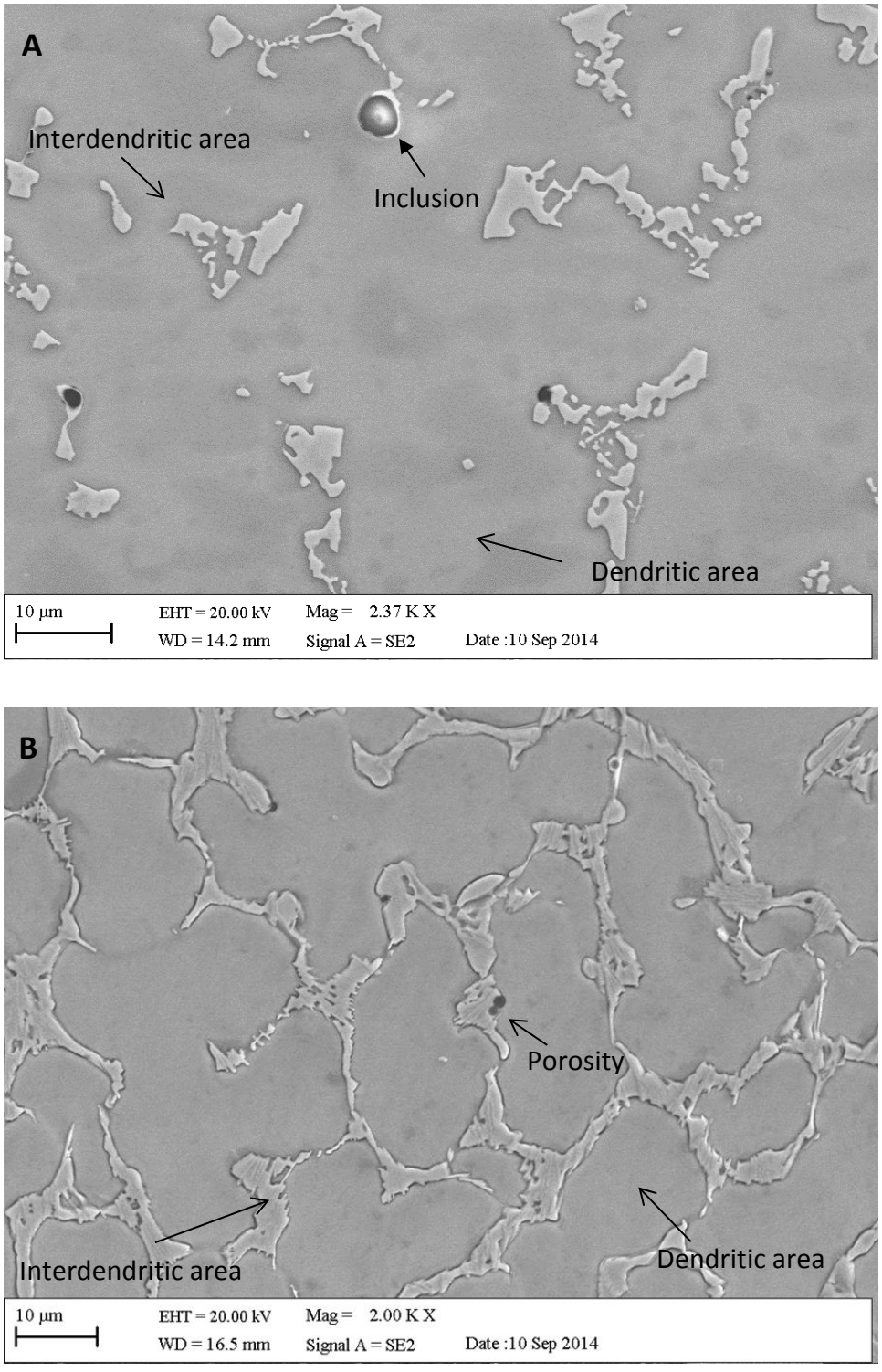

Figure 3-15 Scanning electron micrographs of microstructure of NiCr-100 castings (A), and CoCr-100 casting at 200 X magnification (B)

3.4.3 Quantitative analysis

3.4.4 Mean percentage porosity and pore count

Mean percentage area of pores, mean pore count in an area of 0.45 mm^2 and standard deviations (SD) are presented in Table 3-4 and Table 3-5 for the two alloys tested.

Table 3-4 Mean % area of porosity, pore counts and standard deviations for Co-Cr alloy

Restoration type	Test group (n=5)	% Area of porosity		Pore count (No/ 0.45 mm^2)	
		Mean	SD	Mean	SD
Ceramic bonded (CB) (N=25)	CoCr-CB-0	0.06	0.05	96	8
	CoCr-CB-25	0.04	0.02	94	20
	CoCr-CB-50	0.11	0.01	96	20
	CoCr-CB-75	0.08	0.03	97	14
	CoCr-CB-100	0.27	0.22	94	06
All-metal (AM) (N=25)	CoCr-AM-0	0.04	0.03	50	13
	CoCr-AM-25	0.04	0.03	55	14
	CoCr-AM-50	0.04	0.04	78	19
	CoCr-AM-75	0.04	0.03	74	14
	CoCr-AM-100	0.11	0.03	97	12

Table 3-5 Mean % area of porosity, pore counts and standard deviations for Ni-Cr alloy

Restoration type	Test group (n=5)	% Area of porosity		Pore count (No/ 0.45 mm^2)	
		Mean	SD	Mean	SD
Ceramic bonded (CB) (N=25)	NiCr-CB-0	0.01	0.004	48	04
	NiCr-CB-25	0.02	0.01	48	11
	NiCr-CB-50	0.04	0.04	66	21
	NiCr-CB-75	0.04	0.01	62	15
	NiCr-CB-100	0.06	0.04	81	14
All metal (AM) (N=25)	NiCr-AM-0	0.09	0.01	45	09
	NiCr-AM-25	0.08	0.04	75	05
	NiCr-AM-50	0.15	0.03	84	29
	NiCr-AM-75	0.14	0.06	94	25
	NiCr-AM-100	0.62	0.02	316	57

3.4.4.1 Cobalt-Chromium alloy test groups

Pores were observed in all the test pieces. The mean percentage area values for porosity ranged from 0.04–0.27%. In contrast to the Ni-Cr alloy, the largest mean % area of porosity occurred in the CoCr-CB test groups. CoCr-CB-100 exhibited the maximum mean % area across all test groups at 0.27%. A comparison of results of this test group and the test group containing 75% recycled alloy (CoCr-CB-75) shows that the pore count was similar (97 pores/0.45 mm^2 compared with 94 pores/0.45 mm^2), but the mean % area of porosity was almost three times greater for the test group containing 100% recycled alloy (Table 3-4) (Figure 3-16 and Figure 3-17).

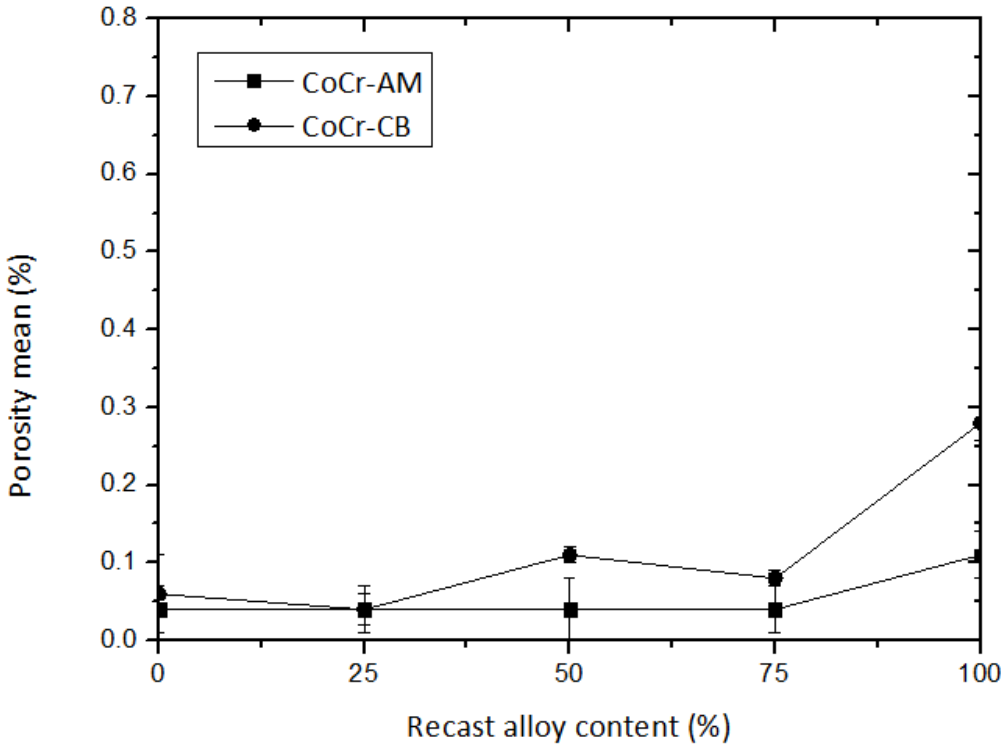

Figure 3-16 Mean porosity of CoCr-AM and CoCr-CB test groups, (error bars represent SD).

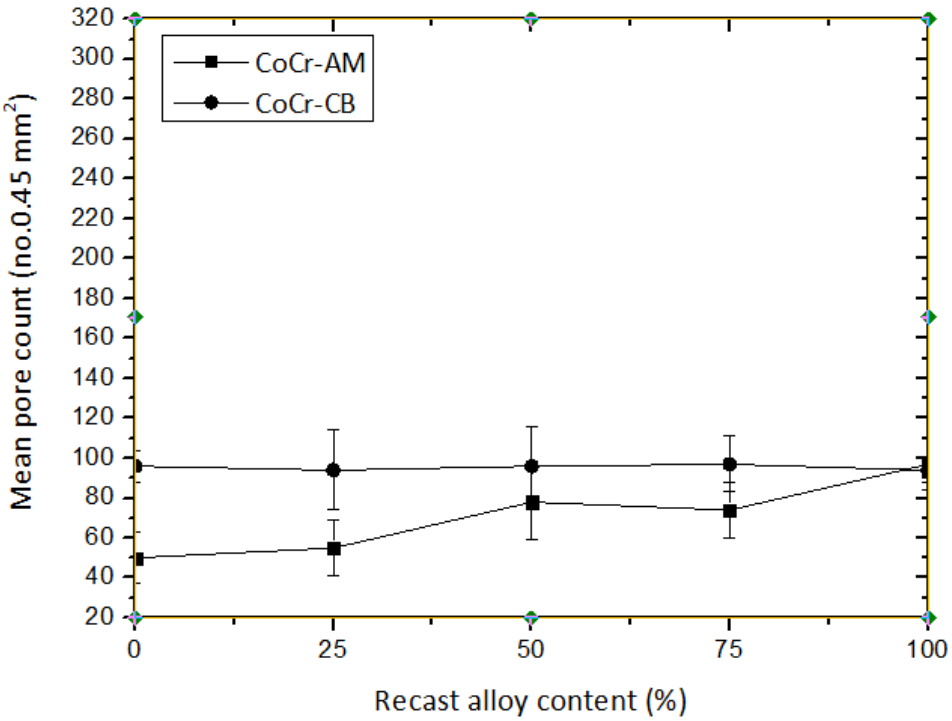

Figure 3-17 Mean pore count of CoCr-AM and CoCr-CB test groups (error bars represent SD).

3.4.4.2 Nickel-Chromium alloy test groups

Pores were observed in all test pieces. The mean percentage area value of porosity values ranged from 0.01–0.62%. In contrast to Co-Cr alloy, the largest mean % area porosity values occurred in the all-metal test groups. NiCr-AM-100 exhibited the maximum mean % area across all test groups at 0.62%. A comparison of results for this test group and the test group containing 75% recycled alloy (NiCr-AM-75) shows that there was a sharp increase in the mean % area of porosity and pore count values of NiCr-AM-100 (Table 3-5) (Figure 3-18 and Figure 3-19)

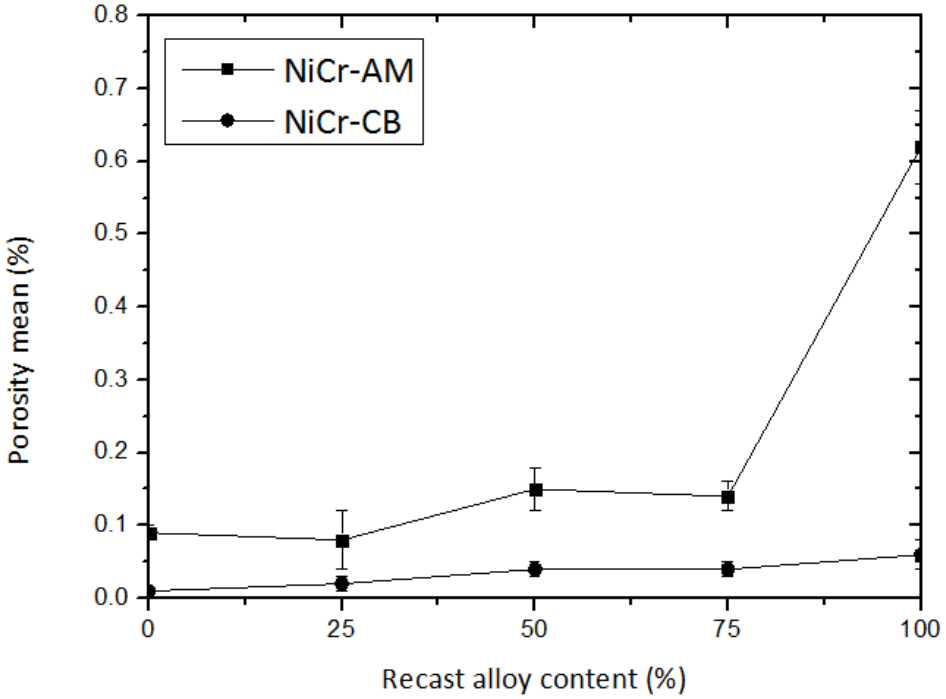

Figure 3-18 Mean porosity of NiCr-AM, and NiCr-CB test groups, (error bars represent SD).

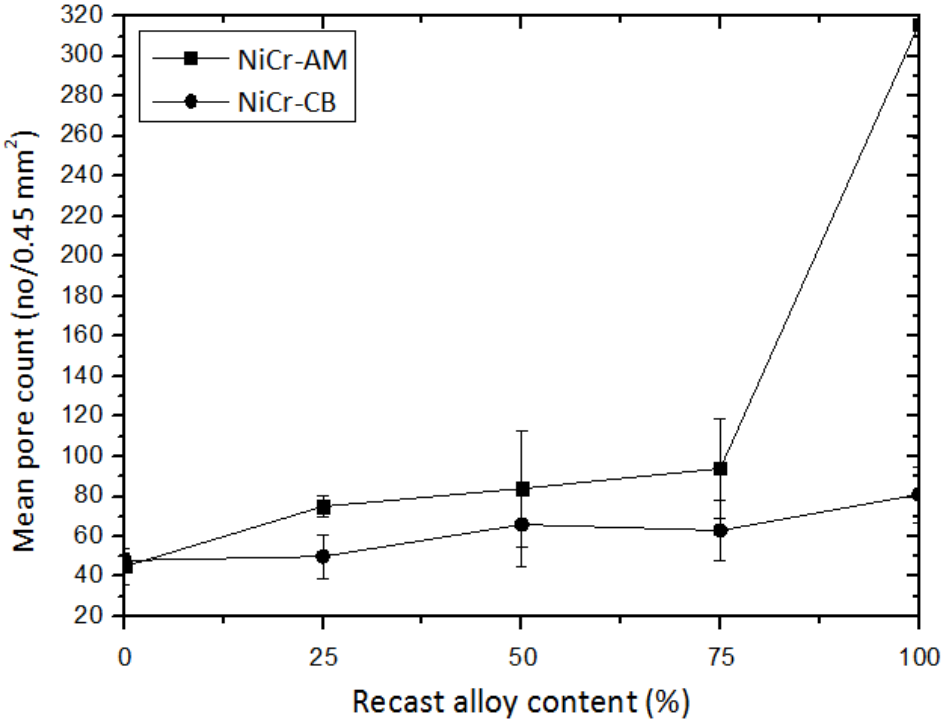

Figure 3-19 Mean pore count of NiCr-AM, and NiCr-CB test pieces, (error bars represent SD).

3.4.4.3 Mean percentage porosity and pore count of ceramic-bonded castings

The plots of mean percentage area of porosity and pore count of ceramic bonded test groups (Figure 3-20 A and B) show that:

Co-Cr test groups exhibited higher mean porosity values than Ni-Cr test groups. CoCr-CB-100 demonstrated a sharp increase in mean porosity values (0.27% ± 0.02%). Whilst NiCr-CB-100 demonstrated a slight and gradual increase (0.06% ± 0.04%) (Figure 3-20 A).

Although Co-Cr test groups demonstrated higher mean pore count values than Ni-Cr test groups, CoCr-CB-100 mean pore count (94 ± 06) was only slightly higher than NiCr-CB-100 mean pore count (81 ± 14) (Figure 3-20 B).

3.4.4.4 Mean percentage porosity and pore count of all-metal castings

The plots of mean percentage area of porosity and pore count of ceramic bonded test groups (Figure 3-21 A and B) show that:

Ni-Cr test groups exhibited higher mean porosity values than Co-Cr test groups. NiCr-AM-100 test groups demonstrated a sharp increase in mean porosity values (0.62% ± 0.02), while CoCr-AM-100 demonstrated a more consistent increase (0.11% ± 0.03) (Figure 3-21 A).

Although Ni-Cr test groups demonstrated slightly higher mean pore count values than Co-Cr test groups, NiCr-AM-100 mean pore count (316 ± 57) was significantly higher than CoCr-AM-100 mean pore count (97 ± 12) (Figure 3-21 B).

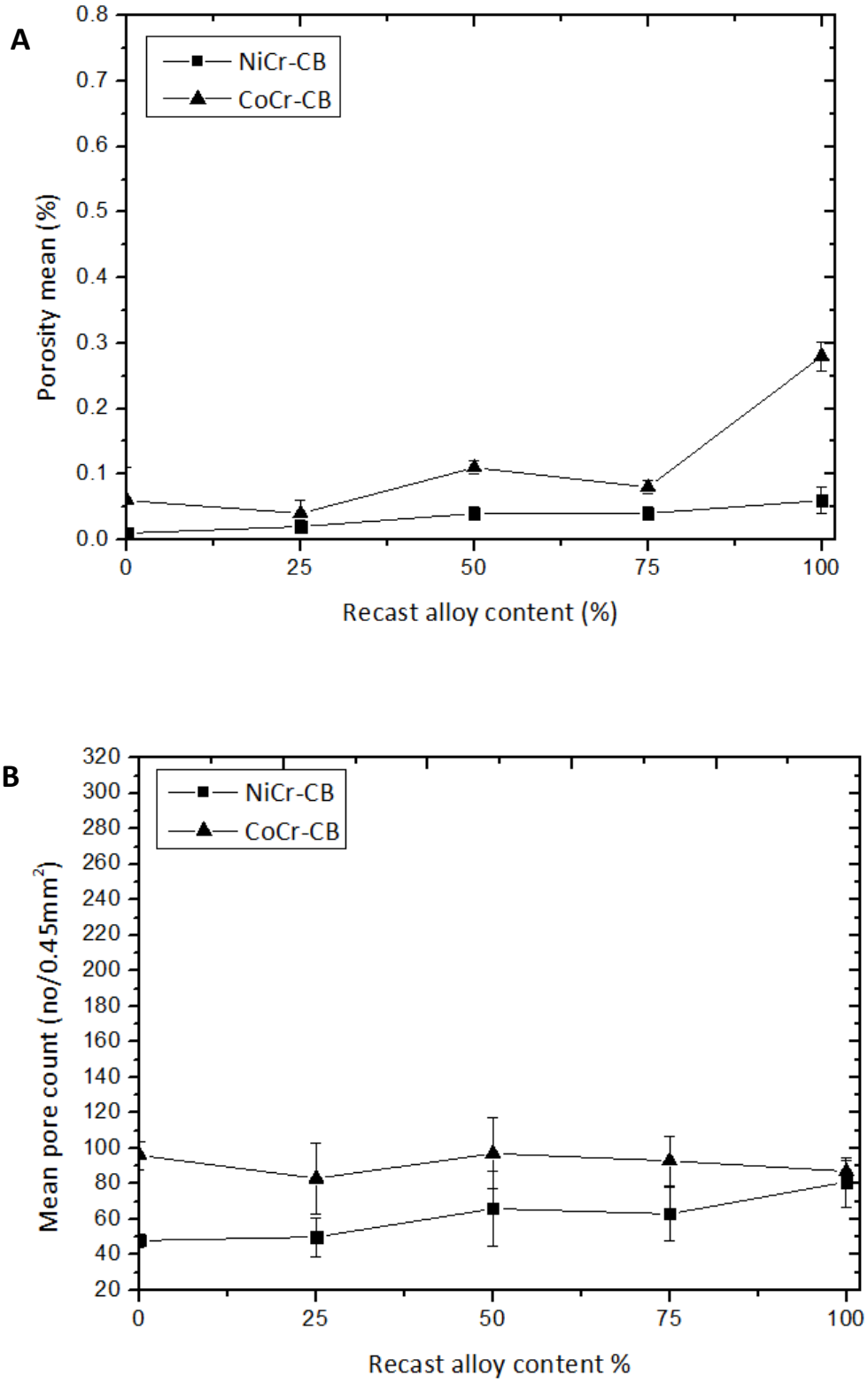

Figure 3-20 Ceramic-bonded castings, mean porosity (A), mean pore count (B), (error bars represent SD).

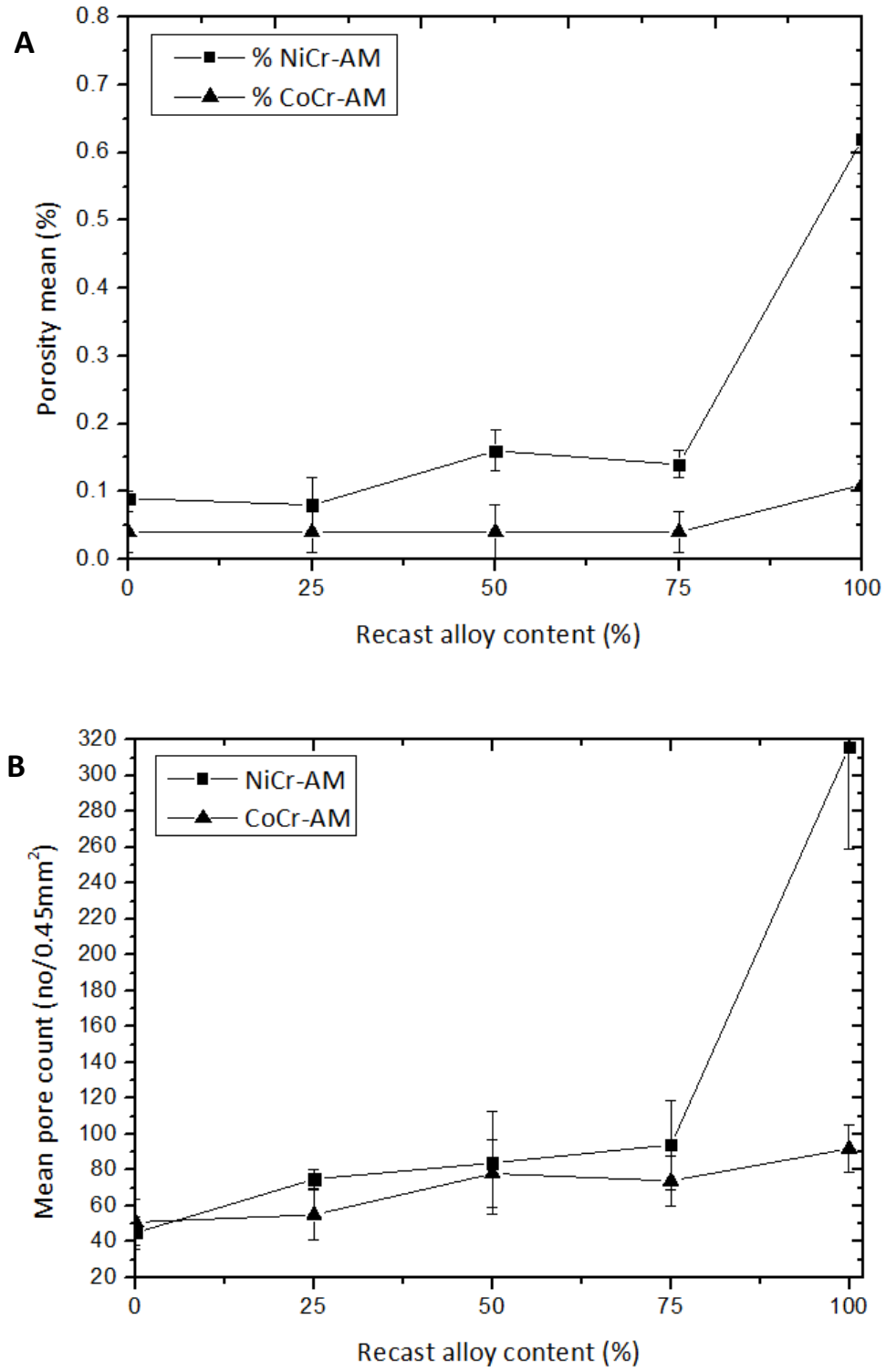

Figure 3-21 All-metal castings, mean porosity (A), mean pore count (B). (Error bars represent SD).

3.4.5 Statistical analysis

3.4.5.1 Mean porosity areas

3.4.5.1.1 Interactions between variables

A two-way ANOVA was conducted to examine the effect of alloy type (Co-Cr and Ni-Cr), restoration type (all-metal or ceramic-bonded) and recycled alloy content on mean % porosity area values. Results indicated a significant main effect of new to recast content of alloy (p= 0.000), there was also a significant main effect of restoration type (p= 0.004). Alloy type (Co-Cr or Ni-Cr) appeared to have less effect (p= 0.055). There was a significant interaction between the effect of alloy type and restoration type levels on porosity occurrence (p= 0.000), the interaction between new to recast content and restoration type was also significant (p= 0.004). The interaction between new to recast content and restoration type only slightly significant (p= 0.043) (Appendix 1, Table 1-1).

3.4.5.1.2 Significances within each alloy test groups

ANOVA test showed that within the same alloy type and restoration type test groups (e,g NiCr-AM), the amount of recycled alloy in castings demonstrated significant differences in mean % area values (Appendix 1, Tables 1-2 and 1-3). Pair Wise comparison test shows a significant difference between the all-metal and ceramic-bonded groups of each alloy (Appendix 1, Table 1.4). Tukey HSD test was used to provide specific information on which means are significantly different from each other (Appendix 1, Tables 1-5 – Table 1-8).

3.4.5.1.3 Co-Cr test groups

For CoCr-AM, no significant differences were demonstrated with up to 75% of re-cast alloy content CoCr-AM-100 demonstrated significant differences with all other test groups (p= 0.000) (Appendix1, Table 1-5). For CoCr-CB test groups, no significant differences were demonstrated with up to 75% of re-cast alloy content (Appendix 1, Table 1-6). Mean percentage values of test groups CoCr-25 and CoCr-50 were slightly different (p= 0.05).

3.4.5.1.4 Ni-Cr test groups

For NiCr-AM test groups, no significant differences were demonstrated with up to 75% of re-cast alloy content. NiCr- AM-100 demonstrated significant differences with all other test

groups (p= 0.000) (Appendix1, Table 1-7). For the NiCr-CB, NiCr-CB-0 demonstrated significant difference with all the other test groups. However, no significant differences were documented between the last three test groups (NiCr-CB-50, NiCr-CB-75 and NiCr-CB-100) (Appendix1, Table 1-8).

3.4.5.2 Pore Count

3.4.5.2.1 Co-Cr test groups

For CoCr-AM, no significant differences were documented with up to 75% content of recast alloy. (Appendix1, Table 1-9). For CoCr-CB, no significant differences were detected with up to 100% content of recast alloy (Appendix1, Table 1-10).

3.4.5.2.2 Ni-Cr test groups

For NiCr-AM, no significant differences were documented with up to 75% content of recast alloy. For NiCr-CB, NiCr-CB-100 test group demonstrated significant difference between the first two test groups (NiCr-CB-0 and NiCr-CB-25). However, no significant differences were demonstrated between this test group (NiCr-CB-100) and test groups containing 50% and 75% recycled alloys (Appendix1, Tables 1-11 and 1-12).

For the surface roughness and the ion release assessments, castings were manually polished and the porosity occurrence data in all-metal (AM) castings will be presented. Finishing and polishing procedures are associated with the removal of material from the casting surface and the resultant exposure of the subsurface structure. However, for metal-ceramic bond strength evaluation, where no polishing was performed, porosity occurrence data in the ceramic-bonded (CB) castings will be presented.

3.4.6 Energy-Dispersive X-Ray Spectroscopy (EDAX) analysis

The chemical compositions of castings were obtained by EDAX analysis. Five determinations were made on each individual test piece. Mean and standard deviation values of the constituent elements (mass%) were reported. The constituents with percentage by mass of 1% or less in the alloys were not included in the EDAX analysis. Table 3-6 and Table 3-7 record results of EDAX analysis.

Table 3-6 Elemental mass percentage means, standard deviation (SD) of Co-Cr test groups.

Restoration type	Test group (n=5)	Element (mass%)							
		Co		Cr		Si		Mo	
		Mean	SD	Mean	SD	Mean	SD	Mean	SD
Ceramic-bonded (CB) (N=50)	CoCr-CB-0	58.91	0.18	32.82	0.18	2.32	0.08	5.85	0.21
	CoCr-CB -25	58.99	0.14	32.80	0.11	2.30	0.02	5.75	0.15
	CoCr-CB -50	59.23	0.29	32.69	0.25	2.30	0.08	5.70	0.23
	CoCr-CB -75	59.00	0.20	32.50	0.21	2.32	0.08	5.88	0.19
	CoCr-CB -100	59.27	0.12	32.59	0.15	2.40	0.17	5.82	0.09
All-metal (AM) (N=50)	CoCr-AM-0	58.88	0.14	32.39	1.02	2.40	0.05	6.16	0.17
	CoCr-AM-25	58.72	0.22	32.39	0.02	2.33	0.92	6.07	0.11
	CoCr r-AM-50	58.91	0.48	32.92	0.24	2.35	0.12	5.90	0.23
	CoCr-AM-75	58.89	0.23	32.44	0.21	2.12	0.11	5.08	0.18
	CoCr-AM-100	58.89	0.38	32.19	0.93	1.77	0.05	4.84	0.18

Table 3-7 Elemental mass percentage means, standard deviation (SD) of Ni-Cr test groups.

Restoration Type	Test group (n=5)	Element (mass%)											
		Ni		Cr		Fe		Mo		Nb		Ta	
		Mean	SD	Mean	SD	Mean	SD	Mean	SD	Mean	SD	Mean	SD
Ceramic-bonded (CB) (N=50)	NiCr-CB-0	58.69	0.46	21.40	0.29	3.82	0.11	9.47	0.25	3.59	0.32	3.02	0.52
	NiCr-CB-25	58.70	0.40	21.33	0.20	3.8	0.08	9.12	0.22	3.48	0.21	3.3	0.22
	NiCr-CB-50	58.69	0.47	21.24	0.20	3.81	0.13	8.12	0.39	3.48	0.21	3.13	0.62
	NiCr-CB-75	58.72	0.40	21.3	0.14	3.81	0.14	8.96	0.25	3.46	0.11	3.00	0.21
	NiCr-CB-100	58.69	0.48	21.36	0.20	3.85	0.08	8.99	0.43	3.29	0.16	2.31	0.32
All-metal (AM) (N=50)	NiCr-AM-0	59.10	0.96	21.20	0.33	3.78	0.060	9.09	1.08	3.44	0.18	3.35	0.17
	NiCr-AM-25	58.55	0.96	21.43	0.14	3.78	0.15	9.18	0.27	3.43	0.11	3.23	0.12
	NiCr-AM-50	58.69	0.44	21.17	0.12	3.83	0.11	9.71	0.24	3.51	0.23	3.07	0.51
	NiCr-AM-75	58.12	0.21	21.32	0.14	3.51	0.11	9.44	0.15	3.5	0.14	3.11	0.11
	NiCr-AM-100	58.69	0.45	19.60	0.24	4.00	0.11	10.01	0.30	3.37	0.17	2.28	0.32

3.4.7 Statistical analysis of chemical composition

3.4.7.1 Chemical composition of Co-Cr alloy

CoCr-AM demonstrated a significant change in the molybdenum content (p= 0.000), from 6.16 % for CoCr-AM-0 to 4.84 % for CoCr-AM-100. Although there was a reduction in the silicon amount, from 2.40 % for CoCr-AM-0 to 1.77 % for CoCr-AM-100 (Table 3-6), this different was not significant (p= 0.171) (Appendix1, Table 1-13).

CoCr-CB demonstrated a significant change in the cobalt and chromium content (p= 0.025 and 0.041, respectively) (Appendix1, Table 1-14). The change in the chromium content (from 32.82 % for CoCr-CB-0 to 32.50 % for CoCr-CB-75) was less than the change in the cobalt content (from 58.91 % for CoCr-CB-0 to 59.27 % for CoCr-CB-100) (Table 3-6).

3.4.7.2 Chemical composition of Ni-Cr alloy

NiCr-AM demonstrated significant changes in the chromium, iron and tantalum content (p= 0.000, 0.000 and 0.001, respectively) (Appendix1, Table 1-15).

NiCr-CB demonstrated significant changes in the molybdenum and tantalum content (p= 0.000 and 0.012, respectively) (Appendix1, Table 1-16). Changes in the elements contents were between the first test group (NiCr-AM-0) and the last test group (NiCr-AM-100) (Table 3-7)

3.4.8 Phase chemical composition analysis (semi-quantitative analysis)

EDAX analysis was conducted on single Co-Cr and Ni-Cr test pieces containing 0% and 100% recycled alloy content.

Figures 3.22 A and 3.22 B indicate the typical Co-rich solid solution (Table 3-8) and the interdendritic area used for analysis of compositions of test pieces at such locations. Interdendritic area was rich in molybdenum and silicone (Table 3-9). Figure 3.22 C shows a region close to a pore corresponded to a silicon rich area (Table 3-10).

Figures 3.23 A and 3.23 B indicate the typical Ni and Cr-rich solid solution (Table 3-11) and the interdendritic area used for analysis of compositions of test pieces at such locations. Interdendritic area was rich in niobium (Table 3-12). Figure 3.23 C shows a region close to a pore corresponded to a silicon rich area and high aluminium and carbon concentrations but low nickel content (Table 3-13)

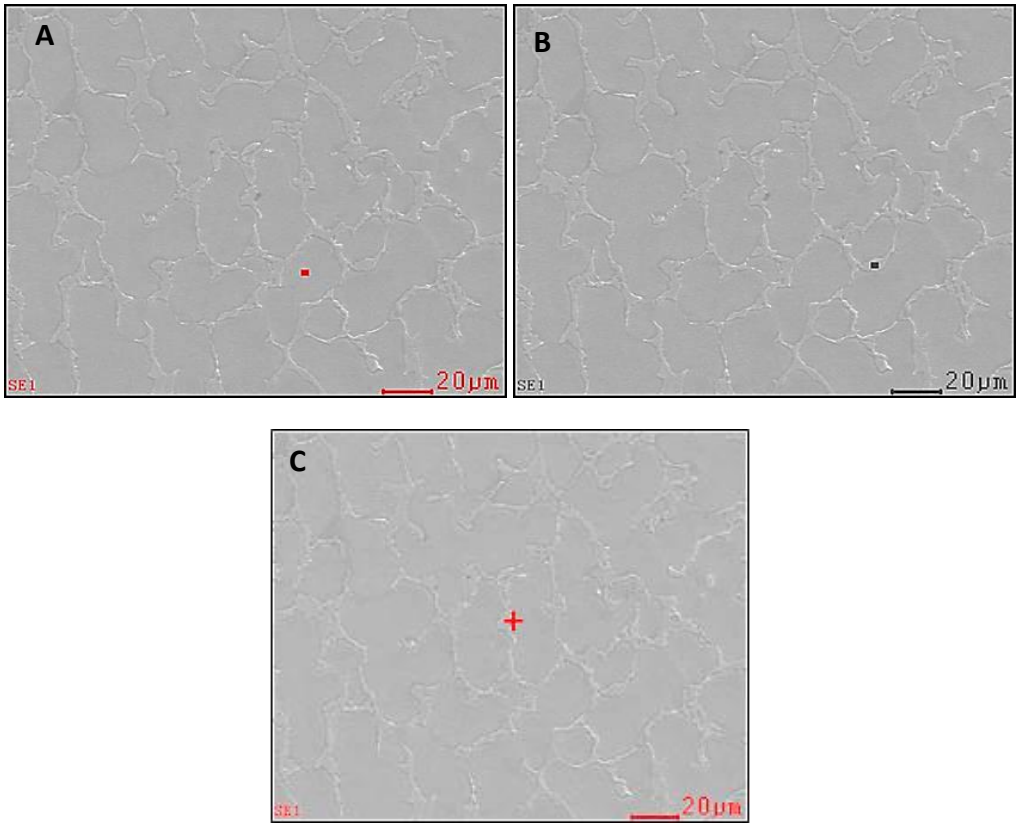

Figure 3-22 Scanning electron micrographs of CoCr-100 test piece showing sites of the EDAX analyses, solid solution area (A), interdendritic area (B), porosity (C)

Table 3-8 Energy-dispersive X-Ray Spectroscopy analysis (mass%) of solid solution area of CoCr-0 and CoCr-100 test pieces

Element (mass%)	Co	Cr	Mo	Si	Mn	Al	O
CoCr-0	53.23	31.41	6.26	02.84	0.26	2.31	3.69
CoCr-100	61.82	31.70	3.29	02.28	0.42	-	1.12

Table 3-9 Energy-dispersive X-Ray Spectroscopy analysis (mass %) of interdendritic area of CoCr-0 and CoCr-100 test pieces

Element (mass%)	Co	Cr	Mo	Si	Mn	Al	O	C
CoCr-0	41.86	36.94	15.10	3.99	0.42	-	1.69	-
CoCr-100	36.37	32.68	04.98	10.76	00.60	1.54	10.5	2.52.

Table 3-10 Energy-dispersive X-Ray Spectroscopy analysis (mass %) of a pore in CoCr-100 test piece

Element (mass%)	Co	Cr	Mo	Si	Mn	Al	O
CoCr-100	28.96	24.21	7.59	18.82	00.70	00.69	18.76

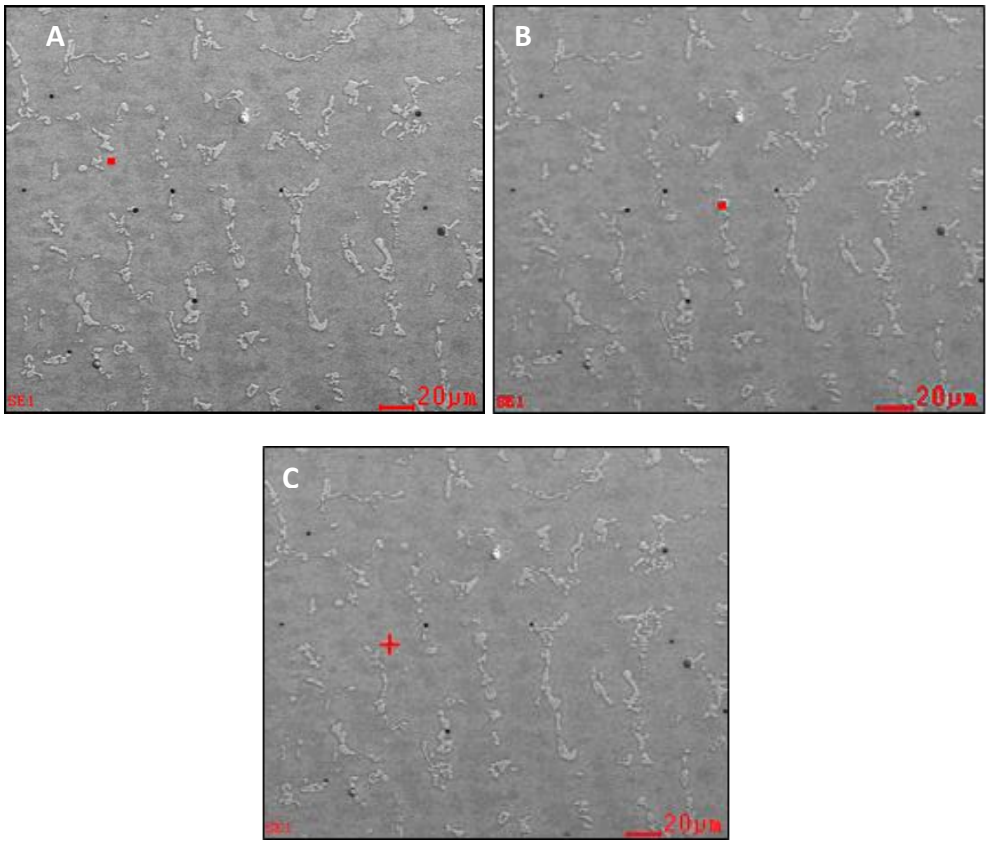

Figure 3-23 Scanning electron micrographs of NiCr-100 test piece showing sites of the EDAX analyses, solid solution area (A), interdendritic area (B), porosity (C)

Table 3-11 Energy-dispersive X-Ray Spectroscopy analysis (mass%) of solid solution area of NiCr-0 and NiCr-100 test pieces

Element (mass%)	Ni	Cr	Mo	Fe	Mn	O	Si	C
NiCr-0	58.14	22.05	9.67	4.49	0.57	3.06	-	-
NiCr-100	62.55	18.77	10.55	3.29	-	-	2.27	1.94

Table 3-12 Energy-dispersive X-Ray Spectroscopy analysis (mass%) of interdendritic area of NiCr-0 and NiCr-100 test pieces

Element (mass%)	Ni	Cr	Mo	Fe	Mn	O	Si	Ne	Nb	C
NiCr-0	45.35	14.76	20.49	-	3.92	1.44	4.93	-	9.11	-
NiCr-100	45.22	16.59	6.32	3.30	0.24	-	-	1.24	15.26	3.38

Table 3-13 Energy-dispersive X-Ray Spectroscopy analysis (mass%) of a pore in NiCr-100 test piece

Element (mass%)	Ni	Cr	Mo	Fe	Mn	O	Si	Nb	C	Al
NiCr-100	16.7	13.41	2.35	1.45	0.83	27.00	20.15	1.87	5.20	7.34

3.5 Discussion

3.5.1 Type of porosity

Porosities detected in specimens were mainly gas porosity and inclusion porosity. Shrinkage porosity is irregular in shape and exists in the large mass of the casting and at the sprue casting junction. Gas and inclusion porosity are spherical in shape and exist throughout the casting [144]. Monroe [57], who investigated porosity occurrence in a variety of casting alloys documented that shrinkage porosity can be controlled better than gas porosity.

In this study, the two types of alloys tested (Co-Cr and Ni-Cr) demonstrated different mean % area of porosity and pore counts values. One explanation could be the microstructure of the alloys. There is a strong relation between microstructure and distribution of pores, where gases are usually trapped between dendrite arms. The dendritic microstructure of Co-Cr alloy was typical in exhibiting primary α-phase and interdendritic areas [14,52]. In this study, similar to other studies [155], pores were found in the white Mo-rich interdendritic regions. The microstructure of nickel-chromium alloy was more complicated; it exhibited cored dendrites with thin, elongated precipitates within the matrix [60].

Inclusions are formed in the interdendritic areas where the liquid is highly enriched with oxides. Moreover, the formation of metal oxide inclusions, such as MnO and Al_2O_3 is highly possible [156], and foreign trapped particles are concentrated at grain boundaries [157]. This could explain the pattern of pore distribution in the castings. Pores in Ni-Cr alloy were found at the dendrite boundaries and throughout the casting (Figure 3.12 A), while pores in Co-Cr alloy were found mainly at the interdendritic areas of the casting (Figure 3-12 B). A similar observation was made by Giacchi [14], in that inclusions were found mainly in the carbides at the dendritic area of re-melted Co-Cr alloys; with inclusions acting as nucleation for porosity occurrence. In this study, chemical analyses of different phases shows that the interdendritic area was a Cr and Mo rich area (Table 3-12 B), and pores demonstrated a silicon rich area with the presence of carbon (Table 3-12 C), which enhances the formation of carbides. The formation of new phases, inclusions and participates reduces the homogeneity of the casting.

3.5.2 Shape and size of pores

The source of porosity may be chemical in nature, when dissolved gases are present in molten metal during melting and pouring. it may also be physical in nature, when trapped gases are unable to escape due to inadequate venting or insufficient porousness of the mould, both types of porosities vary in their characteristics [158].

In the current study, minimal shrinkage porosity was observed. Similar results were documented by Gunasegaram [159], who investigated factors affecting shrinkage porosity occurrence in a variety of cast alloys. This observation might be related to the spruing design used (Figure 3-4). Using an adequate sprue configuration provides complete feeding of the molten metal into the mould during solidification [160]. Reducing the mould-metal temperature difference and smoothing the sprue casting junction, as performed in this study, also contributes to the reduction in shrinkage porosity and incomplete feeding defects [10].

In this study, restorations of different types (CB and AM) demonstrated different mean % porosity values. For example, for NiCr-CB-0, mean % porosity value was 0.01% ±0.004, while for NiCr-AM-0 it was 0.09% ±0.01. In non-sectioned castings (ceramic bonded castings), surface porosity was detected (no surface treatment had been employed except for sandblasting with 50 µm Al_2O_3), while sectioned castings (all-metal castings) contained sub-surface and internal porosity. These types of porosity vary in shape, position and size [144]. Surface pores are usually small pinhole holes, while subsurface and internal pores can be rounded or irregular shaped holes, or of fissure like shape. Inclusion pores are usually rounded and larger in size compared to other rounded gas inclusion porosities [10]. The variation in shape, size and position might explain the difference in porosity surface area and count values in the two types of castings (all metal castings and ceramic bonded castings) and between the two types of alloys.

Another explanation of the difference in mean % area of porosity values between the two different restoration types (CB and AM) can be related to the volume of the castings. A thick casting (0.5-1.5 mm) holds heat for a longer time; hence, complete solidification takes more

time and results in larger grains [161]. In addition, the surface to volume ratio of castings influence their cooling rate; in thicker castings, a smaller surface to volume ratio means these take a longer to cool down, which results in coarse grains, while for thinner castings (0.3-0.5 mm), solidification takes less time and results in finer grains. Pore size is affected by grain size; the finer the grains, the smaller the interdendritic spaces. As a result, fewer and smaller pores develop in the interdendritic spaces [112].

3.5.3 Ingot shape and size

Ingot shape and size have been reported to have an effect on alloy microstructure [144]. The homogeneity of the molten metal and the exact composition of every ingot have a significant effect on casting quality. Cutting and re-using surplus alloy results in having metal pieces of different shapes, sizes, melting points and densities. Consequently, it may not be expected that a casting produced using a quantity of recycled alloy will have a uniform composition and properties [56,143]. In this study, the melting time of cast surplus ingots (which were different in size, shape but approximately similar in weight) was different from that of the new ingots of alloy (which were similar in size, shape and weight). Longer melting time might cause the mould temperature to fall by a few degrees before the molten metal starts to enter the mould; the difference between mould and melting temperature creates rapid cooling of the cast and shortens the time for the gases to escape [10]. This could be an explanation for the increased occurrence of porosity in the re-cast alloys. In addition, overheating of some pieces of surplus alloy means that some alloy remains in the molten state for longer when other parts of the cast have solidified and can cause pores to form between casting and investment material.

3.5.4 Pore count

For CoCr alloy, CoCr-CB pore count stayed about the same, CoCr-AM demonstrated a gradual increase in pore count. For Ni-Cr alloy, NiCr-CB demonstrated gradual increase in pore count, NiCr-AM has also demonstrated an increase in pore count. Internal small pores that are not close to the polished surface, unless the pore size is large or a number of small holes gathering together and act as stress concentration, are not expected to have a negative contribution on some properties, such as corrosion resistance, surface roughness

and bonding to ceramic. The alloy elastic elongation limit, caused by the polishing procedure, may eliminate small surface and subsurface pores [112]. Each alloy has its fatigue limit and so has its critical pore size at which fatigue cracks might be initiated. A previous study by Li [113], who investigated the effect of porosity on fatigue behaviour of silver-palladium (Pd-Ag) alloy, documented that fatigue limit, which occurs when a material is subjected to a cyclic repeated stresses, was reduced for castings when the critical pore size was reduced in the restoration. However, according to Lie, the diameter of pore causing this type of mechanical failure was 280 µm and percentage surface area of porosity was 5% - 10%, which is high in comparison with results documented in this study.

3.5.5 The relationship between pore count and mean % area of porosity

In the current study, the relationship between pore count and pores surface area did not show correlation. For example, for CoCr-CB-75 and CoCr-CB-100, although the number of pores did not exhibit a significant increase (96, 94, 96, 97 and 94); porosity area percentage values exhibited significant increase (0.06%, 0.04%, 0.11%, 0.08% and 0.27%).

In the CoCr-AM test groups, the number of pores increased significantly for the last two test groups (50, 55, 78, 74 and 97); and the porosity area percentage values exhibited a significant change (0.04%, 0.04%, 0.04% and 0.11%). This can be explained by more gas inclusion and localised shrinkage porosity, which mainly occur at the sprue casting junction but can also occur anywhere between dendrites [10], have occurred in the CoCr-AM-100 test groups as these two types of porosity are larger in size than other types of porosities. However, for the NiCr-AM the increase in the number of pores (45, 75, 84, 94 and 316) was combined with an increase in the surface area (0.09%, 0.08%, 0.15%, 0.14% and 0.62%). For NiCr-CB, the relationship between pore surface area and number of pores was more consistent (0.01%, 0.02%, 0.04%, 0.04% and 0.06) and (48, 48, 66, 62 and 81) (Table 3-4 and Table 3-5).

In this study, the highest porosity value documented was 0.62% ± 0.02, followed by 0.27% ± 0.22). Li [113] investigated the effect of casting porosity on fatigue behaviour of 100% new Pd-Ag alloys and reported porosity values of 5%, 10%, and a maximum of 12%. However, unlike the current study, alloys were melted with a gas-oxygen torch, and casted using a

broken-arm casting machine. Galic [64], used an image analysis system (ImageJ), similar to the one used in this study, to evaluate porosity occurrence in 100% new gold alloys. Porosity values reported in Galic's study were of 0.62% and 0.49%. Majidi [162] investigated the effect of fluxing temperature on cast aluminum alloy and documented a porosity range between 2.96%-10.70%. Some of the values documented in these studies are similar to those obtained in this study, However it has to be noted that different types of alloys were used and hence different solidification behaviour may exist.

In the literature, a wide variation in porosity values was obtained by researchers, no perceived threshold values of porosity have been documented with regards to mechanical and physical properties. This variation may be explained by the variation in experimental design, methodology and alloy type. No study was found in the literature similar to the current study and so it was not possible to compare the reported results with other studies. Porosity values obtained in this study fall within the low values found in the literature. This might be due to the controlled laboratory procedures.

In this study, casting was performed in a controlled environment using an induction casting machine, which is recognised to have a positive effect on cast quality in regards to cracks and porosity [54]. In addition, cleaning the recycled alloy by steam water and drying it by an air blast prior to the re-melting procedure can reduce the risk of contamination by the aluminum oxide particles that are used to remove the oxides from the cast surface and act as inclusions. Inclusions suspended in the melt enhance the formation of porosity. Sprue diameter and configuration control the supply of molten metal into the mould, and so play an important role in castings quality in terms of cracks and porosity [160]. Special attention was paid to avoid the contamination resulting from using old crucibles [163]. Grinding debris and slag from old crucibles were avoided.

3.5.6 Energy-dispersive X-Ray Spectroscopy analysis

Elements in dental alloys are present in different concentrations, whether major (< 10%), minor (1-10%) and trace elements (> 1%). The presence and concentration of trace alloying elements, such as silicon, aluminum, manganese and iron contribute largely to the properties of cast alloys. Silicon and manganese, for example, are added to increase fluidity

and castability of alloys, Aluminum, iron and beryllium in bonding alloys act as oxide formation inhibitors.

In the current study, there were changes in the elemental composition of castings containing 100% recycled alloys. These changes varied between an increase of some elements, such as cobalt and chromium (Table 3-6) and reduction in others, such as molybdenum, silicon and tantalum (Table 3-7). The reduction in the amount of tantalum and silicon might be caused by the oxidation. Molybdenum is not oxidised, but the oxide product of molybdenum, e.g. MoO_3, becomes volatile at temperatures exceeding 700°C (the casting temperatures used in this study were 1342°C for the Ni-Cr alloy and 1400°C for the Co-Cr alloy). In noble alloys, losing some trace elements through volatilisation is expected. However, for base metal alloys and due to the high volatising temperatures and lower vapour pressure of the elements, it is not expected that reduction in the amount of some elements is due to volatilisation. Changes in elemental composition might be related to the non-homogeneous distribution of the alloy's elements throughout the casting and the presence of pores, inclusions and precipitates [59].

Phase chemical composition analysis of the matrix area of the two test groups NiCr-0 and NiCr-100, demonstrated a similar trend in the elemental composition (Table 3-11). However, for the interdendritic area, chemical composition varied widely (Table 3-12). The same observation was documented for CoCr-0 and CoCr-100 phase chemical composition analysis (Tables 3-8 and Table 3-9). Podrez [164], who analysed the chemical compossition of the different phases of a Co-Cr alloy demonstrated a high concentration of molybdenum and chromium in the interdendritic area at the participates.

3.5.6.1 Previous studies

It is well documented in the literature that the re-casting procedure affects noble and base-metal alloys' elemental stability. Yavuz [7] evaluated the effects of different surface treatments on the elemental composition stability of as-received and recast Ni-Cr alloys. Changes in the amount of major elements in the alloy, such as nickel and chromium, and other elements, such as molybdenum, silicon, and manganese were documented; Yavus

used gas/oxygen flame melting method, this method is less controlled than the method used in the current study. Presswood [85], analysed the chemical composition of Ni-Cr alloys and demonstrated minor changes in the amount of nickel, iron, chromium and molybdenum. In the previously mentioned study, changes in the amount of the chemical elements were considered minor if they fall within the range of 0.1%-0.01%. Imirzalioglu [106], who evaluated the effect of repeated casting of base metal alloys on gingival fibroblast cytotoxicity, documented a reduction in the amount of chromium in the re-cast Co-Cr alloys, and an increase in the amount of cobalt. Rosenthal [165], investigated the phase characterisation of Co-Cr alloys and observed a high concentration of silicon at the inclusions. Segregation of silicon towards inclusions might explain the change in silicon amount in the re-cast alloy. Segregation is expected to present in cast alloy [164]. In this study, the high amount of silicon detected in the regions close to pores (Table 3.10 and Table 3.13) could be explained by the presence of inclusions at the pores. Type and extent of segregation might change according to solidification conditions and alloy type. Recasting can increase the possibility of having insoluble foreign particles, which can cause the occurrence of micro-segregation [150].

It has to be noted that despite the changes in the amount (mass%) of some elements in castings containing recycled alloys (Table 3-6 and Table 3-7), these amounts were very close to the amounts provided by the manufacturer and the EDAX analysis (Table 3-1 and Table 3-2). For example, the amount of molybdenum in the NiCr-CB-100 test group was 8.99 mass% (Table 3-7); which is very close to the amount detected by EDAX (8.90%) (Table 3-2). The amount of chromium in NiCr-AM-100 test group was 19.60 mass % (Table 3-7); while the amount detected by EDAX was 19.13 mass%. For Co-Cr alloy, the amount of cobalt in the CoCr-CB-100 test group was 59.27 mass% (Table 3-6); which is very close to the amount provided by the manufacturer (59.50%). The amount of molybdenum in the CoCr-AM-100 test group was 4.48 mass% (Table 3-6); while the amount provided by the manufacturer was 5.00 mass% (Table 3-1).

4 Surface roughness and porosity

4.1 Literature review

4.1.1 Surface roughness

Effective polishing of dental restorations is a crucial requirement for the restorations aesthetics and longevity, and oral tissues health and function. Grinding involves removing or reducing bumps, overhangs and excesses of castings; scratches and surface cuts left by grinding are removed by polishing. The ultimate aim of these procedures is to provide a highly smooth, light reflective, and enamel-like surface [10].

4.1.2 Finishing and polishing mechanism

The finishing and polishing mechanism is mainly an abrasive wear procedure. Wear is the accumulative surface damage occurring, where material is removed from a body as small debris particles by a mechanical process. Abrasive wear can be divided into two types, including two body abrasion and three body abrasion. Most laboratory polishing protocols operate in the two body type, in which the bonded abrasive particles are solidly fixed to the substrate. However, dentists and hygienists use the three body abrasives, in which loose abrasive particles in the form of paste move in the interface between the polishing device and the substrate surface and detach debris from the polished surface [166].

4.1.3 Types and composition of abrasives

A variety of abrasives are available for polishing, among which three abrasives are most commonly used, aluminium oxide, carbide compounds and diamond abrasives. Aluminium oxide, due to its adequate hardness, is used with ceramics, alloys and composite resins. Particles are typically bonded to polymer disks and strips, and may also be impregnated into rubber wheels and points. Carbide compounds include silicon carbide, boron carbide and tungsten carbide. Carbide particles are usually pressed with binder into disks, cups, points, and wheels. Diamond abrasives are the hardest, where diamond particles are coated on a rigid matrix, impregnated within a bonded matrix, or used as a polishing paste. In addition, other abrasives, silicon dioxide, zirconium oxide and zirconium silicate, are also in use [166].

4.1.4 Factors affecting the efficacy of finishing and polishing

Surface roughness of a substrate is affected by a variety of factors; (i) type of material being polished, such as alloy, ceramic, acrylic or composite; (ii) size, hardness and shape of particles of abrasive; (iii) physical properties of bonding material used to carry abrasive materials, such as thickness, softness and rigidity; (iv) speed and pressure at which the abrasive is applied; and (v) the use of lubricants during polishing, such as water [167].

4.1.5 Factors affecting casting roughness

A variety of factors have been shown to contribute to the surface roughness and irregularities of castings, including casting technique, melting method, sprue diameter and configuration, investment material type, mould temperature, and finishing and polishing protocols applied.

The manufacturers' recommended liquid/powder ratio for investment materials should be followed. Indeed, increasing the ratio of liquid to powder can enhance surface smoothness; however, it can also cause dimensional changes to castings [10]. The size and length of the sprue former must be relative to the size of the wax pattern, inadequate size leads to the solidification of molten metal in the sprue area before pattern area and results in shrinkage porosity and/or incomplete casting due to incomplete feeding of molten metal. Sprue length should allow the wax pattern to be 6 mm away from the open end of the casting ring to allow gases to escape through the gypsum material. In order to avoid the abrasion and fracture of investment material, a sprue former should be directed away from thin parts of castings. Sprues should be attached to a wax pattern at an angle of 45° to avoid turbulence within moulds [10,43]. Sandblasting with alumina oxide particles is used to clean the casting surface from investment debris and organic contamination, and to enhance mechanical bonding with veneering materials. The size of alumina particles, pressure and duration of exposure affect the surface roughness of castings [78].

4.1.6 Effect of recasting on surface roughness of castings

Recasting dental alloys might have an effect on the surface quality through an increased risk of contamination with oxides and impurities, which form surface flaws in terms of inclusions, micro-cracks and porosity. Surface flaws largely affect the biocompatibility of

castings. They increase plaque accumulation in restorations [109,168], reduce alloys resistance to corrosion, weaken the physical properties and lower fatigue strength and wear resistance [169]. The influence of recasting dental alloys on surface roughness has not been fully investigated.

Although the high initial roughness of castings resulting from the casting process and sandblasting can be reduced by additional finishing and polishing procedures, excessive removal of material is time consuming and labour intensive; it might also affect the fit and thickness of castings [109]. Initial casting roughness has been shown to affect metal to ceramic bond strength. Although a rough surface of casting is essential for mechanical retention between ceramic and metal, inadequate roughness can, however, weaken the interface by causing stress concentrations that could initiate fractures. It can also cause incomplete contact between ceramic and metal. Furthermore, gases can be trapped in the interface, reducing bond strength. Casting roughness also affects metal to cement bond quality, and the ability of luting agent to flow into micro retentions [170,171].

4.1.7 Evaluating surface roughness

The relationship between the average roughness (Ra) values of intra-oral hard surfaces and bacterial adhesion is one way in which clinical acceptability can be determined. A threshold Ra of 0.2 µm value was adopted from the literature [168]. This value is supported by the theory of bacterial adhesion and retention. Ra values below a threshold level of 0.2 µm have been shown to have no effect on supra- and sub-gingival microbial adhesion or colonisation [168,172]. However, one should be aware that the roughness of restorations are prone to change during clinical performance [173].

Some studies have utilised contact profilometer microscopy to assess surface roughness (stylus evaluation) [174]. However, results of these studies cannot be employed for comparison with studies using the laser profilometer [8]. A beam of laser light is about ten times smaller than the stylus used in the stylus-based profilometer, and so resolution is much improved. The radius of the laser is 2 µm, which is small enough to probe into surface flaws that could accommodate bacteria [175].

No study was found in the literature on the consequences of polishing procedure on the surface quality of re-cast base metal alloys. The majority of previous studies have evaluated the effect of components and particle size of abrasives in polishing systems on a variety of restorative materials [169,176].

Other studies have applied complicated and prolonged finishing and polishing procedures to enhance surface smoothness of materials tested. Aydin [174] used a system of seven polishing stages, and described it as the most effective polishing protocol. These polishing protocols are time- and labour-consuming, and therefore, are not expected to be applied in dental laboratories. Simpler protocols are expected to produce comparable results. In addition, excessive polishing reduces the thickness of casting and affects its fitting.

Studies that investigated the effect of sandblasting on surface roughness of castings have provided a good understanding of the effect of particle size of aluminium oxides on the roughness of castings [177–179]. However, sand blasting is usually followed by further surface treatments, including oxidation firing cycles for bonded castings and finishing and polishing for full cast restorations. These treatments change the topography, roughness, and chemical composition of castings [74,180,181]. Controversial conclusions about the effect of alumina oxide have been introduced in the literature [78,182,183]. Variable sizes of alumina particle are expected to result in variations in surface roughness values of castings.

4.2 Aims and objectives

The aim is to assess the initial surface roughness of castings produced from recast base metal alloys in different combinations and evaluate the effects of conventional finishing and polishing procedures on the final surface roughness and porosity.

The surface roughness analysis of the castings in microns (μm) before and after the polishing procedure was assessed and quantified with a light profilometer (Micro XAM, ADE phase shift, Tucson, Arizona). The mean roughness was measured and recorded for each of the test groups. The roughness parameter (Ra) was measured at five different locations, and presented as mean value.

The porosity analysis was evaluated prior to and after the conventional polishing procedure and quantified using Image J software with SEM micrographs. The mean % area of porosity was calculated and presented for each of the test groups.

Qualitative surface characterization of representative sandblasted, finished and polished test pieces was visualised using electron microscopy (SEM) (JEOL, JSM-500 LV, Japan). Test pieces were sputter coated with gold using a sputter coater instrument (EMITECH Ltd, USA).

4.3 Experimental methods

4.3.1 Test pieces fabrication

Wax patterns (0.3-0.5 mm thickness) were duplicated from one silicone mould, as described in Chapter 3, section 3.3.2.1. Wax patterns and sprues were invested and cast as described in Chapter 3, sections 3.3.2.3 and 3.3.2.4.

4.3.2 Test groups

One hundred test pieces were fabricated and divided into two main groups (n=50), Co-Cr and Ni-Cr test groups. Each alloy test group was divided into two groups (n=25), the first group was employed for surface roughness (Ra) assessments. The second group was employed for the porosity assessments. According to its content of recast alloy (mass%), each group was divided into five smaller sub-groups (n=5) (Table 4-1).

Table 4-1 Experimental groups for surface roughness (Ra) and porosity assessments

Assessment type	Surface roughness (μm)	Mean % area of porosity (μm^2)
Co-Cr alloy (N=50)	100% new alloy	100% new alloy
	75% new + 25% re-cast	75% new + 25% re-cast
	50% new + 50% re-cast	50% new + 50% re-cast
	25% new + 75% re-cast	25% new + 75% re-cast
	100% re-cast alloy	100% re-cast alloy
Ni-Cr alloy (N=50)	100% new alloy	100% new alloy
	75% new + 25% re-cast	75% new + 25% re-cast
	50% new + 50% re-cast	50% new + 50% re-cast
	25% new + 75% re-cast	25% new + 75% re-cast
	100% re-cast alloy	100% re-cast alloy

4.3.3 Initial surface treatments

All castings (100) were sandblasted with 50 μm Al_2O_3 particles, placed in a dental ceramic furnace and subjected to oxidising, first and second opaque, dentine and glazing firing cycles to simulate the manufacturing procedure of ceramic fused to metal restorations. For Co-Cr castings (oxidation 980°C in air, opaque 930°C in vacuum, dentine 910°C in vacuum and glaze 890 in air). For Ni-Cr castings (oxidation 980°C in air, opaque 960°C in vacuum, dentine 930°C in vacuum and glaze 920 in air). Details of the ceramic firing cycles are presented in Chapter 5, Table 5-3 and Table 5-4.

4.3.4 Surface roughness evaluation

For test pieces prepared for Ra evaluation (50 test pieces), non-contact white light profilometer (Micro XAM, ADE phase shift, Tucson, Arizona) was used to measure the mean roughness value Ra (μm), which represents the arithmetic mean of the absolute departures of the roughness profile from the mean line. Test pieces were visualised at 50 X magnification. Five measurements in different sites were recorded for the central region of each test piece, and five measurements were recorded for each site (Figure 4-1). The mean Ra value was determined for each specimen and overall mean and standard deviation values determined for the test pieces in each group. Results were statistically analysed with two-way ANOVA and t-tests (p= 0.05).

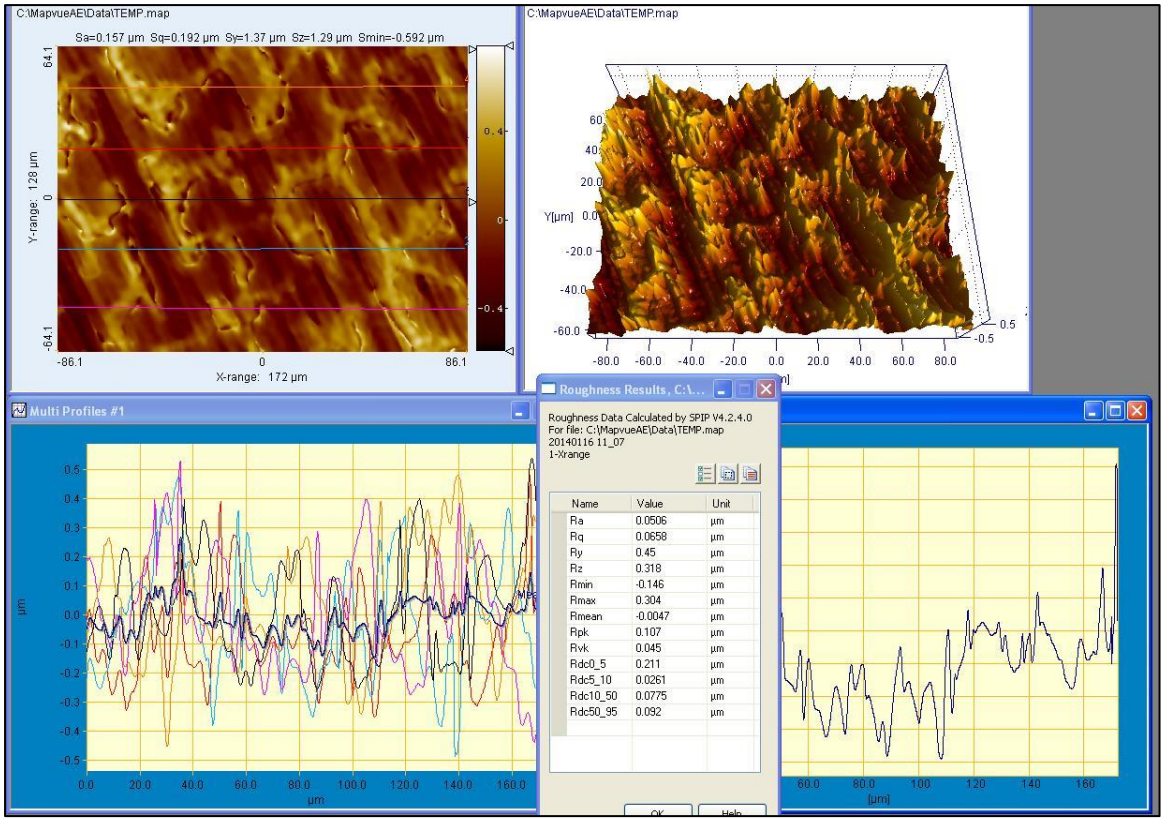

Figure 4-1 Representative 2D and 3D light profilometer images and surface roughness measurements

4.3.5 Porosity evaluation

4.3.5.1 Metallographic polishing and etching

Test pieces prepared for porosity assessment (50) were embedded in a conductive phenolic mounting compound (KonductoMet, USA), which was cured in a mounting machine (Buehler, USA), automatically polished and etched as described in Chapter 3, section 3.3.2.6.

4.3.5.2 Mean porosity assessment

A scanning electron micrograph of each test piece was acquired before the exposure to the automatic polishing procedure. The x-, y-, and z-axis positions of the test piece on the microscope stage were acquired and saved. Micrographs were taken from the central region of each test piece. Five scanning electron micrographs were acquired for each test group. The surface area of pores (μm^2) and the percentage surface area (%) were calculated for

each test piece using ImageJ software as described in Chapter 3, section 3.3.2.7.1. Means and standard deviations of percentage surface area of pores were calculated for each test group with the scanned area being 0.45 mm^2.

4.3.6 Conventional polishing

All test pieces (100) were initially surfaced with sintered aluminium oxide pink stone (Skillbond, UK), treated with medium silicon carbide black rubber polisher points (Dedeco International, USA), followed by a fine silicon carbide green rubber polisher (Dedeco International, USA). A final surface finish used a bristle brush (Buffalo Dental MFG, USA) together with a synthetic diamond polishing compound (BEGO, UK). The polishing system were applied to the specimens using a hand piece rotating at approximately 25.000 rpm (Kavo, Germany), with an intermediate pressure controlled by the operator as much as possible until all specimens looked shiny to the naked eye. New burs were used after the application on five surfaces of a similar test group. At each finishing step, specimens were ultrasonically cleaned (Ultrawave Ltd, Cardiff, UK) with distilled water for three minutes and dried with a blast of air for 20 seconds.

4.3.7 Surface roughness evaluation after the application of conventional polishing

The conventional polishing of the test pieces prepared for surface roughness assessment was followed by a surface roughness evaluation as described in section 4.3.4.

4.3.8 Porosity evaluation after the application of conventional polishing

After the exposure to the conventional polishing, test pieces were prepared for porosity evaluation. A second scanning electron micrograph was acquired for each test piece at the same position on the sample stage used before the polishing procedure; the z-axis had to be slightly adjusted due to the change in test piece height following the polishing procedure. Mean % porosity was evaluated as described in Chapter 3, section 3.3.2.7.1

4.4 Results

4.4.1 Surface roughness assessments

Surface roughness measurements Ra (µm) and standard deviations (SD) were obtained for five test pieces per each test group, before and after the conventional polishing procedure, and calculated as a mean values which are presented in Table 4-2 and Table 4-3.

Table 4-2 Surface roughness means (µm) and standard deviations (SD) of Co-Cr test groups before and after the polishing procedure

Surface treatment	Sandblasted					Polished				
Recast content of alloy	0%	25%	50%	75%	100%	0%	25%	50%	75%	100%
Ra (µm)	1.14	1.08	1.00	1.11	1.13	0.11	0.15	0.14	0.15	0.15
SD (µm)	0.40	0.46	0.29	0.50	0.29	0.04	0.03	0.03	0.03	0.01

Table 4-3 Surface roughness means (µm) and standard deviations (SD) of Ni-Cr test groups before and after the polishing procedure

Surface treatment	Sandblasted					Polished				
Recast content of alloy	0%	25%	50%	75%	100%	0%	25%	50%	75%	100%
Ra (µm)	1.20	1.19	1.18	1.18	1.22	0.10	0.10	0.14	0.14	0.14
SD (µm)	0.56	0.14	0.29	0.32	0.35	0.02	0.02	0.04	0.05	0.03

4.4.1.1 Statistical analysis of surface roughness

The multi-comparison test, two ways ANOVA, indicated that alloy type has no significant effect on surface roughness values before polishing (p= 0.312), or after polishing (p= 0.441). In addition, no significant interaction was found between alloy type and surface treatment before polishing (p= 0.998) or after polishing (p= 0.976). Although test group (new to recast content of alloy mass%) had no significant effect before polishing (p= 0.979), it had a slight but not significant effect after polishing (p= 0.083) (Appendix 1, Table 1-17). For both alloys, polishing procedure has demonstrated a large reduction in Ra values (Table 4-2 and Table 4-3). However, for Co-Cr test groups there were no significant differences in surface roughness values between test groups before polishing (p= 0.982) and after polishing (p=0.194) (Appendix 1, Table 1-18). Similar results were recorded for the Ni-Cr test groups (Appendix 1, Table 1-19).

4.4.2 Surface characteristics

After the surface roughness measurements were taken, representative finished and polished test pieces were used for qualitative SEM analysis (JEOL, JSM-500 LV, Japan).
Figure 4-2 shows the effect of the different surface treatments on the castings surface topography. Low contrast regions, such as surface valleys in Figures A and B, might have been produced by alumina particles during sandblasting. The most obvious defects present in Figure 4-2 C and D are the parallel long continuous scratches and the surface debris left by the abrasive materials used for finishing. Figures E and F represent a smoother surface than Figures C and D with shallower scratches and few pores (Figure 4.2 A-F).

EDAX semi-qualitative analysis was acquired for a representative sandblasted test pieces containing inclusions, with 50 µm alumina particles, analysis revealed the presence of alumina in a high concentration (Table 4-4).

Table 4-4 Chemical composition (mass%) of a representative sand blasted Co-Cr test piece.

Element	Ni	Cr	Mo	Nb	Fe	Al	Si
Mass%	50.22	17.57	7.36	3.56	3.48	16.54	1.28

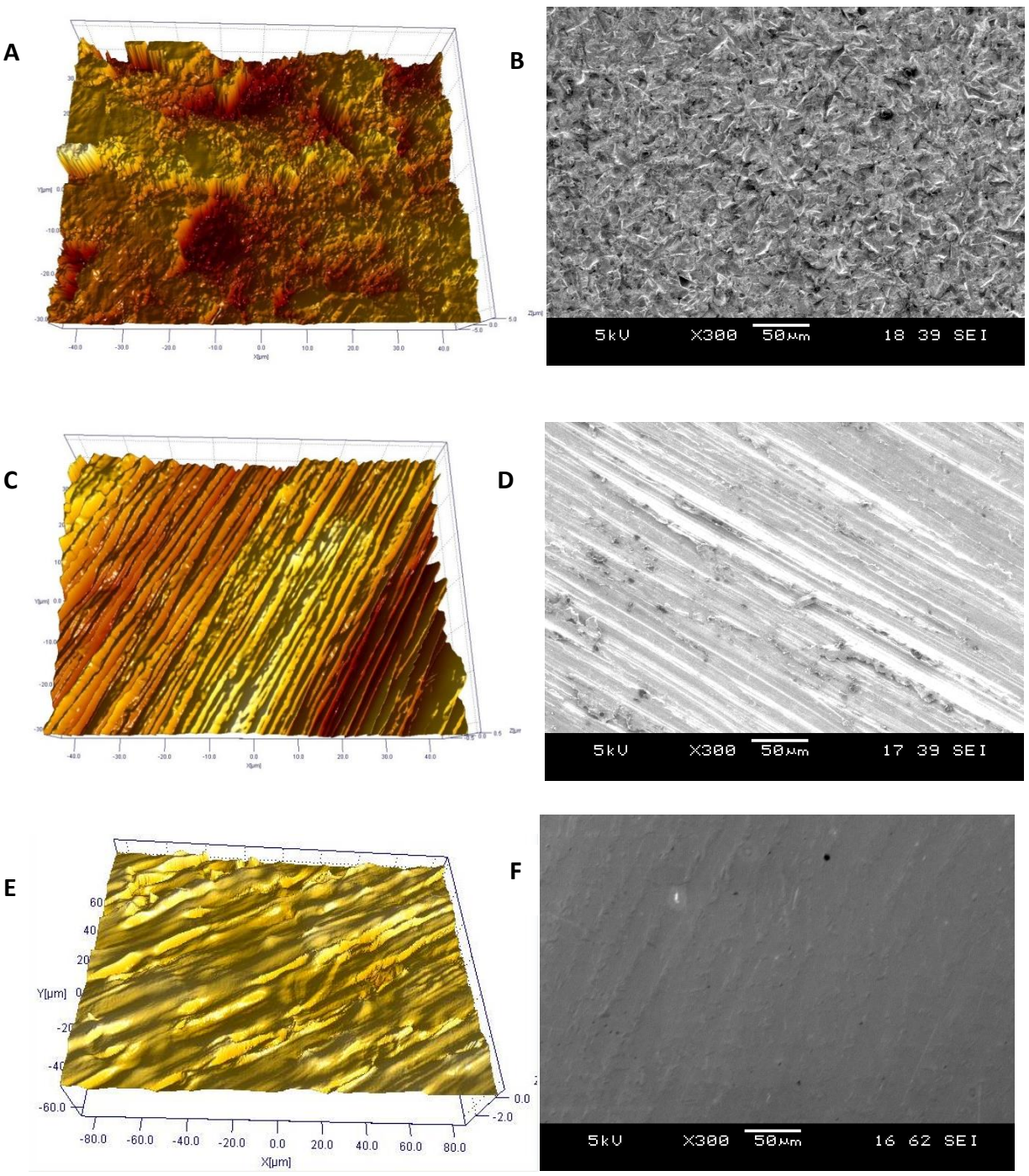

Figure 4-2 Profilometer 3D scans (A, C and E) and scanning electron micrographs (B, D and F) of a Co-Cr castings, sandblasted surface (A), ground surface (B), polished surface (C).

4.4.3 Porosity assessment

The mean percentage area and standard deviations (SD) of pores recorded before and after the conventional polishing procedure are shown in Table 4-5 and Table 4-6.
For both alloys, although the polishing procedure demonstrated only a slight change in the mean porosity values for the first three test groups, it has largely reduced porosity values for the last two test groups compared to those of the first three groups.

Table 4-5 Porosity means (μm^2) and standard deviations (SD) of Co-Cr test groups

Surface treatment	Sandblasted					Polished				
Recast content of alloy	0%	25%	50%	75%	100%	0%	25%	50%	75%	100%
Mean porosity (μm^2 %)	0.04	0.04	0.04	0.10	0.08	0.04	0.04	0.05	0.04	0.04
SD (μm^2)	0.008	0.01	0.01	0.02	0.02	0.009	0.01	0.03	0.01	0.01

Table 4-6 Porosity means (μm^2) and standard deviations (SD) of Ni-Cr test groups

Surface treatment	Sandblasted					Polished				
Recast content of alloy	0%	25%	50%	75%	100%	0%	25%	50%	75%	100%
Mean porosity (μm^2 %)	0.02	0.03	0.05	0.05	0.08	0.02	0.02	0.03	0.02	0.04
SD (μm^2)	0.01	0.01	0.03	0.02	0.06	0.009	0.03	0.01	0.01	0.02

4.4.3.1 Statistical analysis of porosity

For Co-Cr test groups, two ways ANOVA test shows that significant differences exist between the test groups before the polishing procedure (p= 0.024). However, after the polishing procedure, no significant differences were recorded (p= 0.761) (Appendix1, Table 1-20). For Ni-Cr test groups, similar results were reported, significant differences presented between test groups before the polishing procedure (p= 0.011). However, after the polishing procedure, no significant differences were recorded (p= 0.217) (Appendix1, Table 1-21).

A Post Hoc Tukey test was used to determine where significant differences exist (Appendix1, Tables 1-22 and 1-23). For Co-Cr alloys, surface roughness values documented by casting containing 75% recycled alloy were significantly different from those documented by castings containing 0%, 25% and 50% recycled alloys (Appendix1, Tables 1-22). For Ni-Cr alloy, surface roughness values documented by casting containing 100% recycled alloy were

significantly different from those documented by castings containing 0% and 25% recycled alloys (Appendix1, Tables 1-23).

4.5 Discussion

Effective grinding and polishing of dental restorations is essential for the patient′s oral health and restoration's aesthetics [166]. Grinding is removing or reducing bumps, overhangs and excesses in castings. Scratches and surface cuts left by grinding are subsequently removed by polishing [10].

Initial surface roughness of castings is mainly produced by the casting process and sandblasting. In this study, Ni-Cr castings demonstrated higher initial surface roughness values than Co-Cr castings. However, both alloys demonstrated similar roughness patterns after polishing (Table 4-2 and Table 4-3) and the alloy type had no significant effect on the final Ra values documented (Appendix 1 Table 1-17).

The hardness of Co-Cr alloy of 280 VHN, as provided by the manufacturer, is higher than that for the Ni-Cr alloy, 240 VHN. This can cause the Co-Cr to be more resistant than Ni-Cr to the penetration resulting from the sandblasting procedure and demonstrate lower initial surface roughness values (Table 4-2 and Table 4-3). However, the efficacy of the polishing protocol used, allowed both alloys to demonstrate comparable values of Ra. In addition, this observation of having comparable Ra values could be explained in that both alloys were exposed to the same melting method and casting procedure. Similar investment materials and sprue configurations were used and both alloys received the same surface treatment after casting. Another explanation could be that both base metal alloys are categorised into one family of super alloys, whose microstructure and properties of these alloys are comparable. Similar results were obtained by Bezzon [55]; who investigated the surface roughness of three different base metal alloys, Co-Cr, Ni-Cr and titanium, concluded that within the same casting procedure, whether inductions melting with vacuum casting or flame melting with centrifugal casting, no differences in surface roughness values of base metal alloys were found.

Sprue type is one of the important variables in a casting process. Size, length, diameter, configuration and location control the supply of molten metal into the mould, and

contribute to the quality of castings by reducing casting shrinkage, cracks and porosity [43]. The melting method itself is another variable of crucial importance in a casting procedure. In the current study, castings were performed in a controlled environment using induction melting with vacuum pressure casting, which was shown to decrease surface roughness compared to other melting methods [54], such as flame melting. Similar results were observed in Bezzon´s study [55], as the type of alloy did not affect the surface roughness of castings as much as the casting procedure; vacuum casting significantly decreased surface roughness compared to acetylene-oxygen flame casting for Ni-Cr and Co-Cr alloys.

Sandblasting with alumina oxide particles is used to clean the casting surface from investment debris and organic contamination, and to enhance mechanical bonding with veneering materials [78]. In this study, EDAX analysis of an area containing inclusions revealed the presence of Al. Similar results were documented by Al-Jabbari [78], who observed an increase in the amount of aluminium (Al) in the sandblasted Ni-Cr and Co-Cr alloys. It is documented in the literature that sandblasting might change castings surface chemical composition [55,184].

Castings containing recast alloy demonstrated slightly higher surface roughness values after polishing (0.11 µm for CoCr-0, 0.15 µm for CoCr-100, 0.10 µm for NiCr-0 and 0.14 for NiCr-100). Recast alloys are more vulnerable to the formation of carbides and the occurrence of porosity. Nickel, chromium, molybdenum and silicon react with carbon to form carbides, and indeed, the composition, size and distribution of carbides change after recasting [59]. Carbides contribute to the strength and hardness of alloys; however, excessive presence affects the ductility of alloys. Although it is not well understood if carbides are vulnerable areas for porosity or pores enhance carbide formation, there is a suggestion that the presence of pores enhances the accumulation of carbides at the interdendritic areas [75] and, in turn, this might affect mechanical properties of alloys, such as micro-hardness and tensile strength [66]. Changes in mechanical properties of alloy can reduce the efficacy of the abrasive material by affecting its ability to detach debris from castings.

Another explanation for the observation that castings made out of recast alloys have demonstrated higher surface roughness values than castings produced from new alloys can be that air abrasion using Al_2O_3 was able to remove most of the impurities, while grinding

exposed more subsurface pores and inclusions which were hard to remove using the polishing procedures [178]. Surface roughness is not only produced by scratches created by the grinding procedure, but may also be produced by pits, ridges, inclusions and cracks; all these factors contribute to the casting surface roughness [10].

Polishing procedures are associated with the production of heat and residual stress and flaws through the casting being polished [166]. Castings produced from recast alloy or a mixture of recast with new alloy is expected to demonstrate a heterogeneous structure due to the non-homogeneous distribution of the elements of alloys throughout the casting. Re-casting alloys results in a disproportional concentration of elements. The less homogeneous structure of recast alloys make it less affected by the consequences of the polishing procedure [19].

In the current study, the surface roughness parameter is presented as Ra, which is the most commonly used surface parameter to express castings surface roughness. Using Ra make it easier to compare results of this study with others documented in the literature. Ra is defined as average surface roughness or arithmetic mean deviation of the roughness profile, which is the area between roughness profile and its mean line, or the integral of the absolute value of the roughness profile heights (peaks and valleys) and then averaging them all over the entire cut-off/evaluation length. The centreline normally corresponds to the section through the profile, which cuts off the equal areas above and below it [185].

In the current study, all test groups exhibited clinically acceptable topography values as Ra values were less than the threshold value of 0.2 µm [168]. The polishing system applied was able to reduce the surface irregularities and was effective with both alloys.

Factors which are expected to affect the efficiency of the polishing procedure have been controlled by the operator, such as the quality of the abrasive material. A new bur was used after the application on five test pieces of the same group, wear of the abrasive particles might deteriorate their efficacy. Speed and pressure at which the abrasive were applied to the casting have also been controlled by the operator [10].

Bezzon [55], assessed the surface roughness of base metal alloys submitted to different casting techniques. Surface roughness values of castings produced using vacuum casting were 2.43 µm and 2.23 µm for Ni-Cr and Co-Cr respectively. Disc shaped test pieces were used in Bezzon's study. However, using cast test pieces that simulate copings and crowns gives more reliable results. Ravi [177] investigated the effect of various surface treatment procedures on surface roughness of Ni-Cr castings and reported a value of 1.39 µm for sandblasted Ni-Cr castings. However, castings were sandblasted with 110 µm Al_2O_3, surface roughness was measured using a stylus type measuring instrument and the method used to cast wax patterns was not explained. For all the above reasons, comparing results from the current study with those documented by Ravi was not possible.

Castillo-Oyagüe [186], aimed to evaluate the effect of various surface treatments on the surface roughness of cast and laser sintered base metal alloys. Castings which submitted to sandblasting and oxidation cycles exhibited surface roughness values of 3.24µm and 3.31µm for Co-Cr and Ni-Cr respectively. To evaluate the effect of sandblasting on surface roughness, test pieces were submitted to sandblasting with Al_2O_3 particles twice (50µm and 125µm Al_2O_3). Castings produced for metal-ceramic restorations are usually submitted to sandblasting once and one Al_2O_3 particle size is used.

It can be noted that the roughness values obtained in this study, even for castings containing 100% recycled alloy, fall within the low values presented in the literature.

For both alloys, the polishing procedure had no effect on the mean area porosity values of castings with up to 50% recast content of alloys. However, in the casting containing 75% and 100%, significant changes were documented in the porosity values (Table 4-5 and Table 4-6). Polishing results in the removal of a material and the exposure of subsurface microstructure [55]. This result could be explained by homogeneity of casting microstructure and the consistency of the pattern of casting defects presented through castings. Similar to all other casting defects, porosity is linked to the casting procedure and can not be eliminated completely. It can also be stated that due to this homogeneity only a small amount of the material was removed by the polishing procedure with bulk microstructure not being exposed to the surface.

The last two groups of Co-Cr alloys (CoCr-75 and CoCr-100) demonstrated the highest mean porosity values after the sandblasting procedure and before polishing procedure (0.10% ± 0.02 and 0.08% ± 0.02 respectively). However, the polishing procedure produced comparable values of mean porosity of these two groups to the other test groups (Tables 4.5 and 4.6). This can be explained in that the number of pores in the castings containing 75% and 100% recycled alloys has increased but not the surface area of the single pore. This suggestion is supported by the values documented in Chapter 3, (Table 3-5), test group NiCr-CB-100.

Another explanation for the decrease in porosity values in castings containing 75% and 100% recycled alloys after the exposure to the polishing procedure could be that although the surface area of pores in castings containing 75% and 100% has increased; the polishing protocol used was able to remove pores or minimize their surface area.

The ability of polishing to eliminate pores depends on the surface area of the pores and the elongation limit of alloys, (stretch before ultimate failure occurs). The elongation limit of alloys can eliminate small surface and subsurface pores, but might not be able to eliminate pores with larger surface area and other types of porosity, where pores are present in clusters. Polishing pores of greater surface areas might cause the material to exceed its elastic elongation limit and plastic flaws to occur before the large cavity cross-section is removed completely [112]. No study was found in the literature similar to the current study, and so it was not possible to compare the reported results with other studies.

5 Metal-ceramic bond strength

5.1 Literature review

5.1.1 The metal-ceramic bond

Although all-ceramic restorations provide better aesthetics, and are technically less challenging, metal-bonded ceramics are still widely used. The metallic framework provides superior fracture resistance over all-ceramic restorations [187] and are used in long-span fixed partial dentures and restorations in stress-bearing areas. Bonded restorations have proven adequate performance with high overall survival rate in clinical studies [188] and less reported failure rates *in-vivo* than all-ceramic restorations at 10 years in *in-vivo* study [26]. Donovan and Swift [189] recorded a 4-10% failure rate in a 10-year period. Despite the high rate of success, failure still occurs, which can be due to various factors other than inadequate bond strength. These factors include the geometry of preparation, design and thickness of the metal core and occlusal forces and traumas [190,191]. According to Anusavice [192], there is no comprehensive classification system that clearly differentiates between clinical prosthesis failure, and technical and biological complications.

A combination of four factors contributing to the bonding between metal and ceramic have been identified; (i) the chemical bond, which is created by the oxide layer formed on the metal substrate, formed from metallic, ionic, and covalent bonds with oxides in the ceramic opaque; (ii) mechanical interlocking, in which opaque ceramic flows into the undercuts on the metal surface; (iii) Van der Waal's forces, in which attraction between molecules is based on molecular charge; (iv) compressive forces based on coefficient thermal expansion (CTE) of the combined materials. CTE determines the contraction rate of materials during cooling, if the two materials have mismatched CTE, failure via ceramic crack propagation is expected to occur [26,193]. Chemical bonding and mechanical interlocking are considered to have a major contribution to metal-ceramic bond strength. However the role of CTE of metal and ceramic is important.

When ceramic is cooled, leucites contract more than the surrounding glass. This contraction results in the formation of compressive stresses around the crystals due to the transformation from cubic to tetragonal upon cooling. Stress also forms around pores and at

the tips of micro-cracks, which are created within and around crystals [194]. If developed stresses exceed the strength of materials, cracks will move through the materials causing failure in the form of fracture and debonding.

Dental ceramics are brittle materials, i.e. they are stronger when in compression than in tension. Therefore, it is beneficial to have some residual compressive stress through a small CTE mismatch, to take the advantage of this defining property [35]. CTE of metal should be slightly higher (approximately $0.5 \times 10^{-6}/\circ C$) than that of the applied ceramic, putting the ceramic in residual compression upon cooling [195]. Most bonded alloys have a CTE of 13.5-$14.5\times10^{-6}/\circ C$, while Leucite-based ceramics have a CTE of 14.5-$18.0\times10^{-6}/\circ C$ [196]. Opaque ceramic contains leucites to raise CTE close to that of metal. An increased amount of leucites, which can result from repeated firings, can increase the mismatch of CTE of metal and ceramic.

Having achieved a bond, it is important to preserve it, and so design is of crucial importance. Compressive forces depend, to a large extent, on the geometric design of alloy framework that can pull the veneering ceramic toward the metal. For ceramic bonded alloys, the casting temperature of the alloy must be 170 to 280 ˚C above the fusing temperature of the ceramic to avoid distortion in metal frameworks [10].

5.1.2 Metal-ceramic bond strength tests

Bond strength is defined as force per unit area required to break a bonded assembly with failure in, or near the adherent interface [197].

Due to the complexity of the interface and the stress distribution under force, various authors utilise different testing methodologies to evaluate bond strength, and this in turn has limited the ability to compare results of different studies. The International Organisation for Standardisation (ISO) standardised ceramic-metal bond testing through the Schwickerath crack-initiation test; a three-point bending test developed in 1999 [195]. This test is subject to limitations, and only approximates the bond strength. In function, the restoration is subjected to repeated intraoral occlusal forces over long periods of time. In addition, a combination of cohesive and adhesive failure can happen during this test, as it cannot guarantee that the cohesive bond is higher than the adhesive bond [195]. The true bond

strength could only be achieved if the cohesive strength of the feldspathic porcelain exceeded that of the metal ceramic bond, and the CTE of the metal and ceramic were identical [195,198]. Standardising samples and testing methods is crucial to minimise experimental variables, and make it possible for a researcher to compare results with others. In order to categorise a restoration to be clinically acceptable, materials and techniques have to be evaluated prior to the insertion in the patient's mouth, if a metal-ceramic system meets bond strength requirements of ISO 9693 then there is a degree of confidence that restoration will function appropriately. Testing the bond strength of veneered metal core in its crown shape is not possible, because of the challenge of fixing the crown in testing instruments [199].

Even though ISO 9693: 2000 [200] recommends the evaluation of metal alloy bond strength by using the 3-point bending test, a number of studies have evaluated the bond using the shear bond test [201–203]. Della Bona and Van Noort [204] used finite element analysis, and found that using shear interface, test results are governed by the cohesive strength of the ceramic rather than the adhesive bond at the ceramic metal interface. In a 3-point bending test, adhesive failure occurs at the ceramic metal interface this property makes this test more durable for the bond strength test. In addition, the shear bond test is technically more critical than the bending test, shearing force must be put in a way that is perpendicular to the two materials; otherwise, false forces will be delivered.

5.1.3 Recasting and bond strength

Metal-ceramic bond has been described as a complex and illusive mechanism [205]. One of the predominant factors to bond strength is the surface topography of casting. Care must be taken to maintain the surfaces are free of trapped air and contamination. Roughness of different directions and contaminated surfaces affect the mechanical retention of ceramic to castings. It can also affect the wetting ability of ceramic by decreasing the wetting angle, which has to be less than 60° to be effective. All these faults result in porosity at the ceramic metal interface. Porosity and other flaws are stress concentration areas.

As firing of opaque occurs, oxides from the alloy surface can diffuse into the fused ceramic. Remelting of alloy can affect the diffusion of metal oxides into porcelain as the amount and type of oxides change. Remelting of alloy can, for example in CoCr alloy alter the amount of

Al and Be. The reduction in the amount of oxide formation inhibitors, such as Al and Be, result in excessive oxide accumulation and reduction in metal-ceramic bond strength [206]. Diffusion of metal oxides into ceramic might affect the coefficient of thermal expansion. Ceramics are composed of a glassy phase and crystalline phase. Leucite phase transformation at above 625 ˚C is combined with a thermal expansion of 1.2 vol% of the unit cell. Therefore, the thermal coefficient expansion is governed by the amount of crystal phase present, which can be as much as 20% vol. Chemical composition of alloys has an effect on metal-ceramic bond strength; for example, an alloy with higher Cr content has a thicker oxide layer, the presence of elements, such as Al and Be, as oxides in the oxide layer reduce the excessive growth of oxides [207].

Limited literature was found concerning the effect of recasting base metal alloys on metal-ceramic interface quality. Ucar et al [104] evaluated the bond strength of castings made from recast Ni-Cr alloys using the three point bending test. Ucar observed a significant reduction in bond strength of castings containing recast alloys; however, no chemical or microstructural analyses of the interface were employed to support the possible explanation of the results documented.

Kumar [208] examined the bond strength of castings containing recycled Ni-Cr and Co-Cr alloys and documented that the addition of new alloy to recycled alloys enhances the metal-ceramic bond strength. However, similar to Ucar study [104], no chemical or microstructure analyses were conducted. Madani [206] adopted a similar study design, in addition, he examined more variables by using two different types of ceramics to be fused on to one alloy type. Adding more variables to the experiment without conducting further analyses of the composition and thickness of the oxide layer, or analysing the chemical composition of the interface, and assessing the presence of defects in the ceramic side or in the metal side, makes analyses of results difficult.

5.1.4 Factors affect metal-ceramic bond strength

Bond strength is a result of a number of interrelated and overlapping factors, which can be categorised into five groups [193,209];

(i) Factors related to the alloy

- Alloy coefficient of thermal expansion (CTE)
- Chemical composition
- Surface characterisation, including the presence of pores and cracks and types of oxides formed

(ii) Factors related to the ceramic

- Ceramic coefficient of thermal expansion
- Chemical composition

(iii) Factors related to features of ceramic-metal interface,

- Width of interfacial region
- Chemical and phase composition

(iv) Technical factors

- Handling of materials
- Adherence to the manufacturer's instructions.

(v) Other factors

- Methods and materials used for alloy melting and casting
- Surface treatments and cleaning of castings
- Ceramic firing cycles, temperature and pressure of ceramic furnace.

The literature available has focused on the metal–ceramic interface rather than the metal surface or ceramic composition after the multiple preparation stages. A study that analyses the quality of the interface with regard to the presence of pores, and analyses the elemental composition and its variation through the interface, could provide a better understanding of the effect of recasting on bond quality.

5.2 Aims and objectives

This chapter aims to evaluate the effect of reusing surplus alloy on the metal-ceramic bond strength and investigate the thickness of the interfacial region and its chemical composition.

Twenty test pieces were prepared for each test group following the requirements of ISO 9693: 2000 [200]. Test pieces were subjected to 3 point bending test using a universal testing machine (Hounsfield H10KS, Tinius Olson, USA). The mean bond strength of each test group was calculated. Failure occurrence at the metal-ceramic interface was evaluated using light stereomicroscopy (S-1000, Spectrographic, UK).

Elements distribution across the metal-ceramic interface was investigated. Analyses were performed at five different sites across, and at either side of the interface. Thickness of the metal-ceramic interface (μm) was measured using ImageJ software.

5.3 Experimental methods

5.3.1 Test groups

Metal-ceramic bond specimens were prepared using Co-Cr and Ni-Cr alloy of 0%, 25%, 50%, 75% and 100 % recycled alloy content. Twenty test pieces for each composition were fabricated, in accordance with ISO 9693: 2000 methods [200].

5.3.2 Metal substrates

Test pieces were fabricated according to ISO 9693:2000 specifications [200] (

Figure 5-1).

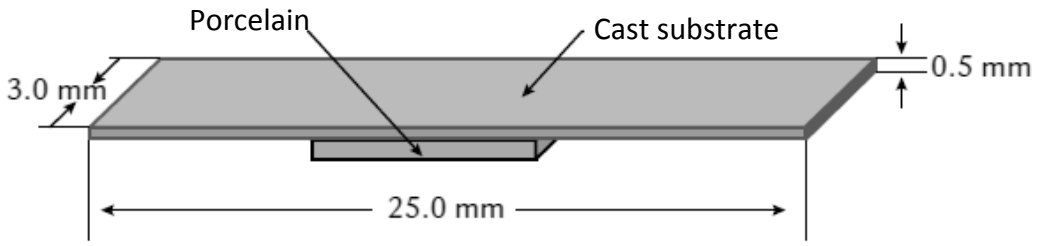

Figure 5-1 Test pieces configuration [200]

Plastic strips (25 mm × 3 mm × 0.5 mm) were cut from a plastic sheet of 0.5 mm thick (Bracon, UK). Five plastic strips were mounted in one casting ring, invested and cast, following the procedure described in sections 3.3.2.4. Castings were bench cooled to room temperature, divested and abraded with 50 µm Al_2O_3 and steam cleaned to remove aluminium oxide particles and other contaminants. The thickness of each test piece was measured using a digital gauge (Dura Tool, UK) and adjusted by grinding the non-working side with aluminium oxide pink stone (Skillbond, UK). Substrates were then steam cleaned and oxidised following the manufacturer's recommendations. Degassed test pieces were sandblasted with 50 µm Al_2O_3 at 4 bars.

5.3.3 Ceramic application

Duceram porcelain (Duceram, Dental-Gesellschaft, Germany) was used with the Co-Cr alloy and Matchmaker porcelain (Davis Ltd, UK) with the Ni-Cr alloy (Table 5-1 and Table 5-2).

Table 5-1 Chemical composition of Duceram porcelain (mass%) as provided by the manufacturer and the EDAX analysis

Element (Mass%)	Manufacturer (Duceram, Dental-Gesellschaft, Germany)	EDAX (Dentine)	EDAX (Opaque)
Si	43-66	27.43	19.85
Al	13-21	7.56	5.61
Na	02-11	4.39	2.04
Ba	0-12	-	-
Sn	0-12	-	7.60
Fe	0-2	-	-
Zr	-	-	15.46
K	-	7.23	7.25
Ca	-	0.47	-
C	-	12.00	8.30
O	-	40.88	33.89

Table 5-2 Chemical composition of Matchmaker porcelain (mass%) as provided by the manufacturer and the EDAX analysis

Element (Mass%)	Manufacture (Davis Ltd, UK)	EDAX (Dentine)	EDAX (Opaque)
Si	45-67	20.80	15.13
Al	8-20	-	-
B	1-12	-	-
Sn	0-15	-	2.88
K	-	3.98	3.39
Na	-	5.41	04.43
Ca	-	0.71	-
Br	-	11.70	11.01
Zr	-	-	11.05
C	-	12.39	10.25
O	-	44.93	41.32

The ceramics were chosen due to their CTE compatibility with the alloy. Two layers of opaque ceramic were applied to a rectangular area of 8.0 mm × 3.0 mm in the centre of each casting strip. The first layer was thin (< 0.01mm) and uniform, while the second layer applied was 0.15 mm. One layer of body ceramic was subsequently applied forming a total

ceramic layer thickness of 1.00 ± 0.1 mm. A rectangular plastic jig was used as a custom made mould to standardise ceramic dimensions. Thicknesses of ceramic layer were determined by measuring the metal strip thickness before the ceramic application and then after by using a digital gauge (Dura Tool, UK).

Excess porcelain was ground with a fine diamond point (Bracon, UK) using a hand piece rotating at approximately 15.000 rpm (Kavo, Germany), with a low pressure controlled by the operator as much as possible. Careful attention was paid not to bend the test piece while grinding. Each porcelain layer was fired in a furnace (Chaperlin & Jacobs Ltd, UK) at a setting recommended by the manufacturers (Table 5-3 and Table 5-4).

Table 5-3 Duceram porcelain firing temperatures as recommended by the manufacturer

Stage	Preheating temperature	Drying time	Preheating time (min)	Heating rate (˚C /min)	Firing temperature (˚C)
Degassing	575	0	3	55	980
Opaque ($1^{st}/2^{nd}$)	575	6	2	55	930
Dentine	575	4	1	55	910
Glaze	600	4	1-3	55	890

Table 5-4 Matchmaker porcelain firing temperatures as recommended by the manufacturer

Stage	Preheating temperature	Drying time	Preheating time (min)	Heating rate (˚C /min)	Firing temperature (˚C)
Degassing	450	0	3	80	980
Opaque ($1^{st}/2^{nd}$)	450	6	2	80	960
Dentine	450	6	1	60	930
Glaze	450	1	1	60	920

5.3.4 Evaluation of metal-ceramic bond strength

Test pieces were subjected to three-point bending using a universal testing machine (Hounsfield H10KS, Tinius Olson, USA). Each test piece was placed on the testing apparatus where the distance between the two supports was 20 mm. The ceramic surface was placed facing down and opposite to the applied load (Figure 5-2). The force was applied at a constant rate of (1.5 ± 0.5 mm/min) and recorded up to failure.

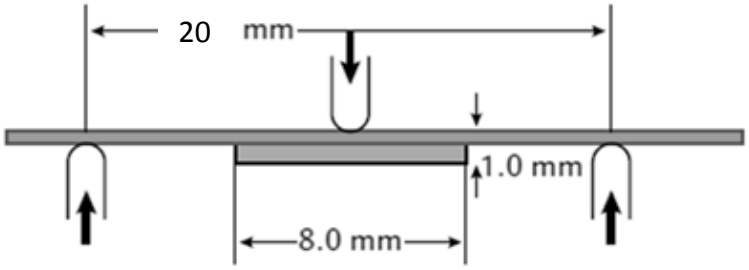

Figure 5-2 Three-point bending test [200]

The fracture force (F_{fail}) for each test piece corresponded to the occurrence of a debonding crack at one end of the ceramic layer, which was observed as a sudden drop in loading force in the load deflection curve (Figure 5-3). The failure load was recorded digitally using software provided by the manufacturer of the testing machine.

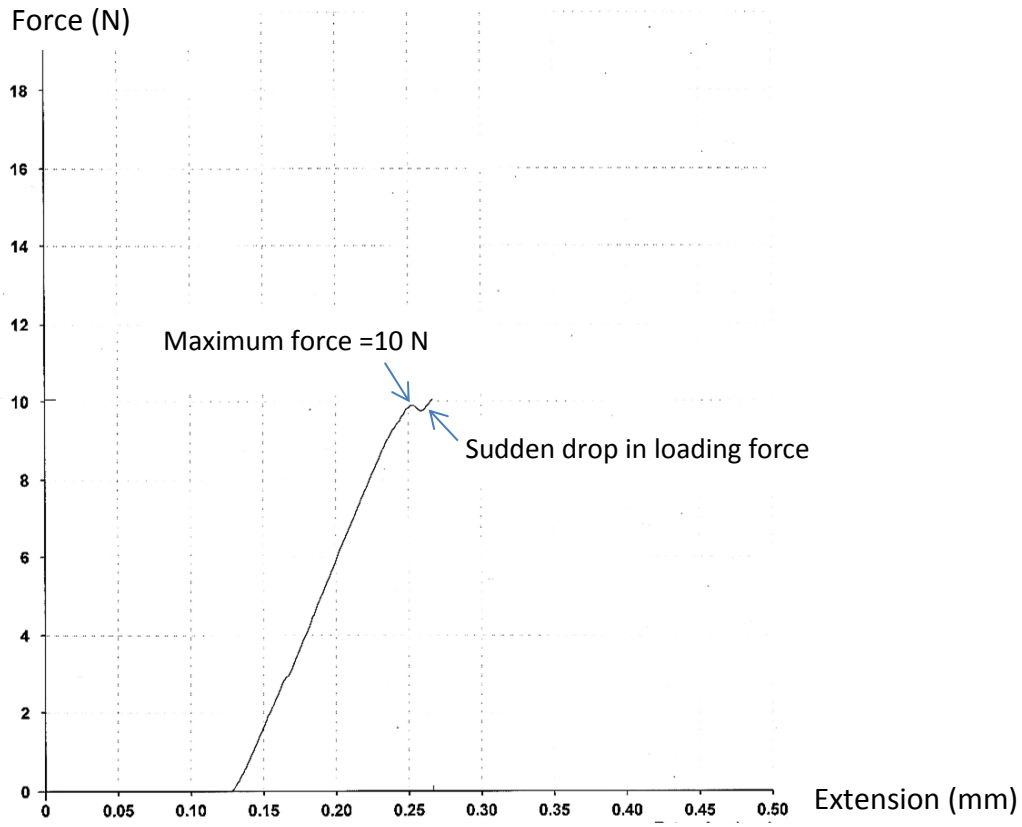

Figure 5-3 Load deflection curve example

5.3.5 Calculation of bond strength

Bond strength was calculated using the following equation:

$$\tau_b = K.F_{fail}$$

where F is the maximum force applied in Newton before de-bonding (failure load) and k is a constant, which can be determined from a graph provided by ISO 9693: 2000 [200] with units of mm^{-2}. The value of k depends on the thickness of the metal substrate and the elastic modulus of the alloy (Figure 5-4).

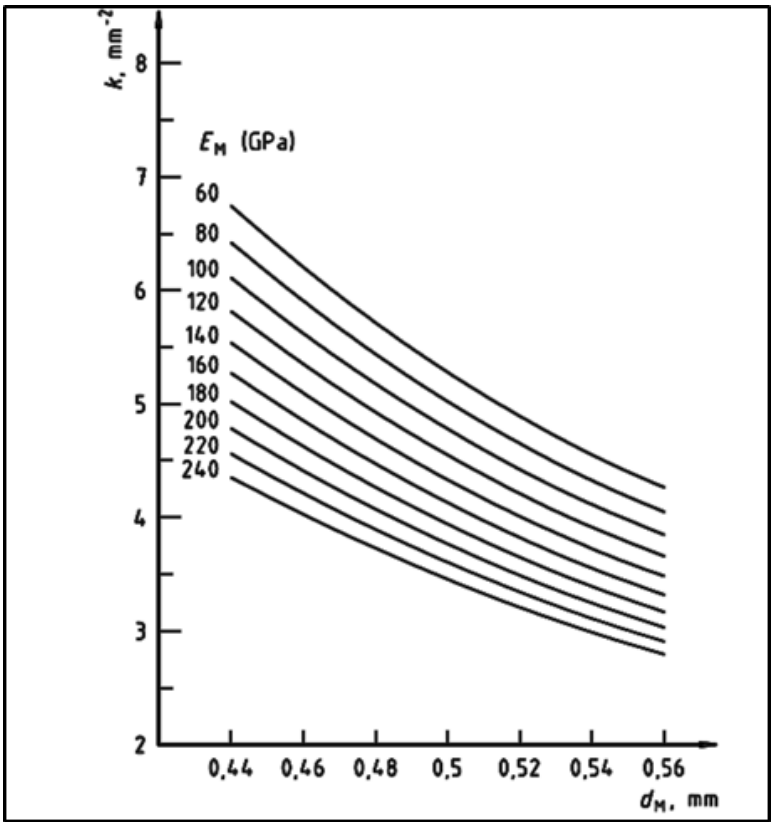

Figure 5-4 Diagram to determine the coefficient k as a function of metal substrate thickness d_M and modulus E_M of the metallic material (ISO 9693: 2000) [200].

5.3.6 Analyses of metal-ceramic interfacial region

5.3.6.1 Mounting and metallographic polishing

Metal-ceramic test pieces were embedded in conductive filled phenolic mounting compound (KonductoMet, USA) and cured in a mounting machine (Buehler, USA). Test pieces were finished automatically (Motopol12, Buehler, UK) using fine grit sandpapers to

produce a flat surface, free of grooves and scratches. Grinding began with 240 grit paper followed by 2500 grit paper. Samples were then polished with 3 µm diamond paste, followed by 1µm diamond paste (MetaDi, Buehler, USA). The final polishing step was performed using 0.05 µm colloidal silica (Buehler, Lake Bluff, Illinois, USA).

5.3.6.2 Carbon coating

The test pieces were coated with a carbon layer using a sputter coating instrument (EMITECH Ltd, USA). The argon gas supply and sputter coater were turned on, and pressure was set at around 0.7 bar. After operating the coating instrument, chamber pressure was reduced to below atmospheric. Pressure was allowed to reach 4 mbar, at that stage, voltage was set to 7 V, and the pulse button was pressed and held for 10 seconds. It was released for 3 seconds, and then pressed again for 10 seconds. When coating was completed, the voltage was turned to zero and chamber evacuation was stopped.

5.3.6.3 Quantitative analysis

The elemental composition in the metal-ceramic interface region was investigated by using EDAX at five different sites across, and at either side of the interface (Figure 5-5 A to E). These analyses were repeated five times for each test group. The interface was imaged at 150 X; the accelerating voltage was set at 20 kilovolts (kV) with a working distance of 9-14 mm. For consistency purposes, acquisition time was set to 20 seconds. Three analyses were acquired for each test piece. The mass percentage of each element was presented as the mean value.

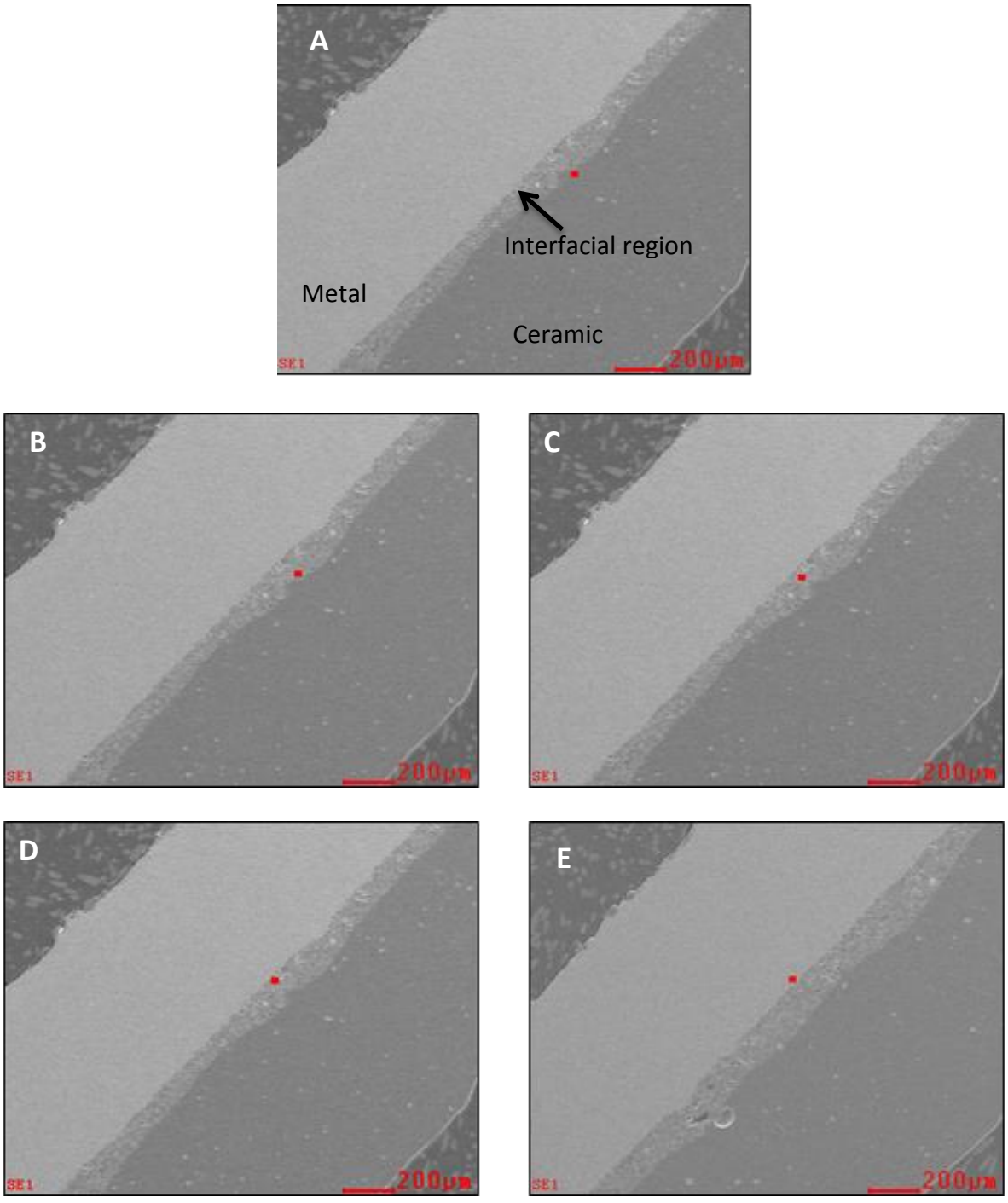

Figure 5-5 Sites of Energy-dispersive X-Ray Spectroscopy area analysis across and at either side of the interfacial region. Squares indicate areas used for EDAX analyses.

5.3.6.4 Qualitative analysis

Variations in the distribution of elements at the ceramic-metal interface were investigated by line scan analysis. The interface was imaged at 5000 magnifications; based on the size of the cross-section of the test piece, a line profile covering the ceramic, interfacial area and the alloy was drawn.

5.3.6.5 Thickness of interface area

The thickness of the ceramic-metal interface was measured using ImageJ software. Straight lines across the interface were drawn and measured (Figure 5-6) for each test group; fifty lines were drawn; the mean and standard deviation of line lengths were recorded (µm).

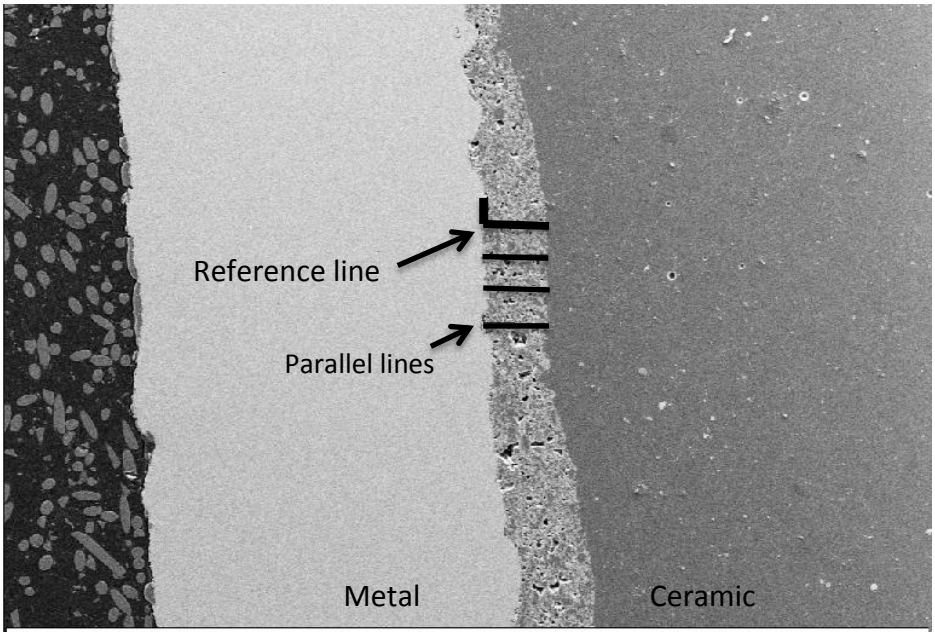

Figure 5-6 Thickness of metal-ceramic interfacial region

5.4 Results

5.4.1 Metal-ceramic bond strength

5.4.1.1 Calculation of bond strength

The fracture force, F_{fail}, was multiplied with a coefficient k, read from Figure 5-4. The coefficient k is a function of the thickness of the metal substrate d_M (0.5 ± 0.05) mm, and the value of Young's modulus, $E_{M,}$ of the metallic material used. Young's modulus E_M is 280 GPa for the Co-Cr and 160 GPa for the Ni-Cr alloy. In order to read the value k for a certain thickness d_M, the curve for the proper value E_M is determined, and then the corresponding value of k is selected from the curve for the selected thickness d_M. The debonding/crack-initiation strength is then calculated using the equation.

Ni-Cr test groups demonstrated higher mean bond strength values than CoCr test groups (Table 5-5 and Table 5-6). For both types of alloys, test groups made out of reused alloys demonstrated a drop in bond strength values. For the CoCr alloy, there was a 26% drop in the bond strength value (from 37.71 MPa to 27.90 MPa for CoCr-0 and CoCr-100, respectively), and a 28.55% drop (from 39.05 MPa to 27.90 MPa for CoCr-75 and CoCr-100, respectively) (Table 5-5).

For Ni-Cr alloy, there was a 19% drop (from 56.17 MPa to 45.35 MPa for NiCr-0 and NiCr-100, respectively) and a 24% drop (from 59.91 MPa to 45.35 MPa for NiCr-75 and NiCr-100, respectively) (Table 5-6).

Figure 5-7 shows that both alloys demonstrated a similar trend for the first two test groups and the last two test groups. However, the behaviour of the two alloys at the transition from the second test group, 25% reused alloy, to the fourth test group, 75% reused alloy, varied widely.

Table 5-5 Fracture force, specimen thickness and bond strength of the Co-Cr test groups

Test group	Fracture force (N)	Metal substrate thickness(mm)		Bond strength (MPa)	
		Mean	SD	Mean	SD
Co-Cr-0	13.16	0.53	0.008	37.71	5.15
Co-Cr-25	12.47	0.52	0.02	37.50	8.89
Co-Cr-50	14.27	0.51	0.02	44.87	8.78
Co-Cr-75	12.71	0.51	0.009	39.05	5.54
Co Cr-100	8.91	0.51	0.01	27. 90	3.29

Table 5-6 Fracture force, specimen thickness and bond strength of the Ni-Cr test groups

Test group	Fracture force (N)	Metal substrate thickness (mm)		Bond strength (MPa)	
		Mean	SD	Mean	SD
Ni-Cr-0	15.64	0.54	0.03	56.17	04.60
Ni-Cr-25	15.50	0.52	0.01	59.45	12.07
Ni-Cr-50	13.85	0.52	0.01	53.22	06.50
Ni-Cr-75	15.84	0.53	0.008	59.91	09.18
Ni-Cr-100	12.20	0.52	0.02	45.35	08.11

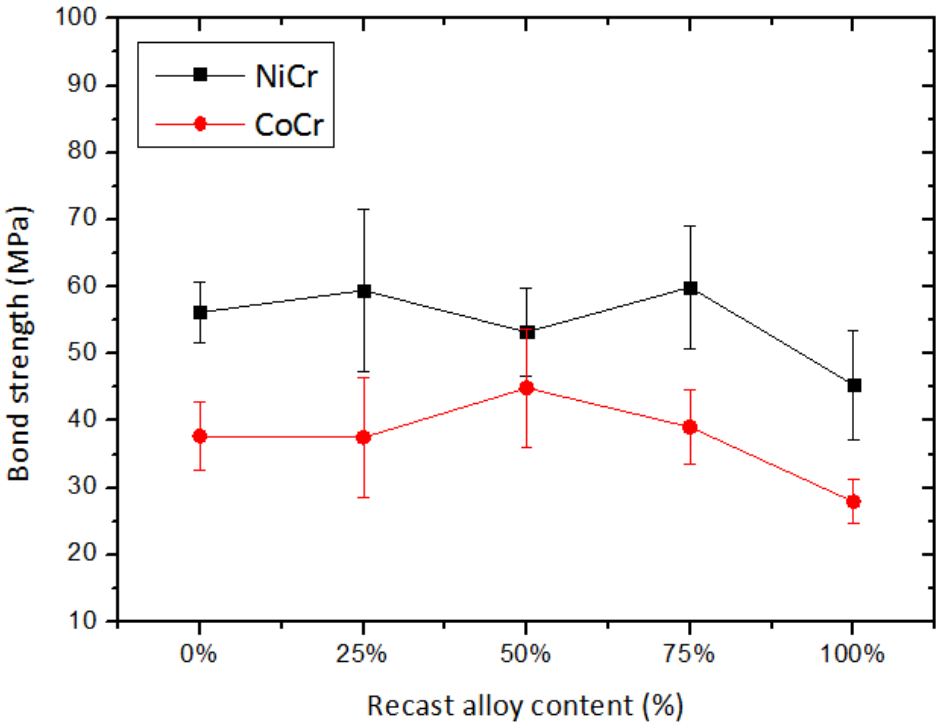

Figure 5-7 Metal-ceramic bond strength of the Co-Cr and Ni-Cr test groups

5.4.2 Thickness of the interfacial region

The thickness of the interfacial region and standard deviations (SD) are presented in Table 5-7 and Table 5-8

Table 5-7 Interfacial region thickness (µm) and standard deviations (SD) of Co-Cr test groups

Recast content of Co-Cr alloy (%)	0%	25%	50%	75%	100%
Mean thickness (µm)	49.44	50.56	47.1	58.8	56.8
SD (µm)	9.37	9.00	7.40	15.34	19.48

Table 5-8 Interfacial region thickness (µm) and standard deviations (SD) of Ni-Cr test groups

Recast content of Ni-Cr alloy (%)	0%	25%	50%	75%	100%
Mean thickness (µm)	48.43	50.00	55.6	63.9	85.4
SD (µm)	7.06	8.43	10.38	10.77	9.32

Figure 5-8 shows that, for the first two test groups, both alloys demonstrated very close values of interfacial area thickness. However, Ni-Cr test groups demonstrated a trend of gradual increase in the values, but ending with a sharp increase for NiCr-100 (85 µm), while Co-Cr values fluctuated more.

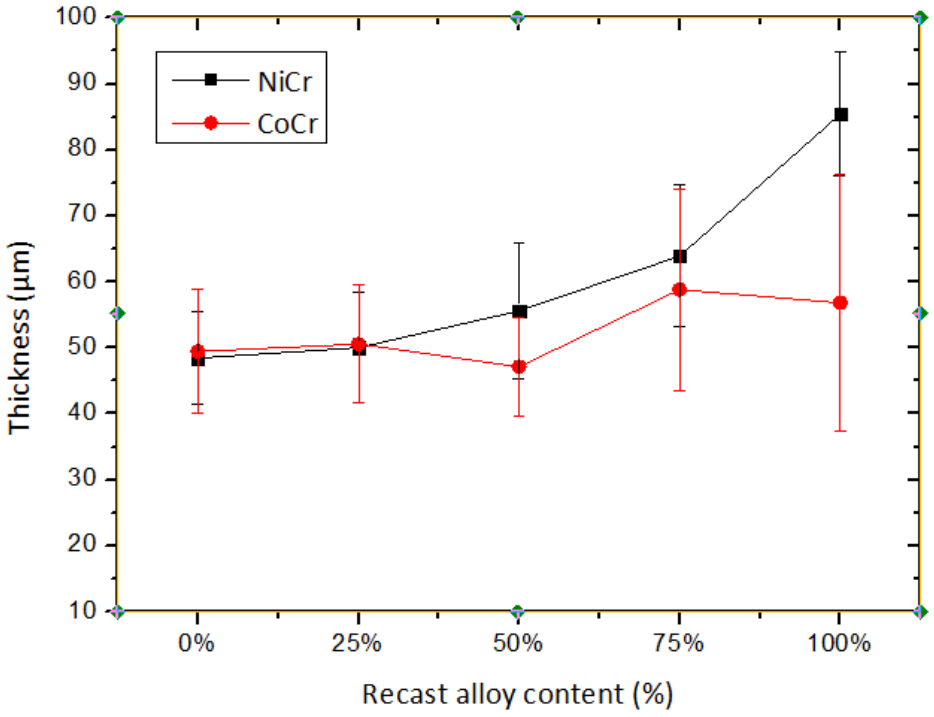

Figure 5-8 Thickness of the interfacial area of the Co-Cr and Ni-Cr test groups

5.4.2.1 Bond strength and interfacial region thickness

Figure 5-9 shows that the first two test groups (CoCr-0 and CoCr-25) demonstrated a balanced relation between bond strength and interfacial area thickness. Opposite relations were demonstrated in the middle region of the graph. For the last two test groups (CoCr-75 and CoCr-100) although the interfacial thickness demonstrated only a slight decrease, the bond strength demonstrated a continuous and significant drop. At 50% recycled alloy content, there was an apparent increase in bond strength coinciding with a reduced interfacial region thickness.

Figure 5-10 shows that the first two test groups (NiCr-0 and NiCr-25%) demonstrated a balanced relation between bond strength and interfacial area thickness. The main feature in Figure 5-10 is at 100% recycled where the large increase in the interfacial area thickness was associated with a significant decrease in bond strength.

Both alloys demonstrated a similar trend for the 0%, 25% and 50% recycled test groups, while the 75% and 100% test groups demonstrated different behaviour (Figure 5-9 and Figure 5-10).

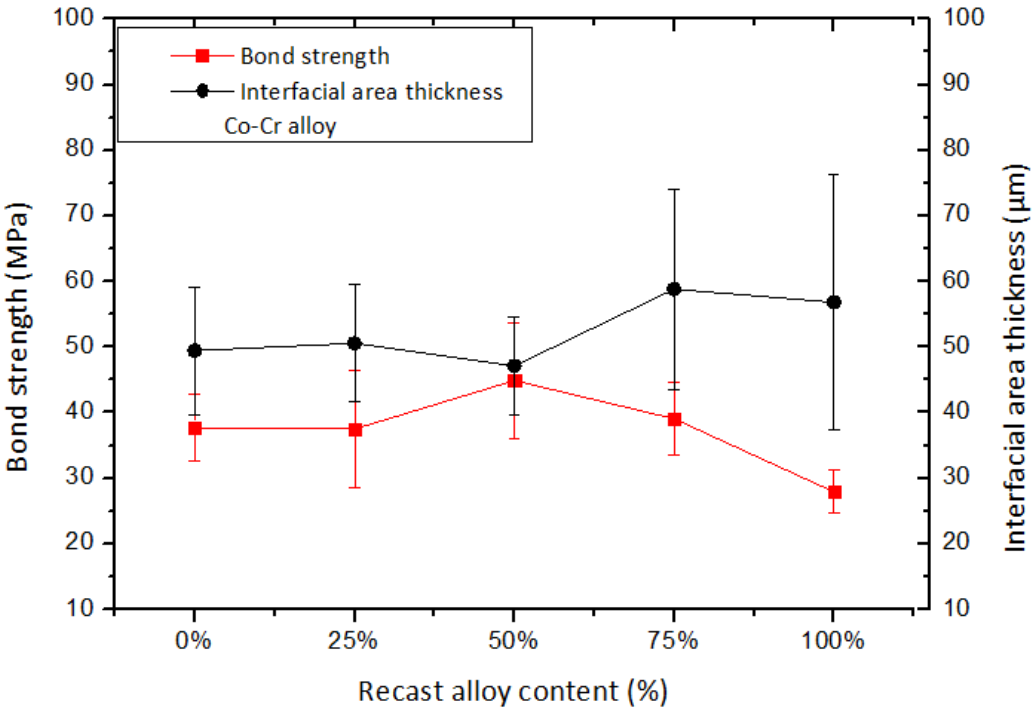

Figure 5-9 Bond strength and interfacial region thickness of Co-Cr test groups

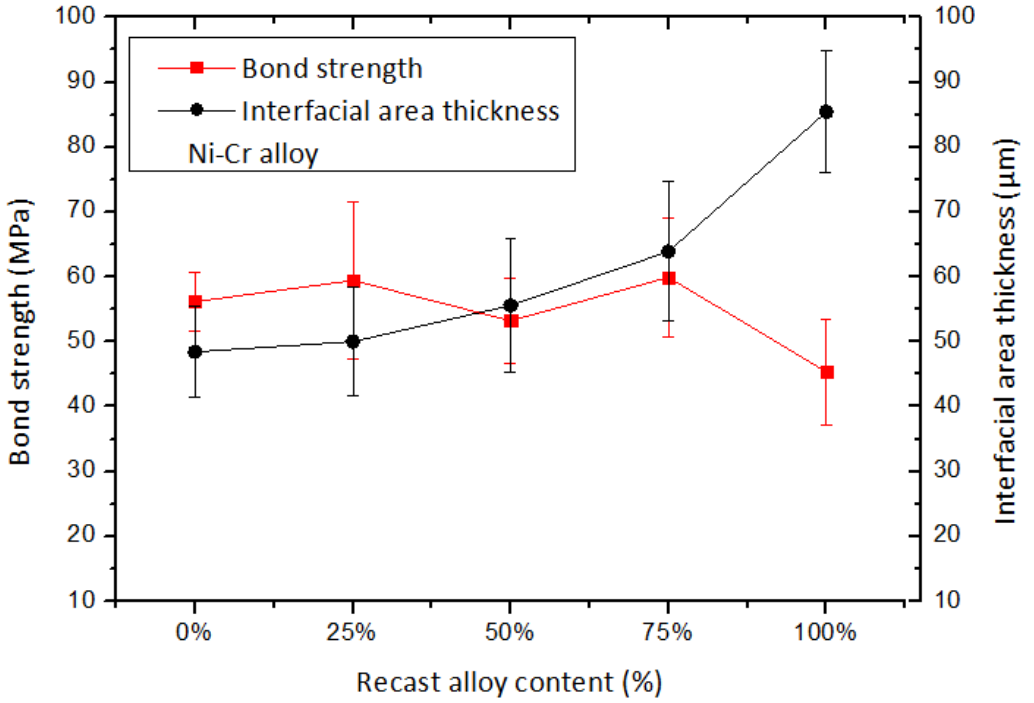

Figure 5-10 Bond strength and interfacial region thickness of Ni-Cr test groups

5.4.3 EDAX assessment of the interfacial region

5.4.3.1 Qualitative assessment

EDAX analyses were conducted on single Co-Cr and Ni-Cr test pieces containing 100% recycled alloy. Mapping of the elements on the surface of metal-ceramic test pieces provided images showing differences in the distribution of elements through the interfacial region. Ceramics and castings show a uniform distribution of the constituent elements. However, the interfacial area shows a heterogeneous distribution of elements (Figure 5-11 and Figure 5-12).

Figure 5-11 shows the high concentration of cobalt and chromium in the Co-Cr alloy. Ceramic was rich with aluminum, sodium, potassium, silicon, and oxygen. The interfacial area contained aluminum, sodium, silicon, oxygen and was rich in zirconium.

Figure 5-12 shows the high concentration of nickel, chromium, molybdenum, and the low concentration of iron in the Ni-Cr alloy. Ceramic was rich in silicon, potassium, sodium, aluminum, tin, and oxygen. The Interfacial region contained silicon, zirconium, potassium, sodium, aluminum, tin and oxygen. Elements present in small amounts were not detected by the X-Ray mapping performed by EDAX.

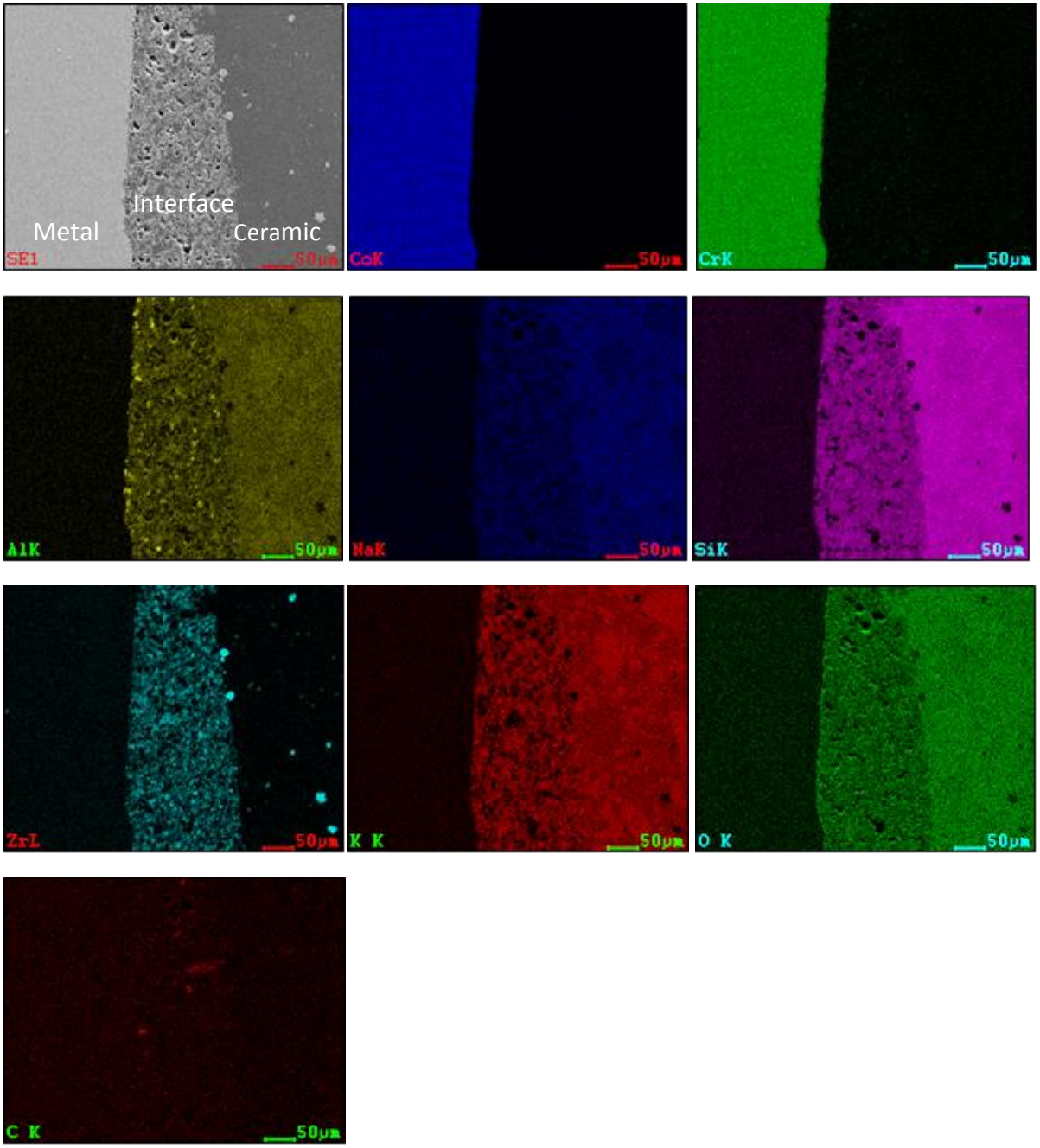

Figure 5-11 Distribution of selected elements through metal-ceramic interface of a Co-Cr test piece.

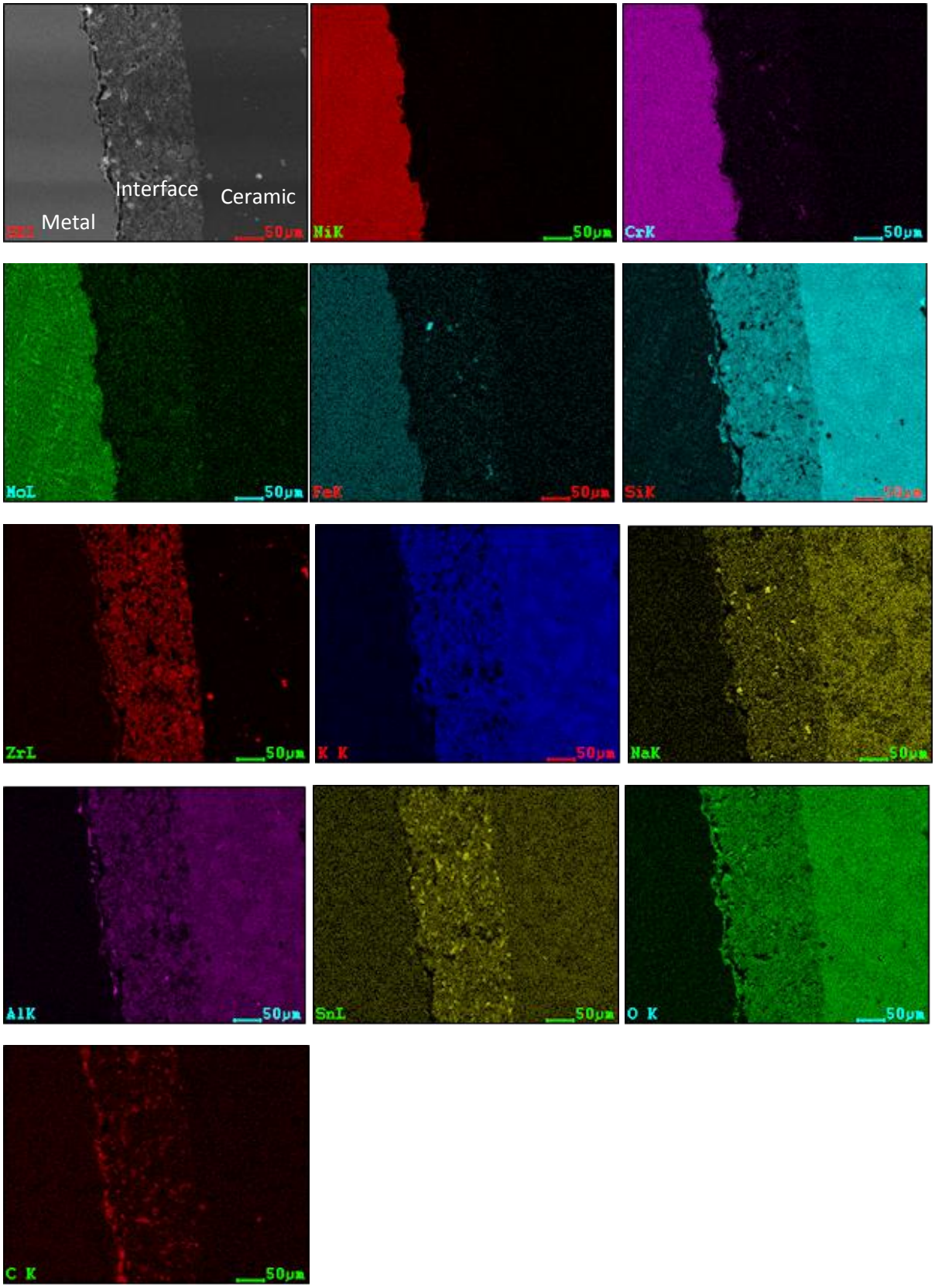

Figure 5-12 Distribution of selected elements through metal-ceramic interface of a Ni-Cr test piece

5.4.3.2 Quantitative assessment

The elemental composition of the ceramic-metal interface region was investigated by using EDAX at five different sites across the ceramic, metal-ceramic interfacial region and the metal (Figure 5-5 A-E). Mean and standard deviation values of the constituent elements (mass%) were reported in Table 5-9 – Table 5-18. Standard deviations are given in brackets (SD).

5.4.3.2.1 Co-Cr alloy

On the ceramic side, trace amounts of Mg and Sb were detected (Table 5-9) whilst within the interfacial region, small amounts of Fe were detected (Table 5-10 and Table 5-11). Although Fe was not detected in the EDAX analysis performed by the researcher, the composition provided by the manufacturer has reported the presence of Fe in a small amount (0-2%) (Table 5-1).

At the interfacial region closer to the ceramic side, a high concentration of Sn was detected, in CoCr-75 and the CoCr-100 test groups, compared to the other test groups (4.98% and 2.42% for CoCr-75 and CoCr-100, respectively) (Table 5-10).

At the interfacial region closer to the metal side, a high concentration of Sn was also detected in CoCr-75 and the CoCr-100 test groups (5.45% and 3.33% for CoCr-75 and CoCr-100, respectively) (Table 5-11). However, according to the ceramic composition provided by the manufacture (Table 5-1), these amounts of Sn are not considered high.

Cr was detected in small amounts (0.15% - 1.34%) on both sides of the interfacial region, closer to the ceramic and closer to the metal (Table 5-10 and Table 5-11).

On the metal side, no traces of elements from ceramic were detected (Table 5-12).

Oxygen amounts have only slightly increased, such as on the ceramic side (37.65 mass% and 38.76 mass% for CoCr-0 and CoCr-100 respectively) (Table 5-9), and at the area closer to the ceramic (35.22% and 34.05% for CoCr-0 and CoCr-100 respectively) (Table 5-10), or decreased, such as in the area closer to the metal (35.61% and 32.69% for CoCr-0 and CoCr-100, respectively) (Table 5-11) and in the area in the middle of the interfacial area (36.39% and 33.23% for CoCr-0 and CoCr-100, respectively) (Table 5-13).

5.4.3.2.2 Ni-Cr alloy

On the ceramic side, trace amounts of Mg, Ce, Ti and Ba were detected (Table 5-14).

At the interfacial area close to the ceramic side and at the middle of the interfacial area, Fe was detected only in the NiCr-100 test group (Table 5-15 and Table 5-18). However, it was detected in all the test groups, except for NiCr-25, in the area closer to the metal side; higher concentrations were recorded in NiCr-75 and NiCr-100 test groups (0.47% and 0.33% respectively) (Table 5-16).

Ba was found in some of NiCr-75 and NiCr-100 test groups. Ni and Cr were detected in the area closer to the ceramic in the NiCr-75 and NiCr-100 test groups only (Table 5-15). In the area closer to the metal, Ni and Cr were detected in all test pieces but; higher amounts were found in the NiCr-75 and NiCr-100 test groups (Table 5-16).

In the area at the middle of the interface, these two elements, Ni and Cr, were detected in the NiCr-75 and NiCr-100 test groups (Table 5-18). On the metal side, no traces of elements from the ceramic were detected (Table 5-17).

Oxygen amounts have increased in all the areas analysed, e.g. in the area closer to the ceramic (28.61% and 33.83% for NiCr-0 and NiCr-100, respectively) (Table 5-15), and in the middle of the interfacial region (26.58% and 32.28% for the NiCr-0 and NiCr-100, respectively) (Table 5-18). However, in the middle of the interfacial area, the highest amount of oxygen was given by NiCr-50 at 34.95% (Table 5-18).

Table 5-9 Elemental mass percentage means and standard deviations (SD) of the Duceram ceramic

Test group	O	Na	Al	Si	K	Ca	Sn	Mg	Sb
CoCr-0	37.65	3.44	8.64	33.85	11.06	0.19	0.00	0.00	0.87
	(1.11)	(1.12)	(0.91)	(1.96)	(2.30)	(0.43)	0.00	0.00	(0.50)
CoCr-25	40.79	3.33	9.53	31.89	10.06	0.43	0.61	0.09	0.44
	(2.42)	(1.41)	(1.57)	(3.97)	(1.60)	(0.60)	(0.36)	(0.20)	(0.82)
CoCr-50	38.86	4.31	8.71	31.47	10.59	0.65	0.00	0.00	0.58
	(0.68)	(0.42)	(0.94)	(3.52)	(0.88)	(1.08)	0.00	0.00	(0.79)
CoCr-75	38.50	3.80	9.57	34.29	11.05	0.00	0.00	0.00	1.11
	(2.41)	(0.61)	(0.62)	(1.83)	(0.96)	0.00	0.00	0.00	(0.88)
CoCr-100	38.76	4.28	9.25	34.95	11.25	0.30	1.37	0.00	0.00
	(0.76)	(0.45)	(0.86)	(1.26)	(0.88)	(0.42)	(0.58)	0.00	0.00

Table 5-10 Elemental mass percentage means, and standard deviations (SD) of the interfacial region (close to ceramic side) of Co-Cr alloy.

Test group	O	Na	Al	Si	Zr	K	Ca	Sn	Fe	Cr	Zn
CoCr-0	35.22	2.35	8.08	22.46	17.05	8.92	0.04	0.80	0.00	0.00	0.00
	(1.84)	(0.97)	(1.46)	(6.05)	(5.25)	(1.86)	(0.09)	(1.45)	0.00	0.00	0.00
CoCr-25	37.63	2.49	7.04	17.50	16.36	8.02	0.00	2.11	1.03	0.00	0.00
	(4.66)	(1.53)	(1.00)	(7.59)	(3.71)	(2.52)	0.00	(0.96)	(1.03)	0.00	0.00
CoCr-50	34.54	2.93	2.93	21.24	22.09	9.65	0.00	1.71	0.00	0.15	0.15
	(1.70)	(0.65)	(0.66)	(1.64)	(3.85)	(1.17)	0.00	(2.46)	0.00	(0.34)	(0.34)
CoCr-75	33.23	2.14	6.94	19.95	21.83	9.57	0.00	4.98	0.58	0.00	0.00
	(1.89)	(0.60)	(1.51)	(1.62)	(4.12)	(2.74)	0.00	(1.99)	(0.81)	0.00	0.00
CoCr-100	34.05	1.84	8.61	18.61	20.81	10.26	0.00	2.42	0.5	0.22	0.94
	(3.50)	(0.95)	(1.73)	(3.38)	(4.62)	(3.35)	0.00	(2.73)	(0.69)	(0.50)	(1.30)

Table 5-11 Elemental mass percentage means, and standards deviations (SD) of the interfacial region (close to metal side) of Co-Cr alloy.

Test group	O	Na	Al	Si	Zr	K	Ca	Sb	Mg	Sn	Fe	Cr	Zn
CoCr-0	35.61	1.81	8.72	18.65	16.01	10.05	0.20	0.00	0.00	0.97	0.54	0.34	0.4
	(5.11)	(0.77)	(2.47)	(5.25)	(3.81)	(4.94)	(0.41)	0.00	0.00	(1.05)	(0.62)	(1.69)	(0.8)
CoCr-25	36.37	2.59	8.98	25.61	11.88	7.82	0.00	0.00	0.00	3.65	0.00	0.77	0.00
	(2.63)	(0.92)	(0.98)	(0.92)	(2.18)	(4.49)	0.00	0.00	0.00	(1.91)	0.00	(0.83)	0.00
CoCr-50	32.8	2.00	6.60	19.0	21.9	2.1	0.00	0.00	2.04	0.00	0.00	0.00	0.00
	(1.16)	(0.58)	(0.85)	(4.14)	(6.74)	(2.04)	0.00	0.00	(3.81)	0.00	0.00	0.00	0.00
CoCr-75	33.01	2.09	7.27	19.10	22.92	9.08	0.00	0.00	0.00	5.45	0.00	0.00	0.00
	(4.65)	(0.34)	(1.43)	(3.04)	(5.38)	(1.89)	0.00	0.00	0.00	(2.74)	0.00	0.00	0.00
CoCr-100	32.69	2.10	7.24	20.21	20.87	9.58	0.00	0.10	0.00	3.34	0.00	0.83	0.00
	(2.91)	(0.59)	(2.08)	(4.77)	(5.95)	(1.70)	0.00	(0.17)	0.00	(2.94)	0.00	(1.16)	0.00

Table 5-12 Elemental mass percentage means, and standard deviations (SD) of the of Co-Cr castings.

Test group	Co	Cr	Mo	Si	Mn	Fe
CoCr-0	40.39	31.09	6.71	1.98	0.55	0.48
	(8.11)	(0.85)	(0.96)	(0.59)	(0.56)	(0.78)
CoCr-25	55.05	33.47	6.80	2.61	0.70	0.14
	(5.82)	(4.68)	(1.80)	(0.39)	(0.26)	(0.21)
CoCr-50	58.39	30.81	3.39	2.07	0.19	0.13
	(2.50)	(4.20)	(3.70)	(0.51)	(0.27)	(0.18)
CoCr-75	58.41	31.15	5.53	2.01	0.25	0.23
	(2.43)	(1.26)	(0.55)	(0.52)	(0.19)	(0.27)
CoCr-100	55.63	30.60	6.77	2.20	0.45	0.64
	(3.32)	(1.16)	(1.29)	(0.75)	(0.41)	(0.68)

Table 5-13 Elemental mass percentage means, and standard deviations (SD) of the interfacial region (in middle of the interfacial area) of Co-Cr alloy

Test group	O	Na	Al	Si	Zr	K	Ca	Sn	Cr	Ba
CoCr-0	36.40	2.01	7.99	17.50	22.59	6.05	0.32	1.19	0.04	0.07
	(4.54)	(0.77)	(2.00)	(3.11)	(4.85)	(2.18)	(0.72)	(2.66)	(0.09)	(0.16)
CoCr-25	38.18	2.27	7.11	21.64	18.972	9.54	0.00	2.28	0.00	0.00
	(3.41)	(0.51)	(2.27)	(4.74)	(6.52)	(1.88)	0.00	(1.85)	0.00	0.00
CoCr-50	33.39	2.091	8.22	21.21	22.048	8.60	0.00	4.01	0.00	0.00
	(2.32)	(0.25)	(0.83)	(3.39)	(3.16)	(2.11)	0.00	(2.29)	0.00	0.00
CoCr-75	35.24	2.47	7.6	20.71	18.61	9.03	0.00	5.01	0.00	0.00
	(2.12)	(0.41)	(2.69)	(3.55)	(3.75)	(1.79)	0.00	(1.52)	0.00	0.00
CoCr-100	33.24	2.33	5.39	17.53	20.39	6.33	0.00	9.73	0.09	0.00
	(3.29)	(0.90)	(2.66)	(3.50)	(5.54)	(2.70)	0.00	(6.25)	(0.14)	0.00

Table 5-14 Elemental mass percentage means, and standard deviations (SD) of the Matchmaker ceramic

Test groups	O	Na	Al	Si	K	Ca	Fe	Zr	Ba	Mg	Ti	B	Ce	Sn
NiCr-0	34.26	3.48	6.92	27.57	9.68	1.34	0.00	2.44	0.00	0.08	0.71	0.00	1.04	2.02
	(2.39)	(0.13)	(0.45)	(2.09)	(1.06)	(0.35)	0.00	(1.99)	0.00	(0.01)	(0.09)	0.00	(0.19)	(1.63)
NiCr-25	32.54	3.57	6.15	27.50	9.56	1.92	0.00	0.00	0.00	0.07	0.52	4.67	1.18	0.73
	(0.36)	(0.16)	(0.68)	(3.22)	(1.82)	(0.50)	0.00	0.00	0.00	(0.05)	(0.29)	(4.09)	(0.27)	(1.12)
NiCr-50	33.53	3.64	6.12	25.68	8.57	1.39	0.00	0.15	0.00	0.05	0.06	0.48	0.06	0.00
	(0.89)	(0.57)	(0.38)	(1.40)	(1.08)	(0.17)	0.00	(0.34)	0.00	(0.08)	(0.14)	(0.29)	(0.14)	0.00
NiCr-75	35.02	3.62	7.81	29.46	8.66	1.31	0.00	0.25	0.03	0.03	0.29	0.00	0.00	0.00
	(0.54)	(0.72)	(1.31)	(1.74)	(1.00)	(0.34)	0.00	(0.36)	(0.06)	(0.04)	(0.27)	0.00	0.00	0.00
NiCr-100	37.02	2.69	6.61	31.34	10.54	0.23	0.03	3.61	0.05	0.00	0.00	0.00	0.00	0.00
	(0.82)	(0.52)	(0.54)	(2.01)	(1.15)	(0.22)	(0.06)	(3.16)	(0.10)	0.00	0.00	0.00	0.00	0.00

Table 5-15 Elemental mass percentage means, and standard deviations (SD) of the interfacial region (close to ceramic side) of Ni-Cr alloy

Test groups	O	Na	Al	Si	K	Ca	Fe	Zr	Ba	Mg	Ti	B	Ce	Sn	Zn	Ni	Cr
NiCr-0	28.62	2.59	4.59	17.05	7.28	1.94	0.00	25.51	0.00	0.06	1.94	0.00	0.18	0.85	0.00	0.00	0.00
	(2.25)	(0.34)	(0.60)	(1.39)	(1.12)	(0.31)	0.00	(5.07)	0.00	(0.06)	(0.31)	0.00	(0.36)	(1.16)	0.00	0.00	0.00
NiCr-25	30.75	3.20	6.57	21.22	8.17	1.85	0.00	15.55	0.00	0.17	2.55	0.28	0.29	0.38	(0.14)	0.00	0.00
	(1.88)	(0.36)	(1.56)	(1.19)	(0.53)	(0.66)	0.00	(6.15)	0.00	(0.18)	(2.51)	(0.39)	(0.26)	(0.53)	0.25	0.00	0.00
NiCr-50	31.12	2.87	4.75	16.29	6.1	1.06	0.00	27.6	0.00	0.06	1.116	0.00	0.34	0.00	0.00	0.00	0.00
	(4.13)	(0.66)	(1.60)	(6.15)	(1.69)	(1.04)	0.00	(12.77)	0.00	(0.06)	(0.80)	0.00	(0.36)	0.00	0.00	0.00	0.00
NiCr-75	29.65	2.68	4.49	15.78	3.99	1.82	0.00	25.73	0.00	0.14	1.39	0.00	0.00	0.00	0.00	0.17	0.10
	(2.19)	(0.39)	(0.61)	(2.64)	(2.12)	(0.86)	0.00	(7.20)	0.00	(0.12)	(0.98)	0.00	0.00	0.00	0.00	(0.12)	(0.21)
NiCr-100	33.83	1.74	4.77	20.53	7.74	0.67	(0.08)	22.41	0.08	0.03	0.00	0.00	0.00	0.00	0.00	0.06	0.00
	(1.55)	(0.28)	(0.71)	(0.49)	(0.48)	(0.63)	0.12	(2.20)	(0.17)	(0.08)	0.00	0.00	0.00	0.00	0.00	(0.13)	0.00

Table 5-16 Elemental mass percentage means, and standard deviations (SD) of the interfacial region (close to metal casting) of Ni-Cr alloy.

Test groups	O	Na	Al	Si	K	Ca	Fe	Zr	Ba	Mg	Ti	B	Ce	Sn	Ni	Cr
NiCr-0	29.10	2.52	5.97	20.55	9.56	1.266	0.096	15.52	0.00	0.18	2.21	0.00	0.24	0.00	0.32	0.09
	(1.10)	(0.22)	(0.12)	(2.25)	(1.56)	(0.46)	(0.19)	(1.39)	0.00	(0.09)	(1.60)	0.00	(0.30)	0.00	(0.34)	(0.18)
NiCr-25	29.78	3.20	5.37	21.14	6.25	1.25	0.00	20.05	0.00	0.09	1.52	0.00	0.00	0.22	1.20	0.69
	(0.74)	(0.46)	(0.64)	(3.31)	(2.31)	(0.25)	0.00	(2.34)	0.00	(0.07)	(0.51)	0.00	0.00	(0.45)	(0.47)	(0.36)
NiCr-50	29.82	2.25	6.30	17.55	4.21	1.30	0.05	19.17	0.00	0.096	1.52	2.24	0.09	0.00	0.40	0.414
	(3.36)	(0.63)	(1.70)	(2.81)	(2.58)	(0.77)	(0.12)	(7.04)	0.00	(0.11)	(0.32)	(5.01)	(0.18)	0.00	(0.26)	(0.34)
NiCr-75	27.67	2.58	5.87	16.62	5.22	1.50	0.47	18.62	0.00	0.07	1.7	0.00	0.43	0.00	3.80	3.85
	(3.08)	(0.85)	(1.34)	(2.77)	(1.59)	(0.58)	(0.28)	(5.57)	0.00	(0.07)	(0.96)	0.00	(0.75)	0.00	(2.01)	(2.36)
NiCr-100	30.94	1.54	4.85	17.28	6.02	0.48	0.33	22.43	0.08	0.00	0.00	0.00	0.00	0.00	2.46	1.86
	(1.56)	(0.30)	(0.97)	(2.03)	(0.79)	(0.45)	(0.25)	(4.50)	(0.17)	0.00	0.00	0.00	0.00	0.00	(2.34)	(1.59)

Table 5-17 Elemental mass percentage means, and standard deviations (SD) of the of Ni-Cr castings.

Test groups	O	Ni	Cr	Mo	Si	Nb	Al	Fe	Mn	Ta
NiCr-0	0.00	60.12	18.44	7.33	1.40	1.44	0.34	3.31	0.00	0.00
	0.00	(3.55)	(0.98)	(1.34)	(0.20)	(1.80)	(0.07)	(0.31)	0.00	0.00
NiCr-25	0.00	58.63	18.78	8.02	1.62	1.44	0.00	3.49	0.122	0.79
	0.00	(2.77)	(0.37)	(0.86)	(0.45)	(1.21)	0.00	(0.34)	(0.12)	(0.34)
NiCr-50	0.38	54.51	19.28	7.56	1.48	2.81	0.00	3.41	0.21	0.63
	(0.24)	(2.39)	(0.75)	(4.02)	(0.28)	(0.20)	0.00	(0.21)	(0.13)	(0.46)
NiCr-75	0.20	53.93	18.87	8.82	1.12	2.29	0.00	3.40	0.20	0.49
	(0.19)	(2.90)	(0.48)	(0.96)	(0.45)	(1.57)	0.00	(0.25)	(0.04)	(0.67)
NiCr-100	0.14	57.22	20.31	8.60	1.54	1.39	0.00	3.74	0.22	0.57
	(0.19)	(1.36)	(1.15)	(0.94)	(0.33)	(1.32)	0.00	(0.10)	(0.02)	(0.53)

Table 5-18 Elemental mass percentage means, standard deviations (SD) of the interfacial region (in the middle of the interfacial area) of Ni-Cr alloy

Test group	O	Na	Al	Si	K	Ca	Fe	Zr	Mg	Ti	Ce	Sn	Zn	Ni	Cr
NiCr-0	26.58	2.74	4.33	16.62	8.95	0.94	0.00	21.52	0.06	2.61	0.24	9.41	0.00	0.00	0.00
	(1.99)	(0.34)	(0.69)	(2.18)	(3.68)	(0.54)	0.00	(7.39)	(0.05)	(0.73)	(0.20)	(4.92)	0.00	0.00	0.00
NiCr-25	30.25	2.49	0.11	5.93	18.45	7.58	0.00	20.74	0.11	2.21	0.00	0.00	0.21	0.00	0.13
	(1.56)	(0.39)	(0.06)	(0.27)	(0.71)	(0.53)	0.00	(3.37)	(0.06)	(0.69)	0.00	0.00	(0.22)	0.00	(0.18)
NiCr-50	34.95	2.47	5.47	16.82	2.54	1.69	0.00	22.82	0.12	0.59	0.34	0.00	0.00	0.00	0.06
	(4.33)	(0.38)	(0.86)	(1.38)	(1.99)	(0.40)	0.00	(1.36)	(0.17)	(0.80)	(0.76)	0.00	0.00	0.00	(0.09)
NiCr-75	29.73	2.57	5.04	15.84	6.11	1.40	0.00	24.62	0.15	2.45	0.00	0.00	0.00	0.11	0.06
	(0.79)	(0.30)	(0.54)	(0.26)	(0.34)	(0.20)	0.00	(3.72)	(0.04)	(1.90)	0.00	0.00	0.00	(0.16)	(0.14)
NiCr-100	32.28	1.94	4.80	18.68	6.07	0.96	0.28	24.90	0.00	0.00	0.16	0.00	0.63	0.21	0.36
	(2.22)	(0.52)	(0.29)	(0.66)	(0.81)	(0.17)	(0.30)	(4.41)	0.00	0.00	(0.12)	0.00	(0.58)	(0.02)	(0.25)

5.4.4 Quality of the metal-ceramic interface

The interface of test pieces made out of new alloys had a relatively even thickness compared to those made from recycled alloys (Figure 5-13 A-C). SD= 9.38µm and 19.48 µm for CoCr-0 and CoCr-100 respectively (Table 5-7). SD= 7.06µm and 9.32 µm for NiCr-0 and NiCr-100 respectively (Table 5-8). In addition, test pieces made out of recycled alloys demonstrated an extensive presence of voids through the interface (Figure 5-14 A and B).

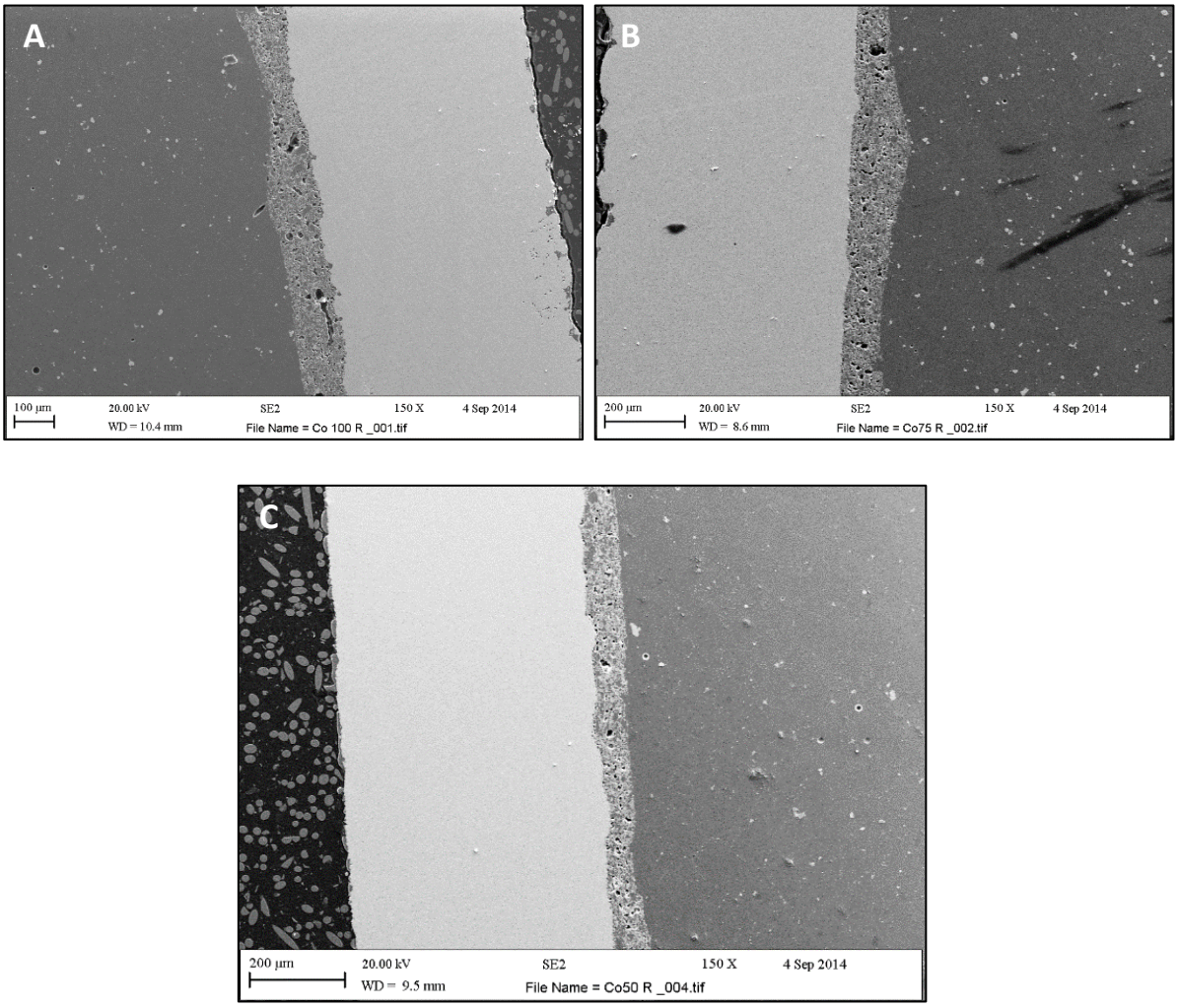

Figure 5-13 Interfacial area of CoCr-100 (A), and CoCr-75 (B), interfacial area of CoCr-50 (C).

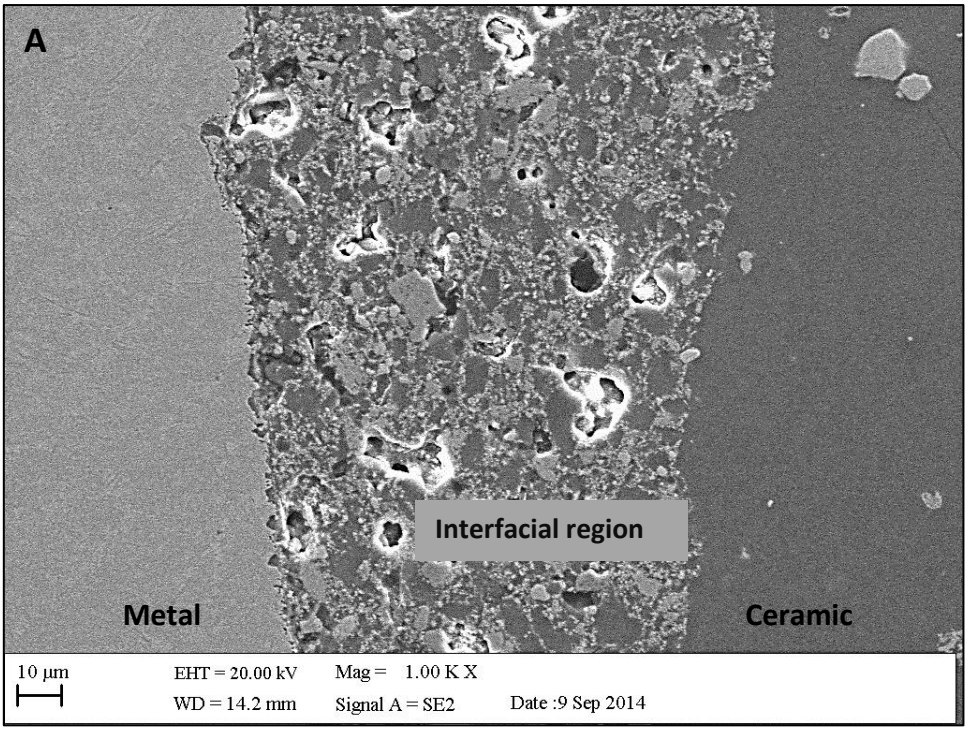

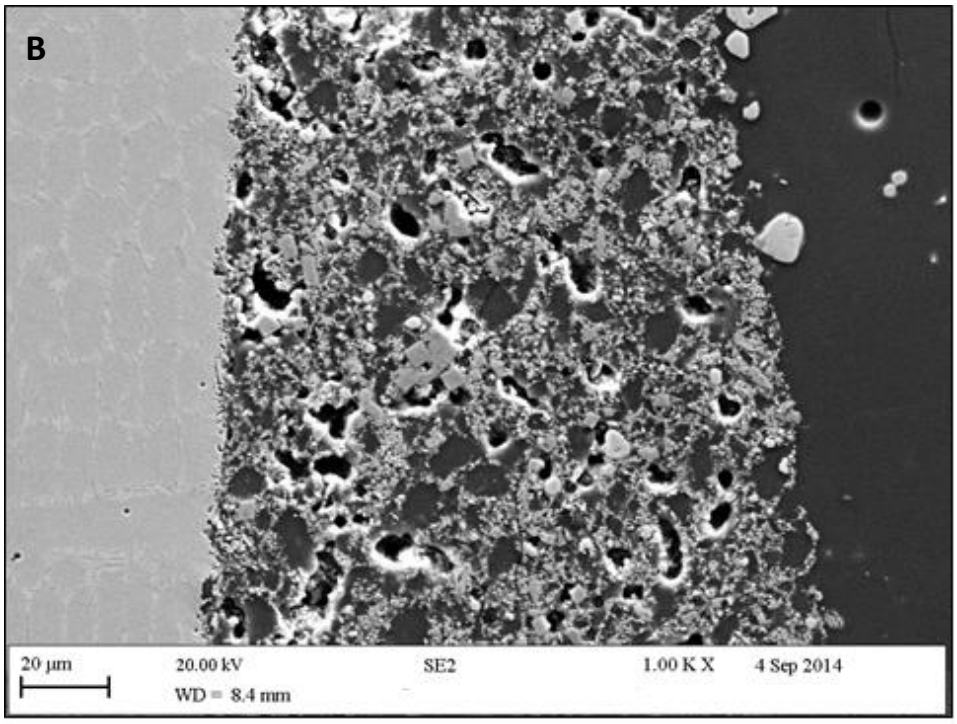

Figure 5-14 Voids in the interfacial region of CoCr-0 (A), CoCr-100 test piece (B)

5.4.5 Type of metal-ceramic bond failure

Following the three points bending test, two test pieces from each test group were selected for examination of the ceramic-metal interface under SEM, fracture lines were located more often between the ceramic and metal for all the groups (Figure 5-15).

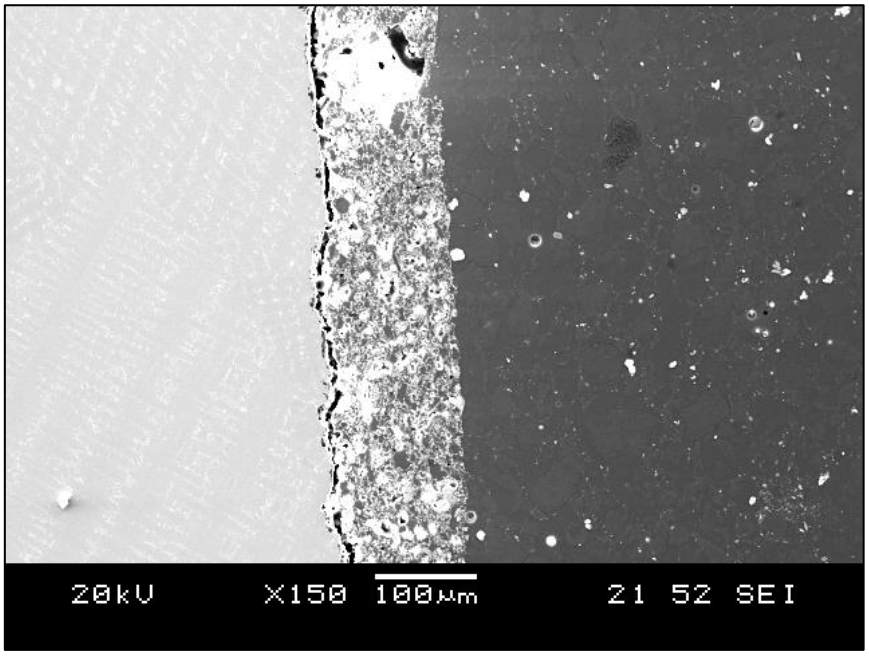

Figure 5-15 Scanning electronic micrograph of a debonded ceramic in a metal-ceramic test piece.

5.4.5.1 EDAX analysis of the fracture surface

Representative SEM micrographs of the fracture surface of CoCr-100 and NiCr-100 test pieces and EDAX analyses indicated a cohesive fracture within the ceramic, where some ceramic was adhering to the casting surface (Figure 5-16).

For CoCr test piece, EDAX analysis revealed the presence of Co (33.32 mass%), Cr (21.56 mass%), Si (11.57 mass%), Al (05.98 mass%), Zr (10.20 mass%), O (16.04 mass%) and C (01.34 mass%) (Figure 5-16 A and B).

For Ni-Cr test piece, EDAX analysis revealed the presence of Ni (5.57 mass%), Cr (32.14 mass %), Al (7.57%), Zr (13.08 mass%), Si (16.84 mass%) and O (24.81 mass%) (Figure 5-16 C and D).

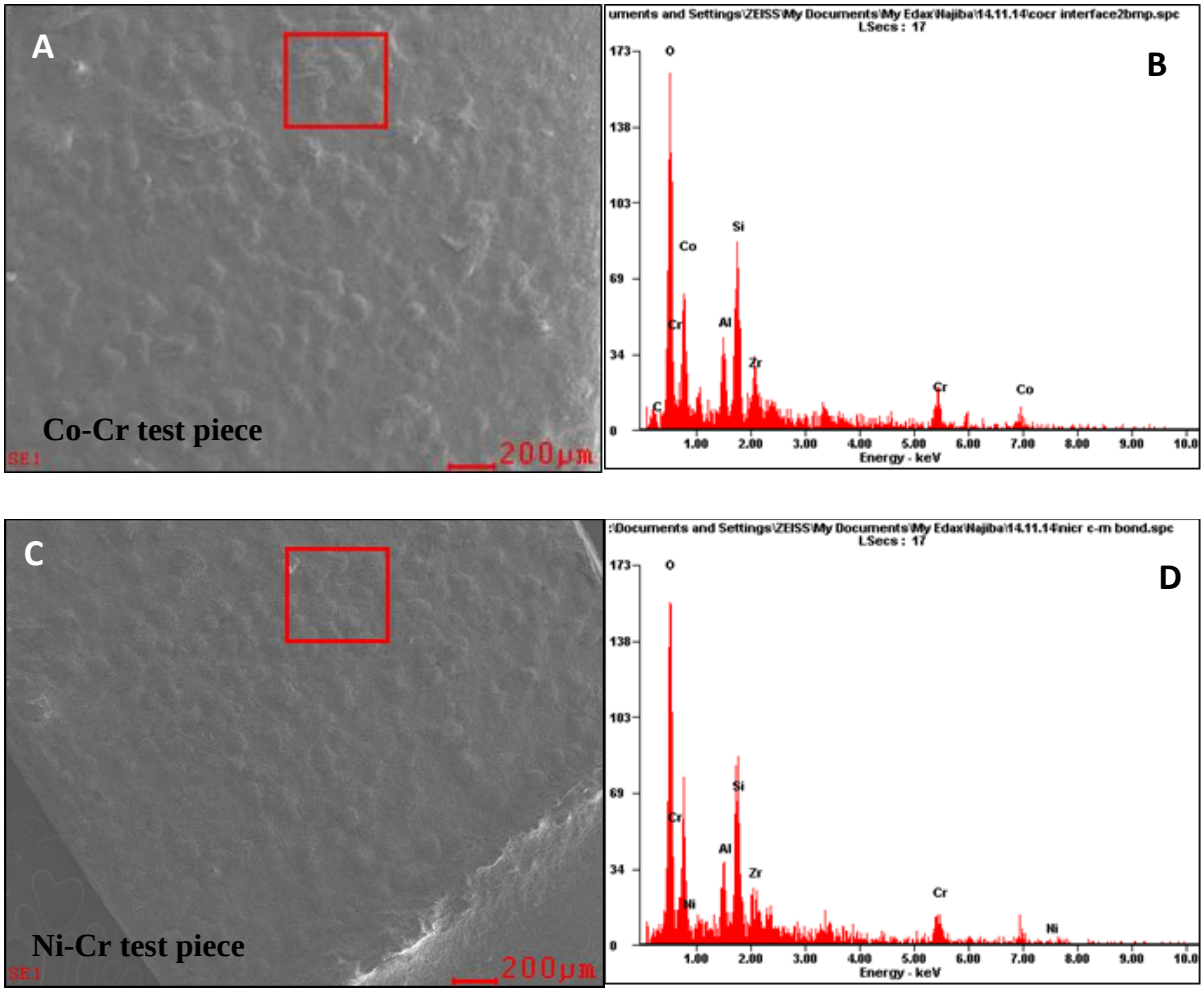

Figure 5-16 Scanning electron micrograph (A, C) and Energy-dispersive X-Ray Spectroscopy analyses (B, D) of the fracture surface of CoCr-100 and NiCr-100 test pieces. Squares indicate the area used for EDAX analyses.

5.5 Discussion

5.5.1 Correlation between metal-ceramic bond strength, surface roughness and porosity occurrence

5.5.1.1 Co-Cr alloy

Castings containing 100% recycled alloy demonstrated low metal-ceramic bond strength (27.90 MPa) compared to the other test groups (Table 5-5), and high interfacial region thickness value (56.8 µm) compared to the first three test groups (CoCr-0, CoCr-25 and CoCr-50), but very close to the value documented by CoCr-75 (58.8 µm) (Table 5-7).

The increase in the interfacial region thickness has not always resulted in a decrease in the metal-ceramic bond strength. For example, the test group containing 75% recycled alloy demonstrated high interfacial region thickness value (58.8 µm) compared to CoCr-0, CoCr-25 and CoCr-50 test groups, however, the metal-ceramic bond strength value was high (39.05 MPa) and close to the value demonstrated by castings produced from new alloy (37.71 MPa) (Table 5-5).

Surface roughness values (Ra) of CoCr-100 (1.13 µm) (Table 4-2) is not expected to contribute to the reduction in metal-ceramic bond strength value. No significant differences were documented between surface roughness values documented by the different test groups (p= 0.982) (Appendix 1, Table 1-18).

The decrease in metal-ceramic bond strength in casting produced from recycled alloy (100% recycled) can be related to the porosity values demonstrated by the CoCr-CB-100 castings (0.27%), which is significantly higher than all the mean porosity values demonstrated by the other test groups (p= 0.00) (Table 3-4) (Appendix 1, Table 1.6).

Mean % area of porosity values documented by CoCr-75 (0.08%) was not significantly different from those documented by CoCr-0 (0.06%) (Table 3-4) (Appendix 1, Table 1-6). However, it was significantly different from the value documented by CoCr-100 (0.27%). This observation suggests an effect of porosity occurrence on metal-ceramic bond strength.

CoCr-50% demonstrated the thinnest interfacial region (47.10 µm) (Table 5-7) and the highest metal-ceramic bond strength (44.87 MPa) (Table 5-5). Surface roughness of this test group was not significantly different from the other test groups. Mean % area of porosity value documented by this test group (0.11%) was less and significantly different from CoCr-100.

5.5.1.2 Ni-Cr alloy

Castings containing 100% recycled alloy gave the lowest metal-ceramic bond strength (45.34 MPa) compared to the other test groups (Table5.6), and the largest interfacial region thickness (85.4 µm) (Table 5-8). However, for the castings containing 75% recycled alloys although there was an increase in the interfacial region thickness (from 48.43 µm for NiCr-0 to 63.9 µm for NiCr-75), this test group gave a mean metal-ceramic bond strength (59.91 MPa) comparable to that of NiCr-0 (56.17 MPa).

Surface roughness values (Ra) of NiCr-100 (1.22 µm) (Table 4-3) can not account for the reduction in metal-ceramic bond strength. The recycled content of alloy (mass%) had no significant effect on surface roughness values after sandblasting and before polishing (p= 0.998) (Appendix 1, Table 1-19).

The decrease in metal-ceramic bond strength using fully recycled alloy does coincide with the highest observed mean % porosity value (0.06%), which is significantly higher than the mean % porosity values demonstrated by NiCr-CB-0 (0.01%) and NiCr-CB-25 (0.02%) (p= 0.00) (Table 3-4) (Appendix 1, Table 1-8). This observation suggests an effect of porosity occurrence on metal-ceramic bond strength.

Porosity value documented by NiCr-CB-75 (0.04%) was not significantly different from the value documented by NiC-CB-0 (0.01%). This observation demonstrates the effect of porosity occurrence on metal-ceramic bond strength and the importance of adding small amount of new alloy to enhance restoration properties.

No study was found in the literature investigating the correlation between metal-ceramic bond strength and factors evaluated in this study.

5.5.2 Discussion and interpretation of results documented in this study

The lowest average metal-ceramic bond strength for Co-Cr and Ni-Cr alloys occurred with 100% recycled material. Highest mean % area of porosity also resulted in casting containing 100% recycled alloys.

An explanation of the reduction in metal-ceramic bond strength of CoCr-100 and NiCr-100 could be the porosity occurrence. Depending on the shape of pores, porosity can increase the surface area available for bonding with ceramic. However, it can create stress concentration areas and trap gases and organic contaminants. In turn, this affects the ceramic's wettability by reducing its ability to flow into the valleys and crevices. Intimate contact is essential for good adhesion to occur, and inadequate wettability is associated with premature failure at the ceramic-metal interface. Hence, interfacial flaws must be minimised to allow adequate wetting [37]. The size of contact angle, which is the angle between the interface and the horizontal plane at the edge of ceramic, is critical for successful ceramic-metal bond [190].

Another factor in the decrease in metal-ceramic bond strength of CoCr-100 and NiCr-100 could be the presence of defects on the metal surface [210]. In this study, the metal-ceramic interfaces demonstrated the presence of this form of porosity (Figure 3-12 A and B); the resulting stress concentration areas are highly vulnerable regions of failure, they decrease fracture resistance of ceramics and lower adhesive material's strength. In addition, for CoCr-100, the interface of test pieces made out of recycled alloys had relatively un-even thickness compared with those made from new alloys, SD=9.38 µm and 19.48 µm for CoCr-0 and CoCr-100, respectively (Figure 5-13).

On more explanation could be the strength of ceramic. Air bubbles and contaminants can be trapped into the scratches on the casting surface, during ceramic firing cycles, air bubbles and contaminants might emerge from the casting surface to the ceramic and within the interfacial region causing the occurrence of porosity within the interfacial region, resulting

in the reduction in ceramic strength [37] and the occurrence of fracture within the ceramic [209,211]. This explanation is supported by the observations documented in this study; representative SEM micrographs of the fracture surface of CoCr-100 test pieces exhibited a cohesive fracture within the ceramic where some ceramic was adhering to the casting surface (Figure 5-14 B and Figure 5-16).

Segregrants and contaminants often weaken the interface region [212]. They affect the distribution of elements through the bulk and surface of casting and in turn, this affects the amount and types of oxides formed on the casting surface. In this study, changes in the chemical composition of castings produced from recast alloys (Table 3-6 and Table 3-7) and the presence of heterogeneous structure are reported (Figure 3-2 A & B).

The reason for contamination can be that the production of these castings containing high amount of recycled alloy involves further treatments, such as cleaning the thick oxide layer formed on the cast surplus alloy and cutting them into adequate sizes and weights.

5.5.3 Oxygen amount and interfacial region thickness

Oxygen concentration measurements were taken to identify the relationship between oxygen concentration and metal-ceramic interfacial thickness. Thickness of the metal-ceramic interfacial region is related to the amount and diffusion rate of oxidized elements [213].

In the current study, for Co-Cr, oxygen amounts in the interfacial region have only slightly changed (Tables 5-10, Table 5-11 and Table 5-13). However, it could be the type of oxides rather the amount of them which affect the metal-ceramic bond strength. Desirable oxides which form a stable bond with ceramic are not only on the surface of the metal, but may be traced to a particular depth in the casting [214]. However, type of oxides formed in the interfacial region was not investigated in this study.

For Ni-Cr test groups, oxygen amounts have increased, interfacial region of NiCr-100 test groups demonstrated higher amounts of oxides (mass%) than other test groups (in the area closer to the ceramic side and in the area closer to the metal side) (Table 5-15 and Table 5-16), this test group demonstrated the highest interfacial region thickness value (85.4 µm) (Table 5-8).

In base metal dental alloys, most of the elements are able to exist in an oxide form. Excessive formations of oxide and the related increased thickness of interfacial layer expose the ceramic metal bond to failure due to the fracture that might happen through the weak interfacial oxide region. In the alloys used in this study, manganese and silicon were added to the Co-Cr alloy by the manufacturer and detected by EDAX analyses of alloy ingots (Table 3-1) and EDAX analyses of metal side of the ceramic bonded test pieces (Table 5-12). Manganese, silicon and aluminium were included in the Ni-Cr alloy and detected by EDAX analyses of alloy ingots (Table 3-2) and EDAX analyses of metal side of the ceramic bonded test pieces (Table 5-17). These element inhibit excessive formation of other oxides, such as NiO and Cr_2O_3 [206,207]. For Ni-Cr alloy, Al was only detected in the NiCr-0 test group (Table 5-17); this might explain that this test group demonstrated the lowest interfacial region value (48.43 μm).

In the current study, small amounts of Ni and Cr were detected in the interfacial regions of casting containing 75% and 100% recycled alloys. (Table 5-15, Table 5-16 and Table 5-18). For example, CoCr-100 contained amounts of 0.22% Cr (Table 5-10), 0.83% Cr (Table 5-11) and 0.09% Cr (Table 5-13). NiCr-100 contained amounts of 1.86% Cr (Table 5-16) and 0.36% Cr (Table 5.18). The oxide products of chromium, such as Cr_2O_3 can change the CTE of ceramic and so induce internal stresses which can decrease the metal-ceramic bond strength [213]. This may explain the low metal-ceramic bond strength exhibited by CoCr-100 (27 MPa). However, NiCr-75% exhibited high bond strength mean value (59.91 MPa) despite the presence of these elements in the interfacial region.

In the current study, no definitive trend in the relation between interfacial region thickness and metal-ceramic bond strength was observed. However, amongst all the test groups, castings containing 50% recycled alloy demonstrated the lowest interfacial region thickness value (47.10 μm) (Table 5-7) and the highest metal-ceramic bond strength value (44.87 MPa) (Table 5-7). In addition, castings produced from CoCr new alloy and those containing 25% recycled alloy demonstrated close interfacial region thickness values (49.44 μm and 50.56 μm respectively) and similar metal-ceramic bond strength values (37.71 MPa and 37.50 MPa respectively).

5.5.4 Other factors affecting metal-ceramic bond strength

The 100% recycled Co-Cr alloy gave the lowest observed metal-ceramic bond strength values. Factors other than interfacial region thickness and castings surface roughness might have contributed to the lowest metal-ceramic bond strength value obtained for the CoCr-100 test group. The changes in the CTE of metal or ceramic or both materials might have contributed to the results documented. For example, if CTE of ceramic is higher than metal, ceramic will contract more than metal, metal will resist ceramic contraction, and so the ceramic will be under surface tensile stresses which will cause the formation of surface cracks [37]. Similar to decreased mismatch of CTE, increased mismatch (more than $0.5x10^{-6}$ /◦C) can equally have an adverse effect on bond strength. When dental ceramic cools down, the leucite crystals contract more than the glass matrix surrounding them, this leads to the formation of compressive stresses around the crystals, the increase in these stresses results in the formation of micro-cracks within and around the leucite. However, this variable (CTE) was not investigated in this study.

Recycling alloys can affect its modulus of elasticity; porosity occurrence changes alloy density and the presence of contaminants and the formation of new phases affect mechanical properties including modulus of elasticity [215]. In his study, Kumar [215] indicated that precipitation of intermetallic phases leads to an increase in modulus of nickel base alloys. This in turn increases the strain forces on the interface and cause bond failure, not because of a weak bond but because of excessive stresses on the interface. However, modulus of elasticity of alloys was not investigated in this study.

Although these variables, CTE and modulus of elasticity, were not tested, the production of test pieces was performed in such a way that these factors would not be changed negatively. For example, recommendations from manufacturers, in terms of casting temperatures and ceramic firing cycles, were followed. The casting process was performed in a controlled environment and test pieces were not submitted to repeated ceramic firing cycles.

5.5.5 Previous studies on interfacial region thickness

Mirković [216], evaluated the thickness of the interfacial region of Co-Cr and Ni-Cr alloys and documented values of 56.67 µm and 53.33 µm, respectively. In the current study, Co-Cr and Ni-Cr casting containing 50% recycled alloys gave mean values of 47.10 µm and 55.60 µm, respectively. The method used to measure the interfacial region thickness was similar to the method used in this study (SEM together with PC Software for quantification of visual information). It was documented that recasting the alloys (castings contained 50% new alloy and were melted repeatedly, up to twelve times) resulted in a reduction in the interfacial region thickness. However, the effect of this reduction on metal-ceramic bond strength was not investigated. And with the absence of a threshold value of the interfacial region thickness the conclusion driven by this study is not considered accurate.

Rokni [79] evaluated the effect of oxidation technique and ceramic firing cycles on the thickness of interfacial region and investigated the relationship between oxide layer thickness and metal-ceramic bond strength of Ni-Cr alloys. The interfacial area thickness was 73 µm for castings exposed to oxidation under vacuum and sandblasted, thicknesses of more than 85 µm resulted in a reduction in bond strength. In the current study, Ni-Cr castings produced from new alloys gave a mean interfacial thickness value of 48.43 µm (Table 5-8). Similar to the observation made by Rokni, interfacial thickness value of 85.4 resulted in a reduction on metal-ceramic bond strength (45.53 MPa) (Table 5-6). Howver in Rokni study, bond strength of metal to ceramic was measured by the three point bend test in a universal testing machine. However test pieces dimensions were not prepared according to the ISO standards. In addition, it has been reported that thickness of interfacial region was measured by SEM, the method used for measuring the thickness was not clearly described and the calculations used to introduce the final mean value was not presented.

Unlike bond strength, no threshold value or range for interface area thickness is required by standards organisations (ISO). ISO 9693: 2000 sets the minimum metal-ceramic bond strength as 25 MPa

In this study, there was a variation in metal-ceramic bond strength. However, all values reported for all test groups, even those made from recycled alloys, were higher than the

threshold value recommended by ISO 9693 (2000) [200] and ANSI/ADA specifications No. 38 [217].

5.5.6 Previous studies on metal-ceramic bond strength

Nieva [218], investigated the effect of sandblasting on the metal-ceramic bond strength of Co-Cr alloy. Metal-ceramic bond strength was 57.15 ± 10.42 MPa, this value is higher than the values documented in this study (37.71 MPa for CoCr-0 test group) (Table 5-5). However, in Nieva's study, ingots of the Co-Cr material were melted and cast (shape and dimensions of castings were not provided), they were then machined to the required shape and size recommended by ISO 9693 using a surface grinder machine. In addition, prior to sandblasting, metal substrates were ground and polished up to 1 micron diamond paste. Machining the castings and polish it before applying sandblasting are unnecessary practices and do not come in accordance with ISO 9693 recommendation and can affect the surface roughness and chemical composition of casting, and hence metal-ceramic bond strength.

In the curent study, casting were sandblasted prior to ceramic application. It has been documented in the literature [219] that sandblasting increases the total surface area of a metallic substrate by up to 6.5 times, and hence increases the area available for bonding, and increases the ceramic-metal bond strength of dental alloys [220]. It has been documented that sandblasted castings demonstrate higher bonding values compared to non-sandblasted ones [218]. In addition Al_2O_3 is a component in dental ceramics, the presence of Al on the casting surface might increase the ceramic adherence to casting surface [74]. This might explain that all test groups demonstrated metal-ceramic bond strength more than the threshold value of 25 MPa.

However, some researchers consider the presence of Al_2O_3 particles as contamination. Grooves formed by air abrasion by Al_2O_3 create tensile stresses at the adjacent surface layers of the material, these stresses will be released on exposure to further thermal treatments [221].

Schweitzer [195], evaluated the effect of using different ceramic types, feldspathic porcelain and pressed ceramic, on the metal-ceramic bond strength of Ni-Cr alloys. Both types of ceramics gave comparable mean metal-ceramic bond strength values at 30.98 MPa -31.81

MPa. This value is lower than the value documented in this study (37.71 MPa for NiCr-0). However, sample size in Schweitzer's study was only 10 for each test group. In the current study, as recommended by ISO 9693, sample size was 20 for each test group (new to recycled content of alloy).

Ucar et al [104], investigated the metal-ceramic bond strength of Ni-Cr alloy, and documented a value of 39.8 MPa for castings containing 100% new alloy; for castings containing 100% recycled alloy, the value was 24.4 MPa. These values are far below the values documented in this study (56.17 MPa) (Table 5-6). However, in Ucar's study, test groups were prepared by mixing 50% new alloy to alloy remnants from previous castings, it was not mentioned how many times the alloy remnants were reused. In addition, prior to the 3-point bend test, test pieces were thermal cycled between 5 ˚C and 55 ˚C for 10.000 cycles. This might explain the low values reported by Ucar.

Madani [206], determined the effect of recasting Ni-Cr alloy on metal-ceramic bond strength and documented that adding up to 50% of recast alloy is acceptable. The highest bond strength reported in Madani's study was for castings produced from new alloy (30.75 MPa), the lowest mean value was given by castings containing 75% recycled alloy (21.72 MPa). In the current study, the highest metal-ceramic bond strength was for NiCr-75% test group (59.51 MPa). Madani used Ni-Cr-Be alloys, the Ni-Cr alloy used in the current study does not contain Be, this element acts as an oxide formation inhibitors. This difference between the two types of alloys might affect the amount and type of oxides forming in the interface region and hence, the thickness of interfacial region and the metal- ceramic bond strength.

6 Biomaterials

6.1 Literature review

Biomaterials are in long and intimate contact with living tissues. In dentistry, the primary use of biomaterials was tooth fillings. These have developed over a long period of time in wider applications, such as joint replacements, cardiovascular repairs and dental implants. The requirements of biomaterial are quite arduous, for the material to repair or replace a tissue or an organ; it has to have specific mechanical, physical and chemical properties. The primary requirement is biocompatibility with surrounding tissues, which means that the material is not expected to cause undesirable local or systemic effects, while performing its required function [222]. Dentistry has extensively used biomaterials and largely promoted their development. The main materials used are alloys, ceramics, polymers and composites. Amalgam was the first material to be used, from the 1860s, as cavity filler. Resin-based materials have also been applied, and have undergone continuous development since their first use in the 1960s [10].

6.1.1 Dental alloys

Metals are essential for biological functions and processes. While some of them, such as iron is essential in high concentrations 8.4-14.8 mg a day, others such as nickel, cobalt, chromium and molybdenum are only needed in trace amounts, where higher concentrations can be toxic. Cobalt is essential to form vitamin B12. However, some metals such as mercury, cadmium, lead and uranium are considered toxic even at very low levels, as they have no biological functions [223] . More than 35 metal elements are used in dental cast alloys. Certain elements of casting alloys are considered to cause adverse reactions [224]. Animal studies have demonstrated that cadmium, cobalt, chromium, and nickel are potent inducers of carcinomas and sarcomas in experimental animals administrated a particular compounds [225,226].

Dental alloys contain elements that can cause allergic reactions to some patients and technicians. Although metallic materials are widely used in dental restorations, the release of toxic metallic ions is still a concern and can limit their application. Beryllium, nickel,

copper, palladium and chromium are the most hazard-causing elements. Beryllium is added to alloys to lower the melting point and surface tension, and hence, improve castability. However, beryllium dust can cause biological hazards to technicians, while its vapour form is considered a hazard. In addition, it can cause contact dermatitis, chronic lung disease, lung carcinoma and osteosarcoma. The risk is associated with melting and finishing alloys containing within this metal. The ISO standard limits beryllium content to 0.02% [22].

Nickel is found in cast alloys, bonded restorations and wrought alloys, and is not usually found in removable prostheses. The concentration of nickel in human serum is <1 μg L^{-1} compared to 100 μg L^{-1} for elements, such as copper, iron and zinc. The necessity of this element has not yet been confirmed. Nickel is commonly found in the diet, where daily intake can be up 0.1 mg. However, twenty per cent of females and 6% of males are allergic to nickel [227]. It is, therefore, essential to know if the patient has a history of an adverse effect related to nickel. Nickel was classified by the Agency for Research on Cancer (IARC) as a possible carcinogenic agent to humans [228]. Yet, all other dental biomaterials have been categorised as not carcinogenic to humans (inappropriate cell growth and division due to an alteration in DNA).

Ions have to be released from castings, through the corrosion process to become allergens, ions themselves are not allergenic, but binding to molecules, such as proteins, nucleic acids and carbohydrates, and altering these molecules causes the body to not recognise these complexes. The inflammatory response will be presented as an allergy or toxic mechanism, or a combination of both. It has been reported that Ni-containing alloys and Pa-Cu alloys are prone to causing adverse reactions [224,229].

Biocompatibility is related to a combination of factors; ion release, which is not necessarily proportional to alloy content, but dependent on elements and phases presented in an alloy. Some elements are more prone to be released from dental alloys, such as nickel and silver, than other elements, such as gold and platinum [26,36]. The presence of some elements in an alloy can affect the ability of other elements to be released; for example, in gold alloys, palladium has been shown to reduce the ability of copper ions to be released. Released metal can gain access to the inside of the body through the gingiva and other oral tissues; it is then distributed by diffusion through tissues, lymphatic or blood vessels. The body is able

to eliminate metals through urine and lungs. The rate of elimination is dependent on the chemical form of the metal, and its distribution in tissues [224,229].

6.1.2 Ion release and corrosion

Ionisation of elements in alloy causes corrosion; uncharged elements in alloys lose electrons, and change to positively charged ions in the solution. An aggressive environment, such as the oral cavity, can promote corrosion of alloys; for example, dietary intake, temperature, mechanical fatigue, and pH. Corrosion is the loss of metal ions; these ions can be directly released into solution or progressively dissolute from an oxide or sulphide layers. Two reactions are involved in the corrosion process oxidation and reduction. Oxidation reaction occurs on the casting surface where ions are produced. Reduction occurs at the cathode where hydrogen ions are reduced to hydrogen gas. Dental alloy form an oxide layer to inhibit corrosion occurrence. This film is exposed to passivation process, which is the slow dissolve of the formed film. Rate of passivation is controlled by the environment surrounding casting [230].

6.1.3 Biologic testing

Biologic testing is divided into two stages: *in vitro* tests either in cell culture or animal tests, and *in vivo* tests in human subjects [231]. *In vivo* tests are of particular complexity, as they are difficult to control and interpret, and are ethically and legally complicated [232]. The most widely used biological systems for *in vitro* toxicity of dental materials are cell culture systems. However, comparing data from different studies must be done cautiously; data from particular experiments are affected by the chosen cell culture conditions (e.g. the cell system and the cell culture medium). Two types of cell culture systems are available; permanent cell lines derived from type-culture collections (from commercial sources), and primary cells derived from explants. [222].

Modified short term *in vitro* tests have been developed, making further testing unnecessary. The element release test is one of these tests, where the concentrations of elements released from a casting can be quantified. However, the element release test is only a primary test as environment and conditions in the oral cavity are more complicated, and variable factors can be encountered, such as the quantity and quality of saliva, oral hygiene,

the amount and distribution of occlusal forces and teeth brushing. All these factors influence ion release and hence, cytotoxic effect. Furthermore, saliva wash out and elimination of elements should be considered. In addition to the environmental conditions around the alloy, other factors relating to the alloy itself have a considerable contribution. Multiple phase alloys increase element release, and certain elements inherently have higher tendency to be released from alloys, regardless of the alloy composition.

6.1.4 Measuring ion release

The release of elements from dental casting alloys is measured using either atomic absorption spectroscopy (AAS), inductively coupled plasma atomic emission spectrometry (ICP-AES) or inductively coupled plasma mass spectrometry (ICP-MS). Atomic absorption spectroscopy is used with cell culture medium, where different biological media can be used, such as saline, saline with 3% bovine serum albumin, complete cell culture medium with 3% serum [4] and pH 7 phosphate buffer solutions. ICP-MS is used with artificial oral saliva, while ICP-AES is used with artificial oral saliva cell culture medium pH 3.5, pH 6 phosphate buffer solution and pH 3.5 mixtures of lactic acid and sodium chloride.

6.1.5 Standard systems

Two systems are accountable for standards to evaluate dental alloy quality: the American National Standard Institute/American Dental Association (ANSI/ADA) and the International Standards Organisation (ISO). Both systems do not require certain biologic tests to approve the quality of a new dental material. Indeed, the manufacturer is responsible for presenting a compelling case for approval of their product quality, and must provide evidence to support their claims [233].

6.1.6 Daily intake

In order to evaluate metal ion release, daily dietary intake has been employed by researchers as a reference. Daily intake of elements has been investigated by researchers as well as by the International Committee for Radiological Protection (ICRP). The daily intake of a specific element varies significantly according to different eating and drinking habits, and geographical location [234]. According to ICRP, the daily mercury intake is indicated to be 20

µg/d [235], while Bowen [236] indicates the corresponding value to be within the range 4-20 µg/d.

In most studies, documented values were far below the tolerable upper intake levels for each ion [6], which makes using this reference questionable. In addition, the amount of dietary intake is uncertain. Different values have been presented for single elements. Moreover, existing information about the relation between the dietary intake levels of metals and long term exposure is not sufficient. Wataha [229] estimated that the daily dietary intake of ions is 400 µg for Ni, 240 µg for Cr, and 250 µg for Co, whereas Grandjean [237] estimated the average daily dietary intake of ions as 200 to 300 µg for Ni and 280 µg for Cr.

Manaranche [238] developed a chemical classification system for dental alloys. Three classes were defined; alloys belonging to classes I–III released 10 µg/cm^2 week or less, 10–100 µg/cm^2 week or less and 100–1000 µg/cm^2 week, respectively. Class III alloys released a large quantity of metallic ions, which could induce adverse biological reactions in patients. However, ISO standard 22674:2006 for maximum ion release from a dental alloy after 7 days presented 200 µg/cm^2 as a threshold value [24].

6.1.7 Inductively Coupled Plasma/Optical Emission Spectrometry (ICP/OES)

ICP/OES is an analytical instrument which is used to determine and quantify concentration of trace elements of gases, liquids and solids. There are other instruments used for this purpose, such as atomic absorption spectrometer (AAS) and graphite furnace atomic absorption spectrometer (GFAAS). The advantages of ICP over these instruments are its ability to analyse multiple elements at a time, it has longer linear ranges, which is the linear relationship between absorbance and concentration, the linearity for ICP ranges from 4 to 6 orders of magnitude whereas AAS and GFAAS range is from 2 to 3 orders of magnitude. Moreover, ICP has less chemical interference, due to the high temperature of the plasma and also has less matrix interference due to its mode of sample introduction. In addition, ICP has a variety of emission lines to choose which helps to reduce interference with other elements [239]. ICP can be accomplished using various techniques, including, inductively coupled plasma - optical emission spectroscopy (ICP-OES), and inductively coupled plasma -

mass spectrometry (ICP-MS). The technique is based on the emission of photons from atoms and ions that have been excited.

6.1.7.1 Calibration of the instrument

Before sample analysis, the ICP must be calibrated. Calibration consists of analysing standards and a blank within the linear range of the element being analysed. The linear range for ICP-OES is typically 4 to 6 orders of magnitude of concentration. A standard is analysed and compared to the initial standard response throughout the run.

The wavelength must be selected, it must be appropriate for the concentrations being analysed. For example, when performing trace level analyses, the least sensitive wavelength would not be used. When analysing multiple elements, the wavelength(s) chosen must take into account interference from the other elements being analysed.

6.1.7.2 Introductions of samples

Sample solutions are introduced into the ICP as an aerosol; aerosol is carried into the centre of the plasma, superheated inert gas. Temperature at the core of the ICP is approximately 10.000 K. The plasma converts the aerosol into a solid, vaporizes the solid into a gas, and dissociates the individual molecules into atoms. This high temperature source (plasma) excites the atoms and ions, the excited atoms then relax to the ground state via the emission of a photon.

6.1.7.3 Detecting and quantifying ions

Emitted photons have distinctive energies that are determined by the quantized energy level structure for each atom or ion. The wavelength of the photons can then be used to identify the elements from which they emitted. A portion of the photons emitted by the ICP is collected with a lens. This focusing optic forms an image of the ICP on the entrance space of a wavelength selection device such as a monochromator. The particular wavelength leaving the monochromator is converted to an electrical signal by a photodetector. The signal is amplified and processed by the detector electronics, then displayed and stored by a personal computer [240].

6.2 Aims and objectives

The aim is to evaluate the effect of reusing surplus alloys on the amount of ions released from castings immersed into artificial saliva at pH 4 and 6 for five weeks.

Twenty test pieces were prepared for each alloy test group. Each test piece was put in a plastic container, which was then filled with 25 mL of artificial saliva (PBS). After each week of immersion, 1.00 cm^3 (1.00 mL) of the PBS solution from each sample was taken, placed in an individual sample pot and diluted with distilled water. Solutions were analysed by Inductive Coupled Plasma-atomic Emission Spectroscopy ICP-OES (Thermo Scientific, ICA6300, DUO). Mean of the amounts of elements released were calculated and presented in the unit ($\mu g/cm^2$).

6.3 Experimental methods

Wax patterns (0.3-0.5 mm thickness) were duplicated from one silicone mould, as described in Chapter 3, section 3.3.2.1. Wax patterns and sprues were invested and cast as described in Chapter 3, sections 3.3.2.3 and 3.3.2.4.

Five test groups were prepared for each alloy type as described in Table 6-1. Castings were sandblasted with 50 μm Al_2O_3 particles, cleaned and subjected to heat treatments for ceramic firing cycles as presented in Chapter 5, Table 5-3 and Table 5-4.

Table 6-1 The experimental groups for the ion release assessment

Alloy type	Cobalt-chromium (n=20)	Nickel-chromium (n=20)
Test group	100% new alloy	100% new alloy
	75% new + 25% re-cast	75% new + 25% re-cast
	50% new + 50% re-cast	50% new + 50% re-cast
	25% new + 75% re-cast	25% new + 75% re-cast
	100% re-cast alloy	100% re-cast alloy

6.3.1 Mounting of the test pieces

Each test piece was placed into a plastic mould mounting cup (Buehler, Germany). Cold setting liquid epoxy resin (Buehler Epo Thin 2 Resin, Germany) was mixed with epoxy resin hardener (Buehler Epo Thin 2 Hardener, Germany). The mixing ratio was five parts resin with 1.95 parts hardener. The combined liquid was thoroughly mixed manually, poured around test pieces, and allowed to cure at room temperature for 24 h (Figure 6-1). Mounted test pieces were then manually polished following the procedure described in Chapter 4, section 4.3.6. After polishing, test pieces were rinsed with distilled water, steam cleaned, ultrasonically cleaned for 5 minutes and then rinsed with distilled water. Finally, test pieces were allowed to dry for 12 hours. Cleaning test pieces is essential to ensure that microbial growth will not occur in the extraction medium.

Figure 6-1 Test pieces embedded in mounting resin

6.3.2 Preparation of the solution

The solution used was Phosphate buffered saline (PBS) artificial saliva. The composition of the PBS is shown in Table 6-2. Salts were added to 1000 ml (1.00 dm^3) of distilled water. Two different pH solutions were prepared (pH 4 and pH 6), with concentrated lactic acid and sodium hydroxide used to adjust pH value. The pH was measured using a Denver Instruments PH meter model 225 (Denver, Colorade, UK). The pH meter was calibrated using buffers at pH 4 and 6 (BDH, Dorset, UK) before testing the PBS solution. The pH probe was rinsed with deionised water and dried prior to readings being taken. The PBS solution was sterilised by autoclaving (Rodwell Ensign, Essex, UK) at 121 ˚C for 15 minutes under pressure.

Table 6-2 Composition of phosphate buffered saline (PBS) solution used as artificial saliva

Compound		Weight (g/dm^{-3})
Sodium chloride	(NaCl)	0.400
Potassium chloride	(KCl)	0.400
Potassium hydrogen phosphate	(KH_2PO_4)	0.218
Disodium phosphate	(Na_2HPO_4)	1.192

6.3.3 Element Release

Each test piece was put in a plastic container, which was then filled with 25 mL of the solution using an Eppendorf pipette. All containers were labelled clearly with the alloy and test group names and corresponding pH of the PBS. The plastic containers were placed in an orbital incubator (Model G25, New Brunswick Scientific, NJ, USA) for five weeks' time period at a constant temperature of 37 ˚C.

6.3.4 Immersion time

Test pieces were immersed in solutions at either pH 4 or pH 6 for one week at a time. After the first week of immersion, 1.00 cm^3 (1.00 mL) of PBS solution from each sample was taken, placed in an individual sample pot and run through the ICP/OES to test the amount of ions released. Five mL is needed for the ICP-OES test, and so solutions were diluted with 20% v/v distilled water, 1 mL: 4 mL. To ensure a constant volume and to avoid the possibility of saturation of solution with some elements, PBS solution was replenished after each testing period. This was repeated each week for a total of five weeks.

6.3.5 Detecting trace elements

All the solution samples were analysed by ICP–OES (Thermo Scientific, ICA6300, DUO). For each analysis the instrument performs three measurements and calculates means and SD for each element and the relative S.D (% RSD). Thus, with the four test pieces tested in each group, the total number of the measurements recorded per element was 12. Wave lengths for each of the detected elements are presented in Table 6-3.

Table 6-3 Wave length of each of the detected elements

Element	Wave length (nm)
Co	228.616
Cr	276.716
Fe	238.240
Mn	257.610
Mo	202.030
Ni	231.604

6.3.6 Calculation of the amount of elements released

The surface area of a single test piece was 0.636 cm^2. The surface area of a test piece to the volume ratio of the solution was 0.025 cm^2/mL. Ions released were measured in (µg/L) (elemental solution concentration), and converted to units of µg/cm^2 (element release per surface area) to make it easier to compare results with other research. To give the value in µg/cm^2, the amount in µg/L was multiplied by the volume of the artificial saliva (25 mL) and divided by the area of the test piece (0.636 cm^2). The raw data were multiplied by the dilution factor (1 mL of artificial saliva into 5 mL of the solution).

For the three repeats of each sample, to assess the variation of the three sets of values collected (between-sample variations); the relative standard deviation was calculated (% RSD). If as in some cases the % RSD of the three readings was above 10 %, the sample was automatically re-analysed. For the four test pieces of each test groups, (between-test pieces variations), to identify any outliers (the observation that is distant from other observations), Q test was used, and outliers at 95% confidence level values were rejected.

6.3.6.1 Standard solution and reagent blank

A standard solution was used (qm_x. Essex, UK) so the analyte concentration is accurately known. The absorbance of the standard solutions were measured and used to prepare a calibration curve (Figure 6-2). The software provided calculated calibration curves for each sample as a reference for comparison with the concentrations of eluted elements. The immersion solutions without specimens being immersed was used as a reagent blank. Reagent blank values were measured and subtracted from test results.

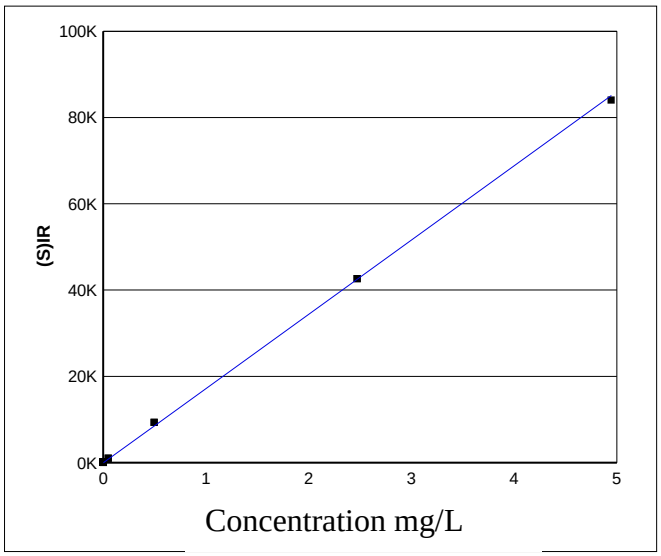

Figure 6-2 An example of calibration graph to calibrate the ICP/OES instrument

6.4 Results of the ion release test

Each test piece was immersed for five weeks in PBS solution at either pH 4 or pH 6. The mean amount of ions released after each week are presented in Tables 6-4, 6-5, 6-8 and 6-9 and Figure 6-3 – Figure 6-12. Data were presented as mean release rate (μg/cm^2) of ions released for each emersion period.

6.4.1 Ion release from Ni-Cr alloy

The cumulative concentrations of Ni, Cr, Mo, Fe, Mn and Co ion metals released in artificial saliva from Ni-Cr castings were measured at different immersion time using ICP/OES, and presented in Table 6-4 and Table 6-5 and Figures 6-3, 6-4, 6-5 and 6-6. Due to the very small amounts of ions released, no graphs were presented for Cr, Fe and Mn.

6.4.1.1 Ions release into solution at pH 4

Table 6-4 shows that the order of the amount of released ions is Ni> Fe> Mo> Co> Mn> Cr. For most of the test groups, the release of elements has decreased over immersion time and was not proportional to the alloy element composition. Although Ni was released more than the other elements in the alloy, only negligible amounts of Cr were released. For all test groups, the amount of ions released was higher at pH 4 (Table 6-4) than pH 6 (Table 6-5). The highest value of ions released was from the NiCr-50 test group at the second week of immersion (7.68 μg/cm^2), which equals 0.55 μg/cm^2 a day. The smallest amount released was from NiCr-25 at week five (1.93 μg/cm^2), which equals (0.06 μg/cm^2) a day.

For Ni, the first three weeks demonstrated the highest release of ions, followed by a trend of a steady or decreased release (Figure 6-3). For Mo and Co, the first two weeks demonstrated the highest release of ions, followed by a trend of a steady or decreased release (Figure 6-5 and Figure 6-7). However, all test groups demonstrated very low release rate

6.4.1.2 Ions release into solution at pH 6

Table 6-5 shows that the order of the amount of released ions is Ni> Mo> Co. Negligible amounts of Cr, Fe and Mn were released. In general, release either has decreased or has slightly increased over the immersion time (Figure 6-4, Figure 6-6 and Figure 6-8).

The highest cumulative amount of Ni release reported was for NiCr-50 in the first week (4.83 μg/cm^2), which equals 0.69 μg/cm^2 a day. The smallest amount of ions released was from NiCr-25 at the end of the third week of immersion (0.53 μg/cm^2), which equals 0.03 μg/cm^2 a day. Trace amounts of Cr were detected in only some of the test groups. Nb and Ta were not detected by the ICP.

Table 6-4 Mean concentrations and standard deviations of the elements released (μg/cm^2) into solution of pH 4 from Ni-Cr castings

Test group	Immersion Time (week)	Ni		Cr		Mo		Fe		Co		Mn	
		Mean	SD	Mean	SD	Mean	SD	Mean	SD	Mean	SD	Mean	SD
NiCr-0	1	2.87	0.01	0.00	0.02	0.25	0.28	0.72	0.32	0.09	0.00	0.04	0.31
	2	3.02	0.02	0.00	0.00	0.26	0.12	0.96	0.10	0.05	0.02	0.04	0.09
	3	2.81	0.01	0.00	0.03	0.20	0.32	0.37	0.34	0.04	0.02	0.04	0.31
	4	2.62	0.01	0.04	0.03	0.14	0.27	0.24	0.33	0.04	0.02	0.02	0.31
	5	2.44	0.01	0.00	0.03	0.11	0.29	0.35	0.29	0.06	0.01	0.05	0.24
NiCr-25	1	1.65	0.05	0.00	0.13	0.16	0.42	0.64	0.48	0.18	0.10	0.06	0.43
	2	2.07	0.04	0.00	0.05	0.17	0.43	0.47	0.63	0.16	0.09	0.06	0.45
	3	2.00	0.03	0.00	0.03	0.14	1.37	1.84	2.07	0.14	0.08	0.09	0.32
	4	1.95	0.03	0.03	0.03	0.09	0.13	0.19	0.16	0.15	0.07	0.05	0.13
	5	1.93	0.03	0.00	0.03	0.07	0.29	0.42	0.41	0.16	0.07	0.07	0.74
NiCr-50	1	7.44	0.02	0.00	0.05	0.55	0.57	0.99	0.63	0.17	0.05	0.05	0.59
	2	7.68	0.02	0.00	0.04	0.52	0.88	1.10	0.96	0.12	0.04	0.06	0.93
	3	5.81	0.07	0.00	0.04	0.37	0.38	0.43	0.41	0.10	0.05	0.09	0.42
	4	6.32	0.03	0.03	0.04	0.26	0.39	0.31	0.47	0.10	0.03	0.05	0.44
	5	5.86	0.03	0.00	0.03	0.18	0.41	0.06	0.41	0.12	0.05	0.09	0.43
NiCr-75	1	5.97	0.01	0.00	0.02	0.46	0.10	0.24	0.09	0.10	0.01	0.07	0.09
	2	6.67	0.09	0.00	0.02	0.39	0.09	0.09	0.10	0.07	0.05	0.13	0.09
	3	6.94	0.08	0.01	0.03	0.41	1.99	2.00	2.24	0.09	0.05	0.24	2.09
	4	6.91	0.19	0.04	0.02	0.32	0.75	0.44	0.85	0.04	0.04	0.23	0.06
	5	6.91	0.26	0.00	0.05	0.30	0.50	0.50	0.57	0.07	0.05	0.30	0.79
NiCr-100	1	5.25	0.00	0.00	0.02	0.50	0.15	1.19	0.27	0.06	0.01	0.04	0.55
	2	5.43	0.00	0.06	0.07	0.49	0.97	2.34	1.13	0.03	0.00	0.05	0.24
	3	4.59	0.02	0.04	0.03	0.40	0.78	1.50	0.87	0.06	0.00	0.06	1.03
	4	4.36	0.02	0.04	0.48	0.39	1.03	1.76	1.15	0.04	0.01	0.06	0.79
	5	3.88	0.02	0.04	0.18	0.24	0.33	0.92	0.32	0.05	0.01	0.07	1.08

Table 6-5 Mean concentrations and standard deviations of the elements released (μg/cm^2) into solution of pH 6 from Ni-Cr castings

Test group	Immersion time (week)	Ni		Cr		Mo		Fe		Co		Mn	
		Mean	SD	Mean	SD	Mean	SD	Mean	SD	Mean	SD	Mean	SD
NiCr-0	1	1.78	0.02	0.00	0.00	0.18	0.06	0.00	0.00	0.09	0.02	0.05	0.06
	2	1.58	0.02	0.01	0.01	0.05	0.10	0.00	0.00	0.04	0.01	0.02	0.12
	3	1.41	0.01	0.01	0.01	0.12	0.14	0.00	0.00	0.00	0.01	0.00	0.00
	4	1.13	0.01	0.01	0.02	0.15	0.13	0.00	0.00	0.01	0.01	0.00	0.00
	5	0.93	0.00	0.00	0.00	0.16	0.23	0.00	0.00	0.03	0.01	0.00	0.00
NiCr-25	1	0.88	0.02	0.00	0.00	0.09	0.35	0.00	0.00	0.06	0.04	0.03	0.37
	2	0.84	0.01	0.01	0.01	0.00	0.25	0.00	0.00	0.06	0.01	0.01	0.19
	3	0.54	0.01	0.00	0.01	0.03	0.23	0.00	0.00	0.00	0.00	0.00	0. 13
	4	0.53	0.01	0.00	0.02	0.07	0.18	0.00	0.00	0.02	0.02	0.00	0. 00
	5	0.55	0.01	0.00	0.00	0.09	0.05	0.00	0.00	0.03	0.01	0.00	0.00
NiCr-50	1	4.86	0.02	0.02	0.03	0.35	0.09	0.00	0.00	0.09	0.06	0.02	0.10
	2	4.43	0.02	0.02	0.01	0.32	0.39	0.05	0.45	0.07	0.01	0.02	0.36
	3	3.39	0.01	0.01	0.03	0.46	0.13	0.00	0.00	0.02	0.01	0.00	0.00
	4	3.46	0.01	0.02	0.01	0.49	0.09	0.00	0.00	0.02	0.01	0.00	0.00
	5	2.95	0.01	0.00	0.02	0.41	0.21	0.00	0.00	0.03	0.01	0.00	0.00
NiCr-75	1	2.24	0.01	0.00	0.02	0.31	0.10	0.00	0.00	0.04	0.01	0.02	0.09
	2	3.38	0.01	0.00	0.03	0.23	0.11	0.00	0.00	0.06	0.02	0.05	0.10
	3	2.89	0.01	0.00	0.02	0.37	0.08	0.00	0.00	0.04	0.03	0.01	0.06
	4	3.30	0.01	0.00	0.00	0.42	0.10	0.00	0.00	0.03	0.02	0.03	0.09
	5	3.12	0.02	0.00	0.00	0.40	0.03	0.00	0.00	0.05	0.02	0.04	0.04
NiCr-100	1	3.99	0.01	0.00	0.00	0.40	0.09	0.00	0.00	0.03	0.02	0.02	0.07
	2	3.94	0.01	0.01	0.01	0.28	0.38	0.18	0.48	0.04	0.03	0.01	0.42
	3	3.02	0.01	0.03	0.01	0.36	0.20	0.16	0.19	0.02	0.02	0.00	0.00
	4	2.78	0.01	0.00	0.00	0.44	0.20	0.00	0.00	0.02	0.01	0.00	0.00
	5	3.17	0.01	0.00	0.00	0.40	0.46	0.00	0.00	0.02	0.01	0.00	0.00

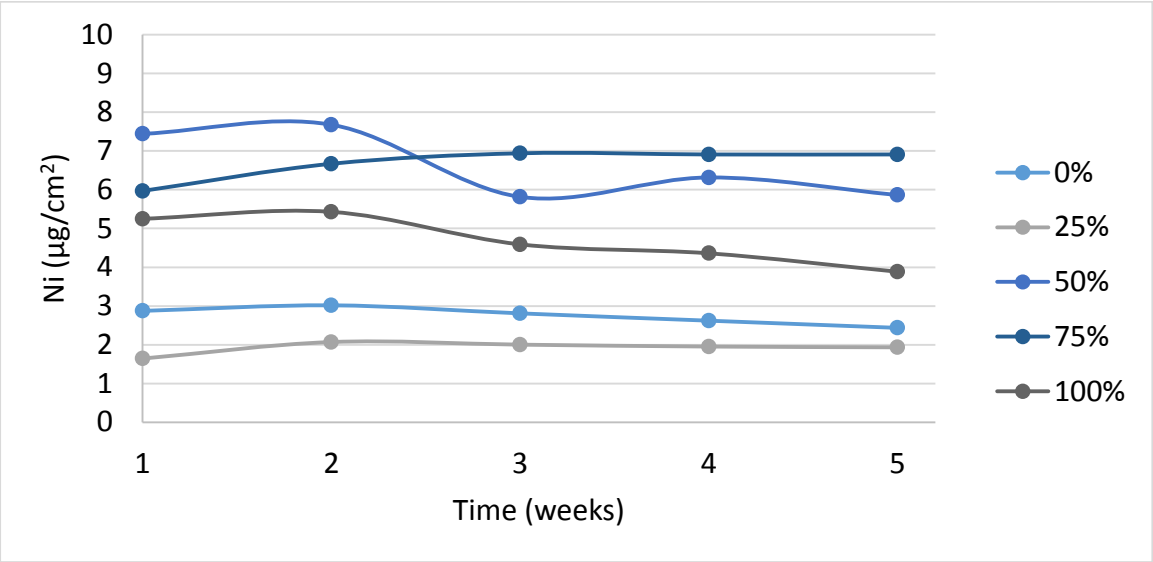

Figure 6-3 Mean amount of Ni released from Ni-Cr castings after immersion into artificial saliva at pH 4 for five consecutive weeks.

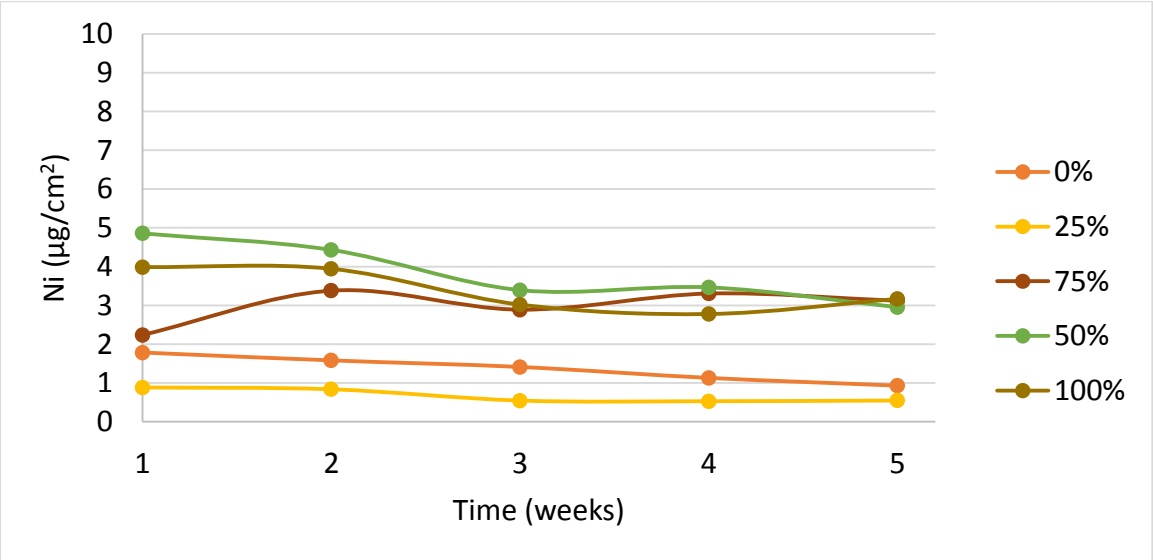

Figure 6-4 Mean amount of Ni released from Ni-Cr castings after immersion into artificial saliva at pH 6 for five consecutive weeks

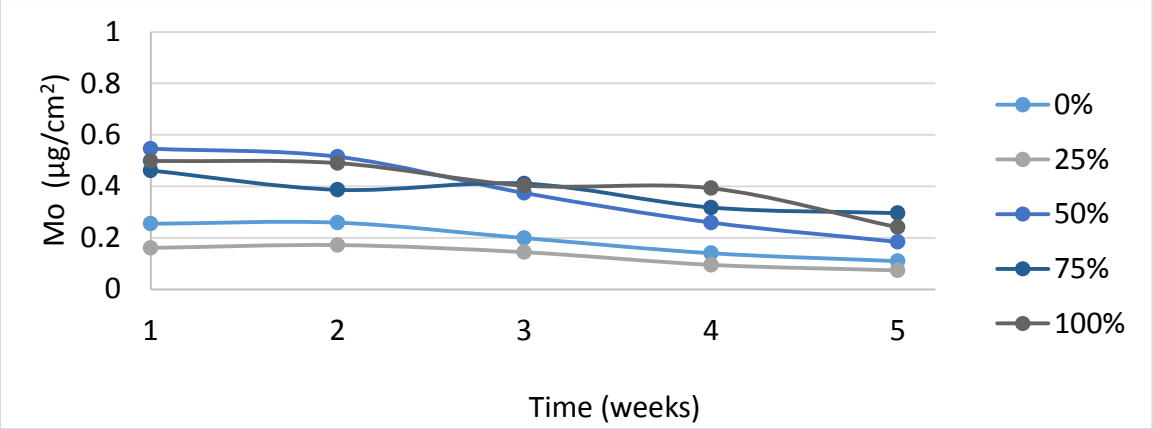

Figure 6-5 Mean amount of Mo released from Ni-Cr castings after immersion into artificial saliva at pH 4 for five consecutive weeks

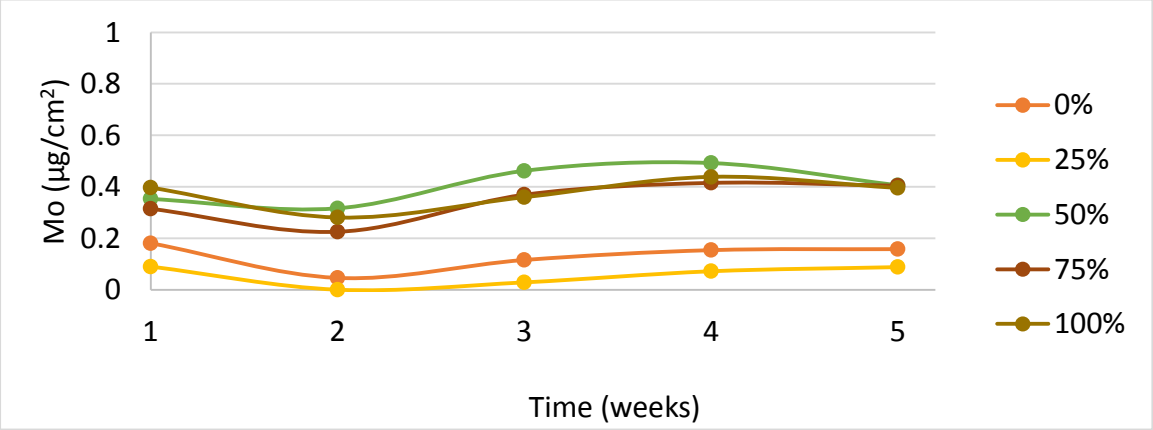

Figure 6-6 Mean amount of Mo released from Ni-Cr castings after immersion into artificial saliva at pH 6 for five consecutive weeks

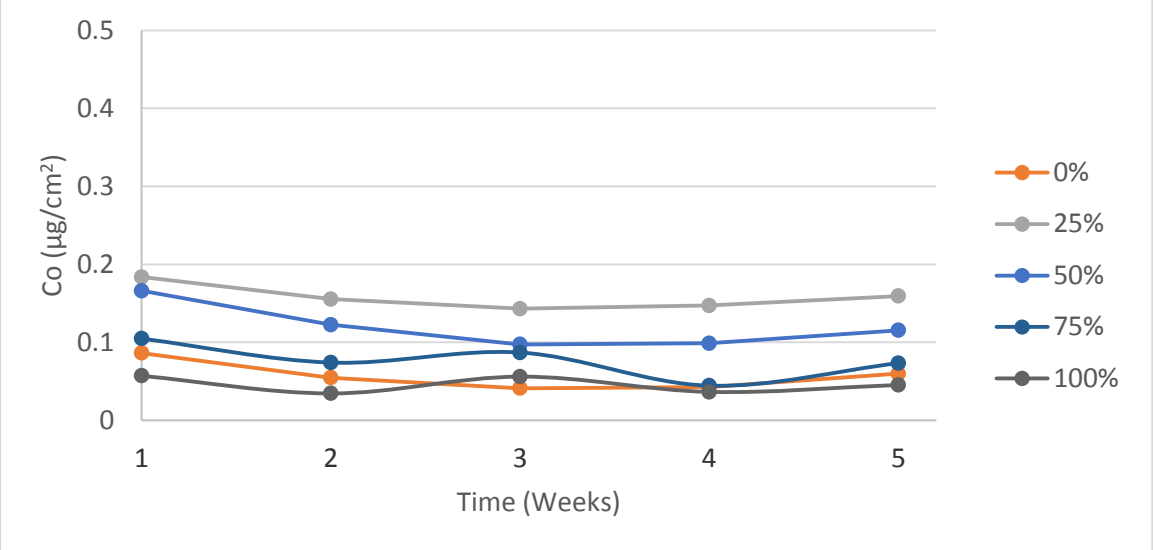

Figure 6-7 Mean amount of Co released from Ni-Cr castings after immersion into artificial saliva at pH 4 for five consecutive weeks

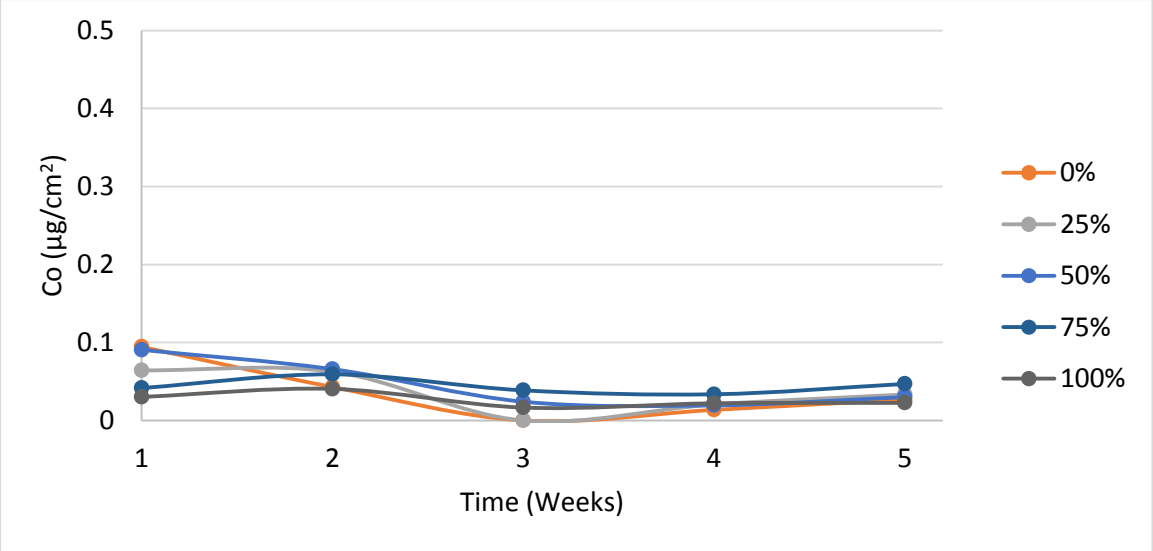

Figure 6-8 Mean amount of Co released from Ni-Cr castings after immersion into artificial saliva at pH 6 for five consecutive weeks

6.4.2 Statistical analysis

6.4.2.1 Nickel release

Data were analysed using a two way analysis of variance (ANOVA), at the 95% confidence level p= 0.05, and the multiple comparisons summary was used to indicate if any combinations differed significantly (Table 6-6). More specific analysis was carried out for the results of each pH value. The Tukey post hoc test was used to distinguish significant differences between mean values. Statistical analyses were carried out for Ni and Mo. Tests of between-subject effects showed that pH value and test group have significant effects on the amount of ions released. However, immersion time does not have a significant effect (Table 6-6).

Table 6-6 Tests of between-subjects effects

Source	Sig (P value)
Immersion time	.437
Test group (recycled content of alloy)	.001
pH value	.000
Immersion time * Test group	1.000
Immersion time * pH value	.999
Test group * pH value	.000
Immersion time * Test group * pH value	1.000

6.4.2.1.1 Solution at pH 4 (Ni ions release)

For the pH 4 solution, data analysis revealed that the test group (recycled content of alloy) has a significant effect on the amount of ions released (p= 0.000). However, within each test group, immersion time has no effect (p= 0.526). In addition, the interaction of test group and immersion type (Test group * immersion time) showed no significant difference (p= 0.943). (Appendix 1, Table 1-24). Tukey HSD revealed that no significant difference was documented between the first two test groups (NiCr-0 and NiCr-25) (p= 0.364). However, significant differences were documented between the first two test group (NiCr-0 and NiCr-25) and all the other test groups (p< 0.000) (Appendix 1, Table 1-25).

6.4.2.1.2 Solution at pH 6 (Ni ions release)

For the pH 6 solution, data analysis revealed that test group (recycled content of alloy) has no effect (p= 0.462). Immersion time has a slight effect (p= 0.044). In addition, the interaction of test group and immersion type (Test group * immersion time) showed no significant difference (p= 0.065) (Appendix 1, Table 1-26). Tukey HSD revealed that no significant difference was documented between the first two test groups (p= 0.608). However, significant differences were documented between the first two test group (NiCr-0 and NiCr-25) and all the other test groups (p< 0.001). No significant differences were documented between the last three test groups (NiCr-50 and NiCr-75 and NiCr-100) (p> 0.05) (Appendix 1, Table 1-27).

6.4.3 Daily release of Ni from Ni-Cr alloy

For the purpose of comparing results with these reported in the literature, the amount of Ni ions released each day is presented in Table 6-7. The release of Ni ions has decreased over time.

The difference between the maximum amount of ions released from NiCr-100 in a pH 4 solution (0.75 µg/cm^2.day), and the maximum amount released from NiCr-0 (0.41 µg/cm^2.day) is only 0.34 µg/cm^2. For the pH 6 solution, the difference between the comparable test groups is very close and equals 0.32 µg/ cm^2 (Table 6-7).

Table 6-7 Mean concentrations and standard deviations of Ni released (μg/cm^2. day) into solutions of pH 4 and pH 6

Test group	Immersion time (Day)	Ni (μg/cm^2. day) (pH 4)		Ni (μg/cm^2. day) (pH 6)	
		Mean	SD	Mean	SD
NiCr-0	7	0.41	0.01	0.25	0.02
	14	0.20	0.02	0.11	0.02
	21	0.13	0.01	0.07	0.01
	28	0.09	0.01	0.04	0.01
	35	0.07	0.01	0.03	0.00
NiCr-25	7	0.24	0.05	0.13	0.02
	14	0.14	0.04	0.06	0.01
	21	0.10	0.03	0.03	0.01
	28	0.07	0.03	0.02	0.01
	35	0.06	0.03	0.02	0.01
NiCr-50	7	1.06	0.02	0.69	0.02
	14	0.51	0.02	0.32	0.02
	21	0.28	0.07	0.16	0.01
	28	0.23	0.03	0.12	0.01
	35	0.17	0.03	0.08	0.01
NiCr-75	7	0.85	0.01	0.32	0.01
	14	0.44	0.09	0.24	0.01
	21	0.33	0.08	0.14	0.01
	28	0.25	0.19	0.12	0.01
	35	0.20	0.26	0.09	0.02
NiCr-100	7	0.75	0.00	0.57	0.01
	14	0.36	0.00	0.28	0.01
	21	0.22	0.02	0.14	0.01
	28	0.16	0.02	0.10	0.01
	35	0.11	0.02	0.09	0.01

6.4.4 Ion release from Co-Cr alloy

The cumulative concentrations of Co, Cr, Mo, Fe, Mn and Ni ion metals released in artificial saliva from Co-Cr casting were measured at different immersion time using ICP/OES, and presented in Table 6-8 and Table 6-9 and Figures 6-9, 6-10, 6-11 and 6-12. Due to the small amounts of ions released, graphs were only presented for Co and Ni.

6.4.4.1 Ions release into solution at pH 4

Co was the highest element to be released; whilst other elements, including Cr, Mo, Fe, Mn were also detected. Surprisingly, Ni was detected in both solutions of different pH values, but in higher amounts in pH 4. Neither the manufacturers, nor the EDAX analysis documented the presence of Ni in the castings. The smallest amount of released Co ions was reported with CoCr-25 in the first week (0.82 μg/cm^2); this equals 0.12 μg/cm^2 a day. The largest amount of released Co ions was reported with CoCr-50 in the second week (1.86 μg/cm^2); this equals 0.13 μg/cm^2 a day (Table 6-8) (Figures 6-9 and Figure 6-11).

6.4.5 Ions release into solution at pH 6

Similar elements were detected, but in smaller amounts. The smallest amount of Co ions released was reported with CoCr-100 in the last week (0.77 μg/cm^2), which equals 0.02 μg/cm^2 a day. The largest amount of Co ions released was reported with CoCr-75 (1.47 μg/cm^2) in the last week, which equals 0.04 μg/cm^2 a day (Table 6-9) (Figures 6-10 and Figure 6-12).

Table 6-8 Mean concentrations and standard deviations of the elements released (μg/cm^2) into solution of pH 4 from Co-Cr castings

Test group	Immersion Time (Week)	Co		Cr		Mo		Mn		Fe		Ni	
		Mean	SD	Mean	SD	Mean	SD	Mean	SD	Mean	SD	Mean	SD
CoCr-0	1	1.53	0.43	0.00	0.04	0.00	0.06	0.00	0.21	0.00	0.01	0.43	0.11
	2	1.56	0.47	0.00	0.00	0.09	0.03	0.02	0.51	0.02	0.01	0.25	0.06
	3	1.61	0.48	0.02	0.04	0.11	0.04	0.04	0.31	0.00	0.04	0.26	0.03
	4	1.57	0.46	0.03	0.04	0.08	0.03	0.00	0.33	0.00	0.01	0.19	0.03
	5	1.48	0.50	0.00	0.06	0.07	0.05	0.01	0.36	0.01	0.01	0.19	0.04
CoCr-25	1	0.82	0.29	0.00	0.03	0.00	0.01	0.00	0.45	0.00	0.01	0.10	0.07
	2	0.91	0.30	0.03	0.02	0.04	0.02	0.05	0.31	0.88	0.02	0.26	0.07
	3	0.92	0.23	0.05	0.03	0.07	0.01	0.03	0.20	0.05	0.01	0.26	0.05
	4	0.93	0.24	0.03	0.02	0.04	0.02	0.01	0.45	0.00	0.02	0.22	0.07
	5	0.91	0.24	0.00	0.04	0.03	0.01	0.02	0.15	0.00	0.02	0.24	0.06
CoCr-50	1	1.65	0.73	0.00	0.02	0.00	0.04	0.00	1.00	0.00	0.01	0.00	0.02
	2	1.86	0.62	0.07	0.02	1.13	0.76	0.70	0.05	0.00	0.99	0.24	0.17
	3	1.70	0.66	0.03	0.03	0.10	0.03	0.03	0.18	0.00	0.01	0.16	0.05
	4	1.67	0.62	0.02	0.02	0.07	0.04	0.01	0.35	0.00	0.01	0.10	0.04
	5	1.67	0.59	0.00	0.03	0.06	0.02	0.02	0.35	0.00	0.01	0.16	0.04
CoCr-75	1	1.26	0.23	0.00	0.02	0.00	0.02	0.00	0.22	0.00	0.01	0.00	0.04
	2	1.38	0.25	0.00	0.02	0.31	0.05	0.06	0.32	0.36	0.01	0.12	0.03
	3	1.43	0.26	0.01	0.02	0.08	0.01	0.05	0.89	0.80	0.01	0.16	0.04
	4	1.39	0.27	0.00	0.03	0.04	0.01	0.01	0.08	0.30	0.00	0.12	0.02
	5	1.41	0.27	0.00	0.02	0.03	0.01	0.04	2.35	1.65	0.01	0.16	0.03
CoCr-100	1	1.61	0.36	0.00	0.04	0.00	0.05	0.00	1.17	0.00	0.01	0.20	0.15
	2	1.43	0.32	0.01	0.01	0.21	0.07	0.04	1.45	1.74	0.01	0.26	0.15
	3	1.54	0.32	0.03	0.04	0.86	0.55	0.27	1.35	1.82	0.27	0.35	0.09
	4	1.56	0.36	0.04	0.05	0.06	0.05	0.00	0.87	0.00	0.01	0.27	0.13
	5	1.57	0.39	0.00	0.03	0.04	0.05	0.02	0.87	0.18	0.01	0.31	0.12

Table 6-9 Mean concentrations and standard deviations of the elements released (μg/cm^2) into solution of pH 6 from Co-Cr castings

Test group	Immersion time (Week)	Co		Cr		Mo		Mn		Fe		Ni	
		Mean	SD	Mean	SD	Mean	SD	Mean	SD	Mean	SD	Mean	SD
CoCr-0	1	1.08	0.31	0.02	0.04	0.09	0.02	0.01	0.00	0.24	0.56	0.19	0.03
	2	0.98	0.27	0.02	0.03	0.04	0.03	0.00	0.00	0.33	0.50	0.13	0.03
	3	0.92	0.27	0.00	0.00	0.00	0.00	0.00	0.01	0.06	0.51	0.10	0.04
	4	0.96	0.28	0.00	0.01	0.10	0.02	0.00	0.00	0.00	0.59	0.12	0.03
	5	0.90	0.25	0.00	0.03	0.11	0.03	0.00	0.01	0.04	0.45	0.29	0.18
CoCr-25	1	0.96	0.32	0.00	0.01	0.06	0.02	0.02	0.01	0.47	0.49	0.21	0.02
	2	0.93	0.35	0.06	0.02	0.00	0.00	0.00	0.01	0.50	0.32	0.19	0.05
	3	0.86	0.30	0.00	0.00	0.00	0.00	0.00	0.01	0.42	0.39	0.11	0.03
	4	1.01	0.27	0.01	0.15	1.16	0.92	0.40	0.54	0.74	0.61	0.18	0.09
	5	0.93	0.32	0.00	0.00	0.06	0.02	0.00	0.01	0.32	0.24	0.15	0.04
CoCr-50	1	0.88	0.14	0.00	0.00	0.04	0.01	0.00	0.00	0.05	0.22	0.09	0.02
	2	0.87	0.08	0.01	0.00	0.00	0.00	0.00	0.00	0.25	0.15	0.04	0.01
	3	0.85	0.15	0.00	0.03	0.00	0.01	0.00	0.00	0.00	0.17	0.00	0.01
	4	0.80	0.15	0.05	0.02	0.43	0.08	0.00	0.00	0.00	0.15	0.01	0.02
	5	0.82	0.18	0.00	0.00	0.07	0.01	0.00	0.00	0.00	0.20	0.05	0.02
CoCr-75	1	1.43	0.56	0.00	0.00	0.07	0.03	0.01	0.01	0.24	0.25	0.10	0.02
	2	1.05	0.70	0.00	0.00	0.00	0.00	0.01	0.00	0.03	0.24	0.04	0.06
	3	1.38	0.52	0.00	0.00	0.00	0.00	0.00	0.00	0.18	0.25	0.08	0.02
	4	1.04	0.09	0.07	0.03	0.26	0.05	0.00	0.00	0.12	0.31	0.05	0.02
	5	1.47	0.60	0.00	0.00	0.94	1.00	0.27	0.38	1.53	1.55	0.17	0.09
CoCr-100	1	0.86	0.50	0.00	0.00	0.05	0.03	0.01	0.00	0.00	0.04	0.17	0.06
	2	0.76	0.36	0.03	0.00	0.00	0.00	0.01	0.01	0.00	0.16	0.09	0.06
	3	0.76	0.47	0.00	0.00	0.00	0.03	0.00	0.01	0.00	0.38	0.06	0.05
	4	0.82	0.53	0.05	0.01	0.17	0.03	0.00	0.01	0.00	0.35	0.02	0.05
	5	0.77	0.53	0.00	0.00	0.55	0.10	0.03	0.03	0.00	0.29	0.16	0.07

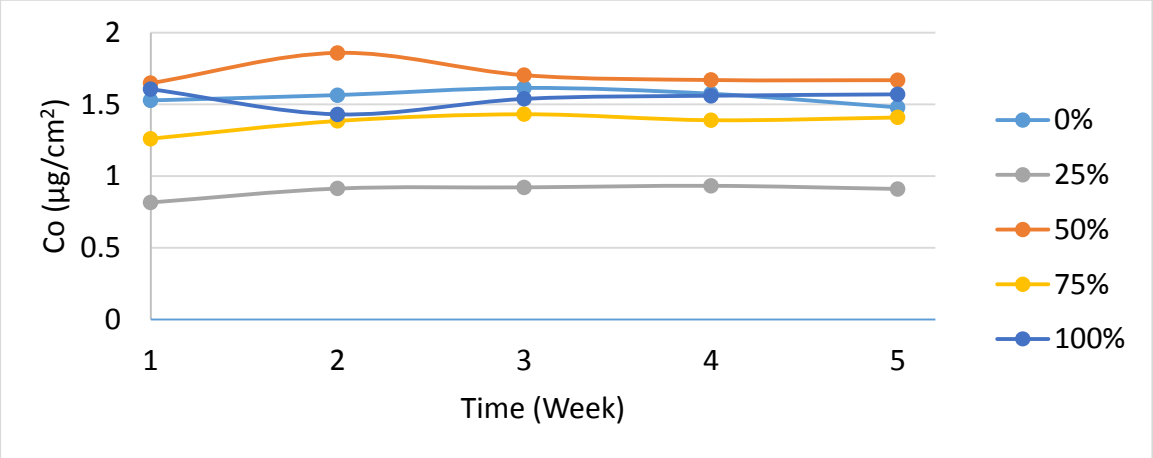

Figure 6-9 Mean amount of Co released from Co-Cr castings after immersion into artificial saliva at pH 4 for five consecutive weeks

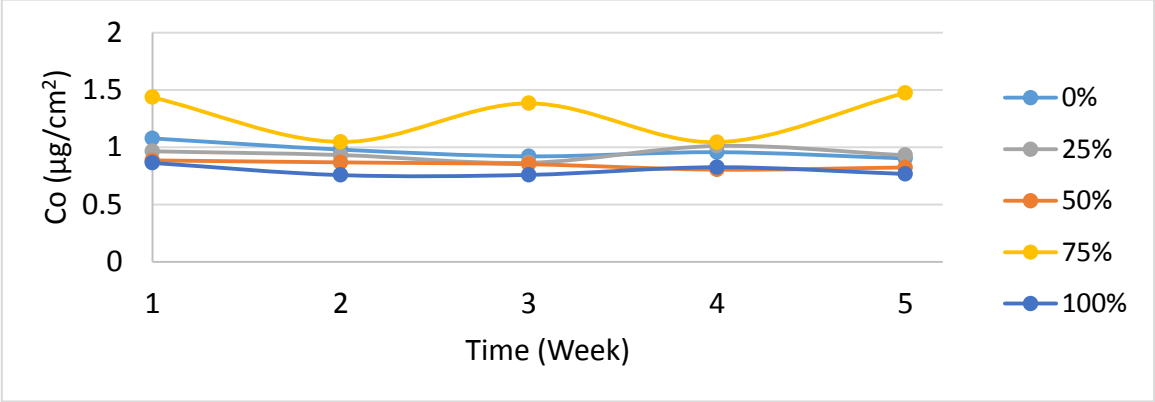

Figure 6-10 Mean amount of Co released from Co-Cr castings after immersion into artificial saliva at pH 6 for five consecutive weeks

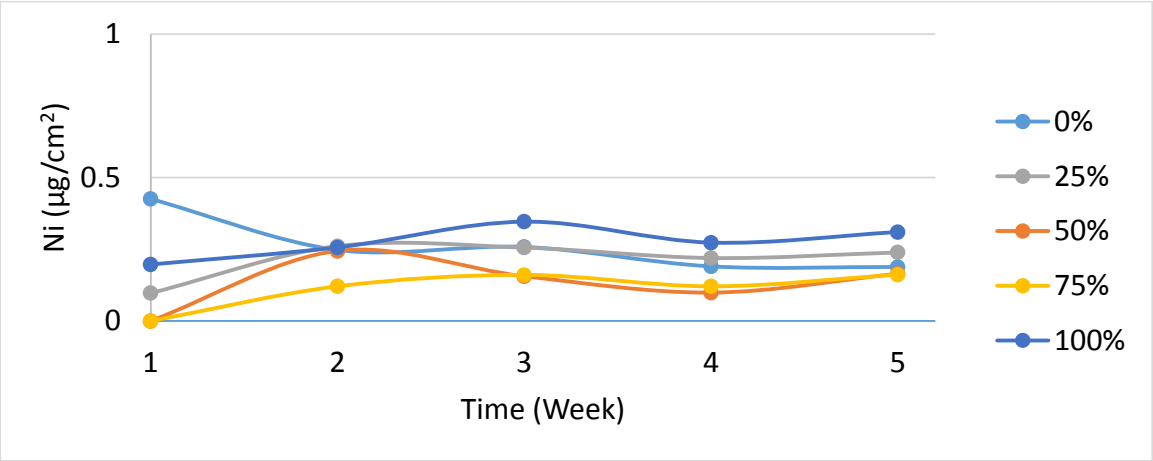

Figure 6-11 Mean amount of Ni released from Co-Cr castings after immersion into artificial saliva at pH 4 for five consecutive weeks

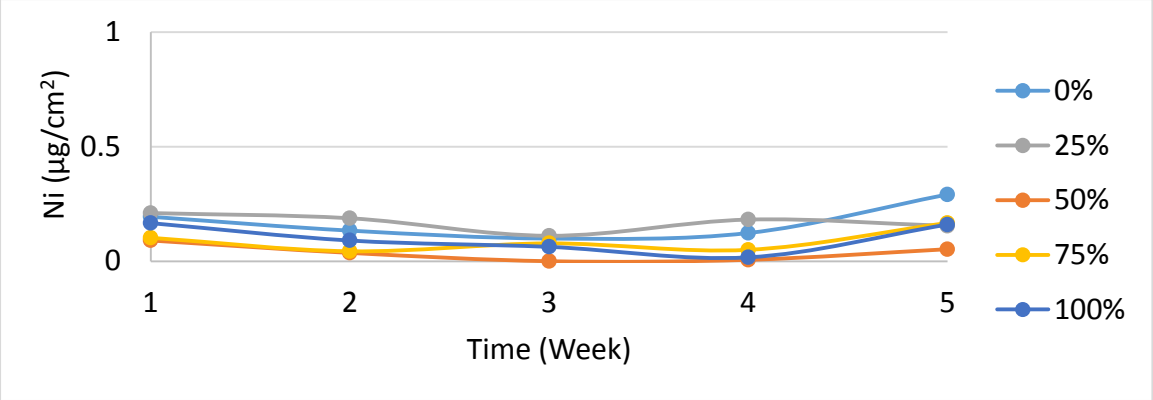

Figure 6-12 Mean amount of Ni released from Co-Cr castings after immersion into artificial saliva at pH 6 for five consecutive weeks

6.4.6 Statistical analysis

Data were analysed using a two way analysis of variance (ANOVA), at the 95% confidence level P= 0.05, and the multiple comparisons summary was used to indicate if any combinations differed significantly (Table 6-10). More specific analysis was carried out for the results of each pH value. The Tukey post hoc test was used to distinguish significant differences between mean values. Statistical analysis was carried out for Co only; negligibly small amounts of the other elements were released. Tests of between-subjects effects showed that pH value and test group have significant effects on the amount of ions released. However, immersion time does not have a significant effect.

Table 6-10 Tests of between-subjects effects

Source	Sig (P value)
Immersion time	.993
pH value	.000
Test group (recycled content of alloy)	.001
Immersion time * test group * pH value	1.000
Immersion time * test group	1.000
Immersion time * pH value	.980
Test group * pH value	.000

6.4.6.1 Solution at pH 4 (Co ions release)

For the pH 4 solution, data analysis revealed that the test group (recycled content of alloy) has a significant effect on the amount of ions released (p= 0.000). However, within each test group, immersion time has no effect (p= 0.994). In addition, the interaction of test group (recycled content of alloy) and immersion type (Test group * immersion time) showed no significant different (p= 1.000) (Appendix 1, Table 1-28). Tukey HSD revealed that the second test group (CoCr-25) documented significant differences with all the other test groups (p< 0.05), while no significant differences were documented between all the other test groups (p> 0.05) (Appendix 1, Table 1-29).

6.4.6.2 Solution at pH 6 (Co ions release)

For the pH 6 solution, data analysis revealed that test group (recycled content of alloy) has a significant effect (p= 0.004). However, within each test group (recycled content of alloy),

immersion time has no effect (p= 0.927). In addition, the interaction of test group (recycled content of alloy) and immersion type (Test group * immersion time) showed no significant difference (p= 1.000) (Appendix 1, Table 1-30). Tukey HSD revealed significant differences were documented between the test group containing 75% recycled alloy and all the other test groups (p< 0.001). However, no significant differences were documented between the other four test groups (p> 0.05) (Appendix 1, Tables 1-31).

6.4.7 Daily release of Co from Co-Cr alloy

For the purpose of comparing results with other results in the literature the amount of Co released per a day is presented in Table 6-11.

The difference between the maximum amount of ions released by CoCr-100 in pH 4 solution (0.23 μg/cm^2.day) and the maximum amount released from CoCr-0 (0.22 μg/cm^2.day) is only 0.01 μg/cm^2. For the solution of pH 6 the difference between the comparable test groups is very close and equals 0.03 μg/cm^2.

Table 6-11 Mean concentrations and standard deviations of Co released (μg/cm^2.day) into solutions of pH 4 and pH 6

Test group	Immersion time (Day)	Co (μg/cm^2.day) pH 4		Co (μg/cm^2.day) pH 6	
		Mean	SD	Mean	SD
CoCr-0	7	0.22	0.43	0.15	0.31
	14	0.11	0.47	0.07	0.27
	21	0.08	0.48	0.04	0.27
	24	0.06	0.46	0.03	0.28
	35	0.04	0.50	0.03	0.25
CoCr-25	7	0.12	0.29	0.14	0.32
	14	0.07	0.30	0.07	0.35
	21	0.04	0.23	0.04	0.30
	24	0.03	0.24	0.04	0.27
	35	0.03	0.24	0.03	0.32
CoCr-50	7	0.24	0.73	0.13	0.14
	14	0.13	0.62	0.06	0.08
	21	0.08	0.66	0.04	0.15
	24	0.06	0.62	0.03	0.15
	35	0.05	0.59	0.02	0.18
CoCr-75	7	0.18	0.23	0.20	0.56
	14	0.10	0.25	0.08	0.70
	21	0.07	0.26	0.07	0.52
	24	0.05	0.27	0.04	0.09
	35	0.04	0.27	0.04	0.60
CoCr-100	7	0.23	0.36	0.12	0.50
	14	0.10	0.32	0.05	0.36
	21	0.07	0.32	0.04	0.47
	24	0.06	0.36	0.03	0.53
	35	0.04	0.39	0.02	0.53

6.5 Discussion

The release of corrosion products is investigated using analytical methods, in which the metal ions released are analysed by analytical instruments, or electrochemical methods, in which polarization tests are used, and corrosion rate is estimated.

Analytical methods have been used in studies on developed alloys, such as Co-Cr alloys containing noble metals [241,242], comparing different types of alloy, investigating the effect of a thermal or surface treatment on castings, such as ceramic firing cycles or finishing and polishing procedures [105], and evaluating the effect of the environment surrounding restorations, such as pH of saliva, and tooth brushing and bleaching [243,244]. In this study, an analytical method was applied to investigate the elements released from castings produced from recycled alloys in different proportions.

For biological tests, where living cells are used, the recommendation of ISO 10933: 2000 is used to determine the test piece to the immersion solution surface area [245], where the recommended test piece surface area to volume ratio is 0.5-6.0 cm^2/mL [244,246]. For other in-vitro non-biological tests, researchers use volumes of solution, which are adequate to the size of their test pieces and design of their methodology.

The surface area of the test piece in this study was 0.636 cm^2. The surface area for fixed restorations varies from about 0.33 cm^2 for the exposed palatal metal collar of a metal ceramic crown to about 1.50 cm^2 for all-metal crown [243]. Some researchers used disc shape test pieces [247], others used plate shape castings in rectangular or square shape [248,249]. Milheiro [250] investigated the influence of test pieces shape on the corrosion of palladium-based dental alloys and found that it has a significant effect on the amount of ions released.

The solution used for immersion varied between the different types of artificial saliva solutions of different pH values [249], NaCl solutions [6], biological mediums [244] and other corrosive solutions, such as hydrogen peroxide [243] . ISO 10271: 2001 [251] was also used in which test pieces are immersed in acetic acid and NaCl solution at pH 2.3 [242].

Researchers presented their results using two types of units of measurement, elemental solution concentration (ppb and ppm) [6] or elemental release per surface area (μg/cm^2) [242]. In this study, for the purpose of comparing the results of the different test groups, data were expressed in μg/cm^2. In order to compare results with other studies, μg/cm^2.day was also used. Most studies introduced the chemical composition of alloys as (mass%), which makes comparison between studies easier, while studies interested in developing new alloys or adjusting the composition of existing ones have used the atomic percentage (at %) [252].

6.5.1 Correlation between ion release, surface roughness and porosity

6.5.1.1 Ni-Cr alloy

Castings containing 50%, 75% and 100% recycled alloys and immersed into solutions of pH 4 and pH 6 exhibited higher ion release values than castings containing 0% and 25% recycled alloys (Table 6-4 and Table 6-5). However, for PH 4, larger amount of ions was released from the NiCr-50 and NiCr-75 test groups than the NiCr-100 test group.

Results of mean % area of porosity evaluation does coincide with the results of the ion release test; casting containing 50%, 75% and 100% recycled alloys demonstrated significantly higher mean % area of porosity values (0.15%, 0.14%, and 0.62% respectively) than those documented by the NiCr-AM-0 and NiCr-AM-25 (0.09% and 0.08% respectively) (Table 3-5). This observation suggests an effect of porosity occurrence on the amount of ions released.

No significant differences in surface roughness values (Ra) were documented between the polished castings of the Ni-Cr alloy test groups (Table 4-3).

6.5.1.2 Co-Cr alloy

For castings immersed into solution of pH 4, no significant differences in the amount of ions released were documented between the CoCr-0, CoCr-50, CoCr-75 and CoCr-100 test groups, casting containing 25% gave lower mean values (Table 6-8). For castings immersed into solution of pH 6, the amount of ions released from the CoCr-75 was higher than the other test groups.

Results of mean % area of porosity evaluation show that CoCr-AM-100 demonstrated higher values than the other test groups at 0.11% (Table 3-4). No significant differences were found between the test groups containing up to 75% recycled alloys. This increase in the mean porosity value did not result in an increase in the ion release from casting.

No significant differences in surface roughness (Ra) values were documented between the test groups of Co-Cr alloy after the application of conventional polishing (Table 4-2).

6.5.2 Chemical composition of castings

A variation in the chemical composition was detected in recast alloys (Table 3-6 and Table 3-7). Lower corrosion resistance and higher ions release for cast alloy is related to local variations in composition and the heterogeneous microstructure with the presence of carbides and different phases. In castings produced from recast alloys, carbon was detected (Table 3-10). Carbon presents in dental alloys in a trace amount (> 1%), and is usually not documented in the alloy composition provided by manufacturers. The presence of carbon in the form of carbides at grain boundaries may deplete the area of potentially important passive elements, such as Cr, which may lead to an acceleration of corrosion in these areas.

Grain boundaries and interdendritic regions are sites of structural discontinuity, microstructural and chemical dissimilarity to the bulk grains. These differences from the bulk affect the corrosion behaviour of casting [105,253]. In this study, dendritic and interdendritic areas in castings produced from surplus alloys varied in their chemical composition (Table 3-8 and Table 3-9). With the presence of precipitates, this leads to preferential corrosion of specific areas of the alloy.

Elements released from castings depend on the structure and composition of alloys, as well as the characteristics of the oral environment [157]. Therefore, alloys, which are to be used in the mouth, should resist the degradation caused by the humidity, temperature and pH changes. Moreover, in the mouth, ions in the interfacial layer are removed continuously with abrasion of food, liquids and toothbrushes [254]. However, in this study, the environment in which test pieces were stored was controlled, and hence, composition of the castings and their surface characteristics is expected to affect the results obtained.

6.5.3 The passive film and its relation to ion release

Co-Cr and Ni-Cr exhibit a passive form of corrosion, where an in-soluble, protective corrosion-product film is formed. With the formation of three-dimensional metal oxide film of limited ionic conductivity, the corrosion reaction rate is slowed to very low levels. The corrosion behaviour of an alloy depends extensively on the integrity, composition, thickness (< 5 nm) and homogeneity of this protective film. If the passive film is broken or dissolves due to mechanical or chemical factors, casting may perform an active corrosion behaviour and dissolution can occur [157]. Casting containing surplus alloys demonstrated changes in the chemical and microstructural characteristics which might change composition of the passive layer and increase in element release.

6.5.4 Surface topography

Castings containing recycled alloys demonstrated higher mean % area of porosity; so for the same test piece, a higher surface area is available for corrosion to occur and more anodic sites within the pores. Castings with surface flaws are more likely to exhibit localized forms of corrosion, such as pitting, and crevice corrosion. Where the bulk of the casting surface is protected by the passive film, corrosion occurs in those areas where the film are broken down or cracked. Pitting corrosion is a localized attack that results in holes on the casting surface. Ions migrate towards these holes and molecules react with water molecules on the metal surface. As a result, metal chloride and hydroxyl ions are produced. This oxidation process is known as metal dissolution. Pores on the casting surface can demonstrate the same behaviour of pits, and so a similar process is expected to occur in porous surfaces. In addition, flaws on the casting surface can cause crevice corrosion, which is a result of the limited diffusion of electrolyte from within a crevice leading to hydrolysis of metal cations, and thus a drop in pH [157].

6.5.5 Ions released over the weeks of immersion

In the current study, for some of the test groups, the amount of Ni and Co ions released was greater in the first 2-3 weeks, and then decreased during the subsequent weeks (Figures 6-4, 6-5, 6-7 and 6-8). For other test groups, the total amount of ions release was steady, decreased or only slightly insignificantly increased over the last two weeks of immersion

(Figures 6-3, 6-6 and 6-9). It can be suggested that there is always a certain amount of ions released. However, two stages of release are suggested to occur; firstly, relatively rapid loss of ions followed by a steady slower process.

The observation that the amount of ions released from castings produced from surplus alloy did not remain high and gradually reduced supports the suggestion that the oxide layer formed on these castings was protective enough as that formed on the castings produced from new alloy. The increase in the amount of ions released from castings produced from surplus alloys in the first week of immersion is mainly due to other factors rather than pitting corrosion, such as the heterogeneous microstructure, chemical characteristic of castings. A similar observation was documented by Sian [249], who investigated Ni release from nickel- based alloys, and found that for most of the alloys tested, a steady rate of Ni release begins after either 2 or 3 weeks.

For other test groups, where the amount of ions released was less in the first two weeks the occurrence of pitting and crevice corrosion is expected to accelerate the rate of corrosion and ions released from castings, as any passive layer formed on the surface would be lost. Thus, the amount of ions released from the castings would be expected to be higher than the first week.

6.5.6 Previous studies

Al-Hiyasat [93] investigated the effect of recycling alloys on the ions release from Ni-Cr alloys, and documented a high level of release compared to the results documented in this study, for fully recycled castings, the range of elements released in Al-Hiyasat' s study was 219 ppb to 501 ppb. However, in Al-Hiyasat' s study, test pieces were stored in a culture medium. In addition, only one combination of new to recast alloy content were used (50% new with 50% recast).

Although Ameer [255] was interested in evaluating the effect of recasting base metal alloys on their biocompatibility, the focus in Ameer's study was on comparing between the chemical and electrochemical methods used to analyse ion release from alloys and observing the effect of altering factors related to measuring corrosion rate rather than evaluating the effect of recycling alloys on corrosion rate.

Differences in alloy composition, solution components, immersion period, detection limit of instrument has to be taken into account when comparing the results of different studies. Comparing results of studies using (ICP-OES), which is sensitive to Ni, Co, Cr and Mo, with results of electrochemical tests estimated by linear polarization may not be reliable. It has been suggested that element release rates estimates by the linear polarization test are usually slightly higher than the respective corrosion rates estimated by ICP-OES. The estimation of corrosion rates is based on the concentrations of the released elements. It is likely that some of the corrosion products might adhere to the alloy surface or the container surface or are lost during sample preparations, and would not be available for detection by the instrumental analysis of the solutes, and thus remain undetectable [256]. However, Al-Hity et al [254], who investigated the correlation between electrochemical and immersion tests, concluded that the corrosion behaviour of dental alloys, noble and base metal, can be predicted using the static immersion tests.

6.5.7 Amount of ions released

In this study, the amount of ions released from all test groups were very small compared to amounts taken in daily diets, which can, for example, include up to 20 µg /L of Ni in drinking water, as well as 87 mg in food per annum [257]. It has to be noted that the amount of elements released from dental restoration will be in addition to the amount consumed in daily diet.

According to the classification developed by Manaranche & Hornbbrger [238], the result of this study is classified as type I, which represents the smallest possible amount of ions released from a dental alloy. A similar observation was documented by Ozdimer & Arikan [120], who investigated the amount of corrosion products released from two Ni-Cr base metal alloys and concluded that recasting has a negligible effect on surface texture and on the amount of corrosion products released from the alloys tested. However, immersion medium (lactic acid and NaCl) and the instrument used to measure the ions release (flame model Atomic Absorption Spectrophotometer) are different from those used in the current study.

Results of the current study are within the lower values compared to other studies in the literature**.** In this study, the highest accumulative amount of Ni release was for the Ni-50

test group in week two in a solution of pH 4 (7.68 μg/ cm^2); this equals 0.55 μg/cm^2 daily. While for pH 6, the highest amount was released from the Ni-50 in the first week (4.86 μg/cm^2), which equals 0.68 μg/cm^2 daily. These results are comparable to those obtained by Al-Salhi [243], who aimed to assess the effect of increasing the concentration of hydrogen peroxide on the ion release of Ni-Cr castings produced from new alloy and documented the results over 24 hours in μg/cm^2, for pH values, 6.41, 5.62, 4.75, and 3.83; the amount of Ni released was, 0.26 μg/cm^2, 0.90 μg/cm^2, 5.05 μg/cm^2 and 8.23 μg/cm^2 respectively.

Oyar [6] investigated the effect of immersion period and media on the ion release of test pieces containing recycled alloys. Oyar documented a value of 0.023 μg/cm^2 of Ni released over three days from a new alloy, in artificial saliva of pH 6.7, which is different from the pH values used in the current study. In this study, Ni released from new alloy in a pH 6 solution ranged from 0.03-0.25 μg/cm^2 a day. For castings containing 50% recycled alloys, Oyar observed a value of 0.05 go/ cm^2. The value documented in this study for a comparable test group was 0.08-0.69 μg/cm^2 .day. For a solution of pH 4, Oyar documented higher values of element release than those documented in the current study. However the immersion media used was NaCl. Composition of the exposing medium affects the amount of ions released even if the pH value is equivalent [244]. In addition, atomic absorption spectrometry (AAS) was used; where detection limit (μg/L) varies between analytical instruments.

6.5.8 Chromium release

In the current study, amounts of Cr released from castings produced from new alloys and castings containing recycled alloys were negligible. The largest amount of Cr ions released from the NiCr-100 test group in solution of pH 4 (0.06 μg/ cm^2 in week two, which equals 0.004 μg/ cm^2 a day) (Table 6-4).

Other studies have also reported similarly low Cr release in artificial saliva solutions [253,256,258]. In our study, there was an increased release of Mo, Ni and Co from Ni-Cr and Co-Cr alloy compared to Cr. This finding is in agreement with previous investigations [105].

Chromium content affects corrosion behaviour of alloy. Cr content in the alloys used in this study was high (22% and 31%). Alloys containing < 20% Cr content demonstrate better

corrosion behaviour. Similar results were documented by Wylie [259], alloys containing 25 mass% Cr demonstrated better results compared to low Cr content alloys (> 20%). This result confirmed the findings of Huang [260], who also showed a lower corrosion resistance for alloys with 12.4–13.6 mass% Cr compared with alloys containing more than 21 mass% Cr [259]. In addition, It has been documented that the amount of Ni released in both acidic and alkaline media increases when the amount of Cr in an alloy drops below 16 to 20 mass% [6].

It has been suggested that Ni-Cr alloys containing at least 16-22% Cr and 9-14% Mo can form a complex stable passive oxide layer that provides adequate corrosion resistance, whereas a low Cr and Mo content in the Ni-Cr-Mo alloy is associated with a high corrosion rate and susceptibility to accelerated corrosion processes [256]. Alloy elements have strong beneficial influence on the corrosion resistance of Ni-Cr and Co-Cr alloys. The passive film of these alloys consists essentially of Cr in its trivalent state which is (Cr III) much less toxic than hexavalent (Cr VI) state. The presence of an inner oxide layer rich in Cr (barrier layer) is a primary factor in enforcing passivity.

6.5.9 Molybdenum release

In the current study, negligible amounts of Mo were released (0.06-0.55 µg/cm^2 for Ni-Cr alloy and 0.00-1.16 µg/cm^2 for Co-Cr alloy) (Tables 6-4, 6-5, 6-8 and 6-9). Beside Cr, Mo is incorporated into the passive film; Mo acts in two different ways, it locates at defects and cervices, which act as anodic sites, and slows the anodic dissolution because of its higher bond strength with metals in alloy. MoO_4 can also form in a solid state in the exterior regions of the film. This MoO_4 layer is positively-charged ions selective, and resists the incorporation of negatively-charged ions, such as Cl^- and OH^-. Thus, the MoO_4 layer reinforces the protectiveness of the high-Cr containing barrier layer by allowing its growth and prevents the breakdown of the passive film, and the subsequent initiation of localized corrosion [261]. In this study, EDAX analysis of casting containing 100% recycled alloys shows a reduction in the amount of Mo (4.48% ± 0.18 in CoCr-AM-100) (Table 3-6). However, for CoCr-CB-100, no change has been documented and the amount of Mo (5.82% ± 0.09) was within the desired amount for adequate corrosion resistance (5.5 mass%) [262].

Studies have shown that the Co–Cr and Co–Cr–Mo alloys are resistant enough to corrosion [254]. Cr ions dissolve as Cr_3, which then combines with NO_3 or other oxidizers to form an

oxide layer (Cr_2O_3) on the surface. This layer slows down the corrosion process [6]. The release of Cr from a dental alloy is an undesirable characteristic in terms of the ability to resist corrosion.

6.5.10 Iron release

In this study, castings containing 100% recycled alloy released more iron ions than the other test groups. For Ni-Cr castings, the largest amount of ions was released from NiCr-100 in the second week (2.34 μg/cm^2 which equals 0.17 μg/cm^2.day). While for Co-Cr castings, the largest amount of ions was released from CoCr-100 in the third week (1.82 μg/cm^2 which equals 0.09 μg/cm^2.day). However, these amounts are far below the recommended dietary allowances for iron.

Corrosion rate is governed largely by the rate at which oxygen reacts with absorbed atomic hydrogen, thereby depolarizing the surface, and allowing the reduction reaction to continue. For pH values below approximately 4, ferrous oxide (FeO) is soluble. Thus, the oxide dissolves as it is formed rather than depositing on the metal surface to form a film. In the absence of the protective oxide film, the metal surface is in direct contact with the acid solution, and the corrosion reaction continues at a greater rate than it does at higher pH values. It is also observed that hydrogen is produced in acid solutions below a pH of 4, indicating that the corrosion rate no longer depends completely on depolarization by oxygen, but also on a combination of the two factors (hydrogen evolution and depolarization).

6.5.11 Effect of pH value of solution

For both types of alloys statistical analyses revealed that pH values had a significant effect on the amount of ions released (Table 6-6 and Table 6-10). The value of pH greatly affects corrosion behaviour for particular metals. Acidic solutions have a greater number of hydrogen ions, and alkaline solutions have a greater concentration of hydroxyl ions. The pH defines the acidity or alkalinity of a solution. It is defined as –log (H+); an increase of one pH unit is equivalent to an order of magnitude, or factor of 10, decrease in hydrogen ion concentration [157].

In this study, the pH values of solutions used were 4 and 6. These values are within the range of pH encountered during the ingestion of various foods and liquids, and under bacterial plaque, which often adheres to dental alloys. pH changes from 2 to 11, where different types of food have different pH levels, and most of them are less than 7 [10].

The pH value of dental plaque decreases for 30 minutes after each meal. These changes may affect ion release from dental alloys. For this reason, pH 4 was chosen. In addition, it is important to assess the corrosion behaviour of dental alloys in acidic solutions due to the low pH encountered in crevices in addition to the variable pH conditions routinely changing in the oral cavity through the variety of foods and liquids ingested [259]. Moreover, the lability of elements appears significant at pH of 4 or below.

The present study verifies previous reports indicating that the release of ions from alloys increases with a decrease in the pH of the immersion media. Wataha [244] investigated the effect of short-term exposure of noble and base metal alloys to reduced pH on the releas of elements. Wataha found that the exposure of cast alloys to acidic environment increases elemental release from Ni-Cr alloys.

6.5.12 Effect of immersion time

In the current study, statistical analyses revealed that immersion time did not have a significant effect on the amount of ions released (Table 6-6 and Table 6-10).

Dental restorations are expected to last for several decades before either a failure occurs or the prosthesis is replaced [263]. Observing the rate of elements released over extended time periods can only give an indication of the alloy behaviour over time in the oral cavity. The environment surrounding a dental restoration, can not easily be simulated in an in-vitro study, such as the continuous flow of saliva which can minimise the accumulation of ions in the oral cavity, fluctuating pH and temperature can affect the release behaviour of a casting. Covington [264] reported significant Ni release (about 2.5 $\mu g/cm^2$) even at pH 6 when the extraction time was 120 days. Another study demonstrated that even 30 minute exposures to these environments increased corrosion behaviour [244]. However, it has to be considered that under dynamic conditions, the release pattern may differ compared with static conditions [265]. A study by Mutlu-Sagesen [266], who investigated the effect of pH value on the ion release of metal-ceramic casting alloys, found that ion release from alloys is

pH dependent and the highest amount of ion release occurred after 60 days of immersion regardless of pH value.

6.5.13 Condition in the mouth and saliva

Natural saliva is a complex compound containing various elements, and varies according to the time of day, diet of the patient and their general and oral health. Thus, it is difficult to simulate natural saliva. However, a simple composition of artificial saliva is preferable to avoid interference with the analysis of element release from alloys. About 60 formulae for artificial saliva solutions are reported in the literature [256]. This reveals the relative difficulty to simulate the chemical composition of natural saliva. In this study, PBS artificial saliva was used, it is easily prepared and its simple composition reduces the possibility of interference with the ICP-OES analysis for element release. In this study, each week saliva was replenished. Non-replenished artificial saliva solutions for extended exposure time may lead to the conclusion that the release rate increases initially, and subsequently remained constant because of the saturation of the immersion solution [256,267].

7 Overall discussion

The quality of dental restorations including alloys as part of a prosthesis, such as composite and ceramic bonded restorations and removable partial dentures, depends extensively on the quality of the cast parts. In this study, combined characteristics of castings, produced partially or completely from surplus alloys, were evaluated. The questions this study sought to answer were how would the recasting process change these characteristics; would these changes, if detected, affect the restoration durability, what effect would laboratory procedures, such as finishing and polishing have on the surface roughness and element release of castings containing surplus alloy.

This research contributes to the global interest in recycling metals. The potential of savings in terms of energy, labour and natural resources caused more interest in recycling and reusing of materials, where costs of extraction, mining and manufacturing procedures can be subtracted, and waste and surplus metals can be reduced. It also contributes to the dental technology economy, where the desire to minimise the cost of dental restoration cost is achieved through different approaches, among them is the reduction of the expense of the materials used which forms, in combination with the labour cost, over 60% of the direct cost in the production of a dental restoration [2].

Minimising the cost of producing a dental restoration becomes more essential in medium and low income countries, where there is limited availability of oral health care, service facilities and dental materials. In such countries, reusing alloys will offset cost and availability limitations of alloys. The research on new biomaterials and advanced manufacturing technologies has grown significantly over the last 10-25 years. However, such materials are mainly feasible in high income and developed countries, and the use of alternative biomaterials may not apply directly to low- and middle income countries [268]. Acceptance of a new material and technology depends on factors far broader than their adequate properties and ease of use, in places where electricity, for example, is expensive and not constantly available, producing a dental restoration relying on digital equipment to produce a dental restoration is not entirely practical nor acceptable [269]. The application of new technologies requires the development in software engineering, dental materials and

digital equipment and the communication between dental laboratories and dental surgeries to be effective and systematised, and this is only available in developed countries.

Applications of base metal alloys vary widely, and hence, to evaluate casting quality (*in-vitro*), microstructure and chemical composition of castings are always crucial in the assessment. However, among the different properties of castings, i.e. mechanical, physical and biological properties, only those which are critical to the application of the casting should be tested. In this study, the combined surface roughness, ion release, and metal-ceramic bond strength were the crucial characteristics to be assessed as they are critical to the success of bonded crowns. Other properties, such as hardness and modulus of elasticity are more critical for cast components of removable metal frames, such as clasps.

The available literature concerning the reuse of base cast alloys either advocated for or against the use of castings containing surplus alloy [5][6][7][8]. However, deviation and changes occurring in characteristics of castings should not automatically cause the complete rejection of the practice of recasting. The materials used to fabricate a restoration are one of two prime factors contributing to the success of a restoration; the manipulation and processing of materials is the other factor. Casting is a multi-stage process requiring the use of many materials and techniques and more than one technician might be involved in the production of a restoration; inappropriate manipulation can lower the quality of a comparable material. On the other hand, careful manipulation can produce the maximum of a less competitive and inferior quality material. In this study, materials were carefully and skillfully used, castings containing surplus alloys demonstrated comparable characteristics to those produced from an entirely new alloy.

It was not possible to use non-destructive methods to evaluate the quality of castings. Firstly, some defects cannot be detected without sectioning the castings. Secondly, testing instruments, such as the 3–point bond strength testing machine requires test pieces of a particular shape and size. In addition, for analytical instruments, such as SEM and EDAX, test pieces have to be flat and exposed to a particular surface treatment. Other analytical instruments, which need less preparation, such as light microscopy and stereoscopy can only be used for primary evaluations.

Analysis of the available literature revealed that the majority of studies conducted on recasting processes used one combination of new to recast alloy (50% new +50% surplus) of disc-shaped test pieces of different thicknesses, which responded differently to the casting procedure of a similar protocol. Using cast test pieces of a size and dimension resembling the restoration type (full crown, core, removable frame, and clasp) can result in more valid data than using test pieces of standardised or conventional size and thickness. In addition no clear correlation was made between the characteristics tested and their contribution to the restoration quality in a particular application.

The methodological approach used was a comprehensive structural evaluation namely (porosity in the microstructure, chemical composition analysis (EDAX), physical (surface roughness), mechanical (bond strength) and biological (ions release) which allowed for a comprehensive evaluation. This approach is expected to be effective for further tests of other types of alloys for different applications, such as alloys for removable frames and alloys for brackets and other metallic components of orthodontic appliances. Adjustments to this approach in the type of properties to be tested and manufacturing procedures protocol to be followed (melting method, casting procedure, sprue design, size of castings) can be made.

Castings containing only 75% new alloy demonstrated comparable results which show that the alloy is retaining its quality by using a small amount of new alloy, This result encourages researchers to move from the conventional way of using three groups of new and 50% new +50% surplus and 100% reused alloy to a more specific combinations such as 75% surplus + 25% new and 85% surplus and 15% new.

The majority of available literature proposes that recasting affects restoration properties. however, it is noted from the results of the current study that recasting did not necessarily negatively change casting properties, and therefore, future researches concerning recasting base metal alloys has to focus more on factors that enhance the quality of castings containing surplus alloy; these include melting duration and temperature, casting method, cleaning of surplus metal prior to recasting, surface treatment of bonded castings and finishing and polishing protocols.

Biocompatibility tests are essential for the initial evaluation of materials to be used in a patient's mouth. Results of this study showed that despite an increase in the amount of ions released from castings containing surplus alloys; this increase was not always significant and was within acceptable amounts. This emphasises the importance of not rejecting the concept of recasting based on the increase in the amount of ions released. For bonded crowns and bridges, only a small area of the metal is exposed to the oral cavity, In addition, these restorations can be fabricated with no metal exposed to the oral cavity. However, for metal frames of removable partial dentures this slight increase might be of significance where a wide area of the patient's palate is in intimate contact with this restoration. The application of the castings should be taken into account; this can be used as a general rule for future research drawn from the observations of this study.

In practice, results of this study can encourage alloys manufacturers to be more specific in regard to their recommendation about reusing their alloys. This needs further investigation to be carried out on the types and brands of the alloys they provide. Technicians, who already reuse surplus alloys, can enhance their practice by following careful procedures in cleaning surplus alloys, adding a weighed amount of new alloy, melting alloys in a controlled environment, and avoid possible organic and non-organic contamination of castings.

This research is expected to draw the attention of people who are interested in the regulations of medical devices. Most regulations are concerned the quality of dental materials before the application of laboratory procedures, where all dental materials must meet ISO standards. However, no regulations control dental restorations, which are classified as medical devices, after the manufacturing process and before they are fitted into the patient's mouth.

The author tried to collect information at a national level on the usage of base metal alloys and the lost wax technique by contacting well-known companies, such as Skillbond. However, no data or figures were revealed and only general information was provided; for example, most laboratories are still using the lost wax technique and the use of base metal alloys is particularly popular with NHS-based services. In addition, a number of laboratories were contacted for information on recasting base metal alloys to evaluate how common this practice is. Nevertheless, no data could be reported, as no precise records are kept by

laboratories. All the published literature, including the most recent (2015) [5], mention that recasting dental alloys is a common phenomenon, however they do not provide data or figures.

7.1 Limitations of this study

In the present study, qualitative and quantitative methods were applied to identify and quantify the effect of recasting process. SEM was used for chemical analysis of bonded castings. However, X-ray photoelectron spectroscopy (XPS) is more appropriate to use for surface analysis. An analysis of the bulk and the surface of castings would have helped to understand the variation in the distribution of elements through the metal ceramic interface. XPS could have also been used to determine the depth of elements (oxides) in the casting at the ceramic-metal interface which can help in explaining the differences in the bond strength between each of the test groups. More quantitative analysis of the phases and participates might have helped in the explanation of the variation in elemental composition of castings containing surplus alloys, X-Ray Diffraction (XRD) analysis provides more details about the structure of different phases.

7.2 Future work

- To use alloys of removable cast frames and investigate the effect of recasting on the micro-hardness and modulus of elasticity, as well as examining casting surplus alloy multiple times.
- To investigate the *in-vitro* toxicity of the ions released from castings containing surplus alloys.
- To evaluate the threshold value of porosity size, and surface area at which a particular property of casting such as ion release is significantly affected.
- To investigate the effect of variables in surface treatment, such as Al_2O_3 size, oxidation cycle duration and temperature on enhancing bond strength to castings containing surplus alloy, and exposing the test piece to mechanical cycling in distilled water or artificial saliva prior to the bond strength test.
- To assess the depth of the oxide layer into the casting and its effect on bond strength

- To evaluate the effect of recasting process on castings' modulus of elasticity, and investigate its relation to metal ceramic bond strength.
- To investigate the different methods of cleaning surplus alloys, such as steam, acidic cleaning and ultrasonic cleaning, and assess its effectiveness in minimising contamination and the presence of inclusions and the occurrence of porosity.
- To assess the time needed to clean surplus metal and getting it ready for re-melting and evaluate the expense in regard to cost, time and labour and evaluate if these expenses outweigh the saving obtained from recasting

8 Conclusions

This work has shown an effect between alloy type and porosity occurrence in castings containing recycled alloys; however casting type (AM & CB) was found to be the significant factors in determining the effect of recycling alloy. Nickel-chromium all-metal castings exhibited the highest porosity occurrence values. In contrast, nickel-chromium ceramic-bonded castings gave in the lowest values of porosity against all the other test groups.

No definitive trend was observed in the relationship between the extent of porosity and pore count; however, irrespective of alloy type or casting size, fully recycled castings exhibited the highest mean % porosity and mean pore count against the other test groups. Adding 25% new alloy resulted in improved porosity values, lower than those exhibited by castings containing 100% recycled alloys, thus providing a beneficial effect on the microstructure in term of porosity occurrence and pore count.

Test groups of each alloy exhibited similarities in the chemical composition with up to 75% recycled alloys. Changes in the constitutions of constituent elements were found in castings containing 100% recycled alloys. However, the chemical composition of this latter group and that provided by the manufacturer and detected by EDAX were similar.

Manual polishing was effective and shown to improve the surface characteristics of castings. The polishing protocol not only reduced surface roughness of castings of the different test groups to comparable values, but also significantly reduced the high mean porosity values of castings containing 75% and 100% recycled alloys to achieve roughness averages less than the threshold value (0.2 μm). The effect of alloy type on initial and final surface roughness was not found to be significant.

Irrespective of alloy type, castings containing 100% recycled alloys exhibited the lowest metal-ceramic bond strength against all test groups. There was some evidence that a reduction in interfacial thickness resulted in an improvement in metal-ceramic bond strength, although this relationship was not linear. Similar to the porosity observations, adding 25% new alloy to castings resulted in a positive effect on bond-strength.

There was a level of interaction between porosity occurrence and metal-ceramic bond strength and porosity was shown to have a strong contribution to the metal-ceramic bond performance. The quality of casting surface and interfacial area in term of porosity is expected to have a great effect on bond strength rather than the thickness of the interfacial region and this view is supported by the type of metal-ceramic bond failure where remnants of ceramic were observed on casting surfaces.

Alloy type and composition were shown to have a significant effect on the distribution of elements through the metal-ceramic region, and hence, bond strength. The most prominent feature of the chemical analysis of the interfacial region is the diffusion of some alloy constituents (Ni and Cr) into the interfacial region. This diffusion was higher in test groups containing 75% and 100% recycled alloys. For Co-Cr alloy, the presence of these elements (Cr) in the CoCr (100%) was associated with a lower metal-ceramic bond strength compared with the other test groups. However, for NiCr-75%, the presence of these elements (Ni and Cr) did not affect the metal-ceramic bond strength value, which was the highest value documented amongst the other NiCr test groups. The increase in the oxygen content in the interfacial region of NiCr-100% compared to NiCr-0% was associated with the increase in interfacial region thickness. However, no definitive trend was observed in this relationship between the oxygen content and the interfacial region thickness of CoCr test groups in the interfacial region.

It was shown that the amount of ions released from castings was dependant on a combined effect of both pH value and casting content of recycled alloy. All test groups showed a low concentration of ion release, even those containing a high amount of recycled alloys, at an extreme pH value. For Ni-Cr alloy, castings containing 0% and 25% exhibited the lowest Ni ions release values against all test groups. There was some evidence that an increase in the extent of porosity resulted in an increase in the ion release, although this relationship was not linear. For Co-Cr alloy, the values of Co ions released from the majority of the test groups were comparable. No definitive trend was observed between the extent of porosity and the amount of ions released from castings.

There are several factors that determine the effect of recycling alloys on the casting's quality. Investigating these factors on the most commonly used alloys allowed it to be

possible to identify the most important factor in determining cast quality. It is suggested that porosity is the most influential factor determining the quality of other characteristics, such as metal-ceramic bond strength and ion release.

Although superior results were produced by test groups produced from exclusively new alloys, all test groups exhibited acceptable results. Based on these findings, it can be concluded that using twice cast base metal alloys is expected to allow castings to perform as required for a dental prosthesis. Adding a small amount of new alloy will be needed to minimise the negative effects of re-melting alloys. In addition, based on the outcomes of this study, dental laboratories are recommended to be consistent and record the amount of reused alloy being used during casting, and to always add a small amount of new alloy. In the current study, alloys were exposed to the melting process only twice, it is recommended for future research to go beyond the double casting and observe its effect on casting quality when mixed with a small amount of new alloy.

9 References

[1] Berry J, Nesbit M, Saberi S. Petridis H. Communication methods and production techniques in fixed prosthesis fabrication: a UK based survey. Part 2: production techniques. British Dental Journal 2014;217:E13.

[2] Oral Health Professional Association. Submission Inquiry IntoThe Supply Of Dental Prosthesis. 2014:1–13. Available from http://www.parliament.act.gov.au/__data/assets/pdf_file/0007/664702/06.-Oral-Health-Professionals-Association.pdf

[3] Northeast SE , Noort van, Johnson A, Winstanley R B, White GE. Metal-ceramic bridges from commercial dental laboratories: alloy composition, cost and quality of fit. British Dental Journal 1992;172:198–204.

[4] Ekblom K, Smedberg JI, Moberg LE. Clinical evaluation of fixed partial dentures made in Sweden and China. Swedish Dental Journal 2011;35:111–21.

[5] Vaillant-Corroy A-S, Corne P, De March P, Fleutot S, Cleymand F. Influence of recasting on the quality of dental alloys: A systematic review. The Journal of Prosthetic Dentistry 2015.

[6] Oyar P, Can G, Atakol O. Effects of environment on the release of Ni, Cr, Fe, and Co from new and recast Ni-Cr alloy. The Journal of Prosthetic Dentistry 2014;112:64–9.

[7] Yavuz T, Acar A, Akman S, Ozturk AN. Effect of Surface Treatment on Elemental Composition of Recast NiCr Alloy. Materials Sciences and Applications 2012;03:163–7.

[8] Ayad MF. Compositional stability and marginal accuracy of complete cast crowns made with as-received and recast type III gold alloy. The Journal of Prosthetic Dentistry 2002;87:162–6.

[9] Knott B. A Study of the Recycling and Recovery Infrastructure for Materials Critical to the UK. Executive Summary Report. Materials KTN. 2011. (Accessed 14 Jul 2014). Available from http://www.iom3.org/news/2011/jun/15/recycling-and-recovery-infrastructure-critical-materials

[10] Anusavice KJ. Phillips' science of dental materials. 12th ed. Philadelphia: W.B. Saunders; 2013.

[11] Thopegowda NB, Shenoy K, Shankarnarayana RK, Kukkila J, Vaddya SB, Gingipalli K. Recycling of Materials used in Dentistry with Reference to its Economical and Environmental Aspects. International Journal of Health and Rehabilitation Sciences 2013;2:140–5.

[12] Nelson DR, Palik JF, Morris HF, Comella MC. Recasting a nickel-chromium alloy. The Journal of Prosthetic Dentistry 1986;55:122.

[13] Hesby DA, Kobes P, Garver DG, Pelleu GB. Physical properties of a repeatedly used nonprecious metal alloy. The Journal of Prosthetic Dentistry 1980;44:291–3.

[14] Giacchi JV, Morando CN, Fornaro O, Palacio HA. Microstructural characterization of as-cast biocompatible Co–Cr–Mo alloys. Materials Characterization 2011;62:53–61.

[15] Cheng H, Zhao W, Chen R, Wu W-Q, Li X-R, Zheng M. Effects of recasting on the composition and microstructure of Ni-Cr ceramic alloy . Journal of Clinical Rehabilitative Tissue Engineering Research 2009;13 :7511.

[16] Khalaf HM, SS A-A, Alsaady AA. The effect of recasting on the Fatigue resistance of Co-Cr alloys. The Marietta Daily Journal (MDJ) 2008;5:205–12.

[17] Zai-xi D, Bao-cheng W, ZHANG S, others. Physical properties of Ni-Cr ceramic alloys after recasts. J Pract Stomatol 2004;20:743–4.

[18] Ruohong Liu, Liu R, Johnston WM, Holloway JA, Brantley WA, Dasgupta T. The effect of metal recasting on porcelain-metal bonding: A force-to-failure study. The Journal of Prosthetic Dentistry 2010;104:165–72.

[19] Peraire M, Martinez-Gomis J, Anglada JM, Bizar J, Salsench J, Gil FJ. Effects of recasting on the chemical composition, microstructure, microhardness, and ion release of 3 dental casting alloys and titanium. The International Journal of Prosthodontics 2007;20:286.

[20] Ayad MF, Ayad GM. Corrosion Behavior of As-Received and Previously Cast Type III Gold Alloy. Journal of Prosthodontics 2010;19:194–9.

[21] Bharti R, Wadhwani KK, Tikku AP, Chandra A. Dental amalgam: An update. Journal of Conservative Dentistry : JCD 2010;13:204–8.

[22] McCabe JF, Walls A. Applied dental materials. Oxford, UK; Ames, Iowa: John Wiley & Sons; 2008.

[23] Van Noort R. The future of dental devices is digital. Dental Materials : Official Publication of the Academy of Dental Materials 2012;28:3–12.

[24] International Organization for Standardization. ISO 22674 (E) Dentistry-Metallic materials for fixed and removable restorations and appliances. Geneva, Switzerland: 2006.

[25] Council on Dental Materials, Instruments and Equipment: Revised ANSI/ADA specification no. 5 for dental casting alloys. The Journal of the American Dental Association 1989;118.

[26] Powers JM, Sakaguchi RL. Craig's Restorative Dental Materials. 12th ed. Elsevier India; 2006.

[27] Wataha JC, Messer RL. Casting alloys. Dental Clinics of North America 2004;48:499–512.

[28] CEN/TC 55. Byrillum in Dental Alloys. Working Group Document N 459. 2005.

[29] Roach M, Zardiackas LD, Dellinger TM, Livingston M. Base metal alloys used for dental restorations and implants. Dental Clinics of North America 2007;51:603–27.

[30] Winkler S, Morris HF, Monteiro JM. Changes in mechanical properties and microstructure following heat treatment of a nickel-chromium base alloy. The Journal of Prosthetic Dentistry 1984;52:821–7.

[31] Morris HF. Veterans Administration Cooperative Studies Project No. 147/242. Part VII: The mechanical properties of metal ceramic alloys as cast and after simulated porcelain firing. The Journal of Prosthetic Dentistry 1989;61:160–9.

[32] Setcos JC, Babaei-Mahani A, Silvio LD, Mjör I a, Wilson NHF. The safety of nickel containing dental alloys. Dental Materials : Official Publication of the Academy of Dental Materials 2006;22:1163–8.

[33] Goyal MR, Goyal VK. Biomechanics of Artificial Organs and Prostheses. CRC Press; 2014.

[34] Niinomi M. Recent Metallic Materials for Biomedical Applications. Metallurgical and Materials Transactions 2002;33:477–86.

[35] O'Brien WJ. Dental materials and their selection. 4th ed. Quintessence Publ. Chicago; 2008.

[36] Wataha JC. Alloys for prosthodontic restorations. The Journal of Prosthetic Dentistry 2002;87:351–63.

[37] Van Noort R. :Introduction to Dental Materials. Elsevier Health Sciences; 2013.

[38] Beeley PR, Smart RF. Investment Casting.London, institute of materials. David Brown Book Company; 1995.

[39] Almughanu M. Spruing, investing and casting. (Accessed 21 Jan 2014). Available from http://www.slideshare.net/mahmoudway/spruingcasting-and-investing?related=1

[40] Chan D, Villa Guillory RB, Chung K. The effects of sprue design on the roughness and porosity of titanium castings. The Journal of Prosthetic Dentistry 1997;78:400–4.

[41] Baltag I, Watanabe K, Kusakari H, Miyakawa O. Internal porosity of cast titanium removable partial dentures: Influence of sprue direction on porosity in

circumferential clasps of a clinical framework design. The Journal of Prosthetic Dentistry 2002;88:151–8.

[42] Johnson A. The effect of sprue design and alloy type on the fit of three-unit metal/ceramic bridges. The European Journal of Prosthodontics and Restorative Dentistry 1995;3:241–5.

[43] Verrett RGG, Duke ESS. The effect of sprue attachment design on castability and porosity. The Journal of Prosthetic Dentistry 1989;61:418–24.

[44] Takahashi J, Kimura H, Lautenschlager EP, Chern Lin JH, Moser JB, Greener EH. Casting Pure Titanium into Commercial Phosphate-bonded SiO2 Investment Molds. Journal of Dental Research 1990;69:1800–5.

[45] Eliopoulos D, Zinelis S, Papadopoulos T. The effect of investment material type on the contamination zone and mechanical properties of commercially pure titanium castings. The Journal of Prosthetic Dentistry 2005;94:539–48.

[46] Oliveira PCG, Adabo GL, Ribeiro RF, Rocha SS. The effect of mold temperature on castability of CP Ti and Ti-6Al-4V castings into phosphate bonded investment materials. Dental Materials : Official Publication of the Academy of Dental Materials 2006;22:1098–102.

[47] Frenzel J, Zhang Z, Neuking K, Eggeler G. High quality vacuum induction melting of small quantities of NiTi shape memory alloys in graphite crucibles. Journal of Alloys and Compounds 2004;385:214–23.

[48] Viennot S, Lissac M, Malquarti G, Dalard F, Grosgogeat B. Influnce of casting procedures on the corrosion resistance of clinical dental alloys containing palladium. Acta Biomaterialia 2 2006;2:321–30.

[49] Mattox DM. Handbook of physical vapor deposition (PVD) processing. Second ed. William Andrew; 2010.

[50] Ivoclar V. Dental alloys processing manual (Accessed 17 Jul 2014). Avaiable from http://www.ivoclarvivadent.co.uk/en/products/alloys/successful-alloy-processing

[51] Brehm P. Bredent Casting Technique. First edit. bredent GmbH & Co.KG; 2007.

[52] Bauer JRDO, Grande RHM, Rodrigues-Filho LE, Pinto MM, Loguercio AD. Does the casting mode influence microstructure, fracture and properties of different metal ceramic alloys? Brazilian Oral Research 2012;26:190–6.

[53] Thompson GA, Luo Q, Hefti A. Analysis of four dental alloys following torch/centrifugal and induction/ vacuum-pressure casting procedures. The Journal of Prosthetic Dentistry 2013;110:471–80.

[54] Bauer J, Costa JF, Carvalho CN, Grande RHM, Loguercio AD, Reis A. Characterization of two Ni-Cr dental alloys and the influence of casting mode on mechanical properties. Journal of Prosthodontic Research 2012;56:264–71.

[55] Bezzon OL, Pedrazzi H, Zaniquelli O, da Silva T. Effect of casting technique on surface roughness and consequent mass loss after polishing of NiCr and CoCr base metal alloys: A comparative study with titanium. J Prosthet Dent 2004;92:274–7.

[56] Chen T J, Wang R Q., Ma Y, Hao Y. Effects of processing parameters on microstructure and ultimate tensile strength of thixoformed AM60B magnesium alloy. Materials Research 2012;15:687–97.

[57] Monroe R. Porosity in castings. AFS Trans 2005;5:10.

[58] Davis JR. Nickel, cobalt, and their alloys. ASM International (OH); 2000.

[59] Davis JR. Handbook of materials for medical devices. ASM International (OH); 2003.

[60] Baran GR. The metallurgy of Ni-Cr alloys for fixed prosthodontics. The Journal of Prosthetic Dentistry 1983;50:639–50.

[61] Lindqvist J, Åkesson U. Image analysis applied to engineering geology, a literature review. Bulletin of Engineering Geology and the Environment 2001;60:117–22.

[62] Diógenes AN, Hoff EA, Fernandes CP. Grain size measurement by image analysis : An application in the ceramic and in the metallic industries. Proceedings of COBEM 2005:6–11.

[63] Krupiński M, Labisz K, Dobrzański LA, Rdzawski Z. Image analysis used for aluminium alloy microstructure investigation. 2010;42:58–65.

[64] Galic I, Zivko-Babic J, Schauperl Z, Vuksic J. Metalographic Properties and Microhardness of Gold-Based Dental Castings. Acta Stomatologica Croatica 2008;42:255–66.

[65] Maksimovic VM, Cairovic a. D, Pantic JR, Cvijovic-Alagic IL. The recasting effects on the high gold dental alloy properties. Journal of Mining and Metallurgy, Section B: Metallurgy 2015;51:55–9.

[66] Karolina BEER, Palka K, Surowska B, Walczak M. A Quality Assessment of Casting Dental Prosthesis Elements Ocena jakościowa odlewanych elementów protetycznych. EKSPLOATACJA I NIEZAWODNOSC 2013;15:230–6.

[67] Goodhew PJ, Humphreys J, Beanland R. Electron microscopy and analysis. CRC Press; 2000.

[68] Schatten H. Scanning electron microscopy for the life sciences. Cambridge University Press; 2012.

[69] Imaging spectroscopy and analysis center. Scanning Electron Microscopy (SEM). (accessed 15 Jan 2014). Available from http://www.gla.ac.uk/schools/ges/research/researchfacilities/isaac/services/scanningelectronmicroscopy/

[70] Goldstein JI, Newbury DE, Echlin P, Joy DC, Fiori C, Lifshin E. Scanning electron microscopy and X-ray microanalysis. A text for biologists, materials scientists, and geologists. Plenum Publishing Corporation; 1981.

[71] My Scope. Australian microscopy and microanalysis research. (Accessed 15 Jan 2014). Available from http://www.ammrf.org.au/myscope/sem/practice/principles/

[72] Limandri SP, Carreras AC, Trincavelli JC. Effects of the Carbon Coating and the Surface Oxide Layer in Electron Probe Microanalysis 2010:583–93.

[73] Humphreys FJ, Materials M, Centre S. Grain and subgrain characterisation by electron backscatter diffraction. JOURNAL OF MATERIALS SCIENCE 2001;6:3833–54.

[74] Johnson T, Noort R van, Stokes CW. Surface analysis of porcelain fused to metal systems. Dental Materials 2006;22:330–7.

[75] Giacchi JV, Fornaro O, Palacio H. Microstructural evolution during solution treatment of Co-Cr-Mo-C biocompatible alloys. Materials Characterization 2012;68:49–57.

[76] Kern M, Thompson VP. Sandblasting and silica-coating of dental alloys: volume loss, morphology and changes in the surface composition. Dental Materials 1993;9:155–61.

[77] Zinelis S. Surface and elemental alterations of dental alloys induced by electro discharge machining (EDM). Dental Materials 2007;23:601–7.

[78] Al Jabbari YS, Zinelis S, Eliades G. Effect of sandblasting conditions on alumina retention in representative dental alloys. Dental Materials Journal 2012;31:249–55.

[79] Rokni SR, Baradaran H. The Effect of Oxide Layer Thickness on Bond Strength of Porcelain to Ni-Cr Alloy. Journal of Mashhad Dental School 2007;31:17–21.

[80] Souza J, Nascimento RM, Martinelli AE. Characterization of dental metal–ceramic interfaces immersed in artificial saliva after substructural mechanical metallization with titanium. Surface and Coatings Technology 2010;205:787–92.

[81] Pinasco M, Cordano E, Giovannini M. X-ray diffraction and microstructural study of PFM precious metal dental alloys under different metallurgical conditions. Journal of Alloys and Compounds 1999;289:289–98.

[82] Lee S-H, Nomura N, Chiba A. Significant improvement in mechanical properties of biomedical Co-Cr-Mo alloys with combination of N addition and Cr-enrichment. Materials Transactions 2008;49:260–4.

[83] Harcourt HJ, Cotterill WF. Induction Melting of Cobalt-Chromium Alloys; a Comparison with Flame Melting. British Dental Journal 1965;20:323–9.

[84] Hong JM, Razzoog ME, Lang B. The Effect of Recasting on the Oxidation Layer of a Palladium Silver Porcelain Alloy. Journal of Prosthetic Dentistry 1988;59:420–5.

[85] Presswood RG. Multiple recast of a nickel-chromium-beryllium alloy. The Journal of Prosthetic Dentistry 1983;50:198–9.

[86] Walczak M, Beer K, Surowska B, Borowicz J. The issue of using remelted co-cr-mo alloys in dental prosthetics. Archives of Civil and Mechanical Engineering 2012;12:171.

[87] Sims CT, Stoloff NS, Hagel WC. Superalloys ii 1987.

[88] Geddes B, Leon H, Huang X. Superalloys: Alloying and Performance. A S M International; 2010.

[89] Song J, Xiao Q, Zang C, Xiao C, Li S, Han Y. Microstructure and Mechanical Properties of Recycled Ni3Al Base Alloy IC6. Chinese Journal of Aeronautics 2002;15:55–60.

[90] Bauer J, Cella S, Pinto MM, Costa JF, Reis A, Loguercio A. The use of recycled metal in dentistry: Evaluation of mechanical properties of titanium waste recasting. Resources, Conservation and Recycling 2010;54:1312–6.

[91] Vaidyanathan TK, Schulman A, Nielsen JP, Shalita S. Correlation Between Macroscopic Porosity Location and Liquid Metal Pressure in Centrifugal Casting Technique. Journal of Dental Research 1981;60:59–66.

[92] Horasawa N, Marek M. The effect of recasting on corrosion of a silver-palladium alloy. Dental Materials : Official Publication of the Academy of Dental Materials 2004;20:352–7.

[93] Al-Hiyasat AS, Darmani H. The effects of recasting on the cytotoxicity of base metal alloys. The Journal of Prosthetic Dentistry 2005;93:158.

[94] Lopes MB, Consani S, Sinhoreti MA, Correr-Sobrinho L. Influence of recasting palladium-silver alloy on the fit of crowns with different marginal configurations. The Journal of Prosthetic Dentistry 2005;94:430–4.

[95] Hesby DA, Kobes P, Garver DG, Pelleu GB. Physical properties of a repeatedly used nonprecious metal alloy. The Journal of Prosthetic Dentistry 1980;44:291–3.

[96] Mosleh I, Abdul-Gabbar F, Farghaly A. Castability evaluation and effect of recasting of ceramo-metal alloys. Egypt Dent J 1995;41:1357–62.

[97] Palaskar JN. Effect of recasting of Nickel-chromium alloy on its Hardness. International Journal of Dental Clinics 2010;2.

[98] Gupta S. The effect of remelting various combinations of new and used cobalt-chromium alloy on the mechanical properties and microstructure of the alloy. . Indian J Dent Res 2012;23 :341.

[99] Kapila S, Reichhold GW, Anderson RS, Watanabe LG. Effects of clinical recycling on mechanical properties of nickel-titanium alloy wires. American Journal of Orthodontics and Dentofacial Orthopedics 1991;100:428–35.

[100] Lee SH, Chang YI. Effects of recycling on the mechanical properties and the surface topography of nickel-titanium alloy wires. American Journal of Orthodontics and Dentofacial Orthopedics 2001;120:654–63.

[101] Huang TH, Yen CC, Kao CT. Comparison of ion release from new and recycled orthodontic brackets. American Journal of Orthodontics and Dentofacial Orthopedics 2001;120:68–75.

[102] Sfondrini M F, Cacciafesta V, Maffia E, Massironi S, Scribante A, Alberti G, Klersy C. Chromium release from new stainless steel, recycled and nickel-free orthodontic brackets. The Angle Orthodontist 2009;79:361–7.

[103] Mohsen SA, Fath-El-Bab I. Effect of recasting and investing materials on surface roughness and microhardness of gold and nickel based alloys. Egyptian Dental Journal 2007;53:2565–70.

[104] Ucar Y, Aksahin Z, Kurtoglu C. Metal Ceramic Bond After Multiple Castings of Base Metal Alloy. The Journal of Prosthetic Dentistry 2009;102:165–71.

[105] Qiu J, Yu W-QQ, Zhang FQ, Smales RJ, Zhang YL, Lu C-HH. Corrosion behaviour and surface analysis of a Co--Cr and two Ni--Cr dental alloys before and after simulated porcelain firing. European Journal of Oral Sciences 2011;119:93–101.

[106] Imirzalioglu P, Alaaddinoglu E, Yilmaz Z, Oduncuoglu B, Yilmaz B, Rosenstiel S. Influence of recasting different types of dental alloys on gingival fibroblast cytotoxicity. Journal of Prosthetic Dentistry 2012;107:24–33.

[107] Zhang CY, Cheng H, Lin DH, Zheng M, Özcan M. Effects of Recasting on the Biocompatibility of a Ni-Cr Alloy. The Chinese Journal of Dental Research 2012;15:105–13.

[108] Palaskar J, Nadgir DV, Shah I. Effect of recasting of nickel-chromium alloy on its porosity. Contemporary Clinical Dentistry 2010;1:237–42.

[109] Swelem AA, Abdelnabi MH, Al-Dharrab A a, Abdelmaguid HF. Surface roughness and internal porosity of partial removable dental prosthesis frameworks fabricated from conventional wax and light-polymerized patterns: A comparative study. The Journal of Prosthetic Dentistry 2014;111:335–41.

[110] Dharmar S, Rathnasamy RJ, Swaminathan T. Radiographic and metallographic evaluation of porosity defects and grain structure of cast chromium cobalt removable partial dentures. The Journal of Prosthetic Dentistry 1993;69:369–73.

[111] Johnson A, Winstanley RB. The evaluation of factors affecting the castability of metal ceramic alloy--investment combinations. The International Journal of Prosthodontics 1995;9:74–8.

[112] Mehl C, Lang B, Kappert, H, Kern M. Microstructure analysis of dental castings used in fixed dental prostheses-a simple method for quality control. Clinical Oral Investigation 2011;15:383–91.

[113] Li D, Baba N, Brantley WA, Alapati SB, Heshmati RH, Daehn GS. Study of Pd-Ag dental alloys: examination of effect of casting porosity on fatigue behavior and microstructural analysis. Journal of Materials Science Materials in Medicine 2010;21:2723–31.

[114] Palaskar J, Nadgir DV, Shah I. Effect of Recasting of Nickel: Chromium Alloy on its Castability. The Journal of Indian Prosthodontic Society 2010;10:160–4.

[115] Nakhaei MR, Ghanbarzadeh J, Goharian R. The effect of recast base metal alloys on crowns marginal accuracy. J Medical Sci 2008;8:599–602.

[116] Hinman RW, Tesk JA, Whitlock RP, Parry EE, Durkowski JS. A technique for characterizing casting behavior of dental alloys. Journal of Dental Research 1985;64:134–8.

[117] Naylor WP, Moore BK, Phillips RW, Goodacre CJ, Munoz C. Comparison of two tests to determine the castability of dental alloys. Int J Prosthodont 1990;3:413–24.

[118] Silva JWJ, Sousa LL, Nakazato RZ, Codaro EN, de Felipe H. Electrochemical and Microstructural Study of Ni-Cr-Mo Alloys Used in Dental Prostheses. Materials Sciences and Applications 2011;2:42–8.

[119] Saji VS, Choe H. Electrochemical behavior of Co-Cr and Ni-Cr dental cast alloys. Transactions of Nonferrous Metals Society of China 2009;19:785–90.

[120] Ozdemir S, Arikan A. Effects of recasting on the amount of corrosion products released from two Ni-Cr base metal alloys. Eur J Prosthodont Restor Dent 1998;6:149–53.

[121] Liu R, Johnston WM, Holloway JA, Brantley WA, Dasgupta T. The effect of metal recasting on porcelain-metal bonding: A force-to-failure study. The Journal of Prosthetic Dentistry 2010;104:165–72.

[122] Shouhua Z, Xunke LI, Zhongyi W. Study on the mechanical property of reusing the surplus alloy of a precious metal ceramic alloy. Journal of Modern Stomatology 2003;2:25.

[123] Mirković N. Effect of recasting on the elastic modulus of metal-ceramic systems from nickel-chromium and cobalt-chromium alloys. Vojnosanitetski Pregled 2007;64:469–73.

[124] Yilmaz B, Ozcelik TB, Johnston WM, Kurtulmus-Yilmaz S, Company AM. Effect of alloy recasting on the color of opaque porcelain applied on different dental alloy systems. The Journal of Prosthetic Dentistry 2012;108:362–9.

[125] Bayne SC. Correlation of clinical performance with “in vitro tests” of restorative dental materials that use polymer-based matrices. Dental Materials 2012;28:52.

[126] Waddell JN, Girvan L, Aarts J. Elemental composition of imported porcelain fused to metal crowns , apilot study. New Zeland Dental Journal 2010;106:50–4.

[127] Ryge, Gunnar and MS. Evaluating the clinical quality of restorations. The Journal of the American Dental Association 1973;87:369–77.

[128] Chatham C, Spencer MH, Wood DJ, Johnson A. The introduction of digital dental technology into BDS curricula. British Dental Journal 2014;217:639–42.

[129] Wong KV, Hernandez A. A review of additive manufacturing. ISRN Mechanical Engineering 2012;2012.

[130] Abduo J, Lyons K. Review Article Rationale for the Use of CAD / CAM Technology in Implant Prosthodontics. International Journal of Dentistry 2013;2013:1–8.

[131] Abduo J, Lyons K, Bennamoun M. Trends in Computer-Aided Manufacturing in Prosthodontics: A Review of the Available Streams. International Journal of Dentistry 2014;2014.

[132] Bajoghli F, Nosouhian S, Badrian H, Goroohi H, Saberian A, Gadesi L. results on the effect of reusing surplus alloys on the quality of castings. The Journal of Contemporary Dental Practice 2013;14:255–8.

[133] Health and Social Care Information centre (HSCIC). NHS Dental Statistics for England - 2012-13. (Accessed 15 Jan 2015). Available from http://www.hscic.gov.uk/catalogue/12370

[134] Health and Social Care Information centre (HSCIC). NHS Dental Statistics for England: 2012/13 Annex 3 – Technical Information. (Accessed 15 Jan 2015). Available at http://www.hscic.gov.uk/catalogue/PUB11625/nhs-dent-stat-eng-2012-13-tech.pdf

[135] Health and Social Care Information centre (HSCIC). NHS Dental Statistics for England: 2013/14 Second Quarterly Report. (Accessed 15 Jan 2015). Available from http://www.hscic.gov.uk/catalogue/PUB13531

[136] Falcon H. Dental Workforce Education and Training Update. 2014. (Accessed 13 Mar 2015). Available from http://thamesvalley.hee.nhs.uk/files/2014/01/16.-HETV-230114_12-Dental-Report.pdf

[137] KITCO. Charts and data 2015. (Accessed 23 Apr 2015). Available from http://www.kitco.com/charts/techcharts_gold.html

[138] Metal Bulletin Research. Base Metals Weekly Market Tracker. http://www.metalbulletin.com/Minor-and-Precious-metals.html#axzz3arqyWHmG 2015.

[139] Katzarov IH. Finite element modeling of the porosity formation in castings. International Journal of Heat and Mass Transfer 2003;46:1545–52.

[140] Hardin RA, Beckermann C. Effect of porosity on the stiffness of cast steel. Metallurgical and Materials Transactions A 2007;38:2992–3006.

[141] Bocchini GF. The influence of porosity on the characteristics of sintered materials. International Journal of Powder Metallurgy 1986;22:185–202.

[142] Deshpande PK, Lin RY. Wear resistance of WC particle reinforced copper matrix composites and the effect of porosity. Materials Science and Engineering: A 2006;418:137–45.

[143] Xunke L, Zhongyi W, Guiwen Z. Metal-ceramic bond of reused surplus alloy of a precious metal ceramic alloy. Journal of Practical Stomatology 2003;2:22.

[144] Vander Voort GF. Metallography, principles and practice. ASM International (OH); 1984.

[145] Campbell J, Harding RA. Solidification Defects in Castings 1994.

[146] Smallman RE, Bishop RJ. Modern physical metallurgy and materials engineering. Butterworth-Heinemann; 1999.

[147] Lewia AJ. Microporosity in casting alloys. Australian Dental Journal 1975;20:161–6.

[148] Tomer A. Structure of metals through optical microscopy. Materials Park, Ohio: ASM International; 1991.

[149] Higgins RA. Engineering Metallurgy, 6Th Edition. Viva Books Private Limited; 1998.

[150] Mitchell BS. An introduction to materials engineering and science for chemical and materials engineers. John Wiley & Sons; 2004.

[151] Atwood RC, Lee PD, Curtis RV, Maijer DM. Modeling the investment casting of a titanium crown. Dental Materials 2007;23:60–70.

[152] Nomoto R, Takayama Y, Tsuchida F & NH. Non-destructive three-dimensional evaluation of pores at different welded joints and their effects on joints strength. Dental Materials 2010;26:246–52.

[153] Nuñez JMC, Takahashi JMFK, Henrique GEP, Nóbilo MADA, Consani RLX, Mesquita M. Radiographic inspection of porosity in pure titanium dumbbell castings. Gerodontology 2011;28:233–7.

[154] Rasband W.S. ImageJ,U.S.National Institutes of Health, Bethesda, Maryland,USA, http://imagej.nih.gov/ij/ 1997. Available to download from http://imagej.nih.gov/ij/

[155] Jabbari YSA. Physico-mechanical properties and prosthodontic applications of Co-Cr dental alloys : a review of the literature. The Journal of Advanced Prosthodontic 2014;6:138–45.

[156] Adolfi S. Slag inclusion formation during solidification of Steel alloys and in cast iron 2007:15–6.

[157] Davis JR. Corrosion: Understanding the basics. ASM International; 2000.

[158] Naro RL. Porosity Defects in Iron Castings From Mold-Metal Interface Reactions. AFS Trans 1999;107:839–51.

[159] Gunasegaram DR, Farnsworth DJ, Nguyen TT. Identification of critical factors affecting shrinkage porosity in permanent mold casting using numerical simulations based on design of experiments. Journal of Materials Processing Technology 2009;209:1209–19.

[160] Verrett RG, Duke ES. The effect of sprue attachment design on castability and porosity. The Journal of Prosthetic Dentistry 1989;61:418–24.

[161] Kaiser R, Browne DJ, Williamson K, O'Brien C. Effects of Section Size And Cooling Rate on Microstructure and As-Cast Properties of Investment Cast CO-CR Biomedical Alloy. Supplemental Proceedings: Materials Properties, Characterization, and Modeling 2012:317–24.

[162] Majidi O, Shabestari SGG, Aboutalebi MRR. Study of fluxing temperature in molten aluminum refining process. Journal of Materials Processing Technology 2007;182.1:450–5.

[163] Nayan N, Saikrishna CN, Ramai, KV, Bhaumik SK, Nair KS, Mittal M. Vacuum induction melting of NiTi shape memory alloys in graphite crucible. Materials Science and Engineering: A 2007;465:44–8.

[164] Podrez-Radziszewska M, Haimann K, Dudziński W, Morawska-Sołtysik M. Characteristic of intermetallic phases in cast dental CoCrMo alloy. Archives of Foundry Engineering 2010;10:51–6.

[165] Rosenthal R, Cardoso BR, Bott IS, Paranhos RPR, Carvalho EA. Phase characterization in as-cast F-75 Co--Cr--Mo--C alloy. Journal of Materials Science 2010;45:4021–8.

[166] Jefferies SR. Abrasive finishing and polishing in restorative dentistry: a state-of-the-art review. Dental Clinics of North America 2007;51:379–97.

[167] Jackson MJ, Ahmed W. Surface engineered surgical tools and medical devices. Springer Science & Business Media; 2007.

[168] Bollen CM, Lambrechts P, Quirynen M. Comparison of surface roughness of oral hard materials to the threshold surface roughness for bacterial plaque retention: a review of the literature. Dental Materials : Official Publication of the Academy of Dental Materials 1997;13:258–69.

[169] Guilherme AS, Pessanha Henriques GE, Zavanelli RA, Mesquita MF, Henriques GEP. Surface roughness and fatigue performance of commercially pure titanium and Ti-6Al-4V alloy after different polishing protocols. The Journal of Prosthetic Dentistry 2005;93:378–85.

[170] Schmage P, Nergiz I, Herrmann W, Özcan M. Influence of various surface-conditioning methods on the bond strength of metal brackets to ceramic surfaces. American Journal of Orthodontics and Dentofacial Orthopedics 2003;123:540–6.

[171] Wagner WC, Asgar K, Bigelow WC, Flinn R. Effect of interfacial variables on metal-porcelain bonding. Journal of Biomedical Materials Research 1993;27:531–7.

[172] Quirynen M, Marechal M, Busscher HJ, Weerkamp AH, Darius PL, Steenberghe D. The influence of surface free energy and surface roughness on early plaque formation. Journal of Clinical Periodontology 1990;17:138–44.

[173] Taylor R, Maryan C & VJ. Retention of oral microorganisms on cobalt-chromium alloy and dental acrylic resin with different surface finishes. J Prosthet Dent 1998;80:592–7.

[174] Aydin AK. Evaluation of finishing and polishing techniques on surface roughness of chromium-cobalt castings. The Journal of Prosthetic Dentistry 1991;65:763–7.

[175] Taylor RL, Verran J, Lees GC, Ward A. The influence of substratum topography on bacterial adhesion to polymethyl methacrylate. Journal of Materials Science Materials in Medicine 1998;9:17–22.

[176] Reddy ES, Patil NP, Guttal SS, Jagadish HG. Effect of different finishing and polishing agents on the surface roughness of cast pure titanium. Journal of Prosthodontics : Official Journal of the American College of Prosthodontists 2007;16:263–8.

[177] Ravi M, Deshraj J. Quantitative determination of changes in texture (roughness) produced on the surface of cast nickellchromium alloy after exposure to various

surface treatment procedures. Journal of Pierre Faucharad Academy (India Chapter) 2010;24:140–5.

[178] Lin H, Zhang H, Li X, Cheng H. Treatment of multiple ceramic alloys before recasting. The Journal of Prosthetic Dentistry 2013;110:29–40.

[179] Louise McGinley E, Coleman DC, Moran GP, Fleming GJPP, McGinley EL. Effects of surface finishing conditions on the biocompatibility of a nickel-chromium dental casting alloy. Dental Materials : Official Publication of the Academy of Dental Materials 2011;27:637–50.

[180] Yavuz T, Acar A, Akman S, Ozturk AN. Effect of Surface Treatment on Elemental Composition of Recast NiCr Alloy. Materials Sciences and Applications 2012;03:163–7.

[181] Li BH, Ye JT, Liao JK, Zhuang PL, Zhang YP, Li JY. Effect of pretreatments on the metal-ceramic bonding strength of a Pd-Ag alloy. Journal of Dentistry 2013;42:319–28.

[182] Külünk T, Kurt M, Ural Ç, Külünk Ş, Baba S. Effect of different air-abrasion particles on metal-ceramic bond strength. Journal of Dental Sciences 2011;6:140–6.

[183] Lahori M, Nagrath R, Sisodia S, Dagar P. The Effect of Surface Treatments on the Bond Strength of a Nonprecious Alloy–Ceramic Interface: An Invitro Study. The Journal of Indian Prosthodontic Society 2013;14:1–5.

[184] Atwood RC, Lee PD & CRV. Modeling the surface contamination of dental titanium investment castings. Dental Materials 2005;21:178–86.

[185] Darvell BW. Materials science for dentistry. Elsevier; 2009.

[186] Castillo-Oyagüe R, Osorio R, Osorio E, Sánchez-Aguilera F, Toledano M. The effect of surface treatments on the microroughness of laser-sintered and vacuum-cast base metal alloys for dental prosthetic frameworks. Microscopy Research and Technique 2012;75Castillo:1206–12.

[187] Shillingburg HT, Sather DA, Stone S. Fundamentals of fixed prosthodontics. Quintessence Publ.; 2012.

[188] Sailer I, Pjetursson BE, Zwahlen M, Hämmerle CH. A systematic review of the survival and complication rates of all-ceramic and metal--ceramic reconstructions after an observation period of at least 3 years. Part II: fixed dental prostheses. Clinical Oral Implants Research 2007;18:86–96.

[189] Donovan TE, Swift E. Porcelain-fused-to-metal (PFM) alternatives. Journal of Esthetic and Restorative Dentistry 2009;21:4–6.

[190] Chowdhuri MAK, Xia Z, Yu D. A study on optimal bonding angles of bi-material interfaces in dental crowns with porcelain fused to metal. Journal of Engineering in Medicine 2011;225:657–68.

[191] Diaz-Arnold AM, Keller JC, Wightman JP, Williams VD. Bond strength and surface characterization of a Ni-Cr-Be alloy. Dental Materials 1996;12:58–63.

[192] Anusavice KJ, Kakar K, Ferree N. Which mechanical and physical testing methods are relevant for predicting the clinical performance of ceramic-based dental prostheses? Clinical Oral Implants Research 2007;18:218–31.

[193] Nicholas MG, Mortimer DA. Assessment Ceramic / metal joining for structural applications. Materials Science and Technology 1985;1:657–65.

[194] Kelly JR. Ceramics in restorative and prosthetic dentistry 1. Annual Review of Materials Science 1997;27:443–68.

[195] Schweitzer DM, Goldstein GR, Ricci JL, Silva NRFA, Hittelman EL. Comparison of Bond Strength of a Pressed Ceramic Fused to Metal versus Feldspathic Porcelain Fused to Metal. Journal of Prosthodontics 2005;14:239–47.

[196] Wilson TG, Kornman KS. Fundamentals of periodontics. Quintessence Publ.; 1996.

[197] Technical specification ISO/TS 11405. Dental materials – testing of adhesion to tooth structure. Switzerland; 2003.

[198] Hammad IA, Talk YF. Designs of bond strength tests for metal-ceramic complexes: review of the literature. The Journal of Prosthetic Dentistry 1996;75:602–8.

[199] Aboushelib MN, de Kler M, van der Zel JM, Feilzer AJ. Microtensile bond strength and impact energy of fracture of CAD-veneered zirconia restorations. Journal of Prosthodontics : Official Journal of the American College of Prosthodontists 2009;18:211–6.

[200] International Organization for Standardization. ISO Standard 9693. Metal-ceramic dental restorative systems. Geneva, Switzerland: 2000.

[201] Al Jabbari YS, Barbagadaki X, Al Wazzan KA, El-Danaf EA, Eliades G, Zinelis S. Shear bond strength and characterization of interfaces between electroformed gold substrates and porcelain. Materials Chemistry and Physics 2013;137:825–33.

[202] Co N, Xie H, Yuan X, Wu F. Effects of Surface Treatments on Bond Strength Between Porcelain and Electroformed Gold Substrates. J Adhes Dent 2009;11:485–91.

[203] Research O. Comparative Evaluation of Metal-ceramic Bond Strengths of Nickel Chromium and Cobalt Chromium Alloys on Repeated Castings : An In vitro Study. Journal of International Oral Health 2014;6:99–103.

[204] Della Bona A, Van Noort R. Shear vs. tensile bond strength of resin composite bonded to ceramic. Journal of Dental Research 1995;74:1591–6.

[205] Bagby M, Marshall SJ, Marshall GW. Metal ceramic compatibility: A review of the literature. The Journal of Prosthetic Dentistry 1990;63:21–5.

[206] Madani AS, Rokni SR, Mohammadi A, Bahrami M. The effect of recasting on bond strength between porcelain and base-metal alloys. Journal Of Prosthodontics 2011;20:190–4.

[207] Huang HH, Lin MC, Lee TH, Yang HW, Chen FL, Wu SC., Hsu C. Effect of chemical composition of Ni-Cr dental casting alloys on the bonding characterization between porcelain and metal. Journal of Oral Rehabilitation 2005;32:206–12.

[208] Kumar CR, Sujesh M, Rao DC and SD. Recasting of Base Metals, Its Effect On Bond Strength Of Porcelein - A Laboratory Study. Indian Journal of Dental Sciences 2012;4:15–9.

[209] Naylor WP, Kessler JC, King AH. Introduction to metal ceramic technology. Quintessence Publishing Company; 1992.

[210] Ebnesajjad S. Handbook of adhesives and surface preparation: technology, applications and manufacturing. William Andrew; 2010.

[211] Graham JD, Johnson A, Wildgoose DG, Shareef MY, Cannavina G. The effect of surface treatments on the bond strength of a nonprecious alloy-ceramic interface. The International Journal of Prosthodontics 1998;12:330–4.

[212] Cao HC, Thouless MD, Evans AG. Residual stresses and cracking in brittle solids bonded with a thin ductile layer. Acta Metallurgica 1988;36:2037–46.

[213] Culha O, Zor M, Ali Gungor M, Arman Y, Toparli M. Evaluating the bond strength of opaque material on porcelain fused to metal restorations (PFM) alloys by scratch test method. Materials & Design 2009;30:3225–8.

[214] Ohno H, Araki Y, Endo K. ESCA Study on Dental Alloy Surfaces Modified by Ga-Sn Alloy. Journal of Dental Research 1992;71:1332–9.

[215] Kumar A, Jayakumar T, Raj B. Relative Influence of Different Factors on Young ' s Modulus in Nickel and Zirconium base Alloy Systems upon Precipitation of Intermetallics. Indira Gandhi Centre for Atomic Research, Kalpakkam, India 2006:1–5.

[216] Mirković N, Draganjac M, Stamenković D, Ristić L. Effect of recasting on the thickness of metal-ceramic interface of nickel-chromium and cobalt-chromium alloys. Vojnosanitetski Pregled 2008;65:365–9.

[217] Council on Dental Material Instruments ans Equipments ANSI/ADA specification No. 38 for metal-ceramic systems. Chicago: American Dental Association; 1991.

[218] Nieva N, Arreguez C, Carrizo RN, Molé CS, Lagarrigue GM. Bonding Strength Evaluation on Metal/Ceramic Interfaces in Dental Materials. Procedia Materials Science 2012;1:475–82.

[219] Oshida Y, Munoz CA, Winkler MM, Hashem A, Itoh M. Fractal dimension analysis of aluminum oxide particle for sandblasting dental use. Bio-Medical Materials and Engineering 1993;3:117–26.

[220] Hautaniemi JA, Juhanoja JT, Herø H. Porcelain bonding on Ti: its dependence on surface roughness, firing time and vacuum level. Surface and Interface Analysis 1993;20:421–6.

[221] Reyes MJD, Oshida Y, Andres CJ, Barco T, Hovijitra S, Brown D. Titanium--porcelain system. Part III: Effects of surface modification on bond strengths. Bio-Medical Materials and Engineering 2001;11:117–36.

[222] Elshahawy W, Watanabe I, Koike M. Elemental ion release from four different fixed prosthodontic materials. Dental Materials 2009;25:976–81.

[223] Foulkes EC. Transport of toxic heavy metals across cell membranes. Proceedings of the Society for Experimental Biology and Medicine 2000;223:234–40.

[224] Schmalz G, Garhammer P. Biological interactions of dental cast alloys with oral tissues. Dental Materials 2002;18:396–406.

[225] Langård S. Chromium carcinogenicity; a review of experimental animal data. Science of the Total Environment 1988;71:341–50.

[226] Costa M. Metal Carcinogenesis In Experimental Animals. Metal Carcinogenesis Testing, Springer; 1981, p. 25–40.

[227] Speidel MO A, Uggowitzer PJ. Materials in Medicine. vdf Hochschulverlag AG; 1998.

[228] International Agency for Research on Cancer and IARC working group on the evaluation of carcinogenic risks tohumans. IARC monographs on the evaluation of carcinogenic risks to humans 1991;49.

[229] Wataha JC. Biocompatibility of dental casting alloys: a review. The Journal of Prosthetic Dentistry 2000;83:223–34.

[230] House K, Sernetz F, Dymock D, Sandy JR, Ireland AJ. Corrosion of orthodontic appliances--should we care? American Journal of Orthodontics and Dentofacial Orthopedics : Official Publication of the American Association of Orthodontists, Its Constituent Societies, and the American Board of Orthodontics 2008;133:584–92.

[231] Nelson SK, Wataha JC, Neme A-ML, Cibirka RM, Lockwoodd PE. Cytotoxicity of dental casting alloys pretreated with biologic solutions. The Journal of Prosthetic Dentistry 1999;81:591–6.

[232] Okazaki Y, Gotoh E. Comparison of metal release from various metallic biomaterials in vitro. Biomaterials 2005;26:11–21.

[233] Elshahawy WM, Watanabe I, Kramer P. In vitro cytotoxicity evaluation of elemental ions released from different prosthodontic materials. Dental Materials : Official Publication of the Academy of Dental Materials 2009;25:1551–5.

[234] Brune D. Metal release from dental biomaterials. Biomaterials 1986;7:163–75.

[235] International Commission on Radiological Protection (ICRP). Publication 30. Recommendations of the International Commission on Radiological Protection. No. 30. 1975.

[236] Bowen HJM. Environmental chemistry of the elements. Academic Press.; 1979.

[237] Grandjean P. Human exposure to nickel. IARC Scientific Publications 1983:469–85.

[238] Manaranche C, Hornberger H. A proposal for the classification of dental alloys according to their resistance to corrosion. Dental Materials 2007;23:1428–37.

[239] Boumans PWJM. Inductively Coupled Plasma Emission Spectroscopy, Applications and Fundamentals. Wiley; 1987.

[240] Hou X, Jones BT. Inductively Coupled Plasma-Optical Emission Spectrometry. Encyclopedia of Analytical Chemistry 2000:9468–9485.

[241] Reclaru L, Lüthy H, Eschler P-Y, Blatter A, Susz C. Corrosion behaviour of cobalt-chromium dental alloys doped with precious metals. Biomaterials 2005;26:4358–65.

[242] Beck K A, Sarantopoulos, DM, Kawashima I, Berzins D. Elemental Release from CoCr and NiCr Alloys Containing Palladium. Journal of Prosthodontics 2012;21:88–93.

[243] Al-Salehi SK, Hatton PV, Johnson A, Cox AG, McLeod C. The effect of hydrogen peroxide concentration on metal ion release from dental casting alloys. Journal of Oral Rehabilitation 2008;35:276–82.

[244] Wataha JC, Lockwood PE, Khajotia SS, Turner R. Effect of pH on element release from dental casting alloys. The Journal of Prosthetic Dentistry 1998;80:691–8.

[245] International Organizatin for Standaratzation. ISO Standard 10933. Biological evaluation of medical devices. Geneva, Switzerland: 2000.

[246] Wataha JC, Craig RG, Hanks CT. Precision of and new methods for testing in vitro alloy cytotoxicity. Dental Materials 1992;8:65–70.

[247] Reddy NR, Abraham AP, Murugesan K, Matsa V. An invitro analysis of elemental release and cytotoxicity of recast nickel-chromium dental casting alloys. Journal of Indian Prosthodontic Society 2011;11:106–12.

[248] Johnson A, Shiraishi T, Hurrell-gillingham K. In vitro biocompatibility of novel Au-Pt-based metal-ceramic alloys. Journal of Oral Science 2011;53:387–91.

[249] Jones SB, Taylor RL, Colligon JS, Johnson D. Effect of element concentration on nickel release from dental alloys using a novel ion beam method. Dental Materials : Official Publication of the Academy of Dental Materials 2010;26:249–56.

[250] Milheiro A, Muris J, Kleverlaan CJ, Feilzer AJ. Influence of shape and finishing on the corrosion of palladium-based dental alloys. J Adv Prosthodont 2015;7:56–61.

[251] International Organizatin for Standaratzation. ISO Standard1071. Dental materials-Corrosion test methods. Geneva, Switzerland: 2001.

[252] Johnson A, Shiraishi T, Al-Salehi SK. Ion release from experimental Au–Pt-based metal–ceramic alloys. Dental Materials 2010;26:682–7.

[253] Viennot S, Dalard F, Lissac M, Corrosion GB. Corrosion resistance of alloys used in fixed prosthetic restorations. European Journal of Oral Sciences 2005:90–5.

[254] Al-Hity RR, Kappert HF, Dalard F, Grosgogeat B, Viennot S. Corrosion resistance measurements of dental alloys , are they correlated ? Dental Materials 2006;3:679–87.

[255] Ameer MA, Khamis E, Al-Motlaq M. Electrochemical behaviour of recasting Ni--Cr and Co--Cr non-precious dental alloys. Corrosion Science 2004;46:2825–36.

[256] Yfantis C, Yfantis D, Anastassopoulou J. Analytical and Electrochemical Evaluation of the in vitro corrosion behavior of Nickel-chrome and Cobalt- chrome casting alloys for metal-ceramic restorations . Eur J Prosthodont Rest Dent 2007;15:33–40.

[257] Biego GH, Joyeux M, Hartemann P, Debry G. Daily intake of essential minerals and metallic micropollutants from foods in France. The Science of the Total Environment 1998;217:27–36.

[258] Darmani H. Elements released from dental casting alloys and their cytotoxic effects. The International Journal of Prosthodontics 2002;15:473.

[259] Wylie CM, Shelton RM, Fleming GJP, Davenport AJ. Corrosion of nickel-based dental casting alloys. Dental Materials 2007;23:714–23.

[260] Huang HH. Surface characterization of passive film on NiCr-based dental casting alloys. Biomaterials 2003;24:1575–82.

[261] Mohamed A , Cahoon J. Oxide Surface Analysis of Nickel Based Chromium Alloys with the Aid of Auger Electron Spectroscopy. International Journal of Engineering Research and Development 2013;7:33–6.

[262] Baran G. Auger chemical analysis of oxides on Ni-Cr alloys. Journal of Dental Research 1984;63:76–80.

[263] Smales RJ, Hawthorne WS. Long-term survival of extensive and posterior crowns. Journal of Dentistry 1997;25:225–7.

[264] Covington JS, McBride MA, Slagle WF, Disney A. Quantization of nickel and beryllium leakage from base metal casting alloys. The Journal of Prosthetic Dentistry 1985;54:127–36.

[265] Canay S, Hersek N, Culha A, Bilgic S. Evaluation of titanium in oral conditions and its electrochemical corrosion behaviour. Journal of Oral Rehabilitation 1998;25:759–64.

[266] Mutlu-Sagesen L, Ergun G, Karabulut E. Ion release from metal-ceramic alloys in three different media. Dental Materials Journal 2011;30:598–610.

[267] Kerosuo H, Moe G, Kleven E. In vitro release of nickel and chromium from different types of simulated orthodontic appliances. The Angle Orthodontist 1995;65:111–6.

[268] Petersen PE, Baez R, Kwan S, Ogawa H. Future use of materials for dental restoration. World Health Organization: Geneva, Switzerland 2009:1–56.

[269] Rekow ED, Fox CH, Watson T, Petersen PE. Future innovation and research in dental restorative materials. Advances in Dental Research 2013;25:2–7.

10 Appendices

10.1 Appendix 1

Table 1-1 Tests of between-subjects effect

Source	Type III Sum of Squares	df	Mean Square	F	Sig.
Corrected Model	1.355[a]	15	.090	7.761	.000
Intercept	1.102	1	1.102	94.719	.000
New to reused content of alloy	.651	4	.163	13.982	.000
Alloy type	.044	1	.044	3.789	.055
Restoration type	.104	1	.104	8.908	.004
New to reused content of alloy * Alloy type	.069	4	.017	1.472	.218
Alloy type * Restoration type	.367	1	.367	31.550	.000
New to reused content of alloy * Restoration type	.120	4	.030	2.587	.043
Error	.978	84	.012		
Total	3.435	100			
Corrected Total	2.333	99			

Table 1-2 ANOVA test for Co-Cr and Ni-Cr all-metal test groups

		Sum of Squares	df	Mean Square	F	Sig.
NiCr-AM	Between Groups	1.023	4	.256	9.453	.000
	Within Groups	.541	20	.027		
	Total	1.565	24			
CoCr-AM	Between Groups	.018	4	.004	20.427	.000
	Within Groups	.004	20	.000		
	Total	.022	24			

Table1-3 ANOVA test for Co-Cr and Ni-Cr ceramic-bonded test groups

		Sum of Squares	df	Mean Square	F	Sig
NiCr-CB	Between Groups	.033	4	.008	14.705	0.000
	Within Groups	.068	120	.001		
	Total	.101	124			
CoCr-CB	Between Groups	.770	4	.193	13.762	0.000
	Within Groups	1.679	120	.014		
	Total	2.450	124			

Table 1-4 Pairwise comparisons between restoration types of Co-Cr and Ni-Cr alloys

Dependent Variable	(I) Restoration type	(J)Restoration type	Mean Difference (I-J)	Std. Error	Sig.[a]	95% Confidence Interval for Difference	
						Lower Bound	Upper Bound
NiCr	CB	AM	-.186*	.043	.000	-.272	-.099
	AM	CB	.186*	.043	.000	.099	.272
CoCr	CB	AM	.057*	.013	.000	.030	.083
	AM	CB	-.057*	.013	.000	-.083	-.030

Table 1-5 Multiple-comparisons of CoCr-AM test groups (Porosity evaluation)

Dependant variable	(I) Test group	(J) Test group	Mean Difference (I-J)	Std. Error	Sig.
CoCr-AM	0% recast	25%recast	.00000	.00938	1.000
		50%recast	-.00200	.00938	.833
		75%recast	-.00200	.00938	.833
		100%recast	-.06800*	.00938	.000
	25%recast	0% recast	.00000	.00938	1.000
		50%recast	-.00200	.00938	.833
		75%recast	-.00200	.00938	.833
		100%recast	-.06800*	.00938	.000
	50%recast	0% recast	.00200	.00938	.833
		25%recast	.00200	.00938	.833
		75%recast	.00000	.00938	1.000
		100%recast	-.06600*	.00938	.000
	75%recast	0% recast	.00200	.00938	.833
		25%recast	.00200	.00938	.833
		50%recast	.00000	.00938	1.000
		100%recast	-.06600*	.00938	.000
	100%recast	0% recast	.06800*	.00938	.000
		25%recast	.06800*	.00938	.000
		50%recast	.06600*	.00938	.000
		75%recast	.06600*	.00938	.000

Table 1-6 Multiple-comparisons of CoCr-CB test groups (Porosity evaluation)

Dependent Variable	(I) CoCrCB	(J) CoCrCB	Mean Difference (I-J)	Std. Error	Sig.
CoCr-CB	0% recast	25%recast	.02200	.03148	.493
		50%recast	-.04400	.03148	.178
		75%recast	-.02000	.03148	.532
		100%recast	-.21000*	.03148	.000
	25%recast	0% recast	-.02200	.03148	.493
		50%recast	-.06600*	.03148	.049
		75%recast	-.04200	.03148	.197
		100%recast	-.23200*	.03148	.000
	50%recast	0% recast	.04400	.03148	.178
		25%recast	.06600*	.03148	.049
		75%recast	.02400	.03148	.455
		100%recast	-.16600*	.03148	.000
	75%recast	0% recast	.02000	.03148	.532
		25%recast	.04200	.03148	.197
		50%recast	-.02400	.03148	.455
		100%recast	-.19000*	.03148	.000
	100%recast	0% recast	.21000*	.03148	.000
		25%recast	.23200*	.03148	.000
		50%recast	.16600*	.03148	.000
		75%recast	.19000*	.03148	.000

Table 1-7 Multiple-comparisons of NiCr-AM test groups (Porosity evaluation)

Dependent Variable	(I) Test group	(J) Test group	Mean Difference (I-J)	Std. Error	Sig.
NiCr-AM	0% recast	25%recast	.01600	.10405	.879
		50%recast	-.05600	.10405	.596
		75%recast	-.04200	.10405	.691
		100%recast	-.52200*	.10405	.000
	25%recast	0% recast	-.01600	.10405	.879
		50%recast	-.07200	.10405	.497
		75%recast	-.05800	.10405	.583
		100%recast	-.53800*	.10405	.000
	50%recast	0% recast	.05600	.10405	.596
		25%recast	.07200	.10405	.497
		75%recast	.01400	.10405	.894
		100%recast	-.46600*	.10405	.000
	75%recast	0% recast	.04200	.10405	.691
		25%recast	.05800	.10405	.583
		50%recast	-.01400	.10405	.894
		100%recast	-.48000*	.10405	.000
	100%recast	0% recast	.52200*	.10405	.000
		25%recast	.53800*	.10405	.000
		50%recast	.46600*	.10405	.000
		75%recast	.48000*	.10405	.000

Table 1-8 Multiple-comparisons of NiCr-CB test groups (Porosity evaluation)

Dependent Variable	(I) Test group	(J) Test group	Mean Difference (I-J)	Std. Error	Sig.
NiCr-CB	0%re-cast	25%re-cast	-.01953*	.00674	.035
		50%re-cast	-.03693*	.00674	.000
		75%re-cast	-.03158*	.00674	.000
		100%re-cast	-.04775*	.00674	.000
	25%re-cast	0%re-cast	.01953*	.00674	.035
		50%re-cast	-.01740	.00674	.080
		75%re-cast	-.01204	.00674	.385
		100%re-cast	-.02822*	.00674	.001
	50%re-cast	0%re-cast	.03693*	.00674	.000
		25%re-cast	.01740	.00674	.080
		75%re-cast	.00536	.00674	.931
		100%re-cast	-.01081	.00674	.497
	75%re-cast	0%re-cast	.03158*	.00674	.000
		25%re-cast	.01204	.00674	.385
		50%re-cast	-.00536	.00674	.931
		100%re-cast	-.01617	.00674	.122
	100%recast	0%re-cast	.04775*	.00674	.000
		25%re-cast	.02822*	.00674	.001
		50%re-cast	.01081	.00674	.497
		75%re-cast	.01617	.00674	.122

Table 1-9 Multiple-comparisons of CoCr-AM test groups (Pore count)

Dependent Variable	(I) Test group	(J) Test group	Mean Difference (I-J)	Std. Error	Sig.
CoCr-AM	0%re-cast	25%re-cast	-5.6000	9.36888	.974
		50%re-cast	-28.0000	9.36888	.050
		75%re-cast	-5.6000	9.36888	.974
		100%re-cast	-45.0000*	9.36888	.001
	25%re-cast	0%re-cast	5.6000	9.36888	.974
		50%re-cast	-22.4000	9.36888	.159
		75%re-cast	.0000	9.36888	1.000
		100%re-cast	-39.4000*	9.36888	.004
	50%re-cast	0%re-cast	28.0000	9.36888	.050
		25%re-cast	22.4000	9.36888	.159
		75%re-cast	22.4000	9.36888	.159
		100%re-cast	-17.0000	9.36888	.393
	75%re-cast	0%re-cast	5.6000	9.36888	.974
		25%re-cast	.0000	9.36888	1.000
		50%re-cast	-22.4000	9.36888	.159
		100%re-cast	-39.4000*	9.36888	.004
	100%re-cast	0%re-cast	45.0000*	9.36888	.001
		25%re-cast	39.4000*	9.36888	.004
		50%re-cast	17.0000	9.36888	.393
		75%re-cast	39.4000*	9.36888	.004

Table1-10 Multiple-comparisons of CoCr-CB test groups (Pore count)

Dependent Variable	(I) Test group	(J) Test group	Mean Difference (I-J)	Std. Error	Sig.
CoCr-CB	0%reast	25%re-cast	1.8000	11.75245	1.000
		50%re-cast	-.8000	11.75245	1.000
		75%re-cast	5.4000	11.75245	.990
		100%re-cast	-.4000	11.75245	1.000
	25%re-cast	0%re-cast	-1.8000	11.75245	1.000
		50%re-cast	-2.6000	11.75245	.999
		75%re-cast	3.6000	11.75245	.998
		100%re-cast	-2.2000	11.75245	1.000
	50%re-cast	0%re-cast	.8000	11.75245	1.000
		25%re-cast	2.6000	11.75245	.999
		75%re-cast	6.2000	11.75245	.983
		100%re-cast	.4000	11.75245	1.000
	75%re-cast	0%re-cast	-5.4000	11.75245	.990
		25%re-cast	-3.6000	11.75245	.998
		50%re-cast	-6.2000	11.75245	.983
		100%re-cast	-5.8000	11.75245	.987
	100%re-cast	0%re-cast	.4000	11.75245	1.000
		25%re-cast	2.2000	11.75245	1.000
		50%re-cast	-.4000	11.75245	1.000
		75%re-cast	5.8000	11.75245	0.987

Table 1-11 Multiple-comparisons of NiCr-AM test groups (Pore count)

Dependent Variable	(I) Test group	(J) Test group	Mean Difference (I-J)	Std. Error	Sig.
NiCr-AM	0%reast	25%re-cast	-29.6000	19.51307	.564
		50%re-cast	-38.0000	19.51307	.326
		75%re-cast	-49.2000	19.51307	.125
		100%re-cast	-270.4000*	19.51307	.000
	25%re-cast	0%re-cast	29.6000	19.51307	.564
		50%re-cast	-8.4000	19.51307	.992
		75%re-cast	-19.6000	19.51307	.850
		100%re-cast	-240.8000*	19.51307	.000
	50%re-cast	0%re-cast	38.0000	19.51307	.326
		25%re-cast	8.4000	19.51307	.992
		75%re-cast	-11.2000	19.51307	.977
		100%re-cast	-232.4000*	19.51307	.000
	75%re-cast	0%re-cast	49.2000	19.51307	.125
		25%re-cast	19.6000	19.51307	.850
		50%re-cast	11.2000	19.51307	.977
		100%re-cast	-221.2000*	19.51307	.000
	100%re-cast	0%re-cast	270.4000*	19.51307	.000
		25%re-cast	240.8000*	19.51307	.000
		50%re-cast	232.4000*	19.51307	.000
		75%re-cast	221.2000*	19.51307	.000

Table 1-12 Multiple-comparisons of NiCr-CB test groups (Pore count)

Dependent Variable	(I) Test group	(J) Test group	Mean Difference (I-J)	Std. Error	Sig.
NiCr-CB	0%reast	25%re-cast	-.6000	9.12842	1.000
		50%re-cast	-18.0000	9.12842	.315
		75%re-cast	-14.6000	9.12842	.515
		100%re-cast	-33.4000*	9.12842	.012
	25%re-cast	0%re-cast	.6000	9.12842	1.000
		50%re-cast	-17.4000	9.12842	.346
		75%re-cast	-14.0000	9.12842	.554
		100%re-cast	-32.8000*	9.12842	.014
	50%re-cast	0%re-cast	18.0000	9.12842	.315
		25%re-cast	17.4000	9.12842	.346
		75%re-cast	3.4000	9.12842	.996
		100%re-cast	-15.4000	9.12842	.464
	75%re-cast	0%re-cast	14.6000	9.12842	.515
		25%re-cast	14.0000	9.12842	.554
		50%re-cast	-3.4000	9.12842	.996
		100%re-cast	-18.8000	9.12842	.275
	100%re-cast	0%re-cast	33.4000*	9.12842	.012
		25%re-cast	32.8000*	9.12842	.014
		50%re-cast	15.4000	9.12842	.464
		75%re-cast	18.8000	9.12842	.275

Table 1-13 ANOVA of CoCr-AM test groups (Chemical composition)

CoCr-AM		Sum of Squares	df	Mean Square	F	Sig.
Co	Between Groups	.123	4	.031	.363	.832
	Within Groups	1.694	20	.085		
	Total	1.817	24			
Cr	Between Groups	4.123	4	1.031	2.042	.127
	Within Groups	10.097	20	.505		
	Total	14.220	24			
Si	Between Groups	1.342	4	.335	1.790	.171
	Within Groups	3.748	20	.187		
	Total	5.090	24			
Mo	Between Groups	7.255	4	1.814	55.706	.000
	Within Groups	.651	20	.033		
	Total	7.906	24			

Table 1-14 ANOVA of CoCr-CB test groups (Chemical composition)

CoCr-CB		Sum of Squares	df	Mean Square	F	Sig.
Co	Between Groups	.531	4	.133	3.505	.025
	Within Groups	.757	20	.038		
	Total	1.288	24			
Cr	Between Groups	.343	4	.086	3.053	.041
	Within Groups	.562	20	.028		
	Total	.906	24			
Mo	Between Groups	.162	4	.040	1.442	.259
	Within Groups	.534	19	.028		
	Total	.696	23			
Si	Between Groups	.036	4	.009	.974	.444
	Within Groups	.186	20	.009		
	Total	.223	24			

Table 1-15 ANOVA of NiCr-AM test groups (chemical composition)

NiCr-AM		Sum of Squares	df	Mean Square	F	Sig.
Ni	Between Groups	2.813	4	.703	1.930	.145
	Within Groups	7.286	20	.364		
	Total	10.099	24			
Cr	Between Groups	11.129	4	2.782	66.414	.000
	Within Groups	.838	20	.042		
	Total	11.967	24			
Fe	Between Groups	.597	4	.149	9.987	.000
	Within Groups	.299	20	.015		
	Total	.896	24			
Mo	Between Groups	2.891	4	.723	1.981	.136
	Within Groups	7.294	20	.365		
	Total	10.185	24			
Nb	Between Groups	.080	4	.020	.646	.636
	Within Groups	.619	20	.031		
	Total	.699	24			
Ta	Between Groups	3.601	4	.900	7.546	.001
	Within Groups	2.386	20	.119		
	Total	5.987	24			

Table 1-16 ANOVA of NiCr-CB test groups (Chemical composition)

NiCr-CB		Sum of Squares	df	Mean Square	F	Sig.
Ni	Between Groups	16.372	4	4.093	.920	.472
	Within Groups	88.993	20	4.450		
	Total	105.365	24			
Cr	Between Groups	.077	4	.019	.404	.803
	Within Groups	.953	20	.048		
	Total	1.030	24			
Fe	Between Groups	.009	4	.002	.160	.956
	Within Groups	.296	20	.015		
	Total	.306	24			
Mo	Between Groups	4.955	4	1.239	12.757	.000
	Within Groups	1.942	20	.097		
	Total	6.896	24			
Nb	Between Groups	.220	4	.055	1.354	.285
	Within Groups	.812	20	.041		
	Total	1.032	24			
Ta	Between Groups	2.912	4	.728	4.222	.012
	Within Groups	3.449	20	.172		
	Total	6.361	24			

Table 1-17 Multi-comparison tests, two ways ANOVA (Effect of polishing)

Source	Dependent Variable	F	Sig.
Corrected Model	Before polishing	.177	.995
	After polishing	1.109	.379
Intercept	Before polishing	457.698	.000
	After polishing	1025.891	.000
Alloy type	Before polishing	1.050	.312
	After polishing	.606	.441
New to reuse content of alloy	Before polishing	.107	.979
	After polishing	2.228	.083
Alloy type * New to reuse content of alloy	Before polishing	.030	.998
	After polishing	.116	.976

Table 1-18 ANOVA test for surface roughness of CoCr test groups (Surface roughness)

CoCr		Sum of Squares	df	Mean Square	F	Sig.
Before polishing	Between Groups	.061	4	.015	.098	.982
	Within Groups	3.134	20	.157		
	Total	3.195	24			
After polishing	Between Groups	.005	4	.001	1.681	.194
	Within Groups	.015	20	.001		
	Total	.020	24			

Table 1-19 ANOVA test for surface roughness of NiCr test groups (Surface roughness)

NiCr		Sum of Squares	df	Mean Square	F	Sig.
Before polishing	Between Groups	.018	4	.004	.033	.998
	Within Groups	2.627	20	.131		
	Total	2.645	24			
After polishing	Between Groups	.004	4	.001	.832	.520
	Within Groups	.022	20	.001		
	Total	.026	24			

Table 1-20 ANOVA test for CoCr test groups (Porosity evaluaion)

CoCr		Sum of Squares	df	Mean Square	F	Sig
Before polishing	Between Groups	.021	4	.005	3.573	.024
	Within Groups	.030	20	.001		
	Total	.051	24			
After polishing	Between Groups	.001	4	.000	.465	.761
	Within Groups	.006	20	.000		
	Total	.007	24			

Table 1-21 ANOVA for NiCr test groups (Porosity evaluation)

NiCr		Sum of Squares	df	Mean Square	F	Sig.
Before polishing	Between Groups	.010	4	.003	4.369	.011
	Within Groups	.012	20	.001		
	Total	.022	24			
After polishing	Between Groups	.020	4	.005	1.585	.217
	Within Groups	.063	20	.003		
	Total	.082	24			

Table 1-22 Tukey HSD test for CoCr test groups

Dependent Variable	(I) CoCr	(J) cocr	Mean Difference (I-J)	Std. Error	Sig.
Before polishing	0 % recast	25%recast	-.01282	.02432	.983
		50% recast	-.00077	.02432	1.000
		75% recast	-.07665*	.02432	.038
		100% recast	-.03920	.02432	.507
	25%recast	0 % recast	.01282	.02432	.983
		50% recast	.01205	.02432	.987
		75% recast	-.06383	.02432	.103
		100% recast	-.02638	.02432	.812
	50% recast	0 % recast	.00077	.02432	1.000
		25%recast	-.01205	.02432	.987
		75% recast	-.07588*	.02432	.038
		100% recast	-.03843	.02432	.526
	75% recast	0 % recast	.07665*	.02432	.036
		25%recast	.06383	.02432	.103
		50% recast	.07588*	.02432	.038
		100% recast	.03745	.02432	.550
	100% recast	0 % recast	.03920	.02432	.507
		25%recast	.02638	.02432	.812
		50% recast	.03843	.02432	.526
		75% recast	-.03745	.02432	.550

Table 1-23 Tukey HSD test for NiCr test groups

Dependent Variable	(I) NiCr	(J) NiCr	Mean Difference (I-J)	Std. Error	Sig.	95% Confidence Interval	
						Lower Bound	Upper Bound
Before polishing	0% recast	25% recast	-.00800	.01523	.984	-.0536	.0376
		50% recast	-.02600	.01523	.452	-.0716	.0196
		75% recast	-.03000	.01523	.316	-.0756	.0156
		100% recast	-.05800*	.01523	.009	-.1036	-.0124
	25% recast	0 % recast	.00800	.01523	.984	-.0376	.0536
		50% recast	-.01800	.01523	.761	-.0636	.0276
		75% recast	-.02200	.01523	.608	-.0676	.0236
		100% recast	-.05000*	.01523	.027	-.0956	-.0044
	50% recast	0 % recast	.02600	.01523	.452	-.0196	.0716
		25%recast	.01800	.01523	.761	-.0276	.0636
		75% recast	-.00400	.01523	.999	-.0496	.0416
		100% recast	-.03200	.01523	.258	-.0776	.0136
	75% recast	0 % recast	.03000	.01523	.316	-.0156	.0756
		25%recast	.02200	.01523	.608	-.0236	.0676
		50% recast	.00400	.01523	.999	-.0416	.0496
		100% recast	-.02800	.01523	.381	-.0736	.0176
	100% recast	0 % recast	.05800*	.01523	.009	.0124	.1036
		25%recast	.05000*	.01523	.027	.0044	.0956
		50% recast	.03200	.01523	.258	-.0136	.0776
		75% recast	.02800	.01523	.381	-.0176	.0736

Table 1-24 Tests of Between-Subjects Effect of NiCr alloy in solution of pH 4

Source	Type III Sum of Squares	df	Mean Square	F	Sig.
Corrected Model	260600.818[a]	24	10858.367	8.147	.000
Intercept	1331894.645	1	1331894.645	999.336	.000
Immersion time	4286.074	4	1071.519	.804	.526
Test group	245797.010	4	61449.252	46.106	.000
Immersion time * Test group	10517.734	16	657.358	.493	.943
Error	99958.485	75	1332.780		
Total	1692453.948	100			
Corrected Total	360559.302	99			

Table 1-25 Tukey HSD test of Ni-Cr alloy in solution of pH 4 (Ni ions release)

(I) test group	(J) test group	Mean Difference (I-J)	Std. Error	Sig.	95% Confidence Interval	
					Lower Bound	Upper Bound
0% recast	25% recast	21.1357	11.54461	.364	-11.1343	53.4058
	50% recast	-98.4490*	11.54461	.000	-130.7191	-66.1789
	75% recast	-99.8951*	11.54461	.000	-132.1652	-67.6250
	100% recast	-49.6164*	11.54461	.000	-81.8864	-17.3463
25% recast	0 % recast	-21.1357	11.54461	.364	-53.4058	11.1343
	50% recast	-119.5848*	11.54461	.000	-151.8548	-87.3147
	75% recast	-121.0308*	11.54461	.000	-153.3009	-88.7608
	100% recast	-70.7521*	11.54461	.000	-103.0222	-38.4821
50% recast	0 % recast	98.4490*	11.54461	.000	66.1789	130.7191
	25%recast	119.5848*	11.54461	.000	87.3147	151.8548
	75% recast	-1.4461	11.54461	1.000	-33.7162	30.8240
	100% recast	48.8326*	11.54461	.001	16.5626	81.1027
75% recast	0 % recast	99.8951*	11.54461	.000	67.6250	132.1652
	25%recast	121.0308*	11.54461	.000	88.7608	153.3009
	50% recast	1.4461	11.54461	1.000	-30.8240	33.7162
	100% recast	50.2787*	11.54461	.000	18.0087	82.5488
100% recast	0 % recast	49.6164*	11.54461	.000	17.3463	81.8864
	25%recast	70.7521*	11.54461	.000	38.4821	103.0222
	50% recast	-48.8326*	11.54461	.001	-81.1027	-16.5626
	75% recast	-50.2787*	11.54461	.000	-82.5488	-18.0087

Table 1-26 Tests of Between-Subjects Effects of Ni-Cr alloy in solution of pH 6 (Ni ions release)

Source	Type III Sum of Squares	df	Mean Square	F	Sig.	Partial Eta Squared
Corrected Model	109289.295[a]	24	4553.721	3.047	.000	.494
Intercept	386892.303	1	386892.303	258.846	.000	.775
Immersion time	5116.543	4	1279.136	.856	.495	.044
Test group	96381.718	4	24095.430	16.121	.000	.462
Immersion time * Test group	7791.034	16	486.940	.326	.993	.065
Error	112101.096	75	1494.681			
Total	608282.694	100				
Corrected Total	221390.392	99				

Table 1-27 Tukey HSD test of Ni-Cr alloy in solution of pH 6 (Ni ions release)

(I) Test group	(J) Test group	Mean Difference (I-J)	Std. Error	Sig.	95% Confidence Interval	
					Lower Bound	Upper Bound
0% recast	25% recast	17.5238	12.22572	.608	-16.6502	51.6977
	50% recast	-63.0905*	12.22572	.000	-97.2644	-28.9166
	75% recast	-41.4627*	12.22572	.010	-75.6367	-7.2888
	100% recast	-51.4636*	12.22572	.001	-85.6375	-17.2896
25% recast	0 % recast	-17.5238	12.22572	.608	-51.6977	16.6502
	50% recast	-80.6143*	12.22572	.000	-114.7882	-46.4403
	75% recast	-58.9865*	12.22572	.000	-93.1604	-24.8126
	100% recast	-68.9873*	12.22572	.000	-103.1613	-34.8134
50% recast	0 % recast	63.0905*	12.22572	.000	28.9166	97.2644
	25%recast	80.6143*	12.22572	.000	46.4403	114.7882
	75% recast	21.6278	12.22572	.399	-12.5462	55.8017
	100% recast	11.6269	12.22572	.876	-22.5470	45.8009
75% recast	0 % recast	41.4627*	12.22572	.010	7.2888	75.6367
	25%recast	58.9865*	12.22572	.000	24.8126	93.1604
	50% recast	-21.6278	12.22572	.399	-55.8017	12.5462
	100% recast	-10.0008	12.22572	.924	-44.1748	24.1731
100% recast	0 % recast	51.4636*	12.22572	.001	17.2896	85.6375
	25%recast	68.9873*	12.22572	.000	34.8134	103.1613
	50% recast	-11.6269	12.22572	.876	-45.8009	22.5470
	75% recast	10.0008	12.22572	.924	-24.1731	44.1748

Table 1-28 Tests of Between-Subjects Effects of CoCr alloy of solution of pH 4

Source	Type III Sum of Squares	df	Mean Square	F	Sig.
Corrected Model	.006	24	.000	1.543	.080
Intercept	.131	1	.131	860.564	.000
Immersion time	3.429	4	8.573E-6	.056	.994
Test group	.005	4	.001	8.851	.000
Immersion time * test group	.000	16	1.330E-5	.088	1.000
Error	.011	75	.000		
Total	.148	100			
Corrected Total	.017	99			

Table 1-29 Multiple Comparisons of Co-Cr alloy of solution of pH 4 (Co ions release).

(I) Test group	(J) Test group	Mean Difference (I-J)	Std. Error	Sig.	95% Confidence Interval	
					Lower Bound	Upper Bound
0% recast	25% recast	.0174*	.00390	.000	.0065	.0283
	50% recast	-.0042	.00390	.813	-.0151	.0067
	75% recast	.0054	.00390	.643	-.0055	.0163
	100% recast	.0017	.00390	.992	-.0092	.0126
25% recast	0 % recast	-.0174*	.00390	.000	-.0283	-.0065
	50% recast	-.0216*	.00390	.000	-.0325	-.0107
	75% recast	-.0120*	.00390	.024	-.0229	-.0011
	100% recast	-.0156*	.00390	.001	-.0265	-.0047
50% recast	0 % recast	.0042	.00390	.813	-.0067	.0151
	25%recast	.0216*	.00390	.000	.0107	.0325
	75% recast	.0096	.00390	.110	-.0013	.0205
	100% recast	.0060	.00390	.546	-.0049	.0169
75% recast	0 % recast	-.0054	.00390	.643	-.0163	.0055
	25%recast	.0120*	.00390	.024	.0011	.0229
	50% recast	-.0096	.00390	.110	-.0205	.0013
	100% recast	-.0036	.00390	.883	-.0145	.0073
100% recast	0 % recast	-.0017	.00390	.992	-.0126	.0092
	25%recast	.0156*	.00390	.001	.0047	.0265
	50% recast	-.0060	.00390	.546	-.0169	.0049
	75% recast	.0036	.00390	.883	-.0073	.0145

Table 1-30 Tests of Between-Subjects Effects of Co-Cr alloy of solution of pH 6 (Co ions release)

Source	Type III Sum of Squares	df	Mean Square	F	Sig.
Corrected Model	.003[a]	24	.000	.874	.633
Intercept	.061	1	.061	460.671	.000
Immersion time	.000	4	2.891E-5	.219	.927
Test group	.002	4	.001	4.230	.004
Immersion time * test group	.000	16	2.626E-5	.199	1.000
Error	.010	75	.000		
Total	.073	100			
Corrected Total	.013	99			

Table 1-31 Multiple Comparisons of CoCr alloy of solution of pH 6

(I) tedtgroup	(J) tedtgroup	Mean Difference (I-J)	Std. Error	Sig.	95% Confidence Interval	
					Lower Bound	Upper Bound
0% recast	25% recast	.0007	.00363	1.000	-.0095	.0108
	50% recast	.0042	.00363	.780	-.0060	.0143
	75% recast	-.0089	.00363	.113	-.0191	.0012
	100% recast	.0038	.00363	.835	-.0064	.0139
25% recast	0 % recast	-.0007	.00363	1.000	-.0108	.0095
	50% recast	.0035	.00363	.872	-.0067	.0136
	75% recast	-.0096	.00363	.073	-.0197	.0006
	100% recast	.0031	.00363	.913	-.0071	.0133
50% recast	0 % recast	-.0042	.00363	.780	-.0143	.0060
	25%recast	-.0035	.00363	.872	-.0136	.0067
	75% recast	-.0131*	.00363	.005	-.0232	-.0029
	100% recast	-.0004	.00363	1.000	-.0105	.0098
75% recast	0 % recast	.0089	.00363	.113	-.0012	.0191
	25%recast	.0096	.00363	.073	-.0006	.0197
	50% recast	.0131*	.00363	.005	.0029	.0232
	100% recast	.0127*	.00363	.007	.0025	.0228
100% recast	0 % recast	-.0038	.00363	.835	-.0139	.0064
	25%recast	-.0031	.00363	.913	-.0133	.0071
	50% recast	.0004	.00363	1.000	-.0098	.0105
	75% recast	-.0127*	.00363	.007	-.0228	-.0025